

Investigation of antimicrobial and cytotoxic actions of plant extracts and essential oils

Doctoral (Ph.D.) thesis



Sourav Das M. Pharm.

Doctoral School of Pharmacology and Pharmaceutical Sciences

Supervisor: Prof. Dr. Tamás Kőszegi, M.D., Ph.D., Dr. Habil.

Doctoral Program "A-143/1993 Optimization of pharmacotherapy"

Leader of Doctoral Program: Prof. Dr. Lajos Botz, Ph.D., Dr. Habil.

Leader of Doctoral School: Prof. Dr. Erika Pintér, Ph.D., Dr. Habil.,

D.Sc.

University of Pécs, Clinical Center

Department of Laboratory Medicine

Pécs, 2020

Table of Contents

List of abbreviations	6
1. Introduction.....	9
1.1. <i>Essential oils and their uses.....</i>	9
1.2. <i>Artemisia annua L. and its secondary metabolites</i>	10
1.3. <i>Usage of arteficial vs. natural preservatives in food industry.....</i>	11
1.4. <i>Candida species-related infections.....</i>	12
1.5. <i>Experimental and application-based problems</i>	13
1.5.1. Issues related to the stability and lipophilicity of EOs	13
1.5.2. Lack of reliable quantitative and qualitative experimental data	15
1.6. <i>Possible solutions to overcome the above issues.....</i>	15
1.6.1. Cyclodextrins (CDs) as drug delivery systems.....	15
1.6.2. Pickering emulsions.....	16
1.6.3. Development of rapid antimicrobial evaluation methods.....	17
2. The major objectives of our study	17
3. Materials and methods used for RAMEB-EO experiments	18
3.1. <i>Reagents and materials used in RAMEB-EO experiments.....</i>	18
3.2. <i>Inclusion complex formation of RAMEB and selected essential oils/components.....</i>	19
3.3. <i>Characterization of encapsulated essential oils and their components.....</i>	19
3.3.1. UV-VIS spectroscopy analysis	19
3.3.2. Photometric titration assay.....	19
3.3.3. Phase solubility studies	19
3.3.4. Thermodynamics of the encapsulation formation of CDs with the essential oils	20
3.3.5. Headspace gas chromatography with flame ionization analysis.....	20
3.3.6. Determination of average molecular weight of the essential oils	21
3.4. <i>Determination of total antioxidant capacity (TAC) of RAMEB-EOs.....</i>	21
3.4.1. DPPH assay.....	21
3.4.2. Enhanced chemiluminescence (ECL) assay	22
3.4.3. ORAC assay.....	22
3.5. <i>Determination of minimum inhibitory concentration (MIC) of RAMEB-EOs.....</i>	23

3.5.1.	Microorganisms used in the studies	23
3.5.2.	Antimicrobial activity against <i>S. pombe</i> , <i>E. coli</i> and <i>S. aureus</i>	23
3.6.	<i>Rapid live/dead fluorescent cellular discrimination assay</i>	24
3.6.1.	Development of a SYBR Green I/propidium iodide microbial viability assay .	24
3.6.2.	Optimization of the fluorescence assay	24
3.6.3.	Staining microbial suspensions with SYBR Green I/propidium iodide for fluorescence microplate reader and flow cytometry testing.....	24
3.6.4.	Rapid viability assay of RAMEB-EOs on <i>S. pombe</i> , <i>E. coli</i> and <i>S. aureus</i> strains	25
4.	Materials and methods used for chamomile EO-Pickering emulsion experiments .	26
4.1.	<i>Synthesis, surface modification, and characterization of Stöber silica nanoparticles (SNPs)</i>	26
4.2.	<i>Preparation and characterization of C_{Pe}, C_{Et}, and C_{T80}</i>	26
4.3.	<i>Materials used for biological experiments for C_{Pe}, C_{Et}, and C_{T80}</i>	27
4.4.	<i>Determination of minimum inhibitory concentration of C_{Pe}, C_{Et}, and C_{T80}</i>	27
4.4.1.	Microorganisms used for the assay	27
4.4.2.	Antimicrobial activity assay	27
4.4.3.	Determination of minimum effective concentration (MEC ₁₀).....	28
4.5.	<i>Determination of microbial free radical generation and killing activity</i>	28
4.5.1.	Quantification of total ROS generation	28
4.5.2.	Detection of peroxide (O ₂ ²⁻) and superoxide anion (O ₂ ^{•-}) generation.....	29
4.6.	<i>Time-kill kinetics assay</i>	29
4.7.	<i>Live/dead discrimination of microbial cells</i>	30
4.8.	<i>Interaction study between the cell model (unilamellar liposomes) and different formulations of chamomile EO</i>	30
4.9.	<i>GC-MS analysis of chamomile EO</i>	31
5.	Materials and methods used for artemisinin and scopoletin related experiments ..	31
5.1.	<i>Materials used for the biological assays</i>	31
5.2.	<i>Instruments used in the biological assays</i>	32
5.3.	<i>Microorganisms and cultural conditions</i>	32
5.4.	<i>Determination of minimum inhibitory concentration (MIC₉₀)</i>	33
5.5.	<i>Determination of minimum effective concentration (MEC₁₀)</i>	33

5.6. Determination of the effects on preformed mature biofilms	34
5.6.1. Evaluation of total fungal biomass in the biofilms	34
5.6.2. Resazurin-derived metabolism assay in the biofilms.....	34
5.6.3. Viability assay of the biofilms and the planktonic <i>Candida</i> species	35
5.7. Determination of the metabolic activity with resazurin assay and colony formation of planktonic fungal cells.....	36
5.8. Detection of peroxide (O_2^{2-}) and superoxide anion ($O_2^{\bullet-}$) generation in planktonic fungal cells	36
6. Materials and methods used for <i>Artemisia</i> essential oil-related biological assays ...	37
6.1. Plant Collection and Extraction of <i>Artemisia</i> Essential Oil.....	37
6.2. GC-MS-FID studies	37
6.2.1. Samples and sample preparation.....	37
6.2.2. GC-MS analysis (performed by Prof. Dr. Luigi Mondello, and Dr. Giuseppe Micalizzi; University of Messina, Italy).....	37
6.2.3. GC-FID analysis (performed by Prof. Dr. Luigi Mondello, and Dr. Giuseppe Micalizzi; University of Messina, Italy).....	38
6.3. Preparation and characterization of Pickering emulsion	38
6.4. <i>In vitro</i> diffusion studies-Static Franz diffusion cell method	39
6.5. Interaction study between the cellular model (unilamellar liposomes) and different formulations of AE.....	39
6.6. Materials used for the biological experiments	39
6.7. Determination of minimum inhibitory concentration (MIC_{90}).....	40
6.8. Determination of minimum effective concentration (MEC_{10})	41
6.9. Quantification of microbial oxidative stress production in the planktonic cells.....	41
6.9.1. Combined ROS generation measurement.....	41
6.9.2. Determination of peroxide (O_2^{2-}) and superoxide anion ($O_2^{\bullet-}$) generation	42
6.10. Microbial cytotoxicity and viability kinetic assays of planktonics	43
6.10.1. Determination of the colony-forming unit (CFU/mL).....	43
6.10.2. Quantification of the planktonics' intracellular ATP and total protein contents	43
6.10.3. Quantification of the planktonics' metabolic activity.....	44
6.10.4. Live/dead discrimination of planktonic microbial cells.....	45
6.11. Determination of the effects on preformed mature <i>Candida</i> biofilms	45

6.11.1. Evaluation of the total fungal biomass.....	45
6.11.2. Metabolic activity in the biofilms	46
6.11.3. Viability assay of the biofilms	46
6.11.4. Determination of the Candida biofilms' intracellular ATP and total protein contents.....	47
7. Statistical analyses	48
8. Results and discussion: RAMEB-EO complexes	48
8.1. Characterization of RAMEB encapsulated essential oils/components.....	48
8.1.1. UV-VIS spectroscopy analysis	48
8.1.2. Determination of average molecular weight of the essential oils	49
8.1.3. Phase solubility studies	50
8.1.4. Encapsulation efficiency	52
8.2. Antioxidant capacity (DPPH, ECL, and ORAC assay)	52
8.3. Antifungal and antibacterial activities.....	53
8.4. Rapid SYBR Green I/propidium iodide live-dead discrimination assay.....	54
8.4.1. Comparison of the plate reader method with flow cytometry	54
8.4.2. Rapid microbial cell live/dead discrimination plate reader assay of <i>S. pombe</i> , <i>E. coli</i> and <i>S. aureus</i>	55
9. Results and discussion: Pickering-chamomile essential oil experiments	56
9.1. Chamomile essential oil and its components	56
9.2. Characteristics of Stöber silica nanoparticles.....	57
9.3. Nanoemulsion stability.....	57
9.4. Anti-bacterial and anti-fungal activities (MICs) of prepared emulsion	57
9.5. Minimum effective concentrations (MEC ₁₀) for tested bacteria and fungi.....	59
9.6. Effects on microbial oxidative stress	61
9.7. Time-kill kinetics study	63
9.8. Live/dead cell viability discrimination.....	65
9.9. Interaction study between cell model and different formulations of chamomile EO....	67
10. Results and discussion: antifungal effects of artemisinin and scopoletin	67
10.1. Antifungal activities (MIC ₉₀) of Ar and Sc.....	67
10.2. Data of minimum effective concentrations (MEC ₁₀) for planktonic Candida species	68
10.3. Effects on mature biofilms	70

10.4. Live/dead planktonic cell viability discrimination.....	72
10.5. Effects on metabolic activity and colony formation of planktonic cells	73
10.6. Effects on planktonics' oxidative balance.....	75
11. Results and discussion: Pickering-Artemisia essential oil experiments.....	77
11.1. Effect of Artemisia essential oil and its components	77
11.2. Preparation and stability studies of O/W type Pickering nanoemulsions	78
11.3. In-vitro diffusion study of Artemisia EO (AE) formulations.....	78
11.4. Interaction studies with unilamellar liposomes as cellular models.....	78
11.5. Antibacterial and antifungal activities of the prepared emulsions.....	78
11.6. Effects of the minimum effective concentration (MEC_{10}) on planktonic microbial cells.....	80
11.7. Effects on the microbial oxidative balance.....	82
11.8. Effects on the microbial planktonics' behavior	84
11.8.1. Colony formation changes	84
11.8.2. Variations in the intracellular ATP to total protein content ratios.....	86
11.8.3. Effects on microbial cell viability and metabolic activity	89
11.9. Effects on mature <i>Candida</i> spp. biofilms	93
12. Conclusions.....	96
13. Future perspectives.....	98
14. Acknowledgements	98
15. Novel findings of the Ph.D. research	99
16. References.....	100
Supplementary materials	116
List of publications and conferences	132
Articles related to this thesis.....	132
Article not related to this thesis	132
Conference presentations related to this thesis	132
Conference presentations not related to this thesis	133
Figure and table legends.....	134
Supplementary figure and table legends.....	138

List of abbreviations

AAPH: 2,2'-azobis (2-methylpropionamidine) dihydrochloride

AE: *Artemisia annua* L. essential oil

AEPs: *Artemisia* Pickering emulsion

AETs: Tween80 stabilized AE

AIDS: Acquired immune deficiency syndrome

Ar: Artemisinin

ATCC: American Type Culture Collection

AUC: Area under curve

BSA: Bovine serum albumin

Cas, Cs: Caspofungin

CBS: Central Bureau of Fungal Cultures

CD: Cyclodextrin

CEt: Chamomile EO in ethanol

CFU: Colony forming unit

CLSI: Clinical & Laboratory Standards Institute

CPe: Pickering emulsion of chamomile EO

CS&T beads: Cytometer Setup and Tracking beads

C_{T80}: Tween 80 conventional emulsion

DCFDA: 2',7'-dichlorofluorescein diacetate

DHE: Dihydroethidium

DHR 123: Dihydrorhodamine 123

DLS: Dynamic light scattering

DMSO: Dimethyl sulfoxide

DNA: Deoxyribonucleic acid

DPPH: diphenyl-2-2 picryl-hydrazyl

ECL: 2.4.2. Enhanced chemiluminescence assay

EE: Encapsulation efficiency

EOs: Essential oils

FD: Fluorescein diacetate

FDA: Food and Drug Administration

FID: Flame ionization detection

FL: Fluorescein

FSC-H: Forward scatter height
FSC-W: Forward scatter width
G: Gibb's free energy
GALT: Gut-associated lymphoid tissue
GC: Gas chromatography
Gc: Growth controls
GC-MS: Gas chromatography and mass spectrometry
GRAS: Generally recognized as safe
H: Standard enthalpy change
HIV: Human immunodeficiency virus
i. d: Internal diameter
IC₅₀: Inhibitory concentration at 50% total antioxidant capacity
ICs: Inclusion complexes
K: Equilibrium constant
K_f: Formation constant
K_s: Stability constant
LB: Lauria-Bertani liquid medium
M cells: Micro-fold cells
Me: Menadione
MEC₁₀: Minimum effective concentration
MHA: Mueller Hinton agar
MIC₉₀: Minimum inhibitory concentration
MOPS: 3-(N-morpholino) propanesulfonic acid
NCCLS: National Committee for Clinical Laboratory Standards
O/W: Oil-in-water
ORAC: Oxygen radical absorbance capacity
PBS: Phosphate-buffered saline
PCR: Polymerase chain reaction
PI: Propidium iodide
PMC: Department of General and Environmental Microbiology, University of Pecs
POD: Horseradish peroxidase
qPCR: Quantitative polymerase chain reaction
R: Ideal gas constant
RAMEB: Randomly methylated β -cyclodextrin

ROS: Reactive oxygen species
RPMI: Roswell Park Memorial Institute Medium
RT-PCR: Reverse transcription polymerase chain reaction
S: Entropy of the system
Sc: Scopoletin
SNPs: Stöber silica nanoparticles
SSC-H: Side scatter height
SSC-W: Side scatter width
SZMC: Szeged Microbial Collection
T: Temperature
TAC: Total antioxidant capacity
TE: Trolox equivalent
TEM: Transmission electron microscopy
TEOS: Tetraethoxysilane
TSB: Tryptic Soy Broth
ULs: Unilamellar liposomes
UV-VIS: Ultraviolet–visible spectroscopy
Van: Vancomycin
W/O: Water-in-oil
XTT: 2,3-bis-(2-methoxy-4-nitro-5-sulfophenyl)-2h-tetrazolium-5-carboxanilide
YES: yeast extract-glucose medium
YPD: yeast extract peptone dextrose agar medium

1. Introduction

The practice of treating various diseases using medicinal plants is as old as an ancient civilization. Secondary metabolites and essential oils present in the plants are predominantly responsible for treating various ailments. These natural compounds exert significant pharmacological and toxicological effects in humankind [1,2]. Folk medicines of almost all civilizations of the world abound in herbal remedies. The majority of the drugs used in traditional medicines is obtained from plants. Despite several advancements in the field of synthetic drug chemistry and production of antibiotics, plants continue to be one of the major raw materials for drugs developed for the treatment of various human ailments. Clinical and pharmaceutical investigations have elevated the status of medicinal plants by identifying the role of active components present in them and elaborating their mode of action in humans and in animals as well [1,3]. Medical systems all around the world, which had been developed thousands of years ago, heavily relied on herbal medicine; a good record of plant usage is available for Traditional Chinese Medicine, Kampo medicine, Ayurvedic medicine, European medicine, and traditional medicines of Africa, Australia, and Americas [2].

The treatment of infections and other health disorders with herbal medicines is usually not or not entirely a placebo medicine but involves active natural products mostly of low molecular weight with great structural diversity (so-called secondary metabolites) and complex mixture of active components e.g. in the form of essential oils, which are found in many plants [2,3]. Since the medicinal herbs are widely used among laymen for various disorders there is an ultimate need to characterize the plant extracts' or their purified components' biological activity including their potential toxicity.

1.1. Essential oils and their uses

Essential oils (EOs) have been widely used in folk medicine throughout the history of humankind. The application of EOs covers a wide range from therapeutic, hygienic, and spiritual to ritualistic purposes. EOs are aromatic, volatile, lipophilic liquids extracted from different parts of plant materials such as barks, buds, flowers, fruits, seeds, and roots [1]. EOs are mixtures of complex compounds with variable individual chemical composition and concentrations that includes primarily terpenoids, like monoterpenes (C₁₀), sesquiterpenes (C₁₅), diterpenes (C₂₀), acids, alcohols, aldehydes, aliphatic hydrocarbons, acyclic esters or lactones, rare nitrogen- and sulfur-containing compounds, coumarin, and homologs of phenylpropanoids [1,2]. The biological effects of EOs cover a wide range of effects, including

antioxidant, antimicrobial, antitumor, anti-inflammatory, and antiviral activity [3]. The increase in demand for the use of aromatherapy as complementary and alternative medicine has led people to believe in the myth that EOs are harmless because they are natural and have been used for a long time [4]. EOs usually recognized as safe (GRAS) are used primarily as flavoring agents in foods, in medicine, and as fragrances in cosmetics [5,6]. However, consumer's recent demand for products extracted from eco-friendly renewable sources, with low toxicity, both for human and animal consumption, and with natural appeal has stimulated the research looking at new applications for EOs [7]. Several studies have demonstrated that some EOs show interesting antimicrobial properties against foodborne pathogens and food spoilage microorganisms. Due to this, their application as a potential green preservative for foods has been considered [5,8–10]. This antimicrobial activity involves their hydrophobic compounds' ability to disrupt microorganisms' cell membranes, which results in a change of cell morphology, alteration of membrane permeability and leakage of electrolytes, consequently leading to cell destruction [11]. In general, essential oils act to inhibit microbial cell growth and the production of toxic metabolites. In case of bacteria most essential oils have a more pronounced effect on Gram-positive bacteria than on Gram-negative species, and this effect is most likely due to differences in the cell wall composition of these microbes [12]. Gram-positive bacteria have only one outer layer, which facilitates penetration of external molecules, promoting interaction with the cytoplasmic membrane and making them more fragile compared with Gram-negative bacteria. Gram-negative bacteria have an additional membrane with a phospholipid bilayer structure responsible for the protection of the inner cytoplasmic membrane, which confers greater resistance to this class of bacteria [13]. The hydrophilic wall hinders the penetration of hydrophobic compounds, for example, essential oils, into the cell. Mechanisms that explain the action of essential oils on microbial cells have been studied, but it is still not possible to say with certainty how the essential oils act on a microbial cell [14]. These bioactive compounds have many components, and the antimicrobial action cannot be confirmed by the action of only a single component or by the activity on a single cell site. The typical hydrophobic characteristics of essential oils is responsible for the breakdown of microbial cell structures, which leads to increased permeability through the microbial cell membrane [14–18].

1.2. Artemisia annua L. and its secondary metabolites

Artemisia annua L. (Sweet Wormwood, Sweet Annie, Sweet Sagewort, Annual Wormwood, or Qinghaosu) is a very important member of the Asteraceae family and is widely

distributed throughout Asia, South Africa, Europe and North America [15,16]. The use of this plant for the treatment of malaria has been recorded before 168 BC in Chinese traditional medicine [15]. Discovery of the artemisinin, a sesquiterpene with the antimalarial property made this plant to have potential commercial importance [17]. The search for other active components has led to the discovery of many phytochemicals including, monoterpenoids, sesquiterpenoids, flavonoids and coumarins, and aliphatic and lipid compounds [18]. Apart from its antimalarial activity, the plant has shown anti-tumor, anti-inflammatory, antipyretic, antimicrobial, antiparasitic, antiulcerogenic, and cytotoxic activities [19]. Several studies on the chemical composition of the *Artemisia annua* L. essential oil (AE) have been performed, and active components like camphor, artemisia ketone, germacrene D, and 1,8-cineole have been found [20]. Variability in the chemical composition of AE depending on the geographical origin and plant's development stages has led to considerable research interests in the investigation of the biological properties of AE [21].

Artemisinin (Ar), belonging to a family of sesquiterpene lactones originally derived from *Artemisia annua* L. is well-known for its anti-malarial actions by forming free radicals through cleavage of intra-parasitic iron-endoperoxide groups and by alkylation of specific malarial proteins mediating eradication of *Plasmodium* species [15]. Protection against cancers and inflammation by artemisinin has also been documented [18]. The Ar has been reported to possess anti-infective activity against viruses (Human *cytomegalovirus*) and fungi (*Cryptococcus neoformans*) [16].

Scopoletin (Sc, 6-methoxy-7-hydroxycoumarin) is a phenolic compound isolated from several plants including *A. annua* L. [22]. Sc possesses anti-tumor and anti-angiogenesis properties by initiating cell cycle arrest and facilitating apoptosis in human prostate tumor cells and leukemia cell lines [23,24]. Although anti-fungal effects including the anti-*Candida* activity of Ar and Sc were already studied, yet no detailed data are found in the literature on *Candida* species' viability and biofilm formation treated with Ar and Sc at their sub-inhibitory concentrations. Because of the diverse biological activities including reactive oxygen species (ROS) generation [22,24–26], the above mentioned secondary active metabolites and essential oil having a wide range of biological actions might exert antimicrobial activity as well.

1.3. Usage of artificial vs. natural preservatives in food industry

Food preservation is a dominant feature in all food sectors and mainly comprises curbing the rise of microorganisms that increase the health-related issues in consumers. The food attributes that attract the attention of the consumer are freshness and their naturalness and

minimal processing. The perception of naturalness drives the consumer towards the food without chemical preservatives. Modernization coupled with the change in the lifestyle of the consumer shifts them towards the use of ready-to-use food. Thermal processing, drying, freezing, refrigeration, irradiation, modified atmosphere packaging (MAP), and addition of antimicrobial agents or salts are some conventional methods to prevent the growth of microbes in foods [27,28]. Some chemical preservatives such as sodium benzoate, potassium sorbate, and nitrites have been used commercially in fruit juices, dairy products, confectionery, meat and meat products, etc. Nitrites and nitrates are applied in the meat industry to inhibit the growth of the microorganisms, retain the red color of the meat, and reduce the oxidation of lipids [29]. However, blue baby syndrome occurs in young children owing to the presence of a high amount of nitrites in their blood [30]. Some chemical preservatives such as sodium benzoate and potassium sorbate used in the fruit juice industry have also constraints like benzoic acid that is converted into benzene in foods [31], and *S. cerevisiae* and *Pichia anomala* can decarboxylate sorbic acid to 1,3 pentadiene which causes kerosene-like off-odor. *Schizosaccharomyces pombe* may produce off-flavors in the presence of sulfite [32]. Due to growing evidence about the harmful effects of chemical preservatives, there is a continuous pressure to reduce the amount of added preservatives in foods.

To avoid the health risks associated with the consumption of chemically enriched foods, natural antimicrobial compounds like bacteriocins, chitosan-fermented ingredients, and plant antimicrobials provide another alternative for preserving food [27]. Spices and herbs are used in food since ancient times, not only for flavoring but also for preservation. Plant extracts, essential oils, and peptides exhibit a broad-spectrum activity [28]. The antimicrobial and antioxidant properties of plants are attributed to secondary metabolites such as phenylpropanoids, terpenes, flavonoids, and anthocyanins [33]. Several studies have been conducted around the globe to prove the efficacy of plant products, and various compounds isolated from these plants are secondary metabolites that possess antimicrobial and other medicinal properties.

1.4. Candida species-related infections

Fungi represent a significant burden of infection to hospitalized patients. The use of broad-spectrum antibiotics, parenteral nutrition, indwelling catheters, or the presence of immunosuppression, or disruption of mucosal barriers due to surgery, chemotherapy, and radiotherapy are among the most important predisposing factors for invasive fungal infection. Fungal biofilms play an important role in numerous infections. They are composed of structural

microbial communities adhering to different surfaces and being enveloped by the exopolymeric matrix [34,35]. The development of biofilms hinders the action of the defense system of the host and increases the resistance to standard antifungal agents [36]. *Candida* species like *Candida albicans* (*C. albicans*), *Candida dubliniensis* (*C. dubliniensis*), *Candida tropicalis* (*C. tropicalis*), *Candida krusei* (*C. krusei*), *Candida glabrata* (*C. glabrata*), *Candida guilliermondii* (*C. guilliermondii*), and *Candida parapsilosis* (*C. parapsilosis*) are fungal species of major medical importance. *Candida* species, members of human microflora, are diploid polymorphic yeasts [37] that can be found in the human gastrointestinal, respiratory, and inside the genitourinary tracts; therefore, *C. albicans* is found in vaginal, mucosal, and deep-tissue infections [38–40]. In certain individuals with immune-compromised status, the *Candida* species might induce consequent infection. Also, *Candida* species can rapidly adapt to the host's micro-environmental circumstances caused by pH and nutritional changes in the gastrointestinal tract [41]. Environmental imbalance because of nutritional change or pH shifting facilitates the abnormal growth of *Candida* species which results in candidiasis [42]. *Candida* species attack the gut epithelium barriers to reach the bloodstream via micro-fold cells (M cells) that are found in the gut-associated lymphoid tissue (GALT) of Peyer's patches in the small intestine promoting intestinal infections [43]. Esophageal candidiasis is one of the major and common infections in people living with HIV/AIDS [41]. Symptoms of candidiasis in the mouth, throat, and esophagus generally include swallowing problems and pain [44,45]. Because of the increasing incidence of candidiasis and the difficulties in its treatment due to the limited options in the use of antifungal drugs with species-specific efficacy [43], there is an ultimate need for at least prevention of fungal infections.

1.5. Experimental and application-based problems

1.5.1. Issues related to the stability and lipophilicity of EOs

Despite the natural appeal and interesting effectiveness against both molds and bacteria, EOs are highly volatile and prone to oxidative damage when exposed to light, oxygen, and temperature [46]. Furthermore, due to their strong odor, the application of EOs in food products may be limited, since undesirable changes in food natural aroma may occur [47]. Chemical component groups of essential oils are readily converted by oxidation, isomerization, cyclization, or dehydrogenation, which are reactions that can be enzymatically or chemically triggered, and these processes are usually associated with a loss of quality. For example, terpenoids tend to be volatile and thermo-labile and can be readily oxidized or hydrolyzed,

depending on their structure [48]. Further, the maintenance of essential oil composition depends strongly on the conditions under which it is processed and how it is handled and stored upon production. Certain factors are crucial for maintaining the stability of essential oils, such as temperature, light, and oxygen availability [49]. Also, there might be several side effects of EOs even if topical administration is applied and, among these, allergic reactions are the most frequent (many EOs can cause, e.g., rashes on the skin). Some of them can be poisonous if absorbed through the skin, breathed, or swallowed. Previous studies also report the interaction of EOs with other drugs [50]. The continuous production of new aroma chemicals and their widespread and uncontrolled usage as alternative therapies together with many carrier diluents have brought serious problems, especially among children. In this regard, it is of utmost importance to study the mode of action of essential oils and to find a proper, harmless formulation. Another serious problem is the highly lipophilic nature of EOs, which makes it impossible to measure their biological effects in an aqueous environment [1,51,52]. Several assays including conventional broth dilution method, disk diffusion method, and bioautography assay are used to measure the antimicrobial activity of EOs. Efforts have been made to overcome the lipophilic nature of the oils usually by application of EOs diluted in seemingly suitable solvents/detergents. In the case of natural lipophilic volatile compounds like EOs, solvents of varying polarity, e.g., DMSO, ethanol, and methanol, are most commonly used. However, previous studies have reported the antimicrobial effects of the solvents themselves (DMSO, ethanol, and other solvents in various microbial assays) or their influence on the true antimicrobial effects of EOs [53]. The usage of solubilizing agents limits the precise determination of the antimicrobial activities of EOs. Also, a major problem might arise in the classical assays due to the evaporation of EOs during the assay or the inability of the test microbes to reach the lipophilic range of the tested EOs (in bioautography, as an example) [54,55].

Therefore, new formulations have been determined to increase the solubility or to emulsify the EOs in an aqueous environment. These efforts help to stabilize the oils, to produce an even release of the active components into the required environment, and to maintain their antioxidant and antimicrobial activities [51,56–58]. Detergents and organic solvents are not welcome in this regard. Attempts have been made to entrap EOs by modified cyclodextrins for the exact determination of their antimicrobial characteristics [59,60].

1.5.2. Lack of reliable quantitative and qualitative experimental data

Another major problem that hinders the measurement of the antimicrobial activity studies is the lack of clearly visible bacterial and fungal colonies which makes precise quantification of the growth, difficult. Lack of a convenient viability testing method has hampered antibiotic testing and new drug discovery [61]. Presently, microscopic counting and quantitative PCR (qPCR) or reverse-transcription PCR (RT-PCR) are the main and reliable assays for rapid assessment. Manual microscopic counting using a counting chamber is mainly used to characterize microbial viability *in vitro*, but it is very time-consuming and is hard to perform in a microtiter plate. Although quantitative PCR (qPCR) can detect very small amounts of DNA and is usually applied for microbial viability assay *in vivo*, it is complex, costly, and not suitable for viability assay of microbes in high-throughput drug screen format. Several rapid colorimetric assays have been used to determine microbial enzymatic activity, cell membrane integrity, cell proliferation, metabolic activity, cell viability and antibiotic susceptibility [62–72]. However, these assays either have limited sensitivity or are cumbersome and cannot be performed in a high throughput format.

1.6. Possible solutions to overcome the above issues

1.6.1. Cyclodextrins (CDs) as drug delivery systems

Cyclodextrins (CDs) approved by the Food and Drug Administration (FDA) and enlisted as GRAS, are one of the most studied host molecules for their use in foods [73]. They are natural oligosaccharides employed for the preparation of inclusion complexes (ICs) with EOs resulting in enhanced oil physical and chemical stability, via reducing volatility and sensitivity against light, heat, and oxidation [74]. They are non-toxic with a hydrophilic outer surface and a hydrophobic core allowing the hydrophobic guest molecule to enter and stay inside. This interaction among the guest molecules and CDs forms a non-covalent inclusion complex in the polar medium. This inclusion complex is in dynamical equilibrium allowing the guest molecule to diffuse out from the CDs complex system [60]. Native CDs are composed of six, seven, or eight glucosyl units and are known as α -cyclodextrin (α -CD), β -cyclodextrin (β -CD) and γ -cyclodextrin (γ -CD), respectively. The diameter of the CDs cavity is measured by the number of glucose units in the CD and this controls the size of the guest molecule for encapsulation (Figure 1). Many CD derivatives including randomly methylated β -cyclodextrins (RAMEB) with enhanced solubility and increased encapsulation performance are of major interest at present [60,75].

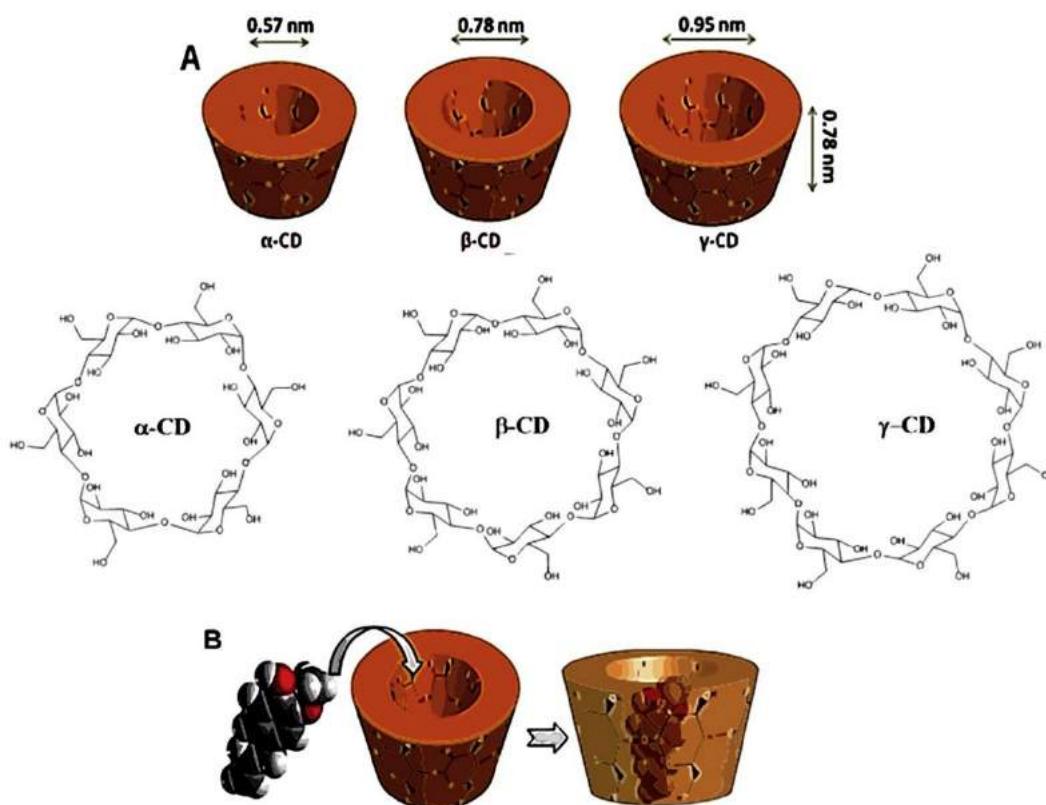


Figure 1. Characteristics of synthetic cyclodextrins. Shapes, dimensions, chemical structures, and complexation of natural cyclodextrins. Cyclodextrins are cyclic oligosaccharides with a lipophilic central cavity and a hydrophilic outer surface. (A): The conical shape, dimensions, and chemical structures of α -, β -, and γ -cyclodextrin are illustrated. The chemical structures of α -, β -, and γ -cyclodextrin show that they are composed of six, seven, and eight glucose units, respectively. (B): Schematic illustration of inclusion complexation. A hydrophobic/amphipathic molecule enters the cyclodextrin cavity to form a reversible inclusion complex. Reproduced from Ref. [75].

1.6.2. Pickering emulsions

The application of Pickering nanoemulsion is also a quite novel approach to stabilize oil-in-water (O/W) and water-in-oil (W/O) emulsions by solid particles instead of surfactants. The mechanism involves the adsorption of solid particles on the oil-water interface, causing a significant decrease in the surface tension that results in high emulsion stability [57] (Figure 2). Previous studies have reported decreased evaporation of EOs from O/W emulsion of nanoparticle-stabilized formulations versus EO–surfactant systems to be a beneficial factor [76,77].

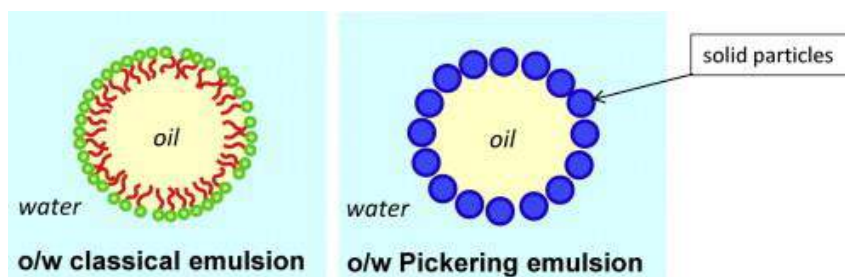


Figure 2. Sketch of a Pickering emulsion and a classical (surfactant-based) emulsion. The solid particles adsorbed at the oil-water interface stabilize the droplets instead of the surfactant molecules. Reproduced from Ref. [78].

1.6.3. Development of rapid antimicrobial evaluation methods

Sensitive viability assays that can be used for rapid viability detection of microbes and for high throughput drug screens to identify new drugs for improved antimicrobial treatment must be developed. The laboratories who do not have the access to expensive instruments will have the possibility to use newly developed reliable and cheaper techniques to perform live/dead antimicrobial assays in a high throughput fashion with a simple multi-plate reader.

2. The major objectives of our study

- **The solubility of the plant-derived secondary metabolites, essential oils, and their active components in the aqueous test systems is usually very poor. That is why the characterization of the antioxidant and antimicrobial properties is often performed by adding detergents, polar protic/aprotic, and non-polar solvents.**

Therefore, we aimed to develop new drug formulations with modified cyclodextrins and nanoemulsions for aqueous test systems that could be used for antioxidant and antimicrobial assays without additives. We also characterized the entrapment efficiency and the thermodynamic properties of the cyclodextrin-captured EOs and pure EO components.

- **There is no existing rapid, high throughput assay for live/dead microbial viability testing.**

We have tried to establish a rapid live/dead microbial viability microplate assay technique using a double-stain fluorescent method.

- **Formation of fungal biofilms is a major problem and there are only a few natural anti-biofilm compounds that could overcome increasing microbial drug resistance. So, there is a need to find some new natural compounds that can compete with microbial drug resistivity in biofilms.**

We aimed to investigate the antimicrobial and biofilm degradation activities of artemisinin and scopoletin (isolated from *Artemisia annua* L.) to reveal their effects on cellular viability, metabolic activity, and oxidative stress balance of microbial biofilms.

- **There are only a few attempts to measure the antimicrobial activity of plant extracts at their concentration below the MIC.**

We aimed to characterize the antimicrobial effects of essential oils and pure plant extracts at their Minimum Effective Concentrations (MEC₁₀) by various methods (metabolic activity, oxidative stress, live/dead discrimination assay, killing activity vs. exposure time).

- **The exact measurement of the antimicrobial assay in the biofilms is still a challenge.**

That is why we have aimed to develop multi-parametric fluorescent techniques to evaluate the possible mode of action of our studied plant extracts in mature biofilms.

3. Materials and methods used for RAMEB-EO experiments

3.1. Reagents and materials used in RAMEB-EO experiments

All chemicals used for the in vitro analysis were of analytical or spectroscopic grade and highly purified water (<1 µS) was applied throughout the experiments. Sterile 96-well plates, 96-well general microtiter plates, and 96-well white optical microtiter plates were from Greiner Bio-One (Kremsmunster, Austria), Sarstedt AG & Co. KG., (Numbrecht, Germany) and PerkinElmer Inc. (MA., USA), respectively. Horseradish peroxidase (POD), 6-hydroxy-2,5,7,8-tetramethylchroman-2-carboxylic acid (Trolox), luminol, para-iodophenol, diphenyl-2,2-picryl-hydrazyl (DPPH, stable free radical), fluorescein Na₂ salt, 2,2'-azobis (2-methylpropionamide) dihydrochloride (AAPH), SYBR Green I, propidium iodide (PI), Lauria-Bertani (LB) liquid medium, yeast extract-glucose (YES, pH 4.5, supplemented with amino acids and Wickerham solution) media and Tryptic Soy Broth (TSB) were from Sigma-Aldrich Chemie GmbH (Steinheim, Germany), and 1 mg/mL bovine serum albumin (BSA, Serva Electrophoresis GmbH, Heidelberg, Germany) in 50 mmol/L phosphate buffer pH 7.4, H₂O₂ (Molar Chemicals Ltd., Budapest, Hungary) diluted with 0.1% citric acid (Ph. Eur 8.0.) were used. Cytometer Setup and Tracking beads (CS&T beads) were from BD Biosciences Co. (M.A., U.S.). Dimethyl sulfoxide (DMSO), ethanol, and methanol (Reanal Labor, Budapest, Hungary) were of spectroscopic grade. In the oxygen radical absorbance capacity (ORAC) assay, 75 mmol/L K-phosphate buffer of pH 7.4 was used. All the EOs/components - RAMEB

(randomly methylated β -cyclodextrin) namely lavender oil, lemon balm oil, peppermint oil, thyme oil, borneol, citral, linalool, menthol, and thymol were obtained from CycloLab Cyclodextrin Research & Development Laboratory, Ltd. (Budapest, Hungary).

3.2. Inclusion complex formation of RAMEB and selected essential oils/components

Twenty-five grams (close to 0.02 mole) of statistically (random) methylated beta-cyclodextrin (having an average degree of methylation of 1.8 methoxy-groups/glucopyranose unit) was dissolved in 30 mL of deionized water at room temperature under nitrogen stream protected from light. Then 1.5 g (close to 0.01 mole) of the essential oils or pure components were fed dropwise to the stirred cyclodextrin solution. The resulting emulsion was sonicated for 3 minutes and stirred for further 2 h protected from light. It was then chilled to - 45 °C in dry ice/ethanol mixture and lyophilized. The resulting light powder was homogenized and used for further studies.

3.3. Characterization of encapsulated essential oils and their components

3.3.1. UV-VIS spectroscopy analysis

The encapsulation formation of the selected essential oils/components to RAMEB was evaluated by UV/VIS spectrophotometry (Hitachi U-3900, Auro-Science Consulting Ltd., Budapest, Hungary). Essential oils were dissolved in acetonitrile (0.5 mg/mL). RAMEB, encapsulated essential oils, components, and a 4:1 mixture of RAMEB-essential oils/components were mixed in acetonitrile at 5 mg/mL and shaken for 10 minutes. The supernatant was separated by centrifugation, diluted hundred times in acetonitrile, and was scanned in the range of 200 – 400 nm to obtain UV-VIS absorption spectra [79].

3.3.2. Photometric titration assay

The photometric titration was performed in acetonitrile. In brief, the oil concentrations were kept constant (1 mmol/L) while the CD concentrations were varied from 1 mmol/L up to 8 mmol/L. Data evaluation was performed as described before [80,81].

3.3.3. Phase solubility studies

Phase solubility plots were obtained to identify and to evaluate the stability of the inclusion complexes [82]. In brief, excess of essential oils was added to 10 mL aqueous solutions of RAMEB in a concentration range of 0 – 10 mmol/L, incubated at 25 °C and 35 °C, shaken at

200 rpm for 24 h and filtered through 0.45 μm syringe filter (Fisher Scientific). The quantity of essential oils remained in the solution was measured spectrophotometrically at 214.5 nm (Hitachi U-3900) and data were compared with the standard curve obtained for the components. The quantity of essential oils in the solution was plotted against RAMEB concentration. The stability constant K_S (L/mole) was calculated from the slope and intercept of the plot from the equation:

$$K_S = \frac{\text{slope}}{\text{intercept} \times (1 - \text{slope})} \quad (1)$$

where K_S (L/mole) represents the stability constant and intercept (mmol/L) is the dissolved guest molecules (essential oil or their pure components) in the aqueous complex medium when no cyclodextrin is present.

3.3.4. Thermodynamics of the encapsulation formation of CDs with the essential oils

The processes associated with the complex formation, thermodynamic parameters were determined using the stability constants measured at different temperatures applying the van't Hoff equation:

$$\ln(K) = \frac{-\Delta G}{RT} = \frac{-\Delta H}{RT} + \frac{\Delta S}{R} \quad (2)$$

where, G, H, K, R, S, and T represent Gibb's free energy, standard enthalpy change, the equilibrium constant, ideal gas constant, the entropy of the system, and temperature, respectively.

3.3.5. Headspace gas chromatography with flame ionization analysis

The formation of inclusion complexes of the selected essential oils, their components, and RAMEB was examined by headspace gas chromatography with flame ionization detection (Agilent 7890A GC system, G1888 Network Headspace Sampler). Encapsulation efficiency for the RAMEB-EO complexes and formation constant (K_f) values of RAMEB/aroma inclusion complexes were determined using the static headspace gas chromatography based on the previous publication [83]. Essential oils (100 ppm) or their components (1 mmol/L) were added to 10 mL deionized water or RAMEB's aqueous solution (20 mmol/L) previously introduced into 20 mL headspace vial. The vial was crimp sealed and thermostated at 25 ± 0.1 °C. After the equilibrium was established (30 minutes), 100 μL of vapor was injected directly into the chromatographic column (DB-ALC2, Agilent J&W Scientific, 30 m x 0.32 mm

internal diameter (i.d.) and a 1.2 μm film thickness). The HS loop and transfer line temperatures were set at 80 $^{\circ}\text{C}$ and 150 $^{\circ}\text{C}$, respectively. The injection port temperature was kept at 230 $^{\circ}\text{C}$ and used in split mode with a split ratio of 1:2. The flame ionization detection (FID) temperature was maintained at 250 $^{\circ}\text{C}$. Nitrogen was used as the carrier gas. The initial GC oven temperature was held at 76 $^{\circ}\text{C}$ for 10 minutes, then the temperature increased at 2 $^{\circ}\text{C}/\text{minute}$ to 128 $^{\circ}\text{C}$ and then ramped at 10 $^{\circ}\text{C}/\text{minute}$ to 218 $^{\circ}\text{C}$ which was kept for 60 seconds. To determine the formation constant (K_f) and the encapsulation efficiency (EE) 3-3 parallel measurements were performed. K_f values (L/mole) and EE (%) were calculated using the following equations:

$$K_f = \frac{\left(\frac{A_0}{A_{RAMEB}}\right) - 1}{C_{RAMEB}} \quad (3)$$

where, A_0 and A_{RAMEB} are the peak areas of aroma components in the absence and the presence of RAMEB, respectively; C_{RAMEB} is the initial concentration of RAMEB, and,

$$EE = \left(\frac{\sum A_0 - \sum A_{RAMEB}}{\sum A_0}\right) \times 100 \quad (4)$$

where, $\sum A_0$ and $\sum A_{RAMEB}$ are the sum of the peak areas of aroma components in the absence and presence of RAMEB, respectively.

3.3.6. Determination of average molecular weight of the essential oils

In brief, the average molecular weight of the experimented essential oils was examined by determining the cryoscopic constants of dimethyl sulfoxide (DMSO, 4.484 K kg/mole) using 1.003654 kg/mole naphthalene. DMSO was used as the media. All measurements were repeated three times.

3.4. Determination of total antioxidant capacity (TAC) of RAMEB-EOs

3.4.1. DPPH assay

DPPH assay has been performed following the procedure described previously [84–86] with modifications. DPPH (2.94 mg) in 25 mL of 96% ethanol (300 μM) was prepared and stored in the refrigerator being stable for one week. Acetate buffer (100 mmol/L, pH 5.5) was used throughout the experiments. Trolox standard of 1 mmol/L was prepared in 50% ethanol. Serial dilutions of Trolox standards ranging from 0-180 μM and EOs - RAMEB dilutions of 1 mg/mL - 0.01 mg/mL % (w/v) were prepared in PBS, pH 7.4. 50 μL of acetate buffer (100

mmol/L, pH 5.5) followed by 50 μ L standard/sample dilutions and 95 μ L DPPH (300 μ M) were pipetted into 96-well general micro-titer plates. The absorbance changes in the wells were measured at 517 nm by the PerkinElmer EnSpire Multimode reader at 25 °C after 90 minutes of incubation in the dark, at room temperature. Measurements were performed in triplicates or more. Antioxidant capacities were calculated in the form of inhibitory concentration at 50% TAC level (IC_{50}) which was obtained from the equation derived from % scavenger activity vs. serial sample dilution concentration graph [85,87,88]. IC_{50} values were referred to as 1 gram dry mass of the samples.

3.4.2. Enhanced chemiluminescence (ECL) assay

We followed the method previously published [89]. The enhanced chemiluminescence reaction was performed in 96-well white optical plates. Ice-cold premixed ECL reagent and POD working solution (200 μ L POD +70 μ L ECL reagent) was prepared freshly. Trolox standards were used in the concentration range of 0 – 100 μ M. 20 μ L Trolox/blank/sample and 270 μ L of POD-ECL reagent were pipetted into each well. For initiation of the ECL reaction, 20 μ L ice-cold H_2O_2 in citric acid was injected into the wells by the automated dispenser of a Biotek Synergy HT Gen5 (Auro-Science, Consulting Ltd., Budapest, Hungary) microplate reader. The chemiluminescence signal was followed for 10 minutes. For the ECL assay, total light output (area under the curve, AUC) data were taken. TAC of the samples was obtained by using the regression equation obtained for the standards, results multiplied by the dilution factor, and expressed as μ M Trolox equivalent (TE). The TE for each sample was further referred to as 1 g of initial essential oil content. Measurements were performed at least in triplicates or more.

3.4.3. ORAC assay

We used a standard procedure described previously [89] with modifications. The working fluorescein (FL) concentration was elevated to 400 nmol/L in 75 μ mol/L phosphate buffer, pH 7.4 while the AAPH oxidant concentration was also increased to 400 mmol/L. Trolox standards were prepared as described above within the concentration range of 0 – 160 μ mol/L. 25 μ L of blank/standard/sample and 150 μ L of working fluorescein solution were pipetted into the wells of 96-well general microtiter plates. The outer wells were filled with 200 μ L phosphate buffer only to have better temperature stabilization. Before the measurements, plates were preheated to 37 °C for 30 minutes in the dark. The reaction was started by an automated injection of 25 μ L AAPH solution into each well by the injector of the Biotek Synergy HT Gen5 microplate

reader. Fluorescence intensities were monitored for 80 minutes using 490/520 nm filter settings. Total light outputs as AUC were calculated. The AUC of the blank was subtracted from that of the standards/samples (net AUC) and was further used in the antioxidant capacity calculations. The total antioxidant capacity (TAC) of the samples was obtained by using the regression equation data obtained for the Trolox standards. The TE was multiplied by the dilution factor and was finally expressed as $\mu\text{mol/L}$ Trolox equivalent. The TE of the samples was referred to 1g of initial essential oils content.

3.5. Determination of minimum inhibitory concentration (MIC) of RAMEB-EOs

3.5.1. Microorganisms used in the studies

Escherichia coli (*E. coli*) PMC 201, *Staphylococcus aureus* (*S. aureus*) ATCC 29213, *Schizosaccharomyces pombe* (*S. pombe*) ATCC 38366 were obtained from the Department of General and Environmental Microbiology, Institute of Biology, University of Pecs, Hungary (PMC).

3.5.2. Antimicrobial activity against *S. pombe*, *E. coli* and *S. aureus*

The antifungal activity was carried out according to the standard protocol suggested by CLSI (Clinical & Laboratory Standards Institute) guidelines [90]. Briefly, *S. pombe* slant agar inoculum stock was prepared from the main stock and was incubated for 16 h at 30 °C in YES media. On the second day, EO-RAMEB and EO component-RAMEB complexes with concentrations ranging from 5 mg/mL to 0.039 mg/mL in square dilution format were added to the yeast population and incubated at 30 °C for 48 h in YES media. 96-well general microtiter plates were used for all experiments. The final population of *S. pombe* per well was 10^3 cells/mL. The absorbance per well was measured by the Perkin Elmer EnSpire Multimode reader at 595 nm.

The antibacterial activity of the samples was evaluated on *E. coli* and *S. aureus* strains according to the protocol described by the CLSI (Clinical & Laboratory Standards Institute) guidelines [70,90]. Briefly, the working population of the bacteria was prepared on the first day, from the stock. For *E. coli* and *S. aureus* we used LB medium and TSB, respectively throughout the experiments. On the second day, the desired population was obtained (0.5 McFarland standards mentioned in NCCLS protocols). The bacterial populations were reduced to 5×10^5 cells/mL and were kept as the final population per well throughout the whole experiment. EO-RAMEB and EO component-RAMEB complexes from 5 mg/mL to 0.0312

mg/mL concentration range were introduced to the inoculated media. The absorbance was measured by the PerkinElmer EnSpire Multimode reader at 600 nm after 12 to 16 h of incubation at 35 ± 2 °C.

3.6. *Rapid live/dead fluorescent cellular discrimination assay*

3.6.1. Development of a SYBR Green I/propidium iodide microbial viability assay

Care has been taken to remove any traces of growth medium before staining the experimented microbial samples with the fluorescent dyes. The nucleic acids and other media components may bind SYBR Green I and propidium iodide in an unpredictable manner, which may result in unacceptable imprecision in the staining procedure. A single wash step with PBS (pH 7.4) was sufficient to remove traces of interfering media components from the microbial suspension. Briefly, 15 mL cultures of either *S. pombe*, *E. coli* or *S. aureus* were grown to log phase in nutrient broth (YES media, LB media, and TSB). Ten milliliters of microbial suspension in each tube was pelleted by centrifugation at 1000g for 5 minutes. The supernatant was removed, and the pellet was re-suspended in 10 mL media (for living microbes) and 2.5-25 % (v/v) of 2-propanol in respective centrifuge tubes for obtaining different ratios of dead/live microbes. All samples were incubated at room temperature for 15 minutes then were centrifuged at 1000g. The supernatants were removed, and the pellets were re-suspended and washed with 5 mL PBS (pH 7.4) followed by centrifugation again. The pellets were finally suspended in 10 mL PBS (pH 7.4).

3.6.2. Optimization of the fluorescence assay

The staining concentration of the two fluorescent dyes has been balanced so that the applied mixture should provide good live/dead cell discrimination in our experimental conditions. For thorough optimization of the staining protocol, we have experimented a wide range of concentrations (5.5 to 5500 times dilution in logarithmic dilution format) of SYBR Green I dye (10,000x stock) each in combination with a concentration range (500 to 5 times in logarithmic dilution format) of propidium iodide (20 mmol/L stock in DMSO).

3.6.3. Staining microbial suspensions with SYBR Green I/propidium iodide for fluorescence microplate reader and flow cytometry testing

The microbial suspensions (live and killed) were adjusted to $\sim 10^6$ cells/mL. One hundred microliters of the above mentioned treated and untreated samples were pipetted into 96-well

transparent flat bottom general plates. One hundred microliters of premixed dye was pipetted into the wells containing the samples and mixed thoroughly. The plates were incubated in the dark for 10 minutes. The outer wells (row A and H and columns 1 and 12) were kept filled with PBS (pH 7.4) to maintain even temperature distribution during the incubation process. For the evaluation of microbial viability, fluorescence intensities of the samples in the 96-well microtiter plates were measured at two monochromatic settings. First, fluorescence intensity was recorded at 490 nm/525 nm excitation/emission wavelengths (emission 1, green). Then the samples were re-measured at 530 nm/620 nm (emission 2, red). Data were analyzed by dividing the fluorescence intensity of the stained microbial suspensions (F_{cell}) at emission 1 by fluorescence intensity at emission 2:

$$Ratio_{G/R} = \frac{F_{cell,em\ 1}}{F_{cell,em\ 2}} \quad (5)$$

Dose-dependent % of dead cells in the microbial suspension was then calculated from the respective $Ratio_{G/R}$ using the following formula:

$$\% Dead\ cells_{Dose} = 100 - \left\{ \left(\frac{Dose_{G/R}}{Control_{G/R}} \right) \times 100 \right\} \quad (6)$$

where $Dose_{G/R}$ is the green to red ratio ($Ratio_{G/R}$) of a specific dose and $Control_{G/R}$ is the green to red ratio of the living control.

In our flow cytometric analysis, we assessed the ratio of living and dead cells using SYBR Green I and propidium iodide double staining as in the case of the plate reader experiments. Flow cytometric measurements were performed on a FACS Canto II instrument (BD Biosciences) using FACS Diva V6.0 software (BD Biosciences). Before sample analysis, the flow cytometer settings were checked using CS&T beads according to the manufacturer's instructions. Doublets were discriminated by a side scatter SSC-H vs. SSC-W plot, and forward scatter FSC-H vs. FSC-W plot. For data analyses, we used FCS express V4.0 software.

3.6.4. Rapid viability assay of RAMEB-EOs on *S. pombe*, *E. coli* and *S. aureus* strains

The viability assay was performed according to the method reported by [61] with modifications. For the discrimination of live and dead cells in 96-well microtiter plates, SYBR Green I and PI were used for staining the nucleic acids of the test microbes. One hundred times dilutions of SYBR Green I (10,000x stock) in DMSO were prepared in aliquots and were stored at -20 °C for future use. In brief, 10 mL microbes with a population of 10^5 cells/mL were incubated (30 °C for *S. pombe* in YES medium, 37 °C for *E. coli* and *S. aureus* in LB media

and TS broth, respectively) for 16 h, treated by different EOs - RAMEB dilutions ranging from 2 mg/mL to 0.06 mg/mL. The treated microbes were centrifuged at 1000g for 5 minutes, washed in PBS (pH 7.4) and were re-suspended in PBS (pH 7.4). Working dye solution was prepared by mixing 18 μ L of SYBR Green I from the aliquots and 2 μ L of propidium iodide (20 mmol/L in DMSO) with 1000 μ L of PBS, pH 7.4. 100 μ L of re-suspended treated microbes were pipetted into each well of 96-well general micro-titer plates. Then 100 μ L of working dye solution was pipetted into each well containing the microbes and the plate was incubated at room temperature in the dark with mild shaking, for 15 minutes. Considering the excitation wavelength of 490 nm for SYBR Green I and 530 nm for PI, fluorescence intensities at 525 nm (green emission) and 620 nm (red emission) were measured for each well by the PerkinElmer EnSpire Multimode reader. Green to red ratios of every sample and for every dose was achieved. The percentage of dead cells with the response to the dose was calculated using the formula described earlier and the percentage of dead cells was plotted against EOs-RAMEB/components-RAMEB doses applied to the cells.

4. Materials and methods used for chamomile EO-Pickering emulsion experiments

4.1. Synthesis, surface modification, and characterization of Stöber silica nanoparticles (SNPs)

This was performed by Barbara Horváth and her colleagues at the Institute of Pharmaceutical Technology and Biopharmacy (Faculty of Pharmacy, University of Pécs). Detailed information regarding the preparation and surface-modification of the silica nanoparticles can be found in Ref. [91] and her PhD thesis “Pickering Emulsions in Pharmaceutical Technology” (in preparation). In brief, the silica nanoparticles were synthesized and surface-modified following the previously reported methods [92,93].

4.2. Preparation and characterization of C_{Pe} , C_{Et} , and C_{T80}

This was performed by Barbara Horváth and her colleagues at the Institute of Pharmaceutical Technology and Biopharmacy (Faculty of Pharmacy, University of Pécs). Detailed information to the preparation and characterization of C_{Pe} , C_{Et} , and C_{T80} can be found in Ref. [91] and her PhD thesis “Pickering Emulsions in Pharmaceutical Technology” (in preparation).

4.3. Materials used for biological experiments for C_{Pe} , C_{Et} , and C_{T80}

In these experiments, the sterile 96-well micro-titer plates were from Greiner Bio-One (Kremsmünster, Austria), potassium phosphate monobasic, glucose, adenine, 96% ethanol (Et), peptone, yeast extract, agar-agar, and Mueller Hinton agar (MHA) were from Reanal Labor (Budapest, Hungary), modified RPMI 1640 (contains 3.4% MOPS, 1.8% glucose, and 0.002% adenine), SYBR Green I 10,000x, propidium iodide, dihydrorhodamine 123 (DHR 123), 2',7'-dichlorofluorescein diacetate (DCFDA), dihydroethidine (DHE) and menadione (Me) were from Sigma-Aldrich Chemie GmbH (Steinheim, Germany), disodium phosphate and dimethyl sulfoxide (DMSO) were from Chemolab Ltd. (Budapest, Hungary), sodium chloride from VWR Chemicals (Debrecen, Hungary), potassium chloride was from Scharlau Chemie S.A (Barcelona, Spain), 3-(*N*-morpholino) propanesulfonic acid (MOPS) was from Serva Electrophoresis GmbH (Heidelberg, Germany), caspofungin (Cas) from Merck Sharp & Dohme Ltd (Hertfordshire, UK), vancomycin (Van) from Fresenius Kabi Ltd. (Budapest, Hungary), 0.22 μ m vacuum filters from Millipore (Molsheim, France) and the cell spreader was from Sarstedt AG & Co. KG (Numbrecht, Germany). All other chemicals used in the study were of analytical or spectroscopic grade. For fungi, we used an in-house nutrient agar medium [94] while phosphate-buffered saline (PBS, pH 7.4) was from Life Technologies Ltd. (Budapest, Hungary). Highly purified water (<1.0 μ S) was applied throughout the studies.

4.4. Determination of minimum inhibitory concentration of C_{Pe} , C_{Et} , and C_{T80}

4.4.1. Microorganisms used for the assay

Escherichia coli (*E. coli*) PMC 201, *Pseudomonas aeruginosa* (*P. aeruginosa*) PMC 103, *Bacillus subtilis* (*B. subtilis*) SZMC 0209, *Staphylococcus aureus* (*S. aureus*) ATCC 29213, *Streptococcus pyogenes* (*S. pyogenes*) SZMC 0119, *Schizosaccharomyces pombe* (*S. pombe*) ATCC 38366, *Candida albicans* (*C. albicans*) ATCC 1001, and *Candida tropicalis* (*C. tropicalis*) SZMC 1368 were obtained from Szeged Microbial Collection, Department of Microbiology, University of Szeged, Hungary (SZMC) and Department of General and Environmental Microbiology, Institute of Biology, University of Pecs, Hungary (PMC).

4.4.2. Antimicrobial activity assay

The antibacterial activity of the tested drugs was separately evaluated on *E. coli*, *P. aeruginosa*, *B. subtilis*, *S. aureus*, and *S. pyogenes* according to our previously published protocol [95]. In brief, bacterial populations of $\sim 10^5$ CFU/mL were inoculated into RPMI

media and incubated for 16 h at 35 ± 2 °C with test compounds chamomile oil-Pickering emulsion (C_{Pe}), chamomile oil-Tween 80 emulsion (C_{T80}), chamomile oil-ethanol solution (C_{Et}), and Van over a wide concentration range (0.3–0.01 $\mu\text{g/mL}$). The absorbance was measured by a Thermo Scientific Multiskan EX 355 plate reader (InterLabsystems, Budapest, Hungary) at 600 nm. The antifungal activity against *S. pombe*, *C. albicans*, and *C. tropicalis* species was also carried out according to our previously published method [95]. Briefly, $\sim 10^3$ cells/mL were incubated for 48 h at 30 ± 2 °C with test compounds (C_{Pe} , C_{T80} , C_{Et} , and Cas) at a wide concentration range (20–0.01 $\mu\text{g/mL}$) in modified RPMI media. The absorbance was measured by a Thermo Scientific Multiskan EX 355 plate reader (InterLab systems, Budapest, Hungary) at 595 nm. Absorbance values were converted to percentages compared to growth control ($\sim 100\%$) and data were fitted by nonlinear dose-response curve method to calculate the dose producing $\geq 90\%$ growth inhibition (MIC_{90}). All the measurements were performed by applying three technical replicates in six independent experiments. The Van and Cas were used as a standard antibacterial and antifungal drug, respectively, throughout the experiments.

4.4.3. Determination of minimum effective concentration (MEC_{10})

The assay has been designed to determine the dose-response curves produced by the effects of the test drugs on the microbial cell population causing sub-minimal killing effects. In brief, a wide concentration range (0.03–80 $\mu\text{g/mL}$) of the test samples was used to treat $\sim 10^6$ cells/mL for one hour. One milliliter of treated and untreated samples was taken and was diluted 10^5 times followed by spreading 50 μL samples onto 20 mL nutrient agar media and incubated for 24 h at 35 °C (bacteria) and 30 °C (fungi) for the colony-forming unit (CFU/mL) quantification. The data were compared with growth control and positive control (Van for bacteria and Cas for fungi) for percentage mortality ($\sim 10\%$ death) determination. It is noteworthy that in the MEC_{10} experiments, the inoculated microbial cell number was 10^3 times higher than was used in the MIC_{90} determinations (10^6 vs. 10^3). However, in both cases, the same formula was used (see Section 7). All the measurements were performed by applying three technical replicates in six independent experiments.

4.5. Determination of microbial free radical generation and killing activity

4.5.1. Quantification of total ROS generation

Total ROS generation was assayed according to previously published protocols [94,96–98]. Briefly, $\sim 10^6$ cells/mL were collected and centrifuged at 1500g for 5 minutes and were

suspended in PBS. The cells were stained with a 20 mM stock solution of DCFDA in PBS (pH 7.4) to achieve an end concentration of 25 μ M, and were incubated at 35 °C (for bacteria) and 30 °C (for fungi) for 30 minutes in the dark with mild shaking. The cells were centrifuged (Hettich Rotina 420R, Auro-Science Consulting Ltd., Budapest, Hungary) and suspended in RPMI media. The cells were treated with C_{Pe}, C_{T80}, C_{Et}, Van (bacteria), and Cas (fungi) at their respective MEC₁₀ concentrations for one hour. The fluorescence signals were recorded at Ex/Em = 485/535 nm wavelengths by a Hitachi F-7000 fluorescence spectrophotometer/plate reader (Auro-Science Consulting Ltd., Budapest, Hungary). The percentage increase in oxidative balance was measured by comparing the signals to those of the growth controls (Gc). Six independent experiments were done with three technical replicates for each treatment.

4.5.2. Detection of peroxide (O₂²⁻) and superoxide anion (O₂^{•-}) generation

The previously described protocol was adapted for peroxide [98,99] and superoxide anion radicals [94,100] with modifications. A positive control, Me (0.5 mmol/L as end concentration), C_{Pe}, C_{T80}, C_{Et}, Van (bacteria), and Cas (fungi) at their respective MEC₁₀ concentrations were used to treat the cell suspensions (~10⁶ cells/mL) for an hour at 35 °C (bacteria) and 30 °C (fungi) in RPMI media. Thereafter, the cells were centrifuged at 1500g for 5 minutes at room temperature followed by resuspension of pellets in PBS of the same volume. DHR 123 (10 μ mol/L, end concentration) and DHE (15 μ mol/L, end concentration) were added separately to the cell samples for peroxide and superoxide determination. The stained cells were further incubated at 35 °C (bacteria) and 30 °C (fungi) in the dark with mild shaking. The samples were centrifuged and re-suspended in PBS followed by the distribution of the samples into the wells of 96-well microtiter plates. The fluorescence was measured at excitation/emission wavelengths of 500/536 nm for peroxides and 473/521 nm for superoxide detection by the Hitachi F-7000 fluorescence spectrophotometer/plate reader. The percentage increase in oxidative stress was measured by comparing the signals to those of the growth controls (Gc). Six independent experiments were done with three technical replicates for each treatment.

4.6. Time-kill kinetics assay

We followed a protocol previously published by T. Appiah et. al., with modifications [101]. In brief, C_{Pe}, C_{T80}, C_{Et}, Van (bacteria), and Cas (fungi) at their respective MEC₁₀ concentrations were used to treat the microbial population of ~10⁶ CFU/mL and were incubated at 35 °C (bacteria) and 30 °C (fungi). One milliliter of the treated and untreated samples was

pipetted at time intervals of 0, 2, 6, 8, 16, and 24 h for bacteria, and 0, 6, 12, 30, 36, and 48 h for fungi, and were diluted 10^5 times followed by spreading 50 μL onto 20 mL nutrient agar media using a cell spreader and incubated at 35 °C (bacteria) and 30 °C (fungi) for 24 h. Van and Cas were used as reference controls for bacteria and fungi. Control without treatment was considered as growth control (Gc). The colony-forming unit (CFU/mL) of the microorganisms was determined, performed in triplicate, and was plotted against time (h). Six independent experiments were done with three technical replicates for each treatment.

4.7. Live/dead discrimination of microbial cells

For live/dead cell discrimination, we followed the protocol published previously [95]. In brief, the cell population of $\sim 10^6$ cells/mL were treated with C_{Pe} , C_{T80} , C_{Et} , Van (bacteria), and Cas (fungi) at their respective MEC_{10} concentrations and were incubated at 35 °C (bacteria) and 30 °C (fungi). Treated and untreated samples were pipetted at time intervals of 0, 2, 6, 8, 16, and 24 h for bacteria, and 0, 6, 12, 30, 36 and 48 h for fungi followed by centrifugation at 1000g for 5 minutes, washed and re-suspended in PBS (100 μL /well). One hundred microliters of freshly prepared working dye solution in PBS (using 20 μL SYBR Green I and 4 μL propidium iodide diluted solutions as described earlier) were added to the samples. The plate was incubated at room temperature for 15 minutes in the dark with mild shaking. The Hitachi F-7000 fluorescence spectrophotometer/plate reader was used to measure the fluorescence intensities of SYBR Green I (excitation/emission wavelengths: 490/525 nm) and propidium iodide (excitation/emission wavelengths: 530/620 nm), respectively. A green to red fluorescence ratio for each sample and each dose was achieved and the % of dead cells with the response to the applied dose was plotted against the applied test compound doses using a previously published formula [95]. All treatments were done in triplicates and six independent experiments were performed.

4.8. Interaction study between the cell model (unilamellar liposomes) and different formulations of chamomile EO

This was performed by Barbara Horváth and her colleagues at the Institute of Pharmaceutical Technology and Biopharmacy (Faculty of Pharmacy, University of Pécs). Detailed information regarding the interaction study between the cell model (unilamellar liposomes) and different formulations of chamomile EO can be found in Ref. [91] and her PhD thesis “Pickering Emulsions in Pharmaceutical Technology” (in preparation). In brief, the unilamellar liposomes (ULs) were prepared by the modified method described before [78].

4.9. GC-MS analysis of chamomile EO

Gas chromatography and mass spectrometry (GC–MS) analyses were carried out on an Agilent Technologies (Palo Alto, CA, USA) gas chromatograph model 7890A with 5975C mass detector. Operating conditions were as follows: column HP-5MS (5% phenylmethyl polysiloxane), 30 m × 0.25 mm i.d., 0.25 µm coating thickness. Helium was used as the carrier gas at 1 mL/minute, injector temperature was 250 °C. The HP-5MS column temperature was programmed at 70 °C isothermal for 2 minutes, and then increased to 200 °C at a rate of 3 °C/minute and held isothermal for 18 minutes. The split ratio was 1:50, ionization voltage 70 eV; ion source temperature 230 °C; mass scan range: 45–450 mass units. The percentage composition was calculated from the GC peak areas using the normalization method (without correction factors). The component percentages were calculated as mean values from duplicate GC–MS analyses of the oil sample.

5. Materials and methods used for artemisinin and scopoletin related experiments

5.1. Materials used for the biological assays

For our experiments, sterile 96-well microtiter plates for antifungal activity, live/dead discrimination and metabolic assays (Catalog number: 30096, SPL Life Sciences Co. Ltd., Gyeonggi-do, Korea), and for biofilm assays (Catalog number: 83.3924.500, Sarstedt AG & Co. KG, Numbrecht, Germany), crystal violet, peptone, yeast extract, agar-agar, potassium phosphate monobasic, acetic acid (Reanal Labor, Budapest, Hungary), resazurin, modified RPMI 1640 medium (containing 3.4% (w/v) MOPS, 1.8% (w/v) dextrose and 0.002% (w/v) adenine) [102], menadione (Me), artemisinin (Ar), scopoletin (Sc), SYBR Green I 10,000x, propidium iodide, dihydrorhodamine 123 (DHR 123) and dihydroethidine (DHE) (Sigma-Aldrich Chemie GmbH, Steinheim, Germany), disodium phosphate, dimethyl sulfoxide (DMSO) from Chemolab Ltd. (Budapest, Hungary), sodium chloride (VWR Chemicals, Debrecen, Hungary), dextrose, adenine, potassium chloride (Scharlau Chemie S.A, Barcelona, Spain), 3-(N-morpholino) propanesulfonic acid (MOPS) (Serva Electrophoresis GmbH, Heidelberg, Germany), 0.22 µm vacuum filters from Merck Millipore (Molsheim, France) were used. All other chemicals in the study were of analytical or spectroscopic grade. Highly purified water (<1.0 µS) was applied throughout the experiments. Caspofungin (Cs) was purchased from Merck Sharp & Dohme Ltd. (Hertfordshire, UK).

5.2. Instruments used in the biological assays

A microbiological incubator (Thermo Scientific Heraeus B12, Auro-Science Consulting Kft., Budapest, Hungary), microtiter plate reader (PerkinElmer EnSpire Multimode plate reader, Auro-Science Consulting Ltd., Budapest, Hungary), benchtop centrifuge (Hettich Rotina 420R, Auro-Science Consulting Kft., Budapest, Hungary) were used throughout the experiments.

5.3. Microorganisms and cultural conditions

All the fungal species were obtained from Szeged Microbiology Collection, University of Szeged, Hungary (Table 1), and were maintained at the Department of General and Environmental Microbiology, Institute of Biology, University of Pécs, Hungary. *C. albicans* 1372, *C. dubliniensis* 1470, *C. tropicalis* 1368, *C. krusei* 779, *C. glabrata* 1374, *C. guilliermondii* 808, and *C. parapsilosis* 8006 were used to evaluate the MIC₉₀, the minimum effective concentration (MEC₁₀) for the planktonic cells and the inhibition of biofilm formation of the test samples. All the fungal species were cultured and maintained in yeast extract peptone dextrose agar medium (YPD: 1% (w/v) peptone, 0.5% (w/v) yeast extract, 2% (w/v) dextrose, 1.5% (w/v) agar-agar in distilled water [94]. Phosphate-buffered saline (PBS, pH 7.4) was from Life Technologies Ltd. (Budapest, Hungary), and highly purified water (<1.0 µS) was applied throughout the experiments.

Table 1. *Candida* species examined in the study.

Species	Collection Code	Origin
<i>C. albicans</i>	SZMC 1372	clinical sample / Debrecen, Hungary
<i>C. dubliniensis</i>	CBS 7987 SZMC 1470	oral cavity of HIV-infected patient / Melbourne, Australia
<i>C. tropicalis</i>	SZMC 1368	clinical sample / Debrecen, Hungary
<i>C. krusei</i>	SZMC 0779	clinical sample / National Institute of Environmental Health (NIEH), Hungary
<i>C. glabrata</i>	SZMC 1374	clinical sample / Debrecen, Hungary
<i>C. guilliermondii</i>	SZMC 0808	clinical sample / Pécs, Hungary
<i>C. parapsilosis</i>	SZMC 8006	clinical sample / Szeged, Hungary

Abbreviations: SZMC, Szeged Microbiological Collection, Szeged, Hungary (http://www.wfcc.info/ccinfo/collection/by_id/987); CBS, Westerdijk Fungal Biodiversity Institute, Utrecht, The Netherlands (<http://www.westerdijkinstituut.nl/>).

5.4. Determination of minimum inhibitory concentration (MIC_{90})

The MIC_{90} was performed according to a previously published method [95] with modifications. Ar and Sc were prepared in DMSO at concentrations ranging from 0.39–200 $\mu\text{g}/\text{mL}$ and 0.01–8 $\mu\text{g}/\text{mL}$ for Cs. A total of 100 μL of fungal suspensions of 10^3 colony forming units (CFU)/mL in modified RPMI 1640 medium was pipetted into each well of sterile 96-well microtiter plates and mixed with 100 μL of dilutions of Ar and Sc. The final solvent concentration for the dilution of the drugs was restricted up to 2.5% v/v in the wells. Inoculated growth medium without any treatment was considered as the growth control. The sterile medium was taken as the blank. After 48 h of incubation at 30 °C in a microbiological incubator, the absorbance was measured at 595 nm. Absorbance values were converted to percentages compared with those of the growth control ($\approx 100\%$) and data were fitted by non-linear dose-response curve method to calculate the dose producing $\geq 90\%$ growth inhibition (MIC_{90}). All the measurements were performed by applying three technical replicates in six independent experiments. The Cs was used as a standard antifungal drug throughout the experiments.

5.5. Determination of minimum effective concentration (MEC_{10})

The MEC_{10} measurement was performed according to our previously published protocol to estimate the dose-dependent survival rate of the cells [91,103,104] with modifications. Briefly, Ar and Sc were prepared in DMSO at concentrations ranging from 0.25–400 $\mu\text{g}/\text{mL}$ and 0.5–32 $\mu\text{g}/\text{mL}$ for Cs. A total of 100 μL of fungal suspensions of mid-log phased 10^5 colony-forming unit (CFU)/mL in modified RPMI 1640 medium were pipetted into each well of sterile 96-well microtiter plates and mixed with 100 μL of dilutions of Ar and Sc. The final solvent concentration for the dilutions of the drugs was restricted up to 2.5% (v/v) in the wells. Inoculated growth medium without any treatment was considered as the growth control. The sterile medium was taken as the blank. After 60 minutes of incubation at 30 °C in a microbiological incubator, 1 mL of treated and untreated samples was pipetted and were spread in nutrient agar media for 24 h at 30 °C for colony-forming unit (CFU/mL) quantification. CFU/mL values were converted to percentages and data were fitted with a non-linear dose-response curve to achieve drug concentrations producing approximately 90% fungal cell growth (MEC_{10}) compared to the untreated culture after a one-hour treatment. All the measurements were performed by applying three technical replicates in six independent experiments. Cs was used as a standard antifungal drug throughout the experiments.

5.6. Determination of the effects on preformed mature biofilms

The protocol for the measurement of the effects on the mature biofilms and treatment was adapted from the literature [44,105] with modifications. A total of 200 μL samples of 24 h old late-log *phased C. albicans* and non-*albicans* species in the modified RPMI 1640 medium (10^6 CFU/mL) were used to culture biofilms without treatments for 24 h at 30 °C. The microtiter plates were washed carefully with sterile PBS (pH. 7.4) and were re-incubated with 200 μL culture medium containing Ar and Sc to be examined at MEC_{10} concentrations ($\mu\text{g/mL}$) for further 24 h at 30 °C. Modified RPMI media as blank, inoculated growth media as growth control (Gc), and Cs-treated samples were considered as controls throughout the experiments. The percentage (%) of inhibition was measured based on the comparison of the values with those of Gc. Treatments were performed with three technical replicates in six independent experiments.

5.6.1. Evaluation of total fungal biomass in the biofilms

To determine the changes in the biofilms, a previously published crystal violet assay protocol was used [106] with modifications. After 24 h incubation, the crystal violet-stained and PBS-washed biofilms were treated with 200 μL of 33% (v/v) acetic acid in double-distilled water. Finally, after 20 minutes the acetic acid-dissolved dye from the biofilm matrix was pipetted into the wells of a new microtiter plate and the absorbance was measured at 590 nm. Cs at MEC_{10} concentration was used as the positive control. The % biofilm biomass reduction measurement was based on growth control (Gc) values which were assigned to be 100% fungal biofilm mass. Six independent experiments were done with three technical replicates for each treatment.

5.6.2. Resazurin-derived metabolism assay in the biofilms

A resazurin-based fluorescent assay published by Kerekes et al. was adapted [106] and was used to estimate the metabolically active (viable) cell number in the biofilm matrix treated with Ar and Sc at MEC_{10} concentrations. Briefly, after 24 h of treatment, the supernatants were removed and the wells were rinsed with PBS. Resazurin (12.5 $\mu\text{mol/L}$) in 200 μL of sterile PBS was added to each well containing the biofilm. After 40 minutes of incubation at 30 °C, the fluorescence was measured at excitation and emission wavelengths of 560/590 nm respectively. The % metabolic activity measurement was estimated based on the growth control (Gc) fluorescence values which were considered to be 100%. The PBS was taken as blank

throughout the experiments. Six independent experiments were performed with three technical replicates for each treatment.

5.6.3. Viability assay of the biofilms and the planktonic *Candida* species

For the determination of live/dead microbes in the preformed mature biofilms we followed the method previously published [95]. Briefly, after 24 h of treatment with Ar, Sc, and Cs (positive control) at MEC₁₀ concentrations in the wells of a microplate, the modified RPMI 1640 medium, and the non-attached planktonic cells were removed, and the wells were rinsed and filled with 100 μ L PBS. A working dye solution containing 20 μ L SYBR Green I (from 10,000 \times stock in DMSO, diluted 100 times in PBS) and 4 μ L propidium iodide (500-fold dilution of working stock in DMSO prepared from 20 mmol/L in DMSO) in 1000 μ L of PBS was used. A total of 100 μ L of this working solution was added into the wells of the microplate. The plates were incubated at room temperature in the dark with mild shaking for 15 minutes.

For the evaluation of the long-term effects of Ar, Sc, and Cs at their MEC₁₀ on the tested *Candida* spp., a previously published live/dead planktonic cell discrimination [91] was optimized and used. A wide concentration range of SYBR Green I (5.5-5500-fold logarithmic dilutions) and propidium iodide (5-500-fold logarithmic dilutions) was examined. For the discrimination of live/dead cells, mid-log phased cell populations of 10⁵ CFU/mL were treated by Ar and Sc with a dose assigned for MEC₁₀ concentrations and incubated at 30 °C for 16 h. Sampling was done at 0, 8, and 16 h time points for the measurements. The samples were centrifuged at 1000g for 5 minutes, washed in PBS, and re-suspended in PBS (100 μ L in each well). Then 100 μ L of freshly prepared working dye solution in PBS (using 20 μ L SYBR Green I and 4 μ L propidium iodide diluted solutions as described earlier) was added to the samples. The plate was incubated at room temperature for 15 minutes in the dark with mild shaking.

A PerkinElmer EnSpire multimode plate-reader was used to measure the fluorescence intensities of SYBR Green I (excitation/emission wavelengths: 490/525 nm) and propidium iodide (excitation/emission wavelengths: 530/620 nm), respectively. A green to red fluorescence ratio for each sample and each dose was achieved and the % of dead cells with the response to the applied dose was plotted against the applied Ar and Sc doses using the previously published formula [91]. In the case of biofilms, the measurements were done by the area scan mode of the instrument. All treatments were done in triplicates and six independent experiments were performed.

5.7. Determination of the metabolic activity with resazurin assay and colony formation of planktonic fungal cells

The metabolic activity of the cells under treatment conditions was performed by the widely accepted resazurin fluorescence method [107–109]. The experiments had to be optimized because the resazurin concentration, the cell number and the incubation time are crucial to increase the signal to noise ratio. Fluorescence data were corrected by subtracting background fluorescence (resazurin in PBS). The initial *Candida* cell density, resazurin levels, and duration of incubation time were varied by using resazurin concentrations ranging from 1.6 $\mu\text{mol/L}$ to 25 $\mu\text{mol/L}$ in the cell suspensions. The proper incubation time for resazurin exposure at an optimized concentration (12.5 $\mu\text{mol/L}$) was performed by 60 minutes incubation and sampling at intervals. The appropriate *Candida* species cell density was obtained by exposing a serial dilution of cells to 12.5 $\mu\text{mol/L}$ resazurin in PBS. The PBS without resazurin but with identical cell density to the investigated samples was used as blank.

For fungal colony-forming unit measurements, we followed a previously published protocol [109]. Briefly, 1 mL of untreated and Ar, Sc, and Cs-treated sample was pipetted at 0, 8, and 16 h time intervals and was diluted 10^5 times followed by spreading 50 μL onto 20 mL YPD agar medium using a cell spreader and incubated at 30 °C for 24 h. The Cs was used as a reference control. Fungal colony forming units (CFU/mL) were determined, performed in triplicates, and were plotted against time (h). Six independent experiments were done with three technical replicates for each treatment

5.8. Detection of peroxide (O_2^{2-}) and superoxide anion ($\text{O}_2^{\bullet-}$) generation in planktonic fungal cells

We adapted the protocols previously described [98] for peroxide anion radicals (O_2^{2-}) determination and superoxide detection in the cells [94] with modifications. The final cell population for the experiment was set to mid-log phased 10^5 CFU/mL. An end concentration of 0.5 mmol/L of menadione (Me) in cell suspensions was added as the positive control. The cell suspensions were treated with MEC_{10} concentrations of test samples. The treatments were done for 60 minutes at 30 °C in the modified RPMI 1640 medium. Thereafter, the cells were centrifuged for 5 minutes at 1500g at room temperature. The pellets were re-suspended in PBS in the same volume. DHR 123 at a final concentration of 10 $\mu\text{mol/L}$ for peroxides determination and DHE at a final concentration of 15 $\mu\text{mol/L}$ for $\text{O}_2^{\bullet-}$ determination were added separately to the cell samples. The stained cell samples were further incubated for 60

minutes at 30 °C in the dark condition with mild shaking. The samples were centrifuged and re-suspended in PBS followed by distribution of the samples into the wells of 96-well microplates. The fluorescence was measured at excitation/emission wavelengths of 500/536 nm for peroxides and 473/521 nm for O₂^{•-} detection, respectively by a PerkinElmer EnSpire multimode plate-reader. The percentage increase in oxidative stress was measured by comparing the signals to those of the growth controls. Six independent experiments were done with three technical replicates for each treatment.

6. Materials and methods used for *Artemisia* essential oil-related biological assays

6.1. Plant Collection and Extraction of Artemisia Essential Oil

The plant samples were collected in 2017 from Békés county, Orosháza-Nagyszénás, Hungary, from a local farm in the autumn and were dried in the dark, under moisture-free conditions for two months. The plant parts were ground to farinose form and were sieved down. The powdered form of the plant was stored in airtight containers for future use.

The extraction of the *Artemisia annua* L. (*A. annua*) essential oil was done by the steam distillation method as described earlier [3,59]. Briefly, 500 mL of distilled water was added to 50 g dried powder of *A. annua*. The steam distillation was done for 30 minutes, and the reading in the graduated tube was recorded for the essential oil yield. The yield value was converted to the percentage (%) w/w of 1 g of the powdered plant's part.

6.2. GC-MS-FID studies

6.2.1. Samples and sample preparation

The *Artemisia* essential oil samples (10 µL) were dissolved in 990 µL of *n*-heptane and injected on the GC-MS and GC-FID systems.

6.2.2. GC-MS analysis (performed by Prof. Dr. Luigi Mondello, and Dr. Giuseppe Micalizzi; University of Messina, Italy)

The sample analyses were carried out on a GCMS-QP2020 (Shimadzu, Milan, Italy) equipped with a split-splitless injector, an AOC-20i autosampler, and a quadrupole MS detector. MS parameters were as follows: mass range 40–650 amu, scan speed: 2000 amu/s. Ion source temperature: 220 °C, interface temperature: 250 °C. An SLB-5ms 30 m × 0.25 mm id × 0.25 µm film thickness column (Supelco, PA, USA) (silphenylene polymer virtually equivalent in polarity to poly (5% diphenyl/95% dimethylsiloxane phase) and a Supelcowax-

10 30 m × 0.25 mm id × 0.25 μm (Supelco) (polyethylene glycol phase) were used for a comprehensive characterization of the volatile fraction. Both columns operated under a programmed temperature: 50 °C to 280 °C at 3.0 °C/minute. Injection volumes: 0.5 μL; Split ratio: 10:1. Helium was used as a gas carrier at a constant linear velocity of 30 cm/s and the inlet pressure of 26.7 kPa. The GCMSsolution software (version 4.30 Shimadzu, Milan, Italy) was used for data collection and handling. A homologous series of n-alkanes (C7-C30) (Supelco, PA, USA) standard solution has been used for Linear Retention Indices (LRIs) calculation that supported the identification of analytes on the SLB-5ms column; relative to the Supelcowax-10 column, a Fatty Acid Methyl Esters (FAMES) C4-C24 (Supelco, PA, USA) standard solution was used for LRI determination. The peaks assignment was carried out based on a double filter, namely the MS similarity spectra (over 85%) and an LRIs between ± 5 and ± 10 ranges (respectively on SLB-5ms and Supelcowax-10) compared to the values reported in a spectral library. For mass spectral identification, Shimadzu FFNSC 3.01 was mainly used.

6.2.3. GC-FID analysis (performed by Prof. Dr. Luigi Mondello, and Dr. Giuseppe Micalizzi; University of Messina, Italy)

Sample analyses were carried out on a GC-2010 Plus (Shimadzu, Milan, Italy) equipped with a split-splitless injector (280 °C), an AOC-20i autosampler, and a flame ionization detector (FID). An SLB-5ms 30 m × 0.25 mm id × 0.25 μm film thickness column (Supelco) and a Supelcowax-10 column operated individually under programmed temperature: 50 °C to 280 °C at 3.0 °C/minute. Injection volume: 0.5 μL; Split Ratio: 10:1. Helium was used as the carrier at a constant linear velocity of 30 cm/s and an inlet pressure of 99.5 KPa. The FID temperature was set at 280 °C (sampling rate 40 ms) and gas flows were 40 mL/minute for hydrogen, 30 mL/minute for makeup (nitrogen), and 400 mL/minute for air, respectively. Data were processed through LabSolution software (Shimadzu). Quantification was performed using the GC-FID data. Each sample was injected in triplicate for a major precision of data.

6.3. Preparation and characterization of Pickering emulsion

This was performed by Barbara Horváth and her colleagues at the Institute of Pharmaceutical Technology and Biopharmacy (Faculty of Pharmacy, University of Pécs). Detailed information to the preparation and characterization of *Artemisia* EO (AE) can be found in Ref. [21] and her PhD thesis “Pickering Emulsions in Pharmaceutical Technology” (in preparation). Briefly, the synthesis and surface-modified spherical silica nanoparticles were done following previously published methods [57].

6.4. In vitro diffusion studies-Static Franz diffusion cell method

This was performed by Barbara Horváth and her colleagues at the Institute of Pharmaceutical Technology and Biopharmacy (Faculty of Pharmacy, University of Pécs). Detailed information to the in vitro diffusion studies-Static Franz diffusion cell method can be found in Ref. [21] and her PhD thesis “Pickering Emulsions in Pharmaceutical Technology” (in preparation). In brief, the experiments were carried out following the previously published protocols [110].

6.5. Interaction study between the cellular model (unilamellar liposomes) and different formulations of AE

This was performed by Barbara Horváth and her colleagues at the Institute of Pharmaceutical Technology and Biopharmacy (Faculty of Pharmacy, University of Pécs). Detailed information to the interaction study between the cellular model (unilamellar liposomes) and different formulations of AE can be found in Ref. [25] and her PhD thesis “Pickering Emulsions in Pharmaceutical Technology” (in preparation). In brief, unilamellar liposomes (ULs) were prepared as described previously [91].

6.6. Materials used for the biological experiments

Promega BacTiter-Glo microbial cell viability assay kit (Bio-Science, Budapest, Hungary), glass beads (Sigma-Aldrich Chemie GmbH, Steinheim, Germany, reference number: G-8772), sterile petri-dishes (Greiner Bio-One, Kremsmunster, Austria), sterile petri-dishes for the biofilm assays (Sarstedt AG & Co. KG, Numbrecht, Germany, reference number: 83.3900.500), 0.22 μm vacuum filters (Millipore, France), cell scraper (Sarstedt AG & Co. KG, Numbrecht, Germany), sterile microplates (Greiner Bio-One, Kremsmunster, Austria), sterile microplates for the biofilm assays (Sarstedt AG & Co. KG, Numbrecht, Germany, catalog number: 83.3924.500), 96-well optiplates (Perkin Elmer, Waltham, Massachusetts, USA), bovine serum albumin (BSA; Biosera, Nuaille, France), potassium phosphate monobasic, ethanol 96% (Et), methanol, peptone, yeast extract, agar-agar and Mueller-Hinton agar (for the maintenance of the tested bacteria’s health, used throughout the experiments) (Reanal Labor, Budapest, Hungary), modified RPMI 1640 (contains 3.4 w/v% MOPS, 1.8 w/v% glucose and 0.002 w/v% adenine), menadione (ME) (Sigma Aldrich, Budapest, Hungary), disodium phosphate, dimethyl-sulfoxide (DMSO) from Chemolab Ltd. (Budapest, Hungary), sodium chloride (VWR International Ltd., Debrecen, Hungary), potassium chloride (Scharlau Chemie S.A, Spain), 3-(N-morpholino) propanesulfonic acid (MOPS) (Serva

Electrophoresis GmbH, Heidelberg, Germany), Caspofungin (CAS) from Merck Sharp & Dohme Ltd., Netherlands, vancomycin (VAN) from Fresenius Kabi Ltd., (Budapest, Hungary), SYBR Green I 10,000x, propidium iodide, dihydrorhodamine 123 (DHR 123), 2',7' – dichlorofluorescein diacetate (DCFDA) and dihydroethidine (DHE) were purchased from Sigma Aldrich (Budapest, Hungary) and from the above-mentioned sources. All other chemicals applied for the study were of analytical or spectroscopic grade. For fungi, we used an in-house nutrient medium containing 1 w/v% yeast extract, 2 w/v% peptone, 2 w/v% glucose, and 2 w/v% agar-agar (for the colony-forming unit assay in the Petri-dishes) [17], while phosphate-buffered saline (PBS, pH 7.4) was obtained from Life Technologies Ltd., Hungary. Highly purified water (<1.0 µS) was applied throughout the studies.

Escherichia coli (*E. coli*) PMC 201, *Pseudomonas aeruginosa* (*P. aeruginosa*) PMC 103, *Bacillus subtilis* (*B. subtilis*) SZMC 0209, *Staphylococcus aureus* (*S. aureus*) ATCC 29213, *Streptococcus pyogenes* (*S. pyogenes*) SZMC 0119, *Schizosaccharomyces pombe* (*S. pombe*) ATCC 38366, *Candida albicans* (*C. albicans*) SZMC 1372, *Candida tropicalis* (*C. tropicalis*) SZMC 1368, *Candida dubliniensis* (*C. dubliniensis*) SZMC 1470 and *Candida krusei* (*C. krusei*) SZMC 0779 were obtained from Szeged Microbial Collection, Department of Microbiology, University of Szeged, Hungary (SZMC) and Department of General and Environmental Microbiology, Institute of Biology, University of Pecs, Hungary (PMC).

6.7. Determination of minimum inhibitory concentration (MIC_{90})

We used a previously published protocol [17,91] for measuring the antibacterial activity separately on *E. coli*, *P. aeruginosa*, *B. subtilis*, *S. aureus*, and *S. pyogenes* and antifungal activity against *S. pombe*, and *Candida* species. In brief, for the antibacterial activity determination, a bacterial population of $\sim 10^5$ CFU/mL was inoculated in modified RPMI 1640 medium followed by incubation for 16 h at 35 ± 2 °C Thermo Scientific Heraeus B12 microbiological incubator (Auro-Science Consulting Kft., Budapest, Hungary) with AEP, AET, AEE and VAN over a wide range of concentrations (26.2—0.01 µg/mL). The absorbance was measured by a Thermo Scientific Multiskan EX 355 microplate reader (InterLabsystems, Budapest, Hungary) at 600 nm.

The antifungal activity against *S. pombe* and *Candida* species were also performed according to our previously published method [17]. Briefly, $\sim 10^3$ cells/mL were incubated with AEP, AEE, AET, and CAS at a wide concentration range (26.2 - 0.01 µg/mL) in modified RPMI 1640 medium for 48 h at 30 °C (Sanyo MIR-154 microbiological incubator, Auro-Science Consulting Kft., Budapest, Hungary). The absorbance values obtained by the

microplate reader at 595 nm were converted to percentages and were compared to the growth control (100%). The data were fitted by a non-linear dose-response curve fitting method to estimate the dose producing $\geq 90\%$ growth inhibition (MIC_{90}). All measurements were performed by applying three technical replicates in six independent experiments. The VAN and CAS were used as the standard antibacterial and antifungal drug controls, respectively throughout the experiments.

6.8. Determination of minimum effective concentration (MEC_{10})

The MEC_{10} concentration was obtained according to our previously published protocol [91]. In brief, a wide concentration range (105–0.2 $\mu\text{g/mL}$) of AEP, AET, and AEE was used to treat mid-log phased $\sim 10^5$ cells/mL in modified RPMI 1640 medium for an hour, incubated at 35 ± 2 °C and 30 °C for the bacteria and the fungi, respectively, in an orbital incubator (Sanyo MIR-220RU orbital incubator, Auro-Science Consulting Kft., Budapest, Hungary). Inoculated growth medium without any treatment was considered as growth control. For the colony-forming unit (CFU/mL) quantification, 1 mL of the treated and untreated samples were pipetted out and 10^5 times dilutions were prepared followed by spreading 50 μL of the test samples onto 20 mL respective nutrient-rich agar media containing Petri-dishes and were incubated for 24 h at 35 ± 2 °C and 30 °C in the case of bacteria and fungi, respectively. The colony formation data (CFU/mL) were converted to percentages and the data were fitted using a non-linear dose-response curve fitting method to evaluate the drug concentrations producing approximately 90% microbial cell population growth (MEC_{10}) when compared to the untreated microbial cell populations after one hour of treatment. Three technical replicates in six independent experiments were performed in all the measurements. The VAN and CAS were used as the standard antibacterial and antifungal drug controls throughout the experiments, respectively.

6.9. Quantification of microbial oxidative stress production in the planktonic cells

6.9.1. Combined ROS generation measurement

For the quantification of the combined (not specified separately) reactive oxygen species (ROS) generation, we have followed our previous protocol [17]. In brief, for the ROS measurements, mid-log phased $\sim 10^5$ cells/mL were collected and centrifuged at 1500g (Hettich Rotina 420R bench-top centrifuge, Auro-Science Consulting Ltd., Budapest, Hungary) for 5 minutes and were re-suspended in PBS. The staining of the cells was done with 2',7' – dichlorofluorescein diacetate (DCFDA) stock solution (20 mM in DMSO) with a final

concentration of 25 μM in each well, followed by incubation at 35 ± 2 °C for the bacteria and 30 °C for the fungi in the dark with mild rotation in a test tube rotator (Cole-Parmer Roto-Torque Variable Speed Rotator, InterLabsystems, Budapest, Hungary) for 30 minutes. The cells were re-suspended in modified RPMI 1640 medium after centrifugation followed by treatment with AEP, AET, and AEE at their respective MEC_{10} concentrations for one hour. The fluorescence data were recorded by a fluorescence spectrophotometer/microplate reader (Hitachi F-7000 fluorescent spectrophotometer, Auro-Science Consulting Ltd., Budapest, Hungary) at Ex/Em = 485/535 nm in 96-well Optiplates. VAN and CAS were used as the standard antimicrobial controls in the case of bacteria and fungi. The ME treated samples were considered as the positive controls. The percentage increase (%) in the ROS generation was measured by comparing the signals obtained from the growth controls (GC). Six independent experiments with three technical replicates in each treatment were performed.

6.9.2. Determination of peroxide (O_2^{2-}) and superoxide anion ($\text{O}_2^{\bullet-}$) generation

Our previously described protocol was adapted for the peroxide and the superoxide anion radicals' measurements [17,96]. AEP, AET, and AEE at their respective MEC_{10} concentrations were used to treat the mid-log phased ($\sim 10^5$ cells/mL) microbial cell suspensions followed by incubation in an orbital incubator at 35 ± 2 °C and 30 °C for the bacteria and fungi in modified RPMI 1640 medium for an hour, respectively. The VAN and CAS were used as the standard antimicrobial controls in the case of bacteria and fungi. Menadione (ME) (0.5 mmol/L, end concentration) was used as a positive control throughout the experiments. The cells were centrifuged at 1500g for 5 minutes at room temperature and were re-suspended in PBS at the original volume of the samples. DHR 123 (10 $\mu\text{mol/L}$ end concentration) and DHE (15 $\mu\text{mol/L}$) were used to stain the microbial cell samples for the peroxide and superoxide determination and were further incubated at 35 ± 2 °C for the bacteria and 30 °C for the fungi in the dark with mild shaking. The samples were centrifuged again and were re-suspended in PBS, followed by even sample distribution into the 96-well microplates. For the peroxide measurements, the fluorescence was measured at Ex/Em: 500/521 nm, whereas, Ex/Em: 473/521 nm was used to detect the superoxide generation by a fluorescence spectrophotometer/microplate reader in 96-well Optiplates. The percentage increase (%) in the oxidative stress was measured by comparing the signals obtained from the growth controls (GC). Six independent experiments were performed with three technical replicates for each treatment.

6.10. *Microbial cytotoxicity and viability kinetic assays of planktonics*

The cytotoxicity and the viability of the microbial cells were performed with our previously published method [17,91]. Briefly, AEP, AET, AEE, VAN (bacteria) and CAS (fungi) at their respective MEC₁₀ concentrations were used to treat the mid-log phased microbial cell populations (~10⁵ cells/mL) in modified RPMI 1640 medium followed by incubation in an orbital shaker-incubator at 35 ± 2 °C and 30 °C for the bacteria and fungi in modified RPMI 1640 medium. After that, the multi-parametric cytotoxicity and viability kinetic studies were performed (Sections 6.10.1 – 6.10.4).

6.10.1. Determination of the colony-forming unit (CFU/mL)

We followed our previously published protocol for determining the changes in colony formation (CFU/mL) [91]. Briefly, 1 mL of the treated and the untreated samples were pipetted at the 0, 2, 6, 8, 16 and 24 h for the bacteria, and 0, 6, 12, 30, 36 and 48 h for the fungi, and were diluted 10⁵ times followed by spreading 50 µL onto 20 mL nutrient agar media with a cell spreader and incubation at 35 ± 2 °C (bacteria) and 30 °C (fungi) for 24 h. VAN and CAS were used as the reference controls for the bacteria and fungi. Controls before the treatment at 0 h were considered to be 100% and sigmoidal time interval vs. % CFU decrease was established for each test sample. Three technical replicates for each treatment in six independent experiments were performed.

6.10.2. Quantification of the planktonics' intracellular ATP and total protein contents

The instructions provided by the manufacturer were followed for the intracellular ATP measurement of the microbial planktonics. In brief, 1 mL of both treated and untreated aliquots were sampled at time intervals of 0, 2, 6, 8, 16 and 24 h (for bacteria), and 0, 6, 12, 30, 36 and 48 h (for fungi) and were centrifuged at 1000g for 5 minutes. The pellets were washed and were re-suspended in 1 mL PBS. An equal volume of the freshly prepared BacTiter-Glo reagent was pipetted to 100 µL of PBS containing the planktonic cells in 96-well Optiplates. The microplates were shaken in the dark at 4 °C for 15 minutes on an orbital shaker and the luminescence was measured using a Perkin Elmer EnSpire Multimode plate reader (Perkin Elmer, Waltham, Massachusetts, USA). All the measurements were calculated in terms of nmol/L from an ATP standard calibration curve and were converted to intracellular ATP over total protein content ratio (nmol/mg) followed by comparison with the controls before the treatment at 0 h. The PBS, VAN (for bacteria), and CAS (for fungi) were considered as the

blank and standard antimicrobial controls throughout the experiments. Three technical replicates were performed for each treatment in six independent experiments [80,89].

For the total protein content of the planktonics, we adapted the Bradford protein assay method [80,111]. One mL of AEP, AET and AEE treated samples were collected at time intervals of 0, 2, 6, 8, 16 and 24 h (for bacteria), and 0, 6, 12, 30, 36 and 48 h (for fungi) and were centrifuged at 1000g for 5 minutes. The pellets were washed and were re-suspended in 1 mL NaOH (1 M) containing 100 mg of glass beads (425-600 μm) [112]. The collected samples were stabilized on ice for 5 minutes followed by 5 minutes vortexing with a mechanical cell disruptor (Scientific Industries SI analog cell disruptor (InterLabsystems, Budapest, Hungary), consecutively. The cycle was repeated three times and then the samples were centrifuged at 20,000g for 10 minutes at 4 °C (Heraeus Multifuge 3 S-R bench-top centrifuge, Kendo Laboratory products, Osterode, Germany). The supernatants' microbial cell lysates were collected in separate 1.5 mL centrifuge tubes. Two hundred microliters of the freshly prepared Bradford reagent were added to a new 96-well general microplate containing 20 μL of the test samples' lysates. The absorbance was measured at 595 nm by a multimode plate reader. NaOH, VAN, and CAS treated samples were used as the blank, standard antibacterial and antifungal controls, respectively. Three technical replicates for each treatment in six independent experiments were performed. All the measurements were calculated in terms of mg/L from a BSA standard calibration curve and were compared to the 0 h samples [80,89].

6.10.3. Quantification of the planktonics' metabolic activity

For the metabolic activity measurements, AEP, AET, and AEE treated samples were pipetted at time intervals of 0, 2, 6, 8, 16 and 24 h (for bacteria), and 0, 6, 12, 30, 36 and 48 h (for fungi) and were centrifuged at 1000g for 5 minutes. The pellets were washed and were re-suspended in 200 μL PBS containing resazurin (12.5 $\mu\text{mol/L}$) followed by 40 minutes of incubation at 30 °C. The fluorescence was measured with a fluorescence spectrophotometer/microplate reader in 96-well Optiplates at an Ex/Em: 560/590 nm wavelengths. The percentage (%) metabolic activity was estimated based on the fluorescence intensities of samples before the application of the treatment at 0 h which were considered to be 100%. A sigmoidal time interval vs % metabolic activity was established for each test sample. The PBS, VAN (for bacteria), and CAS (for fungi) were considered as the blank and standard antimicrobial controls throughout the experiments. Three technical replicates for each treatment in six independent experiments were performed [17].

6.10.4. Live/dead discrimination of planktonic microbial cells

Briefly, both untreated, AEP, AET and AEE treated samples were taken at 0, 2, 6, 8, 16 and 24 h (for bacteria), and 0, 6, 12, 30, 36 and 48 h (for fungi) following centrifugation at 1000g for 5 minutes, washed and re-suspended in PBS (100 μ L/mL). Freshly prepared 100 μ L of the SYBR Green I/PI working solutions [95] were added to the samples. For 15 minutes, the plates were incubated in the dark with mild shaking at room temperature. Fluorescence intensities of the SYBR Green I and PI were measured in 96-well Optiplates at an Ex/Em: 490/525 nm and 530/620 nm wavelengths, respectively, by a fluorescence spectrophotometer/microplate reader. The green to red fluorescence ratio for each sample and each dose was established and the % of the dead (non-viable) microbial cells with the response to the applied dose were plotted against the applied test compounds using our previous formula [17,95]. The VAN and CAS were considered as the standard antimicrobial controls, whereas, PBS was used as the blank. All the treatments were done in triplicates and six independent experiments were performed.

6.11. Determination of the effects on preformed mature *Candida* biofilms

The effects (Sections 6.11.1–6.11.4) on the mature *Candida* species biofilms and the treatment conditions were adapted from our previously published work [17]. Briefly, 200 μ L of 24 h-old late-log phased ($\sim 10^6$ cells/mL) *C. albicans* and non-*albicans* species in modified RPMI 1640 medium were used to culture biofilms in the microplates before the treatments for 24 h at 30 °C. The microplates were washed in PBS followed by re-incubation in 200 μ L modified RPMI 1640 medium containing AEP, AET, and AEE at MEC₁₀ concentrations (μ g/mL) for further 24 h at 30 °C. Modified RPMI 1640 medium, untreated growth sample, and CAS treated samples were considered as the blank, growth control (GC), and standard antimicrobial control (CAS), respectively. The biofilm degradation percentage (%) was measured based on the comparison of the values with those of the GC. All the treatments were performed in three technical replicates in six independent experiments.

6.11.1. Evaluation of the total fungal biomass

The change in the biofilm biomass was determined by our previously published crystal violet assay [17]. After 24 h of incubation, the supernatant containing the test samples was pipetted out and the wells were washed with PBS. Two hundred microliters of methanol were added to each well to fix the biofilms. The supernatant was removed and 200 μ L of 0.1% crystal violet in absolute ethanol was pipetted into each well. The crystal violet solution was pipetted

out and 200 μL of acetic acid (33% v/v in double distilled water working stock) was pipetted to the crystal violet pre-stained biofilms to release the bound stains. Subsequently, 20 minutes later, the acetic acid-dissolved dye from the stained biofilms was pipetted into the wells of general microplates. The absorbance was measured at 590 nm by a multimode plate reader. The CAS was considered as the standard antifungal control. The change in the percentage (%) biofilm biomass was evaluated from the growth control (GC) values which were taken as 100% fungal biofilm biomass. Three technical replicates in each treatment for six independent experiments were considered.

6.11.2. Metabolic activity in the biofilms

A resazurin-derived fluorescent technique was adapted from our previously published protocol to determine the metabolic activity in the fungal biofilms [17]. Briefly, after 24 h of the treatment with AEP, AET, and AEE at their respective MEC_{10} concentrations, all of the supernatants were removed followed by rinsing the wells with the PBS. Two hundred microliters of sterile PBS containing resazurin (12.5 $\mu\text{mol}/\text{mL}$) were pipetted into the wells and were incubated at 30 $^{\circ}\text{C}$ for 40 minutes. The fluorescence intensities were recorded at an Ex/Em: 560/590 nm wavelengths, respectively, by a fluorescent spectrophotometer/microplate reader. The percentage (%) metabolic activity measurements were evaluated based on the fluorescence values recorded by the growth control (GC), which was considered as 100%. The PBS was taken as the blank throughout the measurements. Six independent experiments were performed with three technical replicates for each treatment.

6.11.3. Viability assay of the biofilms

For the discrimination of the live/dead fungal cells in the biofilms, we have followed a method previously published [17,91,95]. After 24 h of treatment with AEP, AET, and AEE, at their respective MEC_{10} concentrations in modified RPMI 1640 medium, the planktonic cells were pipetted out, followed by rinsing and filling of the biofilm-attached wells with 100 μL PBS. One hundred microliters of SYBR Green I/PI working solutions [17,95] were pipetted into the wells of the microplate. The plates were incubated at room temperature for 15 minutes in the dark with mild shaking. A fluorescence spectrophotometer/microplate reader was used to measure the fluorescent intensities at an Ex/Em: 490/525 nm and 530/620 nm for SYBR Green I and PI, respectively, into 96-well Optiplates. The green to red fluorescence ratio for each sample and each dose was established, and the % of the dead microbial cells with the response to the applied dose was plotted against the applied test compounds using our previous

formula [17,91]. All treatments were done using three technical replicates in six independent experiments.

6.11.4. Determination of the *Candida* biofilms' intracellular ATP and total protein contents

The instructions provided by the company were followed for the intracellular ATP measurement of the *Candida* mature biofilms. In brief, after 24 h of the treatment with AEP, AET, and AEE, the planktonic cells were pipetted out, followed by rinsing the biofilm and pipetting 100 μ L of PBS into every well of the microplate. An equal volume of the freshly prepared BacTiter-Glo reagent was pipetted into the wells containing the biofilms submerged in the PBS. The microplates were shaken in the dark at 4 °C for 15 minutes on an orbital shaker. The content of the microplates was transferred to 96-well Optiplates and the luminescence was measured using a multimode plate reader. All measurements were quantified by using an ATP standard calibration curve and were converted to intracellular ATP over the total protein content ratio (nmol/mg) followed by comparison with the growth control (GC). The PBS and CAS were used as the blank and the standard antifungal controls, respectively. Three technical replicates for each treatment in six independent experiments were performed [17].

For the measurement of the total protein content in the biofilms, parallel to the microplate cultures the biofilms were produced and treated in 35 mm diameter sterile Petri-dishes with identical surface properties to those of the microplates. We have adapted the Bradford protein assay method [111]. Briefly, after 24-hour treatment of the mature biofilms with AEP, AET, and AEE, the planktonic cells were pipetted out and biofilms were rinsed with PBS. The biofilms were scraped out from the Petri-dishes using a cell scraper into sterile 1.5 mL centrifuge tubes containing 1 mL NaOH (1 M) and 100 mg of glass beads (425–600 μ m). The collected samples were stabilized on ice for 5 minutes, followed by 5 minutes vortexing, consecutively. The cycle was repeated three times and then the samples were centrifuged at 20,000g for 10 minutes at 4 °C. The supernatants' fungal cell lysates were pipetted out and were diluted in NaOH (1 M) up to the initial volume used for biofilm growth. Two hundred microliters of the homemade freshly prepared Bradford reagent were added to a new 96-well general microplate containing 20 μ L of the test sample lysates. The absorbance was measured at 595 nm by a multimode plate reader. All the measurements were calculated in terms of mg/L from a BSA standard calibration curve. Total protein contents were referred to as the surface area of the microplates to obtain the valid ATP/TP values. The NaOH and CAS treated samples were used as the blank and the standard antifungal controls, respectively. Three technical

replicates for each treatment in six independent experiments were performed. All the measurements were calculated in terms of mg/L from a BSA standard calibration curve and were compared to the growth control (GC).

7. Statistical analyses

All data were given as mean \pm SD. Graphs and statistical analyses were conducted using OriginPro 2016 (OriginLab Corp., Northampton, MA, USA). All experiments were performed independently six times in triplicates and data were analyzed by a one-way ANOVA test. *P*-values of <0.05 were considered statistically significant. The minimum inhibitory concentrations (MIC₈₀ and MIC₉₀) and the minimum effective concentration (MEC₁₀) were calculated using a non-linear dose-response curve function as follows:

$$y = A_1 + \frac{A_2 - A_1}{1 + 10^{(LOG_x0 - x)p}} \quad (7)$$

where A_1 , A_2 , LOG_x0 , and p as the bottom asymptote, top asymptote, center, and hill slope of the curve have been considered. Either MIC₈₀ or MIC₉₀ were calculated depending on our methodological requirements.

8. Results and discussion: RAMEB-EO complexes

8.1. Characterization of RAMEB encapsulated essential oils/components

8.1.1. UV-VIS spectroscopy analysis

The UV absorption spectra of investigated essential oils, active components, and RAMEB are shown in Figure 3. The maximum absorption of the essential oils was found to be in the range of 210 – 220 nm which is attributed to the active components. The absorption peak of essential oils at 250 nm corresponding to 1,8-cineole. The spectral analysis of the physical mixture of RAMEB with essential oils and with components before complexation was found to be harmonious with the essential oils and components. The absorbance spectra of the physical mixture of essential oils with RAMEB with components were in symmetry with the essential oil spectra and components. In the case of complexation, the absorption peaks disappear in RAMEB complexation spectra. The active compounds from the encapsulation were recovered by dissolving the complexes in 95% acetonitrile [113]. The compounds were released from the RAMEB cavity and were separated by centrifugation. The solutions were diluted to hundred times in acetonitrile and the absorbance was measured. In this line, beside the active compounds, 1,8 cineole, cis- β -ocimene, α - pinene, α -terpineol, *p*-cymene, and β -

caryophyllene were also observed at 210 nm and 240 nm respectively. We are aware of the complexity of EOs which makes our absorbance spectroscopic analysis to be an approximation only however, it indicates the successful formation of complexation of essential oils and their components with RAMEB.

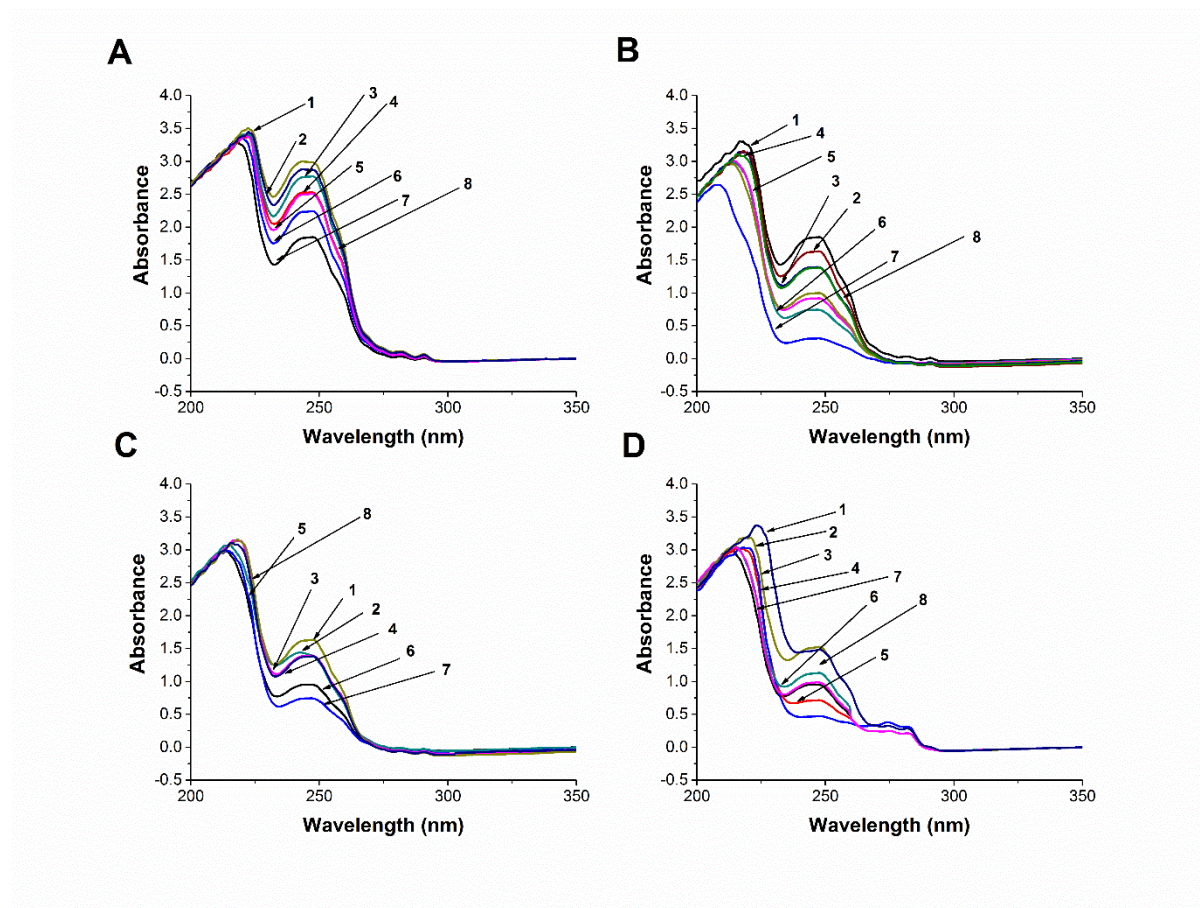


Figure 3. The UV absorption spectra of the physical mixture of essential oil-RAMEB (1), physical mixture of component-RAMEB (2), essential oil (3), active component (4), encapsulated essential oil-RAMEB (5), encapsulated component-RAMEB (6), RAMEB (7) and chemicals extracted from encapsulated essential oils. The four graphs are the UV spectra of the followings: (A): lavender oil, linalool, RAMEB, (B): peppermint oil, menthol, borneol, RAMEB, (C): lemon balm oil, citral, RAMEB and (D): thyme oil, thymol, RAMEB. Six independent experiments with three technical replicates were performed (mean \pm SD).

8.1.2. Determination of average molecular weight of the essential oils

The evaluated average molecular weight of the examined essential oils are as follows in decreasing order: peppermint oil (237.19), lemon balm oil (236.64), lavender oil (225.44) and thyme oil (182.84). All measurements were repeated three times showing less than 1% imprecision.

8.1.3. Phase solubility studies

The y-intercept is referred to as the concentration of solubilized guests without a host in the solution medium. The plot indicates the type of inclusion complex. Positive slopes < 1 with a linear relationship among the concentration of dissolved essential oil or active components and RAMEB were obtained in every case (Figure 4). The complexes thus may be classified as an AL type (1:1 molar ratio of guest to host) [82]. Major entrapped compounds are mono- and sesquiterpenoids and phenylpropane derivatives (average molecular weight: 120-160 g/mole), thus a 1:1 complex formation can be expected [114]. K_s (stability constant) is an important parameter to measure the difference in the equilibrium between free and complex formulation. Low K_s were obtained in case of essential oils while for the active components they are in the order for those of RAMEB complexes (Figure 4). This may be because of the competition or affinity of other compounds with the active components used in the study to form RAMEB complexes. The decrease in K_s with an increase in temperature reflects an exothermic process [115]. The phase solubility study (Figure 4) shows that the aqueous solubility of essential oils used in the study can be increased with increasing RAMEB concentration. The complex stabilities for thymol with cyclodextrins vary from 152 L/mole [73] to 3337 L/mole [83]. One possible reason for this variation of the complex stability constants is the encapsulation of water molecules by the host cyclodextrins and also the microsolvation of guest molecules by water [116]. This property highly affects the complex formation due to the modified structure of the solvation shell of guests and the exit of the solvent water molecules from the CD cavity before the formation of the complexes. Studies performed previously on the host-guest interactions of calixarenes with similar-sized aromatic guests, the protic character of water should be considered, as the entropy change associated with the complex formation is also highly affected by the processes [117]. Furthermore, the large difference of complex stabilities obtained in protic aqueous and non-protic acetonitrile media for the main components of essential oils also highlights the role of micro-solvation during the complex formation (Figure 4).

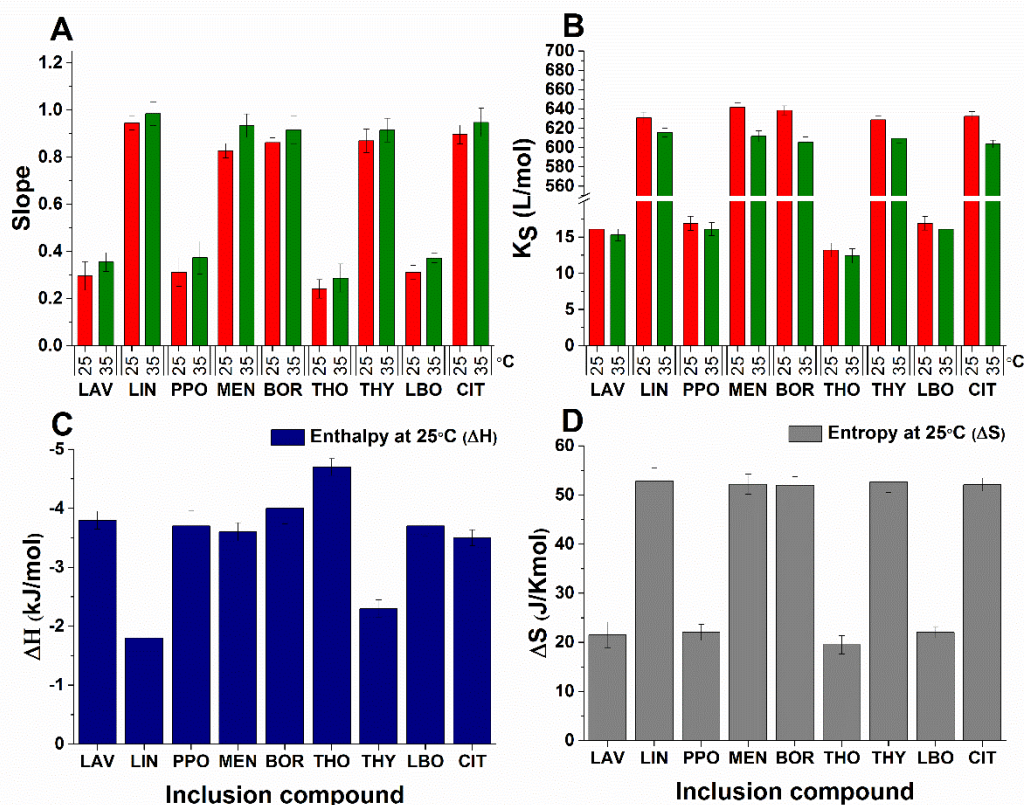


Figure 4. The A, B, C, and D represents slope, stability constant (K_s , L/mol), enthalpy (ΔH , kJ/mol), and entropy (ΔS , J/Kmol) changes of encapsulated essential oils and active components at specified temperatures. Data in parentheses reflect stability constants determined in acetonitrile (mean \pm SD, n = six independent experiments). R^2 is higher than 0.86 for all components.

The thermodynamic data show clearly that the complex formation is an entropy-driven process. The enthalpy changes associated with the complex formation are about 2-4 kJ/mole which value is just the average kinetic energy associated according to the equipartition theorem. This stabilization energy is far to be responsible for complex formation. In contrast, entropy gain plays a determinant role to improve complex stability. It is doubled in some cases (for main components) resulting in a huge increase of the calculated stabilities compared to those related to the essential oils. Comparing the complex stabilities derived from the measurements performed in aqueous or acetonitrile media the probable determinant process responsible for the complex formation is the leave of solvent molecules from the CD cavity before the complex formation (Supplementary Figures S1-S6). The hydrophobic interior of the cavity supports the exchange of water molecules with the guest essential oils while this process is just blocked when the essential oils want to replace the acetonitrile molecules in the CDs cavity. As a result, the enhanced freedom of water molecules after the formation of complexes manifest the entropy gain while no similar process can be obtained in acetonitrile media. As a

result, much lower stabilities can be obtained in acetonitrile. It is worth mentioning here the much larger stability derived for the main component compared with the appropriate oil: the components of oil other than the main component only weakly can replace the water molecules in the CD interior resulting in much lower entropy gain during complex formation.

8.1.4. Encapsulation efficiency

Encapsulation efficiency (EE) expressed in % of RAMEB-EO complexes is based on GC analyses (Supplementary Figure S7). Peppermint oil showed the highest encapsulation efficiency ($94.95 \pm 0.57\%$) followed by thyme oil ($93.30 \pm 1.58\%$), lemon balm oil ($93.13 \pm 1.04\%$) and lavender oil ($87.38 \pm 2.28\%$) respectively. Several EO components, including pinene, can polymerize in low-permittivity solutions [118]. In such cases, the large polymer adducts are not able to form complexes with the RAMEB molecules. As a result, the concentration of the components which are active in the complex formation is much lower than it can be assumed from the physical amount of EO used in the experiments.

The Formation constant (K_f) values of RAMEB/aroma inclusion complexes are as follows (L/mole): linalool 688, neral (Z-citral) 399, geranial (E-citral) 416, menthol 1464, iso-borneol 1689, borneol 1784 and thymol 1206 (SD <10%).

8.2. Antioxidant capacity (DPPH, ECL, and ORAC assay)

We have quantified the antioxidant properties of EOs - RAMEB and their components by DPPH, ORAC, and ECL assay methods. As reported previously [119] cyclodextrin may influence the ORAC fluorescence assay for antioxidant activity evaluation. However, we could not find any interference or measurable antioxidant activities of RAMEB at the applied concentrations (1 to 100 mg/mL) on the emission intensity of fluorescein used in the ORAC assay. Also, EOs are strongly lipophilic molecules with limited effect in aqueous antioxidant tests therefore, entrapment by RAMEB was essential for our TAC assays. Consequently, it was postulated that EOs -RAMEB complexes being water-miscible enable the use of fewer amounts of entrapped EOs than the free oils alone. The antioxidant activity obtained by thyme oil and its component thymol was found to be the highest followed by lemon balm oil, lavender oil, and peppermint oil (Figure 5). Previous data [84,86,120,121] reported a higher concentration of EOs than were used in our experiments to produce suitable antioxidant activity. We found, that when EOs are captured by RAMEB, a remarkable antioxidant activity is achieved despite the use of smaller amounts of them.

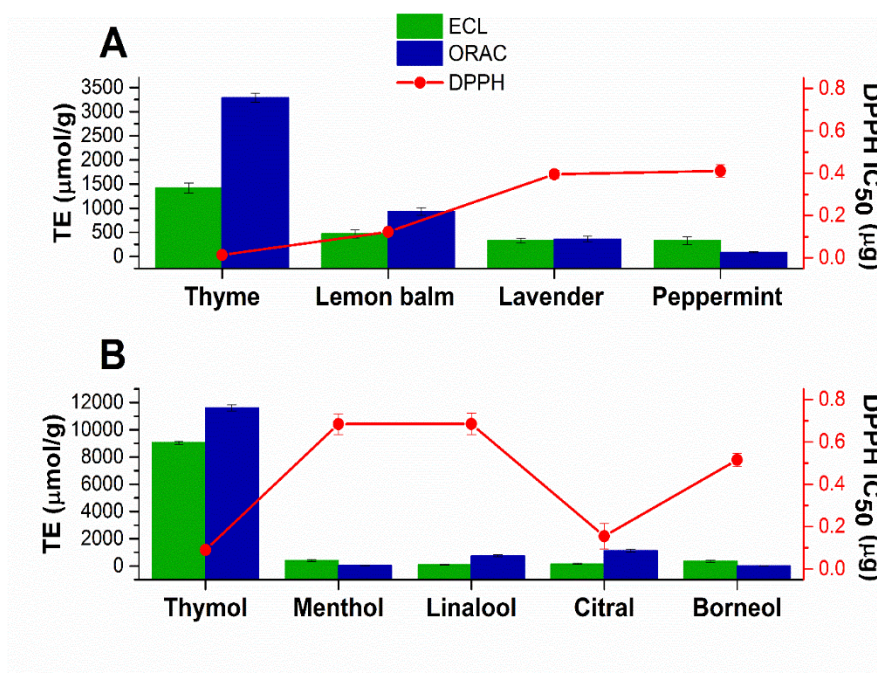


Figure 5. Antioxidant activities of investigated EO-RAMEB (A) and EO components RAMEB (B) complexes. The effects of selected RAMEB packed EOs and their components on ORAC, ECL, and DPPH assays. Six independent experiments with three technical replicates were performed (mean \pm SD). The activity of RAMEB was not shown as the data were outside the acceptable ranges.

8.3. Antifungal and antibacterial activities

Different EOs-RAMEB inclusions were tested against *S. pombe* cultured for 48 hours at 30 °C, *E. coli* and *S. aureus* cultured for 24 hours at 37 °C. Antifungal and antimicrobial effects were expressed as a minimum inhibitory concentration (MIC₈₀) which is the first concentration where 80% of microorganisms are inhibited (Figure 6). All the inclusion complexes showed antifungal and antimicrobial activity. However, RAMEB-thyme oil was found to have the best MIC (MIC₈₀ = 0.125 – 0.25 mg/mL, 0.156 – 0.312 mg/mL, 0.5 – 1 mg/mL) against *S. pombe*, *E. coli*, and *S. aureus* respectively, followed by lemon balm oil, peppermint oil, and lavender oil, in this order (Figure 6). RAMEB-EO components also showed antifungal and antimicrobial activity. Antimicrobial and antifungal effect of RAMEB-citral (MIC₈₀ = 0.0078 – 0.156 mg/mL, 0.125 – 0.25 mg/mL, 0.078 – 0.156 mg/mL) was close to RAMEB-thymol (MIC₈₀ = 0.078 – 0.156 mg/mL, 0.125 – 0.5 mg/mL, 0.25 – 0.5 mg/mL) under our test conditions.

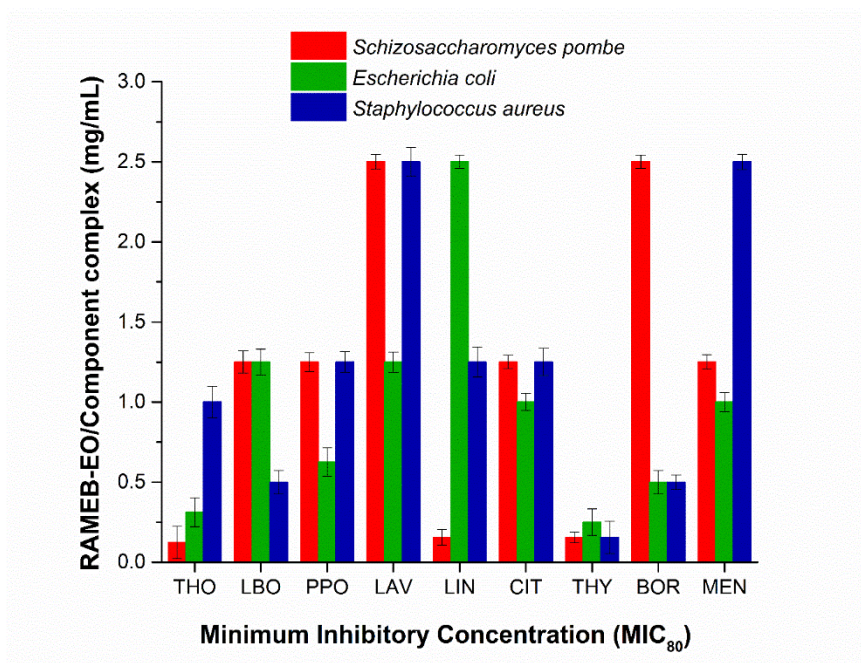


Figure 6. Anti-fungal and anti-microbial activity of investigated EO-RAMEB and EO component-RAMEB complexes and on *S. pombe*, *E. coli* and *S. aureus*. The effects of selected RAMEB packed EOs (THO: thyme, LBO: lemon balm, PPO: peppermint, LAV: lavender, LIN: linalool, CIT: citral, THY: thymol, BOR: borneol and MEN: menthol) and their components are found to be variable on the gram (+)ve, gram (-)ve and fungus used in the study. Six independent experiments with three technical replicates were performed (mean \pm SD).

Free thyme oil and thymol with MIC of 0.64 mg/mL and 0.73 mg/mL have been reported by several authors [122,123]. Our study shows MIC of 0.156 mg/mL and 0.125 mg/mL against *E. coli*. When applied against both *E. coli* and *S. aureus*, free peppermint oil showed MIC at 0.6 mg/mL [60]. Both free linalool and lavender oil have MIC at higher concentrations [124]. Our data suggest that RAMEB encapsulated lavender oil and linalool have MIC at lower concentrations 1.25 mg/mL and 0.078 mg/mL, respectively. It has been reported that inclusion complexes with RAMEB may elevate aqueous solubility of the encapsulated guests resulting in better antimicrobial efficiency of the essential oils and their components at lower concentrations [10,115]. Our obtained MIC values are different from those of previously published results by other authors that may be due to differences in media composition, methodology, and strains of bacteria and fungus used in the studies [115].

8.4. Rapid SYBR Green I/propidium iodide live-dead discrimination assay

8.4.1. Comparison of the plate reader method with flow cytometry

To evaluate if the SYBR Green I/propidium iodide staining can be used for rapid plate reader viability assay, *S. pombe* was subjected to treatment with different concentrations of 2-

propanol (see section 3.6.4). Also, we assessed the ability of SYBR Green I/propidium iodide assay to determine the viability of *S. pombe* by flow cytometry. In summary, we have evaluated the microbial viability to compare the percentage of dead cells by both plate reader and flow cytometry methods. We found the optimized SYBR Green I/propidium iodide assay to be reliable for the rapid estimation of the viability of microbes using the plate reader technique (Figure 7).

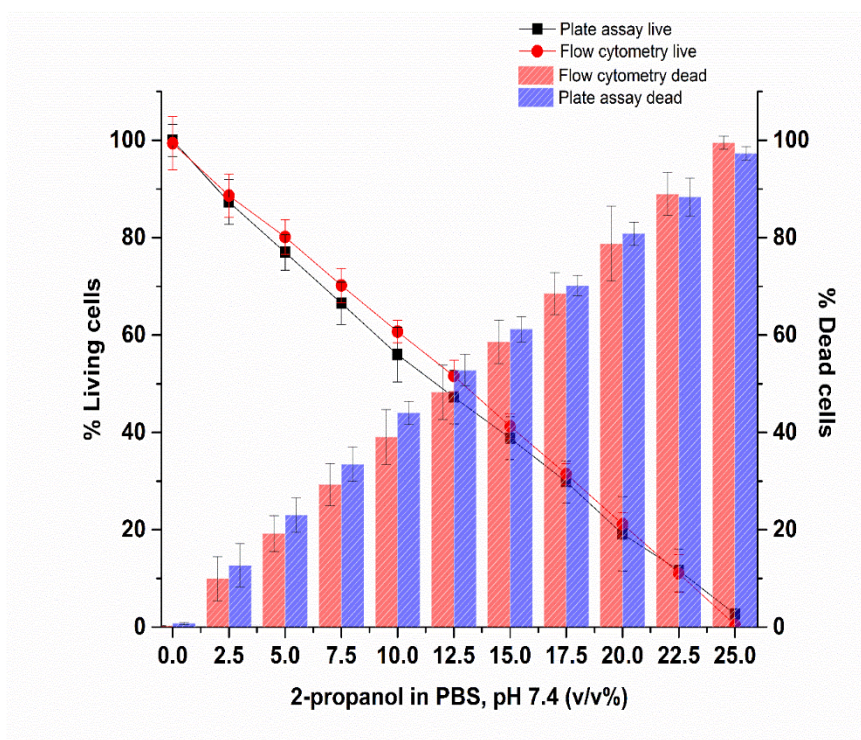


Figure 7. Comparison of the live/dead discrimination results between the plate reader assay and the flow cytometric assay using SYBR Green I/propidium iodide double staining on *S. pombe* (six independent experiments). Six independent experiments with three technical replicates were performed (mean \pm SD).

8.4.2. Rapid microbial cell live/dead discrimination plate reader assay of *S. pombe*, *E. coli* and *S. aureus*

This viability assay was attempted for the fast evaluation of the susceptibility of different concentrations of EOs - RAMEB on *S. pombe*, *E. coli*, and *S. aureus*. Our findings suggest that complexed peppermint oil is less effective in killing *S. pombe* at 2 mg/mL when compared to the percentage of dead/compromised cells of *E. coli* and *S. aureus* at the same concentration (Figure 8). Thyme oil was found to be more potent at 0.5 mg/mL, killing 90% of cells in all three cases followed by citral which showed 90% inhibition at 0.25 mg/mL. Lavender oil, although expressing less killing property at 2 mg/mL, was more effective towards *E. coli* and

S. aureus at more than 90% efficiency at the same concentration. Thymol is the active constituent of thyme oil showed high (80% and above) killing/compromising ability at low concentrations starting from 0.25 mg/mL. On the other hand, menthol showed more effectiveness in killing *E. coli* and *S. aureus* at 2 mg/mL. Borneol had no killing or inhibiting properties at all towards both microbes. The validity of our plate reader assay was verified by testing the microbial samples using flow cytometry as well. The two methods can be considered to be equivalent and the plate reader assay offers the advantage of high throughput determinations.

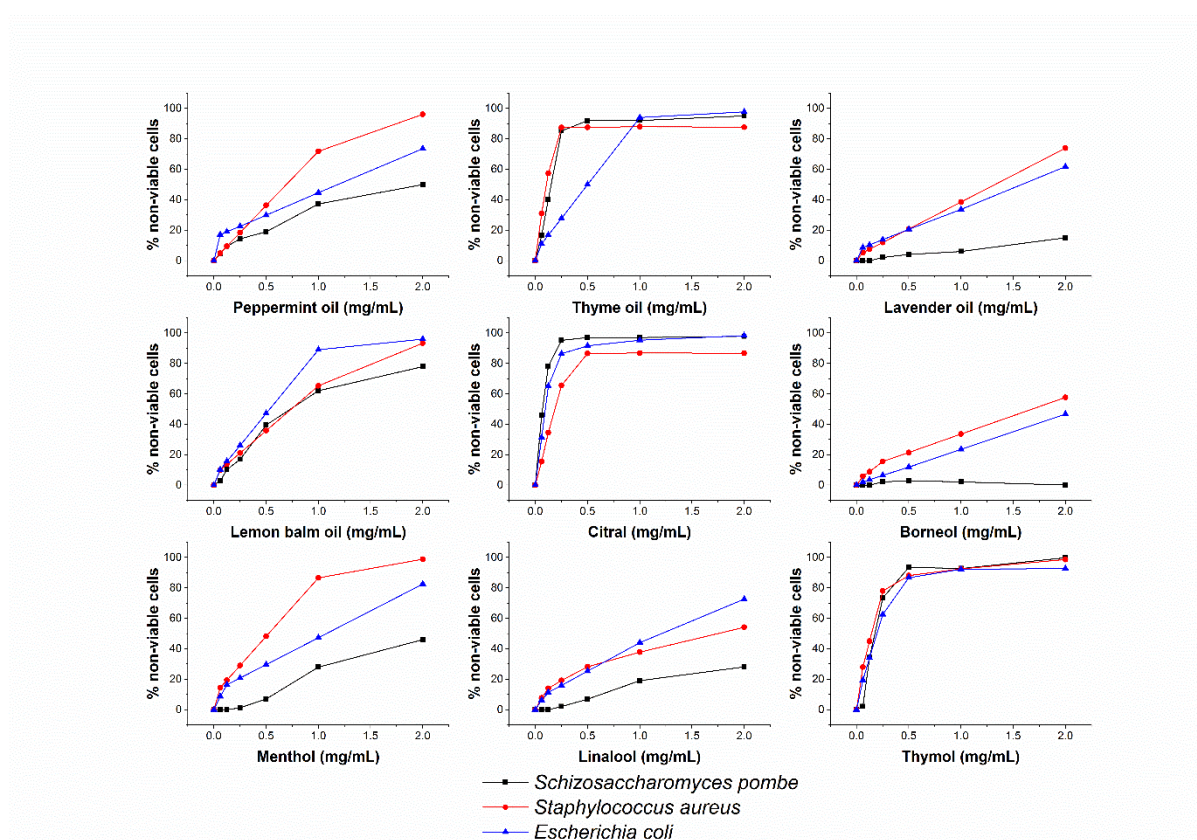


Figure 8. Percentage death of cells using SYBR Green I/PI double-stained plate reader method for live/dead discrimination of the test microbes. Six independent experiments with three technical replicates were performed (mean \pm SD).

9. Results and discussion: Pickering-chamomile essential oil experiments

9.1. Chamomile essential oil and its components

The gas chromatography-mass spectrometry detection (GC-MS) analyses (Supplementary Figure S8 and Table S1) have documented trans β -farnesene (17.93%), germacrene D (1.54%), bicylogermacrene (1.39%), (E,E)- α -farnesene (2.08%), spathulenol (1.88%), bisabolol oxide

B (7.57%), bisabolone (21.83%), chamazulen (3.19%), bisabolol oxide A (10.48%) and vetivazulene (4.94%).

9.2. Characteristics of Stöber silica nanoparticles

This was performed by Barbara Horváth and her colleagues at the Institute of Pharmaceutical Technology and Biopharmacy (Faculty of Pharmacy, University of Pécs). The results of the characteristics of Stöber silica nanoparticles can be found in Ref. [91] and her PhD thesis “Pickering Emulsions in Pharmaceutical Technology” (in preparation). The size distribution obtained by dynamic light scattering (DLS) was confirmed by transmission electron microscopy (TEM), which showed that the mean diameter of silica samples was 20 nm; they are highly monodisperse and have a spherical shape.

9.3. Nanoemulsion stability

This was performed by Barbara Horváth and her colleagues at the Institute of Pharmaceutical Technology and Biopharmacy (Faculty of Pharmacy, University of Pécs). The results of the nanoparticle stability can be found in Ref. [91] and her PhD thesis “Pickering Emulsions in Pharmaceutical Technology” (in preparation). The Pickering nanoemulsion using silica nanoparticles was stable for three months.

9.4. Anti-bacterial and anti-fungal activities (MICs) of prepared emulsion

The effect of chamomile Pickering nanoemulsion, conventional emulsion, and essential oil in ethanol on the growth of some foodborne microbes and opportunistic fungi have been evaluated. The C_{Pe} has been shown to have good antibacterial and antifungal activities (MIC₉₀) on *Escherichia coli* (*E. coli*) (2.19 µg/mL), *Pseudomonas aeruginosa* (*P. aeruginosa*) (1.02 µg/mL), *Bacillus subtilis* (*B. subtilis*) (1.13 µg/mL), *Staphylococcus aureus* (*S. aureus*) (1.06 µg/mL), *Streptococcus pyogenes* (*S. pyogenes*) (2.45 µg/mL), *Schizosaccharomyces pombe* (*S. pombe*) (1.28 µg/mL), *Candida albicans* (*C. albicans*) (2.65 µg/mL), and *Candida tropicalis* (*C. tropicalis*) (1.69 µg/mL), respectively when compared to C_{T80} counterpart ($P < 0.01$). C_{Pe} showed antimicrobial activity on the selected microbes at an average of fourteen fold less concentration compared with free essential oil in ethanol (C_{Et}). Simultaneously, C_{Pe} showed a similar antifungal effect as caspofungin (Cas) on *Candida tropicalis*. The comparative dose-response curves are shown in Figures 9 and 10 for bacteria and fungi, respectively. Based on our antimicrobial activity analyses, C_{Pe} shows higher growth inhibitory action and consequently lower MICs compared to C_{T80} and C_{Et}.

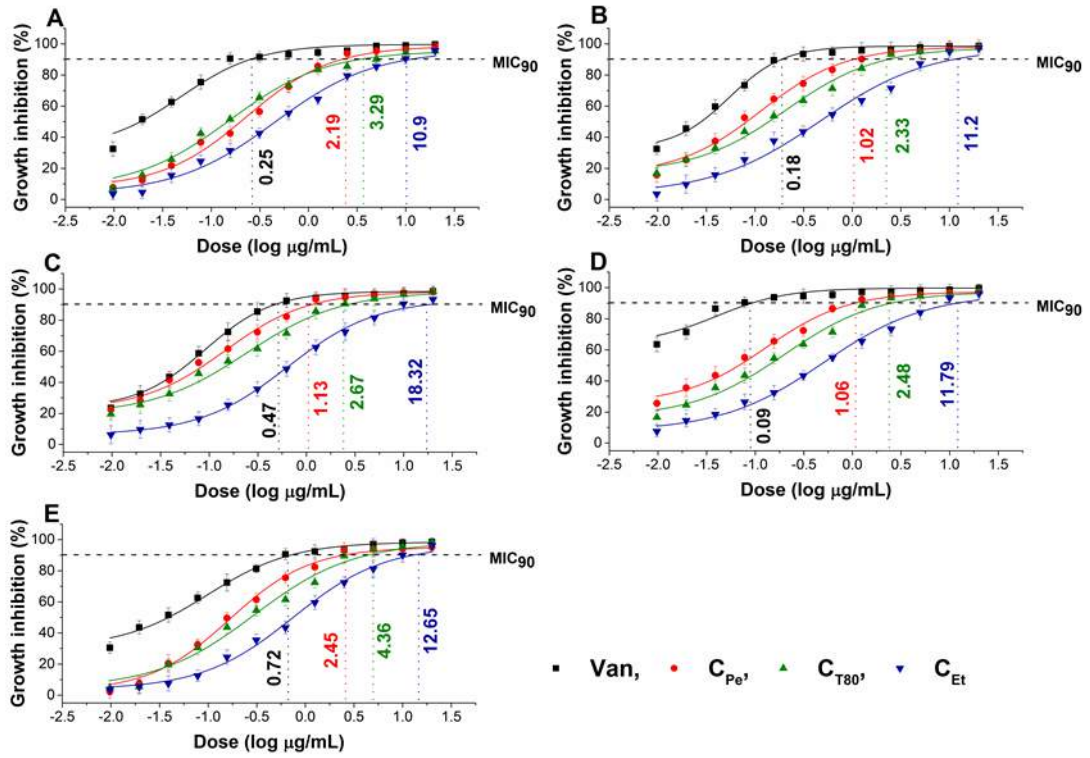


Figure 9. Minimum inhibitory concentration (MIC₉₀) of C_{Pe}, C_{T80}, C_{Et}, and vancomycin (Van, µg/mL) on *E. coli* (A), *S. aureus* (B), *B. subtilis* (C), *P. aeruginosa* (D), and *S. pyogenes* (E). Six independent experiments with three technical replicates were performed (mean ± SD).

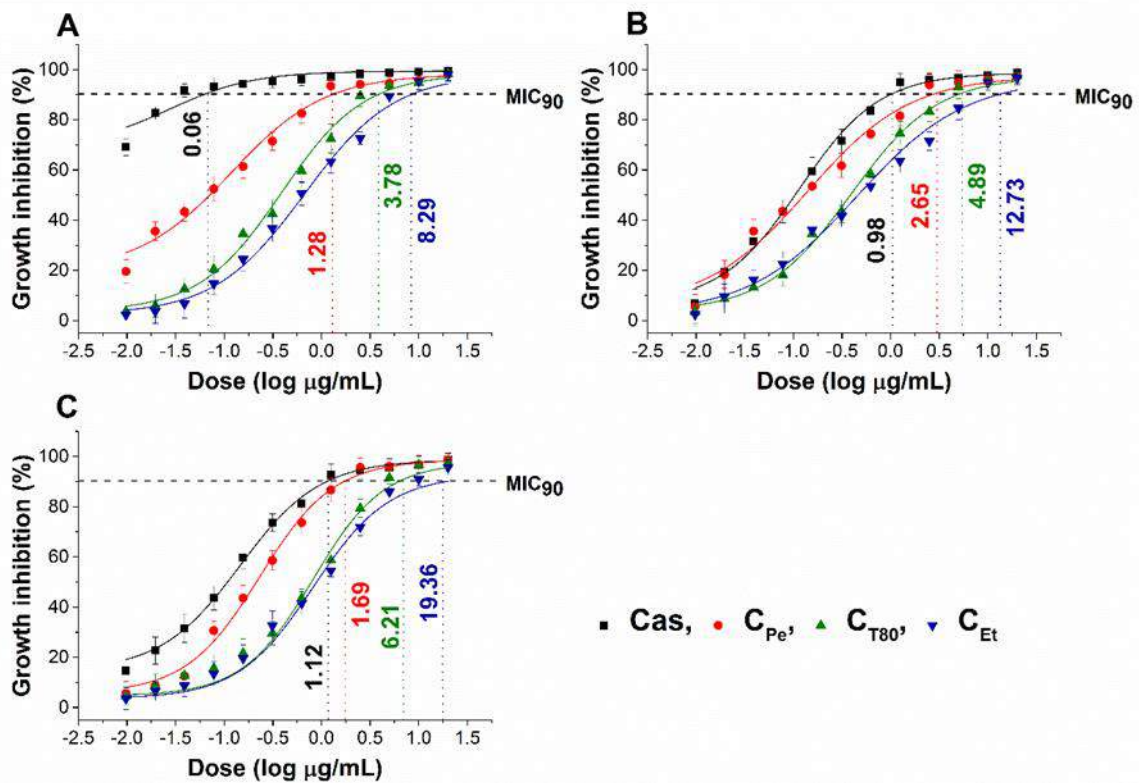


Figure 10. Minimum inhibitory concentration (MIC₉₀) of C_{Pe}, C_{T80}, C_{Et}, and caspofungin (Cas, μg/mL) on *S. pombe* (A), *C. albicans* (B), and *C. tropicalis* (C). Six independent experiments with three technical replicates were performed (mean ± SD).

9.5. Minimum effective concentrations (MEC₁₀) for tested bacteria and fungi

The minimum effective concentration (MEC₁₀) of C_{Pe}, C_{T80}, and C_{Et} on foodborne Gram-positive and Gram-negative bacteria as well as fungi have been determined. The dose-response curve shows a slow killing effect ($\leq 10\%$ of the population) of C_{Pe} after 60 minutes of treatment at a two-fold lower concentration compared with MIC₉₀ data. The MEC₁₀ also highlights the effective killing effect of C_{Pe} when compared to C_{T80} and C_{Et} (Figures 11 and 12) ($P < 0.01$). Many researchers have studied the antimicrobial activity of chamomile oil [3,52,125–127], however, the mechanism of action at sub-inhibitory concentrations has not previously been studied. Our data suggest an effective killing activity of C_{Pe} on selected bacteria and fungi. It is believed that EOs act against cell cytoplasmic membrane and induce stress in microorganisms [96,97,128,129].

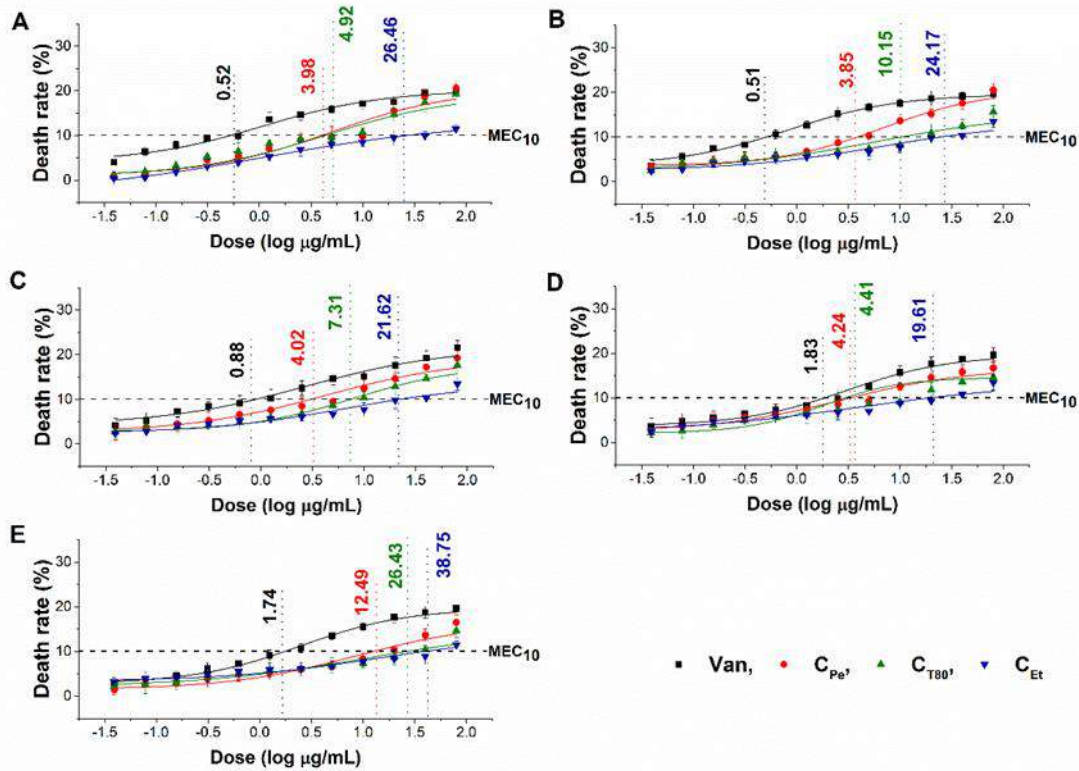


Figure 11. Minimum effective concentration (MEC₁₀) of C_{Pe}, C_{T80}, C_{Et}, and Van ($\mu\text{g/mL}$) on *E. coli* (A), *S. aureus* (B), *B. subtilis* (C), *P. aeruginosa* (D), and *S. pyogenes* (E). Six independent experiments with three technical replicates were performed (mean \pm SD).

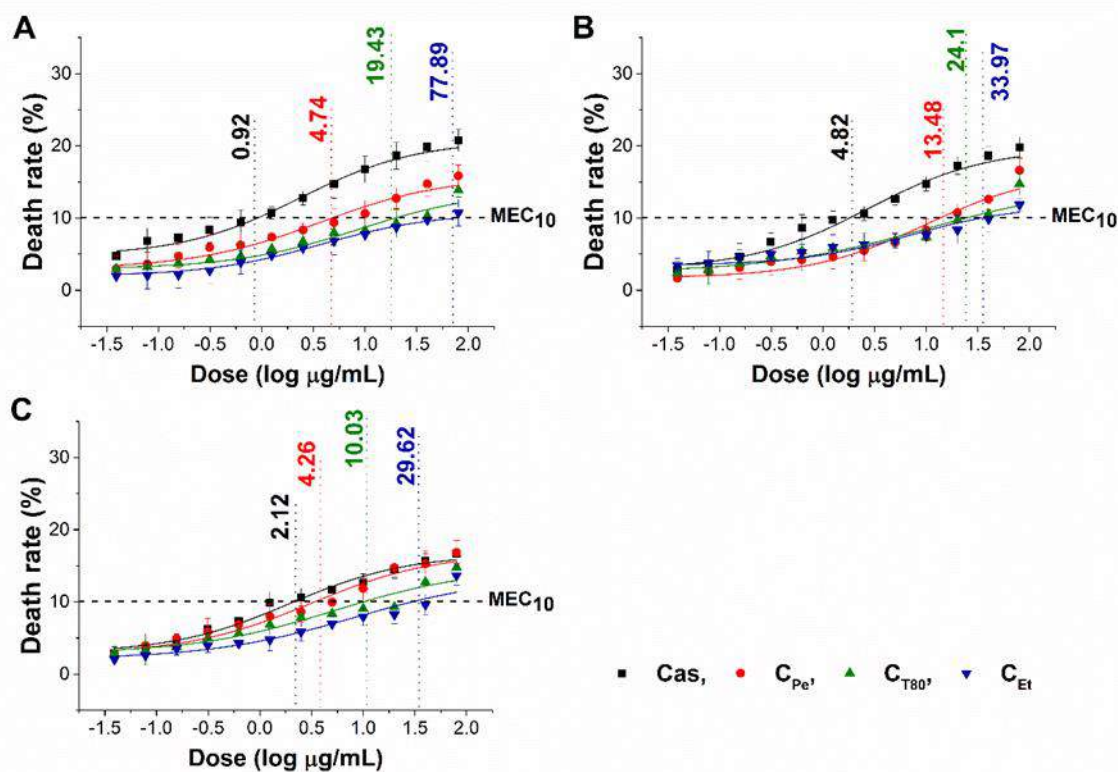


Figure 12. Minimum effective concentration (MEC_{10}) of C_{Pe} , C_{T80} , C_{Et} , and Cas ($\mu\text{g/mL}$) on *S. pombe* (A), *C. albicans* (B), and *C. tropicalis* (C). Six independent experiments with three technical replicates were performed (mean \pm SD).

9.6. Effects on microbial oxidative stress

Reactive oxygen species (ROS) production and accumulation in the cells initiate oxidative stress, leading to cellular structural damage followed by induced apoptosis [51]. We have investigated the relationship between oxidative stress generation after 60 minutes of treatment and microbial killing activity. The results are demonstrated in Figures 13 and 14 for bacteria and fungi, respectively. Data expressed as % of the control are as follows: the ROS (1085.86 ± 126.36), peroxide (1229.86 ± 164.52) and superoxide (1276.86 ± 165.42) generation were the highest in case of *S. aureus*. The C_{Pe} showed an increment of ROS, peroxide, and superoxide generation in both Gram-positive and negative bacteria when compared to C_{T80} and C_{Et} ($P < 0.01$). C_{Pe} showed increased oxidative stress in both bacteria and fungi at least seven-fold higher than the negative control whereas the positive control (menadione) produced an eight- to nine-fold increase in 60 minutes. The C_{Et} has generated a two to four-fold increment in oxidative stress which is the lowest among all tested compounds. The C_{Pe} was able to generate higher oxidative stress compared to the conventional emulsion and ethanolic solution

followed by metabolic interference and cell wall disruption and finally caused cell death at sub-inhibitory concentration [76,93,130–132].

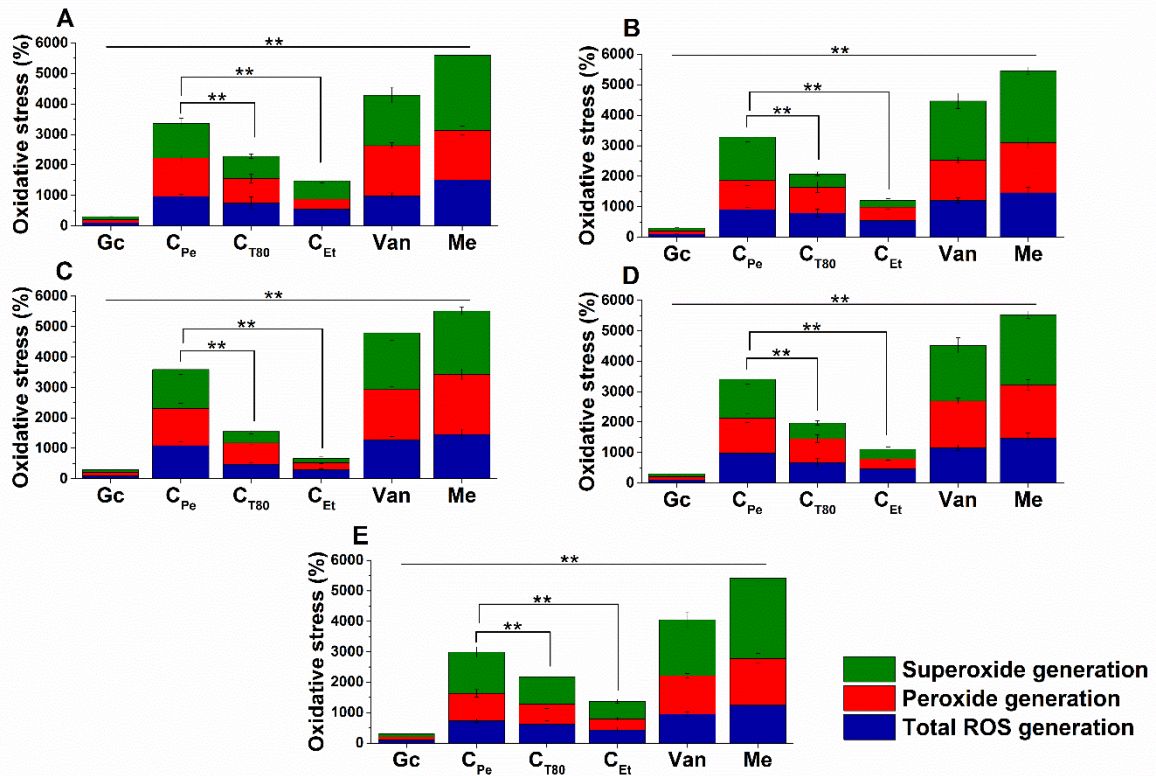


Figure 13. Percentage oxidative stress generation by C_{Pe}, C_{T80}, C_{Et}, and Van on *E. coli* (A), *S. aureus* (B), *B. subtilis* (C), *P. aeruginosa* (D), and *S. pyogenes* (E). Six independent experiments, each with 3 replicates, compared with menadione (Me) and growth control (Gc) as controls after 1 h of treatment (**P < 0.01).

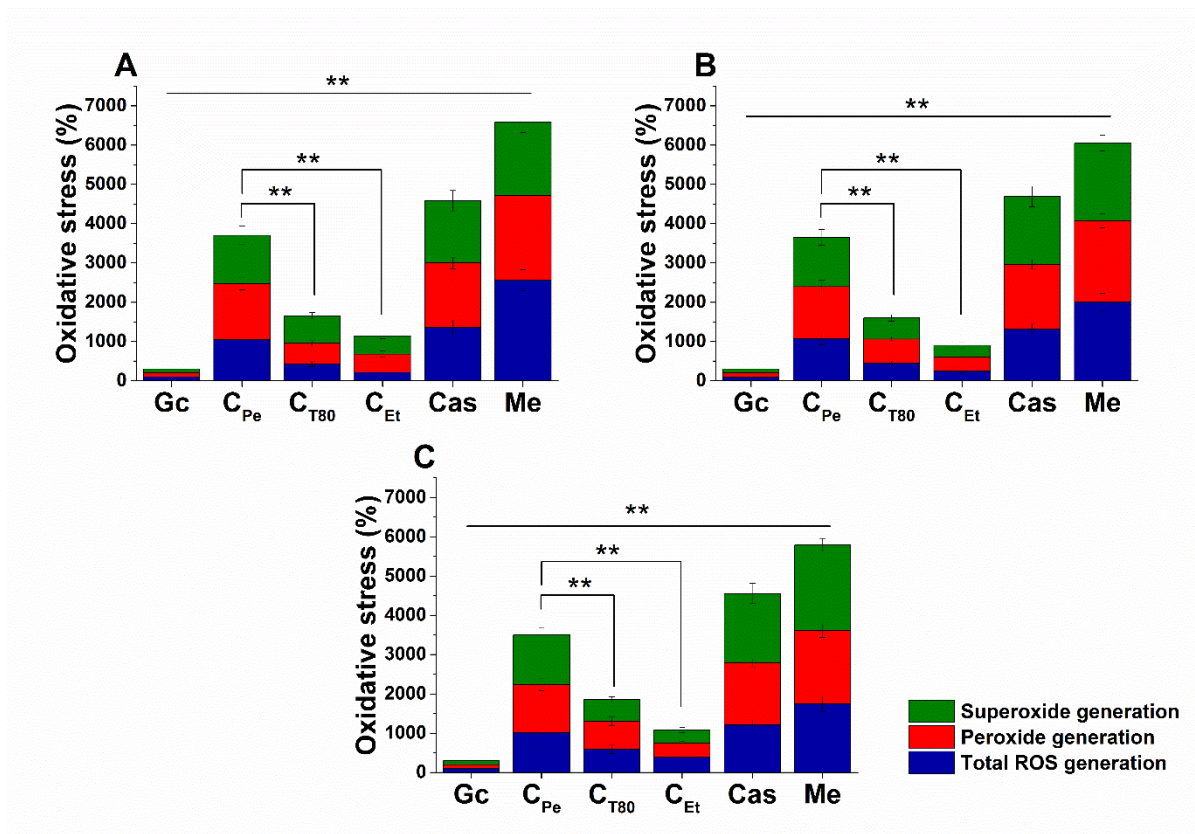


Figure 14. Percentage oxidative stress generation by C_{Pe}, C_{T80}, C_{Et}, and Cas on *S. pombe* (A), *C. albicans* (B), and *C. tropicalis* (C). Six independent experiments, each with 3 replicates, compared with Me and Gc as positive and growth controls after 1 h of treatment (** $P < 0.01$).

9.7. Time-kill kinetics study

The time-kill kinetics curve was performed to quantify living populations after a definite time interval under different sample MEC₁₀ concentrations. A significant reduction (four log-fold) in the cell survivability has been observed in the case of C_{Pe} when compared to Gc ($P < 0.01$) (Figures 15 and 16). Fifty percent of cell death occurred by C_{Pe} at 16 and 36 h in the case of bacteria and fungi and was most effective in reducing living colonies in the case of *C. albicans* (1.73 ± 0.15 CFU/mL) after 48 h of treatment. At an average of a two-fold higher concentration, C_{Et} was able to show a killing effect compared to C_{Pe} ($P < 0.01$).

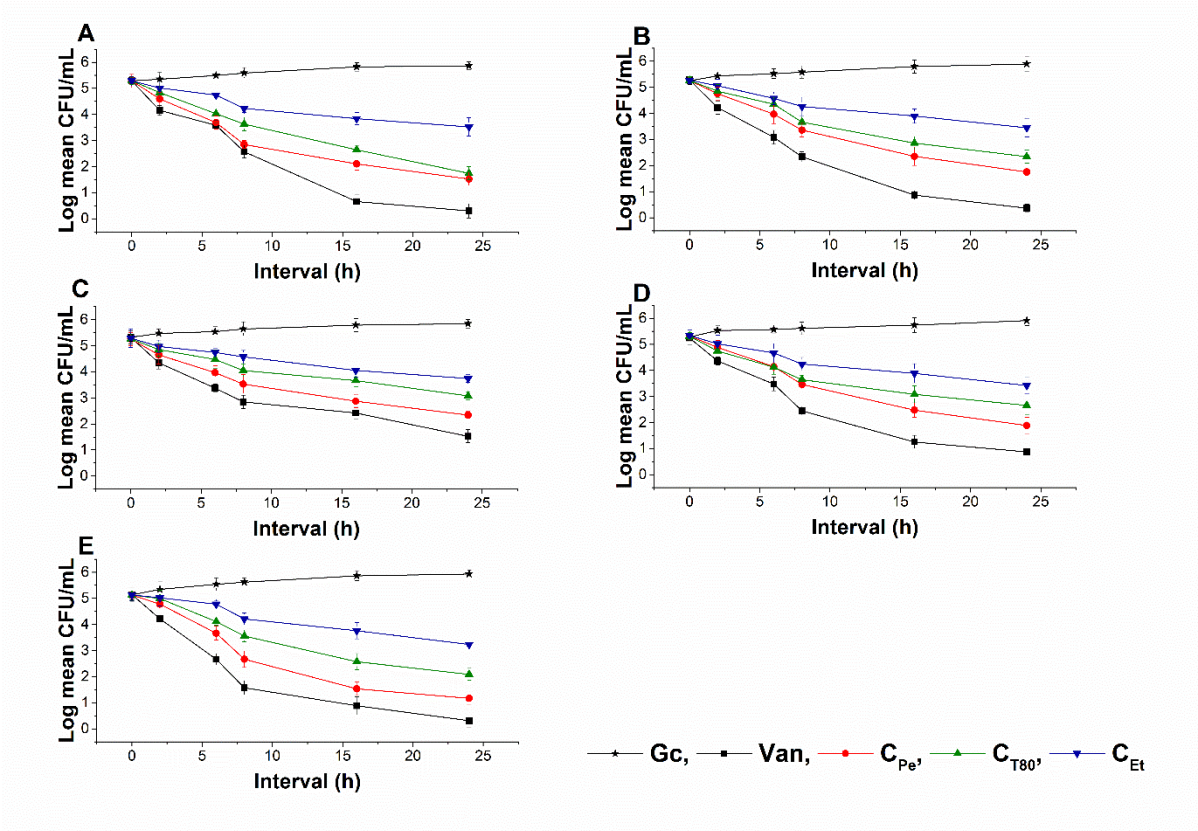


Figure 15. Colony-forming unit (CFU/mL) of C_{Pe}, C_{T80}, and C_{Et} on *E. coli* (A), *S. aureus* (B), *B. subtilis* (C), *P. aeruginosa* (D), and *S. pyogenes* (E). Six independent experiments, each with 3 replicates, compared with Van and Gc as positive and growth controls.

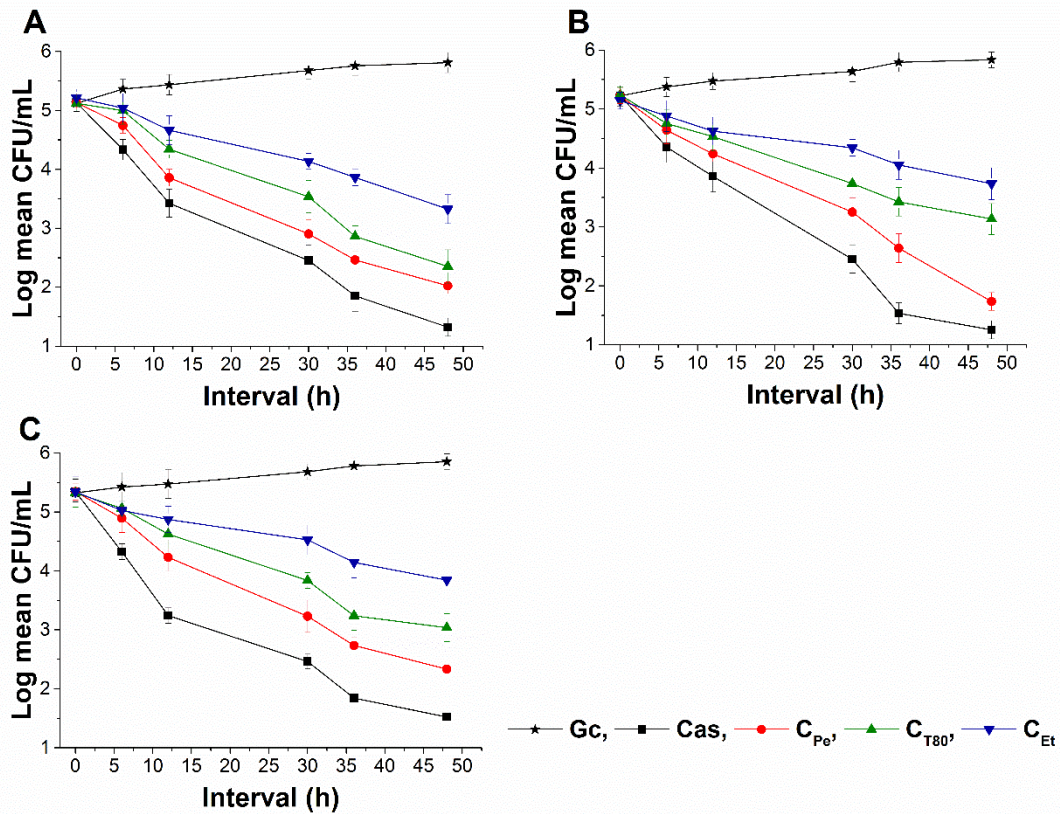


Figure 16. Colony-forming unit (CFU/mL) of C_{Pe}, C_{T80}, and C_{Et} on *S. pombe* (A), *C. albicans* (B), and *C. tropicalis* (C). Six independent experiments, each with 3 replicates, compared with Cas and Gc as positive and growth controls.

9.8. Live/dead cell viability discrimination

The effect of C_{Pe}, C_{T80}, and C_{Et} on the viability of selected bacteria and fungi were tested (Figures 17 and 18). The C_{Pe} decreases the viability of the tested bacteria and fungi with an average viability reduction to $42.36\% \pm 3.74\%$ and $49.62\% \pm 5.25\%$ of mean percentage viability compared to Gc after 16 and 36 h of treatments in bacteria and fungi respectively ($P < 0.01$), whereas C_{T80} and C_{Et} were less effective than C_{Pe} with mean percentage viabilities of $\geq 60\%$ and 70% , respectively.

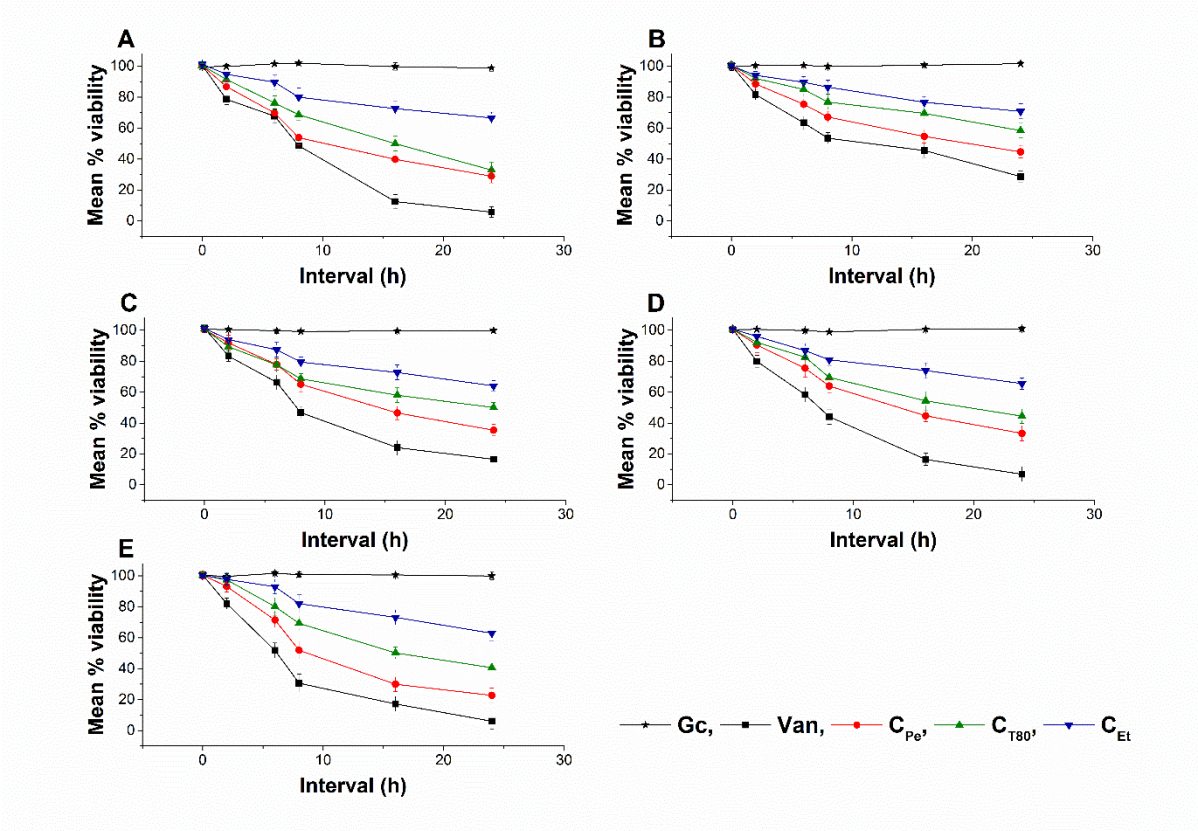


Figure 17. Mean percentage viability of C_{Pe}, C_{T80}, and C_{Et} on *E. coli* (A), *S. aureus* (B), *B. subtilis* (C), *P. aeruginosa* (D), and *S. pyogenes* (E). Six independent experiments, each with 3 replicates, compared with Van and Gc as positive and growth controls.

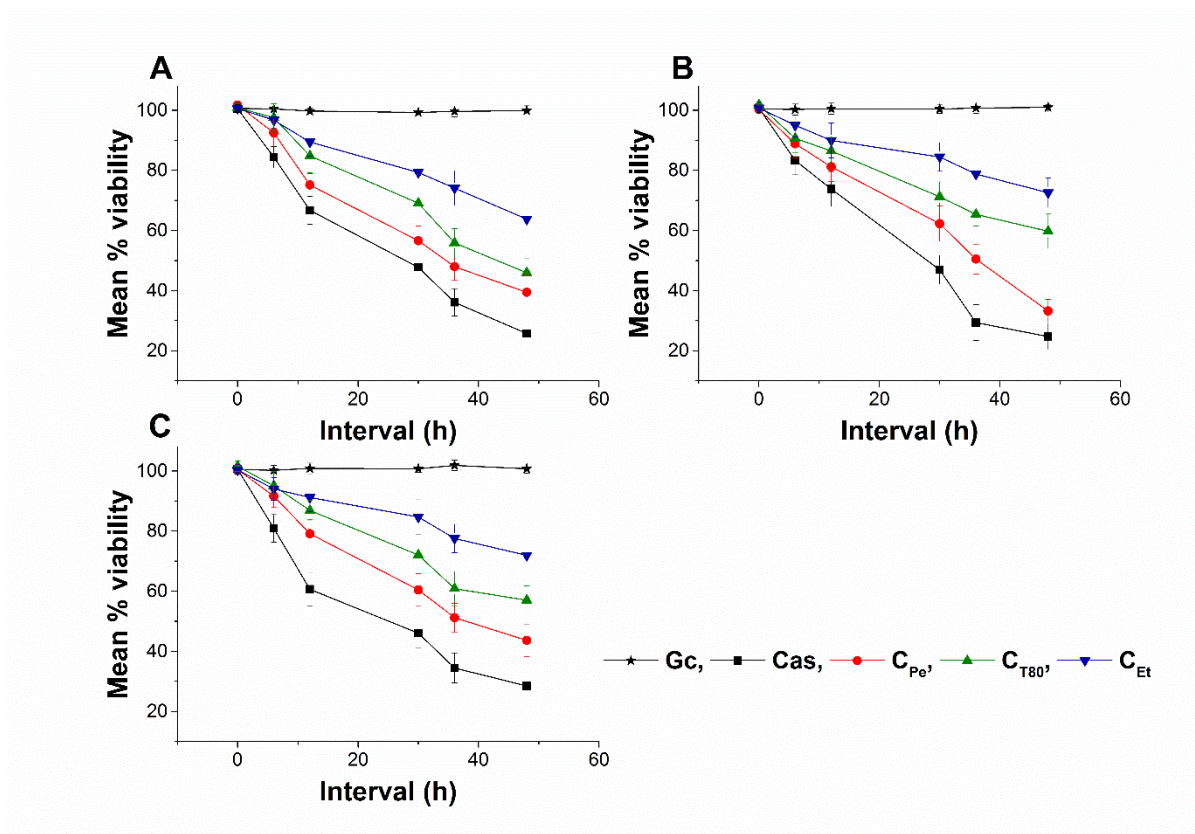


Figure 18. Mean percentage viability of C_{Pe}, C_{T80}, and C_{Et} on *S. pombe* (A), *C. albicans* (B), and *C. tropicalis* (C). Six independent experiments, each with 3 replicates, compared with Cas and Gc as positive and growth controls.

9.9. Interaction study between cell model and different formulations of chamomile EO

This was performed by Barbara Horváth and her colleagues at the Institute of Pharmaceutical Technology and Biopharmacy (Faculty of Pharmacy, University of Pécs). The results of the nanoparticle stability can be found in Ref. [91] and her PhD thesis “Pickering Emulsions in Pharmaceutical Technology” (in preparation). The results obtained in the model experiment show that C_{Pe} is the most effective form for the intracellular delivery of chamomile EO.

10. Results and discussion: antifungal effects of artemisinin and scopoletin

10.1. Antifungal activities (MIC₉₀) of Ar and Sc

Average MIC₉₀ data obtained after 48 h of treatment with Ar and Sc for seven *Candida* spp. are presented in Figure 19. The Ar MIC₉₀ ranged from 21.83 to 142.1 µg/mL, while Sc MIC₉₀ was between 83.43 and 119 µg/mL taking all the tested *Candida* species. The Ar MIC₉₀ values were significantly lower than those of Sc in the case of *C. dubliniensis*, *C. krusei*, and *C. parapsilosis* ($P < 0.01$). *C. glabrata* and *C. tropicalis* were more susceptible to Sc (67.22

and 119 $\mu\text{g/mL}$, respectively). However, in general, Ar expressed higher fungicidal activity than Sc at concentrations in the range of 27 to 80%, less than was seen for Sc. Ar and Sc were effective against the selected *Candida* spp. and their antifungal activities were comparable in every measured parameter to Cs even if the antifungal agent's MIC₉₀ value was much lower than that of our plant-derived test compounds. The susceptibility of selected *Candida* spp. to Ar and Sc has not been reported before. The antifungal activity of Ar and Sc may be attributed to the inhibition of efflux pumps as it was shown for berberine, a natural isoquinoline alkaloid [133]. The measured lower effects of Sc is not known, however, the presence of efflux pump proteins belonging to ABC (ATP Binding Cassette) and MFS (Major Facilitators) superfamily might also be the responsible factors [34,133].

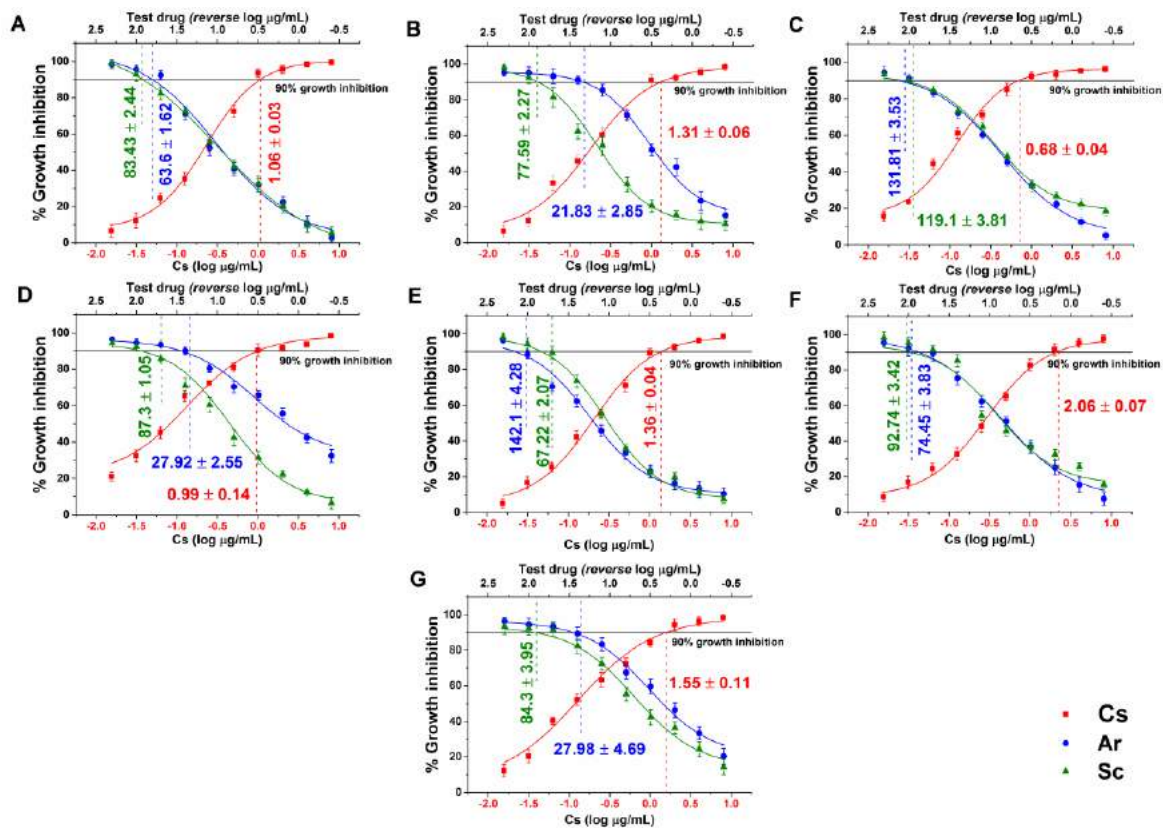


Figure 19. Minimum inhibitory concentrations (MIC₉₀) (mean \pm SD) of artemisinin (Ar) and scopoletin (Sc) on *C. albicans* (A), *C. dubliniensis* (B), *C. tropicalis* (C), *C. krusei* (D), *C. glabrata* (E), *C. guilliermondii* (F) and *C. parapsilosis* (G) species. Six independent experiments, each in three replicates, compared with caspofungin (Cs) as positive control and comparison of Ar and Sc treatments ($\mu\text{g/mL}$).

10.2. Data of minimum effective concentrations (MEC₁₀) for planktonic *Candida* species

Dose-response curves regarding the minimum effective concentrations (MEC₁₀) for Ar and Sc on the selected opportunistic *Candida* species are shown in Figure 20. For Ar the obtained

MEC₁₀ concentrations are as follows: *C. albicans* 84.04 ± 2.92; *C. dubliniensis* 71.26 ± 3.81; *C. tropicalis* 89.95 ± 3.62; *C. krusei* 233.14 ± 4.72; *C. glabrata* 324.97 ± 4.42; *C. guilliermondii* 180.9 ± 3.36; and *C. parapsilosis* 171.86 ± 4.24 (in µg/mL). For Sc the MEC₁₀ values were: *C. albicans* 132.17 ± 4.19; *C. dubliniensis* 132.17 ± 5.08; *C. tropicalis* 134.27 ± 4.66; *C. krusei* 162.01 ± 5.03; *C. glabrata* 215.3897 ± 5.41; *C. guilliermondii* 149.2 ± 5.32, and *C. parapsilosis* 164.7 ± 5.26 (in µg/mL). The curves have expressed a dose-dependent cell survival (CFU count) after 60 minutes of exposure to Ar and Sc. The doses corresponding to MEC₁₀ (meaning an average 90% survival rate of mid-log phased populations, at ~10⁵ CFU/mL) were further used to evaluate their effects on planktonic cells and mature biofilms. Cs, Ar, and Sc have shown an average MEC₁₀ of 6.66 ± 0.14 µg/mL, 165.16 ± 3.87 µg/mL, and 160.84 ± 4.99 µg/mL, respectively for the tested planktonic *Candida* spp. Ar appeared to have the lowest MEC₁₀ in the case of *C. dubliniensis* (21.83 ± 2.85 µg/mL), *C. krusei* (27.92 ± 2.55 µg/mL), and *C. parapsilosis* (27.98 ± 4.69 µg/mL), respectively.

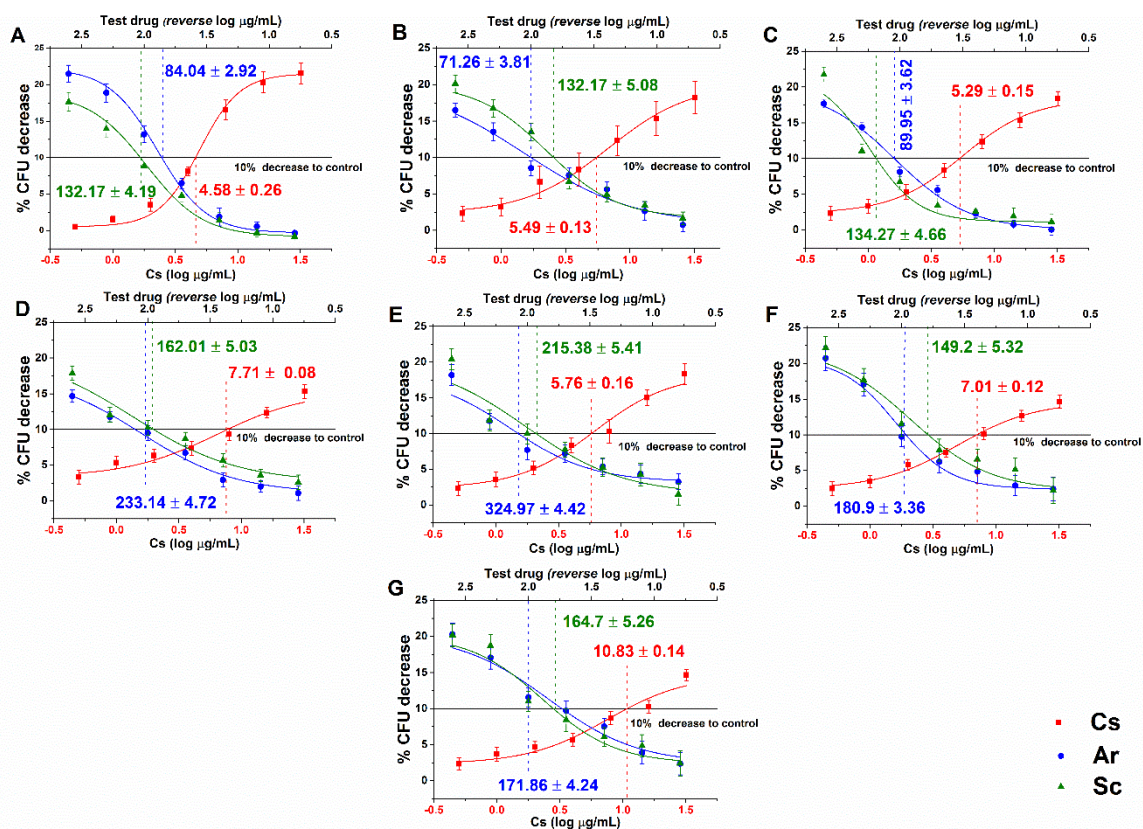


Figure 20. Minimum effective concentrations (MEC₁₀) (mean ± SD) of artemisinin (Ar) and scopoletin (Sc) on *C. albicans* (A), *C. dubliniensis* (B), *C. tropicalis* (C), *C. krusei* (D), *C. glabrata* (E), *C. guilliermondii* (F) and *C. parapsilosis* (G) species. Six independent experiments, each in three replicates, compared with caspofungin (Cs) as positive control and comparison of Ar and Sc treatments (µg/mL).

10.3. Effects on mature biofilms

Variable response to Ar, Sc, and Cs at MEC₁₀ doses has been found. Although no changes in the biomass have been observed in the case of Ar treatments, yet an average $55.04 \pm 9.46\%$ and $46.32 \pm 12.62\%$ reduction in metabolic activities and non-viable cells were seen in the case of *C. albicans*, *C. dubliniensis*, *C. tropicalis*, and *C. glabrata* when compared to growth control ($P < 0.01$). A significant reduction up to an average of 60% in the total biomass on Sc-treated *C. albicans*, *C. dubliniensis* and *C. glabrata* ($P < 0.01$) was found when compared with growth control (Gc) and Cs treatments. However, the data obtained from metabolic activity testing and non-viable cell numbers are invalid for the above species because of the significant biomass loss. *C. guilliermondii* has shown significantly higher resistance to Ar and Sc compared with the other species. The highest cell death (>60%) detected by the double fluorescence staining assay and the reduced metabolic activities (<50%) for *C. krusei*, and *C. parapsilosis* were found in the case of Sc treatment (Figure 21). Our results demonstrated that Ar is more effective in disrupting the preformed complexed, extracellular matrix-covered biofilm structure and killing the sessile (surface-attached) cell population as well compared to Sc at their respective MEC₁₀ concentrations after 24 h exposure. This may be due to the abilities of the sesquiterpenoids to have action on amyloid proteins, which are one of the major building blocks of microbial biofilms [134,134–136]. On the other hand, Sc treatment showed a dramatic decrement in the total biomass including cell loss from the polystyrene surface in case of *C. albicans*, *C. dubliniensis*, and *C. glabrata*, which might be due to the action of coumarin derivatives on the chemical pathways such as quorum sensing resulting in biofilm dispersion [106,137–141]. However, the higher metabolic activities and the less cell death rate found in the case of *C. guilliermondii* indicates the presence of other drug resistance mechanism factors apart from poor drug penetration into *Candida* biofilms. The alternate mechanism might be related to the expression patterns of genes coding for multidrug efflux pumps [142–144]. Moreover, this might be the reason why the surviving cells can adapt to stressful microenvironment by decreasing their metabolic activities [145,146]. Though the adapted cell populations with reduced metabolic activities might survive the toxicity of both test drugs, Ar exerts higher cell-killing properties than those of Sc in the mature biofilm, whereas Sc might cause changes in the biofilm adherence factors to the polystyrene surfaces. The adaptation of *Candida* species under various conditions has already been described [145,147]. The widely accepted crystal violet assay was used to investigate the effects of the tested compounds on the changes of *Candida* biofilm biomass [148]. This chemically basic dye stains fungal cells including

negatively charged surface molecules and polysaccharides in the biofilm extracellular matrix enabling a rapid quantification of biofilm mass before labor-intensive microscope analysis [149]. Although, the poor correlation between biofilm biomass reduction, metabolic activities, and cellular viability remains a major limitation of this method because of the non-selective staining of the biofilm matrix including viable and dead cells as well [68]. Therefore, results obtained from the crystal violet assay must be combined with other multi-parametric techniques such as intracellular ATP, ATP/protein ratio, live/dead cell discrimination and selective visualization of the biomass matrix [150–152]. Our novel multi-parametric evaluations have more precisely highlighted the planktonic fungal susceptibility, killing ability inside the mature biofilm than the classical proliferation assays [153–156].

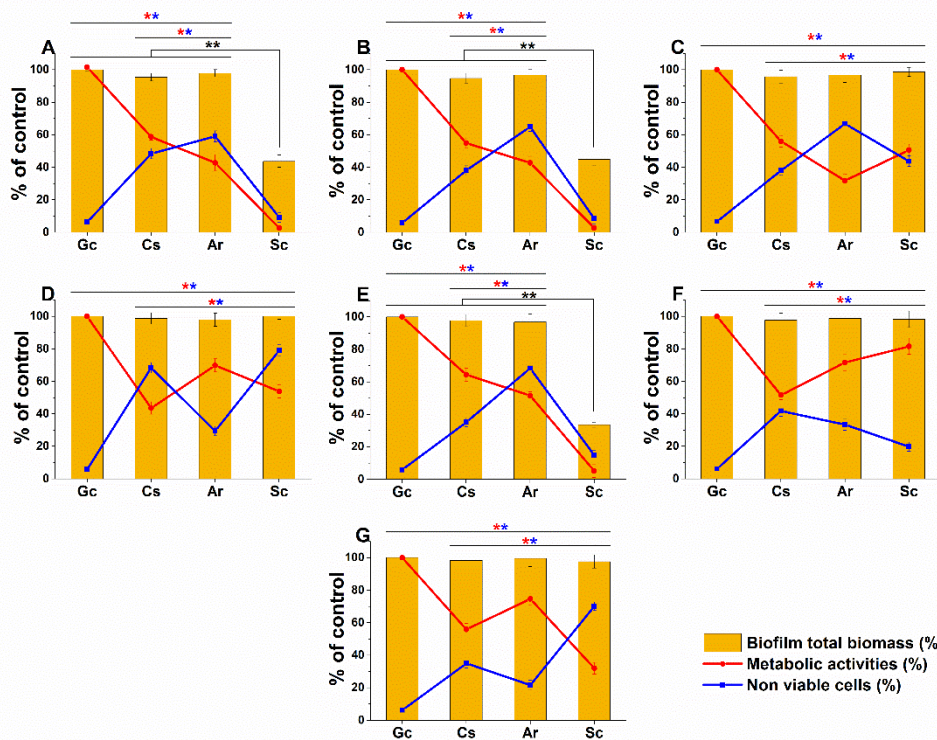


Figure 21. Effects of artemisinin (Ar) and scopoletin (Sc) at their MEC₁₀ concentrations on the metabolic activity, amount of biofilm biomass, and viability of *C. albicans* (A), *C. dubliniensis* (B), *C. tropicalis* (C), *C. krusei* (D), *C. glabrata* (E), *C. guilliermondii* (F), and *C. parapsilosis* (G) cell populations (mean ± SD, n = 6 independent experiments, data were compared with untreated controls (Gc) and with casprofungin (Cs)-treated positive controls. The red (*) and blue (*) asterisks represent a significance value of $P < 0.01$ for the metabolic activity and viability measurements, respectively. Whereas, the black double asterisks (**) highlight the changes in the Sc-treated biofilm biomass when compared to Gc, Cs, and Ar treatments at $P < 0.01$ significance level.

10.4. Live/dead planktonic cell viability discrimination

The long-term effects of Ar and Sc on the viability were tested on mid-log phased planktonic *Candida* spp. as well. Ar and Sc decreased the viability of the tested *Candida* spp. with an average viability reduction of $58.2 \pm 3.5\%$ and $58.6 \pm 4.2\%$ after 8 h, whereas $33.6 \pm 3.9\%$ and $32.2 \pm 3.6\%$ were seen after 16 h when compared with their respective controls. *C. glabrata*, *C. guilliermondii*, and *C. parapsilosis* were found to have less than 30% of viable cells in the presence of Ar and Sc for 16 h at their MEC₁₀ concentrations. Ar and Sc showed a reduction in viability around $\leq 50\%$ after 8 h of treatment on *C. parapsilosis* and *C. krusei* compared with the controls (Figure 22). Based on literature data both Ar and Sc may induce time-dependent cell wall and membrane damage enabling propidium iodide to bind to fungal nucleic acids [157]. The double-stain fluorescence assay showed that the longer the exposure time is, the higher the cellular death rate is found in the Ar and Sc-treated fungal populations. The difference in viability among the examined *Candida* species we think is due to the potential difference in the activity of multidrug efflux pumps among the *Candida* spp. The maintenance of metabolic activities at about 50% even in the presence of low planktonic cell populations indicates the adaption of surviving planktonic cells [142].

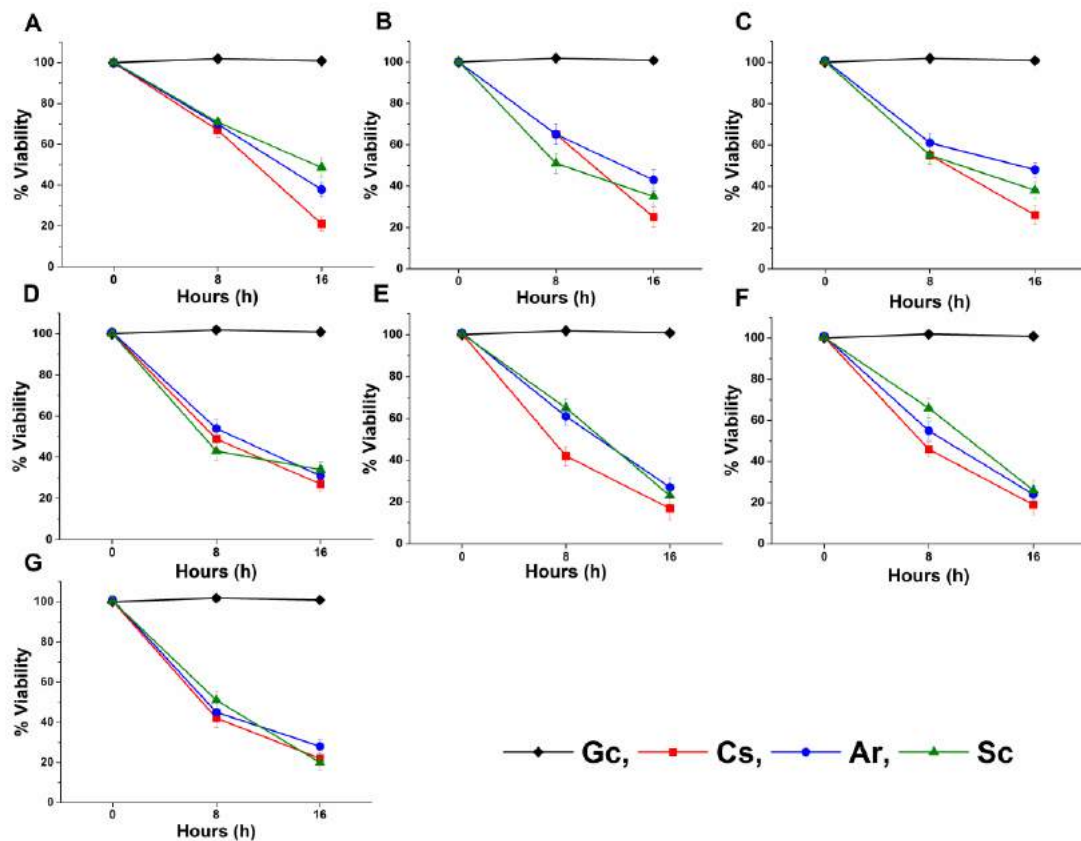


Figure 22. Effects of artemisinin (Ar) and scopoletin (Sc) at their MEC₁₀ concentrations on the viability of planktonic *C. albicans* (A), *C. dubliniensis* (B), *C. tropicalis* (C), *C. krusei* (D), *C. glabrata* (E), *C. guilliermondii* (F), and *C. parapsilosis* (G) species compared with untreated controls (Gc) after 8 and 16 h of treatment (mean ± SD, n = 6 independent experiments, caspofungin (Cs) was used as positive control).

10.5. Effects on metabolic activity and colony formation of planktonic cells

The metabolic activity of the mid-log phased planktonic *Candida* spp. in the presence of Ar and Sc at their MEC₁₀ concentrations was evaluated with resazurin at 0, 8, and 16 h time points (Figure 23). Ar and Sc showed an average reduction in the metabolic activities of tested *Candida* spp. to two-fold after 8 h of treatment followed by three-fold after 16 h of treatment when compared with their respective controls. A less than the two-fold decrease of metabolic activity was found in *C. glabrata*, *C. guilliermondii*, and *C. parapsilosis* planktonic cells in the presence of Ar and Sc after 16 h of treatment.

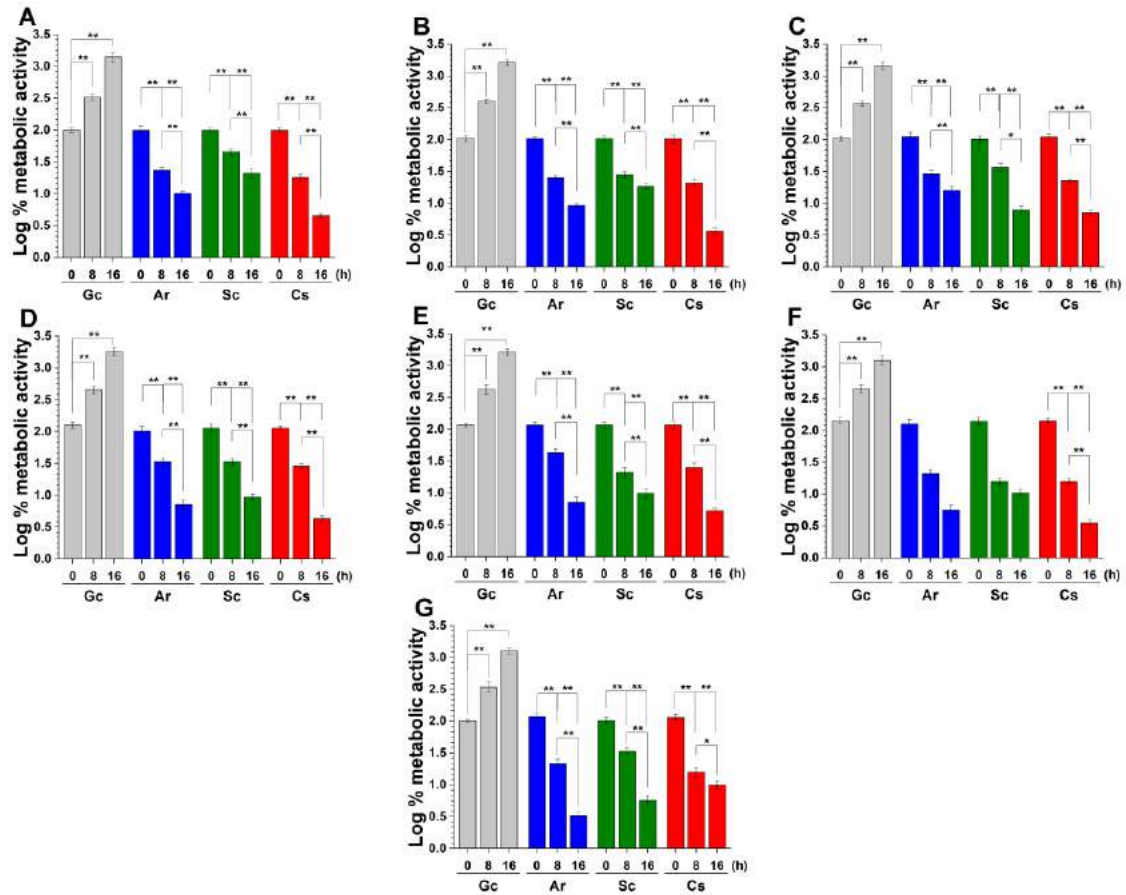


Figure 23. Effects of artemisinin (Ar) and scopoletin (Sc) at their MEC₁₀ concentrations on the metabolic activities of planktonic *C. albicans* (A), *C. dubliniensis* (B), *C. tropicalis* (C), *C. krusei* (D), *C. glabrata* (E), *C. guilliermondii* (F), and *C. parapsilosis* (G) species compared with untreated controls (Gc) and caspofungin (Cs) as positive control after 8 and 16 h of treatment (mean ± SD, n = 6 independent experiments, *P < 0.05 and **P < 0.01).

A significant change in the planktonic cell number reduction compared with the control ($P < 0.01$) was also found after 8 and 16 h of treatment (Figure 24). A prominent reduction of $\leq 50\%$ of the planktonic cell population, when compared to the controls, was found in the case of *C. glabrata*, *C. guilliermondii* and *C. parapsilosis* after 16 h of Ar, Sc, and caspofungin (Cs) exposures. As a limitation of our viability study, it should be mentioned that measuring a single parameter only (e.g., the resazurin assay) does not necessarily reflect total cell viability because cellular ATP levels may change rapidly without significant reduction in intracellular enzyme activities [158].

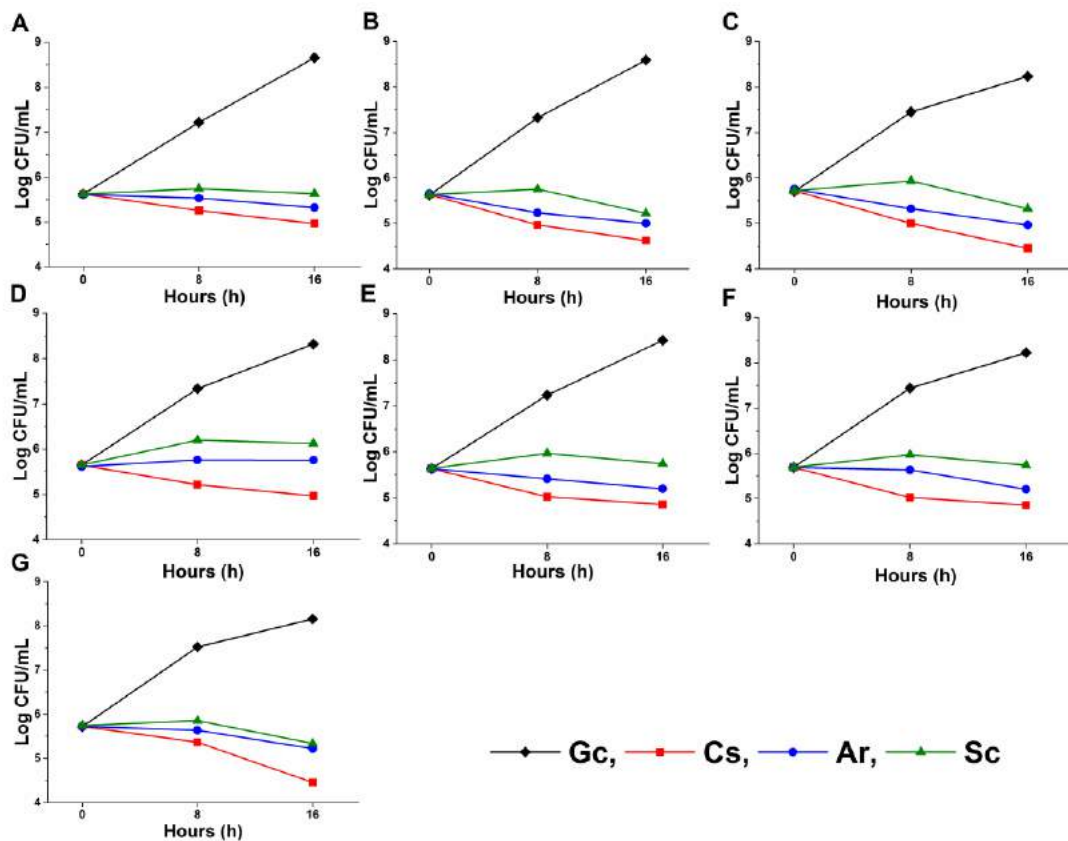


Figure 24. Effects of artemisinin (Ar) and scopoletin (Sc) at their MEC₁₀ concentrations on colony formation of planktonic *C. albicans* (A), *C. dubliniensis* (B), *C. tropicalis* (C), *C. krusei* (D), *C. glabrata* (E), *C. guilliermondii* (F) and *C. parapsilosis* (G) species compared with untreated controls (Gc) after 8 and 16 h of treatment (mean \pm SD, n = 6 independent experiments, caspofungin (Cs) was used as positive control).

10.6. Effects on planktonics' oxidative balance

The effects of Ar and Sc on the induction of the oxidative stress at MEC₁₀ concentrations on respective mid-log phased *Candida* spp. planktonic cell populations are illustrated in Figure 25. Menadione (Me) was used as a positive control. All the test drugs caused significant oxidative stress in the planktonic cells compared with that of the controls ($P < 0.01$). More than 25% and 50% of O₂^{•-} generation was observed in *C. glabrata*, *C. guilliermondii*, and *C. parapsilosis* compared with other tested *Candida* spp. after the treatment with Ar and Sc for 60 minutes. The overall O₂^{•-} generation induced by Ar was found to be $13.4 \pm 1.8\%$ higher than that of Sc. Peroxide generation in *C. glabrata*, *C. guilliermondii*, and *C. parapsilosis* was also found to be higher (an average of 30.2% increment in Ar treatment and 8.4% increment in Sc treatment) compared with the other tested *Candida* spp. An average increment of $64.1 \pm 2.6\%$ was found in oxidative stress induction by Ar when compared to Sc in *Candida* species. In summary, we found that all the tested *Candida* species were susceptible to Ar and Sc

treatments in favor of Ar vs. Sc. Data presented in this study suggest the induction of apoptosis-like processes in the tested *Candida* spp. that may be due to the accumulation of reactive oxygen species (ROS) that induce or regulate the apoptosis in yeasts [145,159]. Using the superoxide and peroxide radicals' fluorescent assays, we showed the accumulation of reactive oxygen species, which are the indicators of lipid damage [98]. It has been postulated that Ar and Sc affect ergosterol synthesis [34,160]. Ergosterol, apart from maintenance and regulation of structural and functional integrity of the membrane, inhibits lipid peroxidation [161]. This can also facilitate the permeability of the cell membrane and incorporation of propidium iodide through the compromised membranes into the cells. Further characterization of the effects of Ar and Sc on the levels of superoxide dismutase and catalase at increased ROS levels must be assessed [160,162]. Moreover, Ar also plays an important role in the electron transport chain by overexpressing nuclear distribution protein nude homolog 1 (NDE₁) that is responsible for encoding mitochondrial NADH dehydrogenases causing sensitivity to Ar followed by membrane disruption resulting in mitochondrial dysfunction by the higher free radical generation when compared to Sc [163,164]. Based on the results of the tested *Candida* planktonic cells, we found that the MEC₁₀ concentrations of our treating compounds are more effective to initiate oxidative imbalance and reducing metabolic activities followed by the death of the planktonic cells when compared to the effects on preformed mature biofilms, which have shown variable results including cell death, biomass loss, and resistance. The reason behind the resistance to the MEC₁₀ concentrations may be due to the extracellular matrix acting as a diffusion barrier [140,165,166] or the up-regulation of the genes coding the efflux pumps [167–169]. Previous studies also reported that the planktonic cells released from the biofilms express subtle genetic changes for producing resistant phenotypes. As a consequence, the resistant new population may form biofilms with an altered phenotype that might be responsible for the hostility in some of the tested *Candida* species [170].

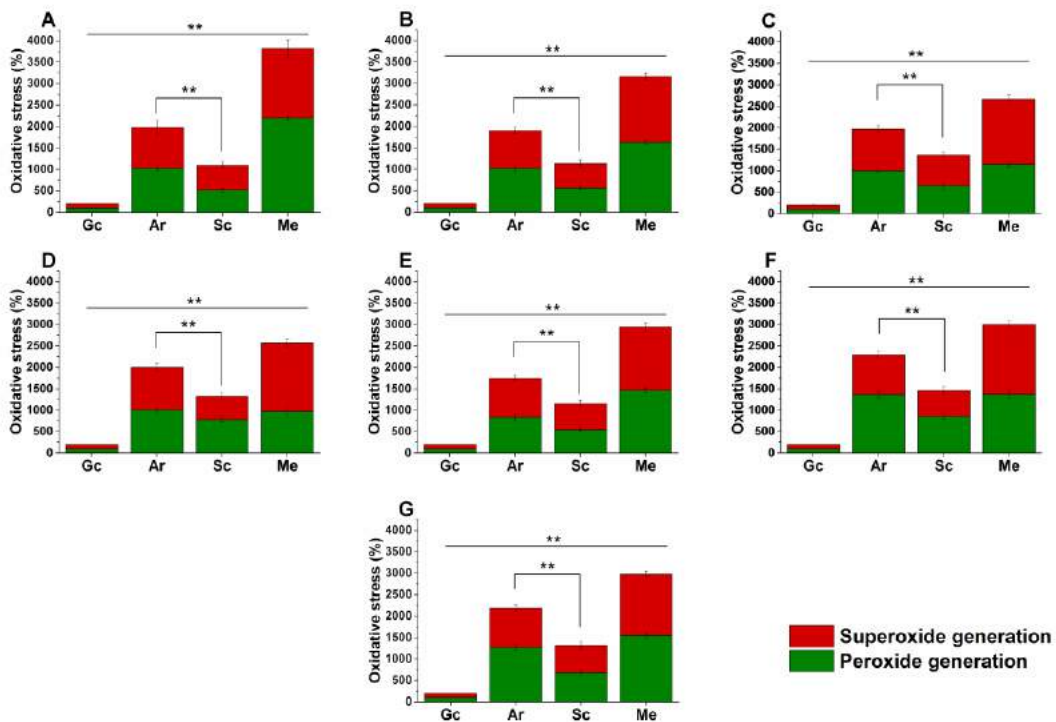


Figure 25. Effects of artemisinin (Ar) and scopoletin (Sc) at their MEC₁₀ levels on peroxide (O₂²⁻) and superoxide anion (O₂^{•-}) generation in planktonic *C. albicans* (A), *C. dubliniensis* (B), *C. tropicalis* (C), *C. krusei* (D), *C. glabrata* (E), *C. guilliermondii* (F), and *C. parapsilosis* (G) species compared with untreated (Gc), with menadione (Me)-treated controls and comparison of Ar and Sc treatments (mean ± SD, n = 6 independent experiments, ** $P < 0.01$).

11. Results and discussion: Pickering-Artemisia essential oil experiments

11.1. Effect of Artemisia essential oil and its components

The amount of the essential oil obtained by steam distillation was 3% w/w of plant powder. Our gas chromatography-mass spectrometry-flame ionization detection (GC-MS-FID) analyses (Supplementary Figures S9-S14 and Table S2) have documented β-pinene (1.25%), artemisia ketone (4.43%), yomogi alcohol (1.29%), artemisia alcohol (1.68%), trans-pinocarveol (7.55%), pinocarvone (3.22%), camphor (7.06%), terpinen-4-ol (1.75%), α-copaene (2.75%), caryophyllene (5.26%), β-farnesene (4.8%), β-selinene (12.27%), spathulenol (1.75%), caryophyllene oxide (8.64%), eudesma-4(15),11-dien-5-ol (1.06%) and mustakone (1.27%) as the major components of the essential oil of *Artemisia annua* L. essential oil, that has been used throughout the experiments.

11.2. Preparation and stability studies of O/W type Pickering nanoemulsions

This was performed by Barbara Horváth and her colleagues at the Institute of Pharmaceutical Technology and Biopharmacy (Faculty of Pharmacy, University of Pécs). The results of the nanoparticle stability can be found in Ref. [21] and her PhD thesis “Pickering Emulsions in Pharmaceutical Technology” (in preparation). The *Artemisia annua* EO Pickering nanoemulsions (AEP) were more stable than the corresponding AET and AEE.

11.3. In-vitro diffusion study of Artemisia EO (AE) formulations

This was performed by Barbara Horváth and her colleagues at the Institute of Pharmaceutical Technology and Biopharmacy (Faculty of Pharmacy, University of Pécs). The results of the in-vitro diffusion study can be found in Ref. [21] and her PhD thesis “Pickering Emulsions in Pharmaceutical Technology” (in preparation). The results obtained from model experiments have highlighted that the Pickering nanoemulsion of the AE oil is the most effective form for the intracellular delivery and the transport of EO through biofilms when compared to AET and AEE.

11.4. Interaction studies with unilamellar liposomes as cellular models

This was performed by Barbara Horváth and her colleagues at the Institute of Pharmaceutical Technology and Biopharmacy (Faculty of Pharmacy, University of Pécs). The results of the interaction studies with unilamellar liposomes can be found in Ref. [21] and her PhD thesis “Pickering Emulsions in Pharmaceutical Technology” (in preparation). The results of the model system suggests that the AEP facilitates the penetration of *Artemisia essential* through the biofilm and the planktonic cells as well.

11.5. Antibacterial and antifungal activities of the prepared emulsions

The effects of the *Artemisia* Pickering nanoemulsion, conventional emulsion, and essential oil in ethanol on Gram-positive and Gram-negative bacteria, and on opportunistic fungi were studied. The AEP showed acceptable antibacterial and antifungal activities (MIC₉₀) on *E. coli* PMC 201 (1.68 ± 0.72 µg/mL), *S. aureus* ATCC 29213 (1.62 ± 0.37 µg/mL), *B. subtilis* SZMC 0209 (1.42 ± 0.64 µg/mL), *P. aeruginosa* PMC 103 (1.46 ± 0.22 µg/mL), *S. pyogenes* SZMC 0119 (3.15 ± 0.16 µg/mL), *S. pombe* ATCC 38366 (2.01 ± 0.46 µg/mL), *C. albicans* SZMC 1372 (3.62 ± 0.65 µg/mL), *C. tropicalis* SZMC 1368 (4.29 ± 0.82 µg/mL), *C. dubliniensis* SZMC 1470 (3.63 ± 0.57 µg/mL) and *C. krusei* SZMC 0779 (3.79 ± 0.57 µg/mL), respectively, when compared to AET ($P < 0.01$). The Pickering *Artemisia annua* EO nanoemulsion (AEP)

showed higher antimicrobial activity at an average of twelve-fold less concentration when compared to the free essential oil in ethanol (AEE). The comparative dose-response curves are shown in Figures 26 and 27 for bacteria and fungi, respectively.

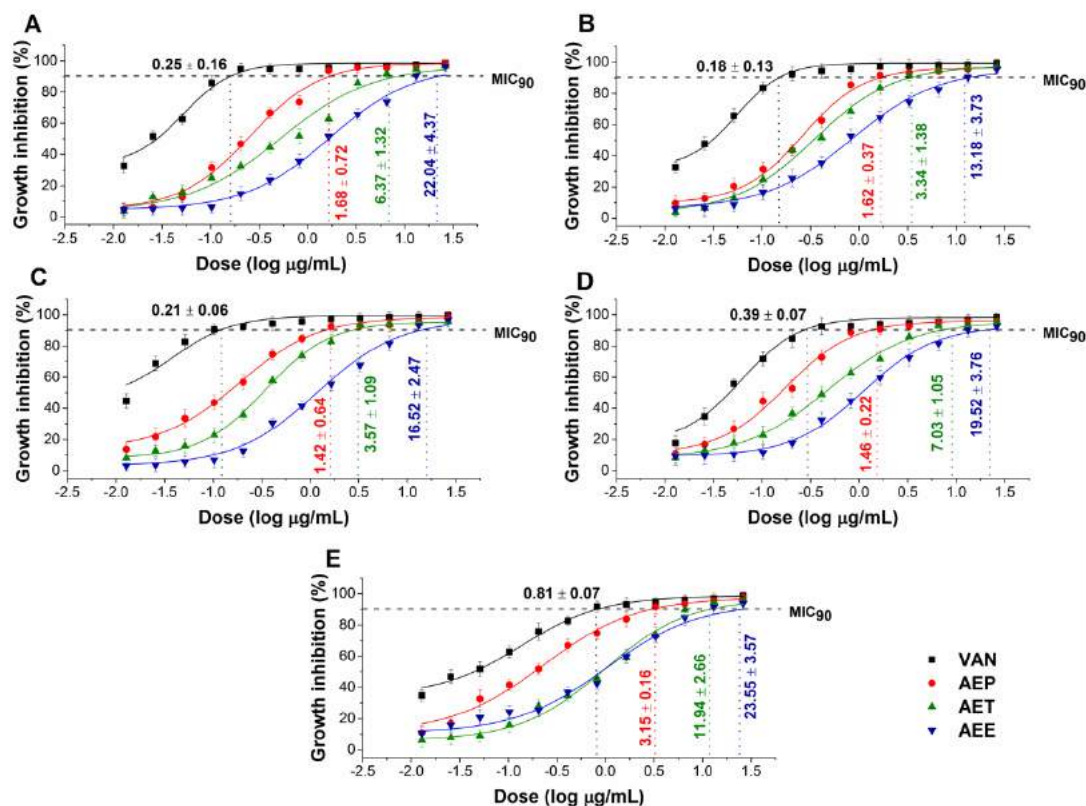


Figure 26. Minimum inhibitory concentration (MIC₉₀) of AEP, AET, AEE, and vancomycin (VAN) in µg/mL on *E. coli* (A), *S. aureus* (B), *B. subtilis* (C), *P. aeruginosa* (D), and *S. pyogenes* (E). Six independent experiments each with three technical replicates were performed (mean ± SD).

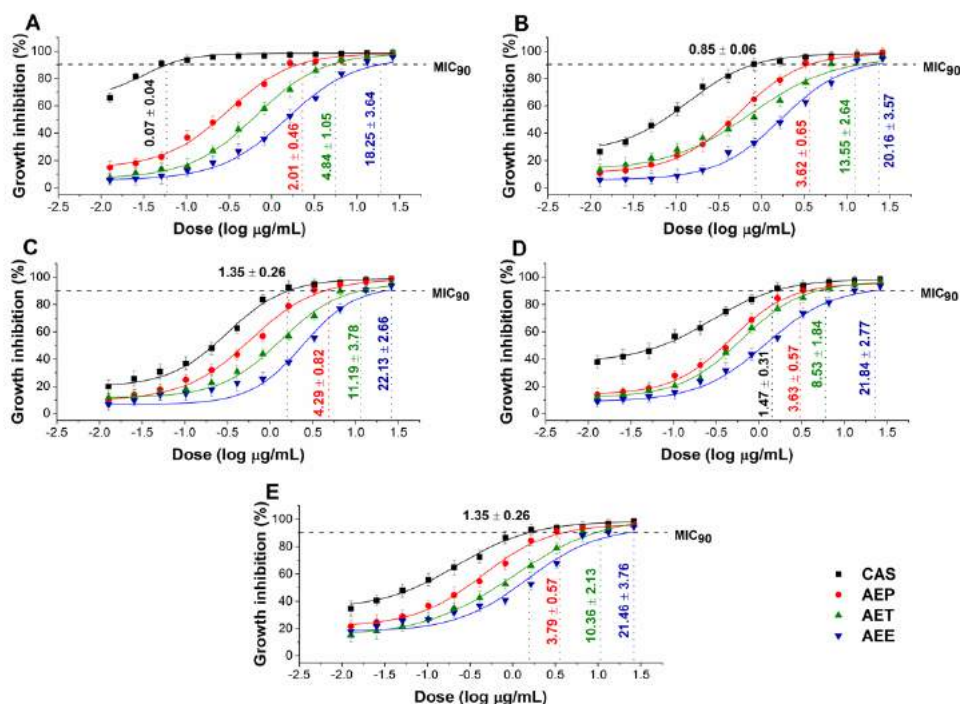


Figure 27. Minimum inhibitory concentration (MIC₉₀) of AEP, AET, AEE, and caspofungin (CAS) in µg/mL on *S. pombe* (A), *C. albicans* (B), *C. tropicalis* (C), *C. dubliniensis* (D) and *C. krusei* (E). Six independent experiments each with three technical replicates were performed (mean ± SD).

11.6. Effects of the minimum effective concentration (MEC₁₀) on planktonic microbial cells

The minimum effective concentration (MEC₁₀) of the *Artemisia* Pickering nanoemulsion, conventional emulsion, and essential oil in ethanol on Gram-positive and Gram-negative bacteria, and on opportunistic fungi are shown in Figures 28 and 29. For the AEP the MEC₁₀ concentrations are as follows: *E. coli* (4.05 ± 0.69 µg/mL), *S. aureus* (4.79 ± 0.84 µg/mL), *B. subtilis* (5.54 ± 1.05 µg/mL), *P. aeruginosa* (6.39 ± 0.95 µg/mL), *S. pyogenes* (9.25 ± 1.03 µg/mL), *S. pombe* (7.02 ± 1.55 µg/mL), *C. albicans* (7.12 ± 2.11 µg/mL), *C. tropicalis* (13.79 ± 2.74 µg/mL), *C. dubliniensis* (10.49 ± 3.77 µg/mL) and *C. krusei* (11.67 ± 3.62 µg/mL). The curves expressed a dose-dependent cell survival rate (by CFU quantification) after 60 minutes exposure to AEP, AET, and AEE. The doses corresponding to MEC₁₀ (average 90% survival rate of the ~10⁵ CFU/mL, mid-log phased cell population) were then used in further study on planktonic cells and on mature biofilms.

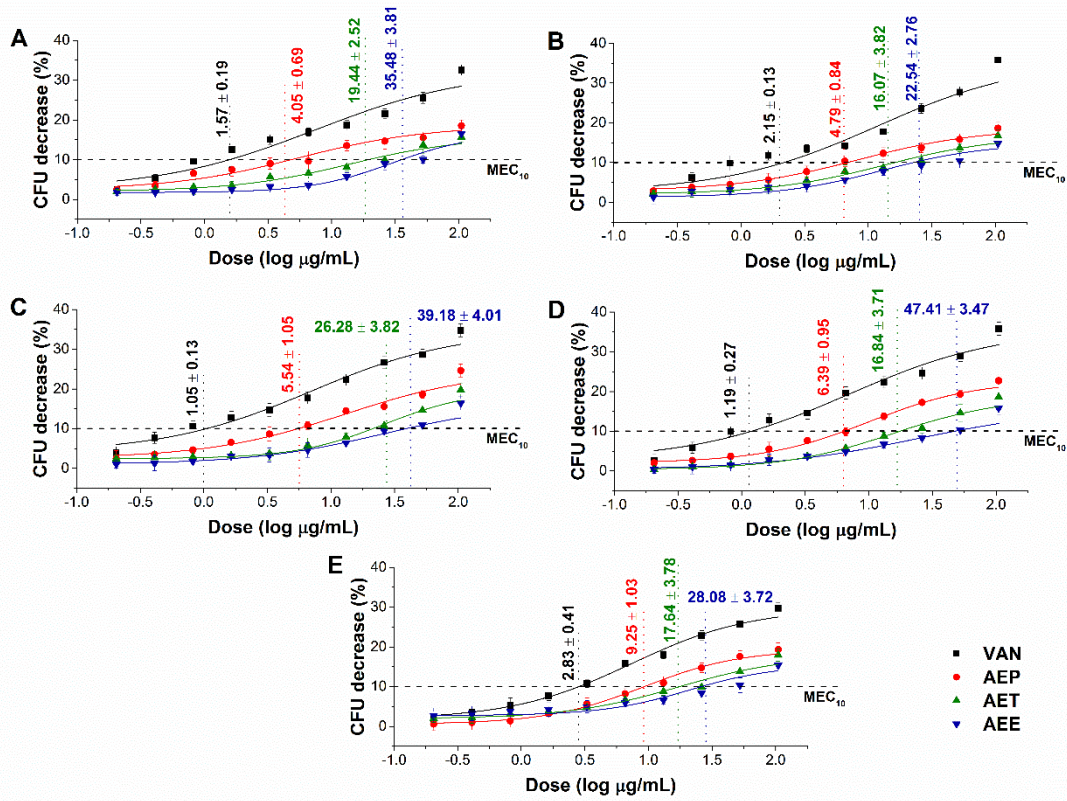


Figure 28. Minimum effective concentration (MEC₁₀) of AEP, AET, and AEE (µg/mL) on *E. coli* (A), *S. aureus* (B), *B. subtilis* (C), *P. aeruginosa* (D), and *S. pyogenes* (E). Six independent experiments, each with three technical replicates, compared to vancomycin (VAN) were considered.

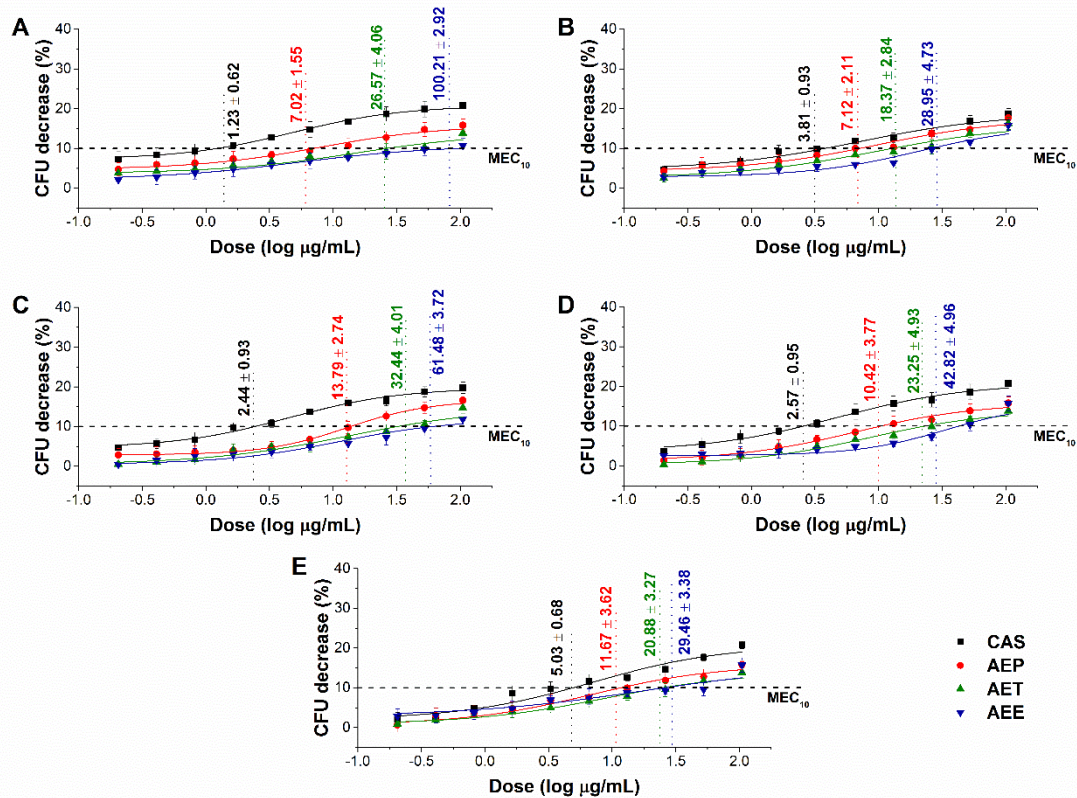


Figure 29. Minimum effective concentration (MEC₁₀) of AEP, AET, and AEE (µg/mL) on *S. pombe* (A), *C. albicans* (B), *C. tropicalis* (C), *C. dubliniensis* (D) and *C. krusei* (E). Six independent experiments, each with three technical replicates, compared to caspofungin (CAS) were considered.

11.7. Effects on the microbial oxidative balance

Various reactive oxygen species (ROS) production and accumulation in the bacterial and fungal cells initiate oxidative stress followed by cellular structural damages and apoptosis induction [159,171]. The oxidative stress generation after 60 minutes of treatment has been investigated (Figures 30 and 31). Data expressed as % of control are as follows: combined ROS detected by DCFDA ($1235.46 \pm 133.63\%$), peroxide by DHR 123 ($1053.74 \pm 146.26\%$) and superoxide by DHE ($1153.84 \pm 142.67\%$) were the highest in the case of *P. aeruginosa*. The AEP caused an effective increase in the combined ROS, peroxide, and superoxide generations as well, in both Gram-positive and negative bacteria and fungi when compared to AET and AEE ($P < 0.01$). The AEE has generated a three to four-fold increment in oxidative stress compared to the growth control (GC), which was the lowest among all treatments.

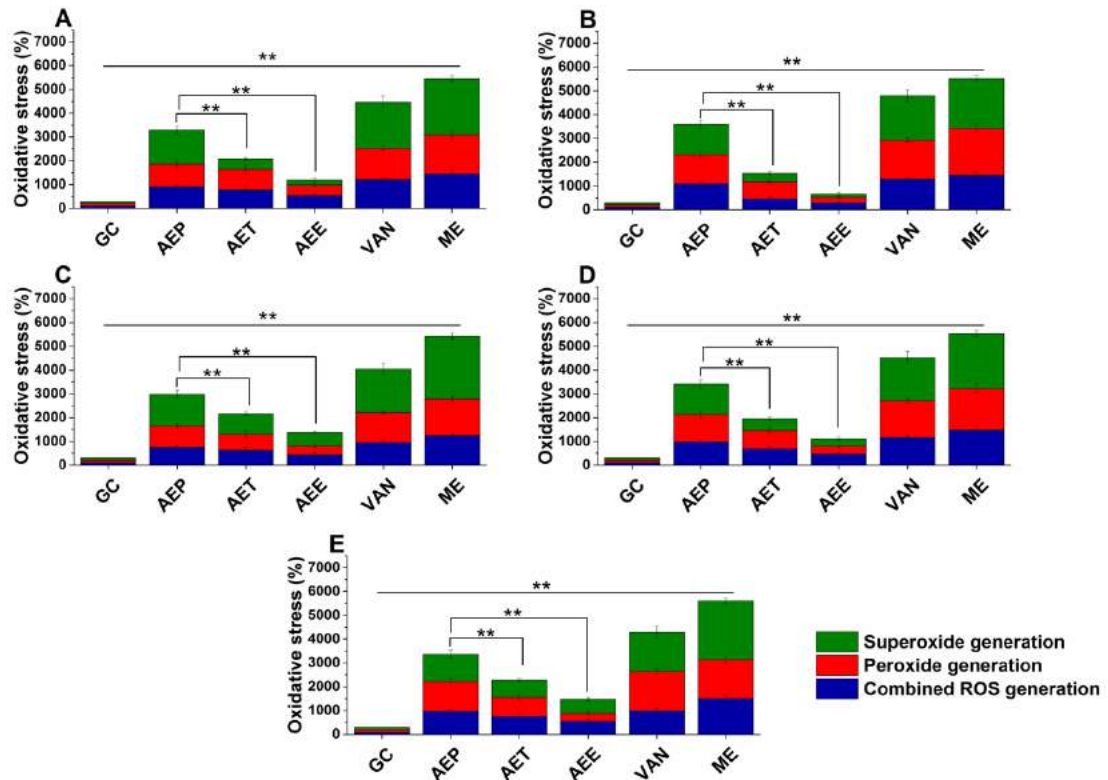


Figure 30. Percentage oxidative stress generation by AEP, AET, AEE, and VAN on *E. coli* (A), *S. aureus* (B), *B. subtilis* (C), *P. aeruginosa* (D), and *S. pyogenes* (E) at their respective MEC₁₀ concentrations after a one-hour treatment. All results were compared to those for menadione (ME) and growth control (GC). The three formulations were evaluated separately as well. Six independent experiments, each with three technical replicates (** $P < 0.01$).

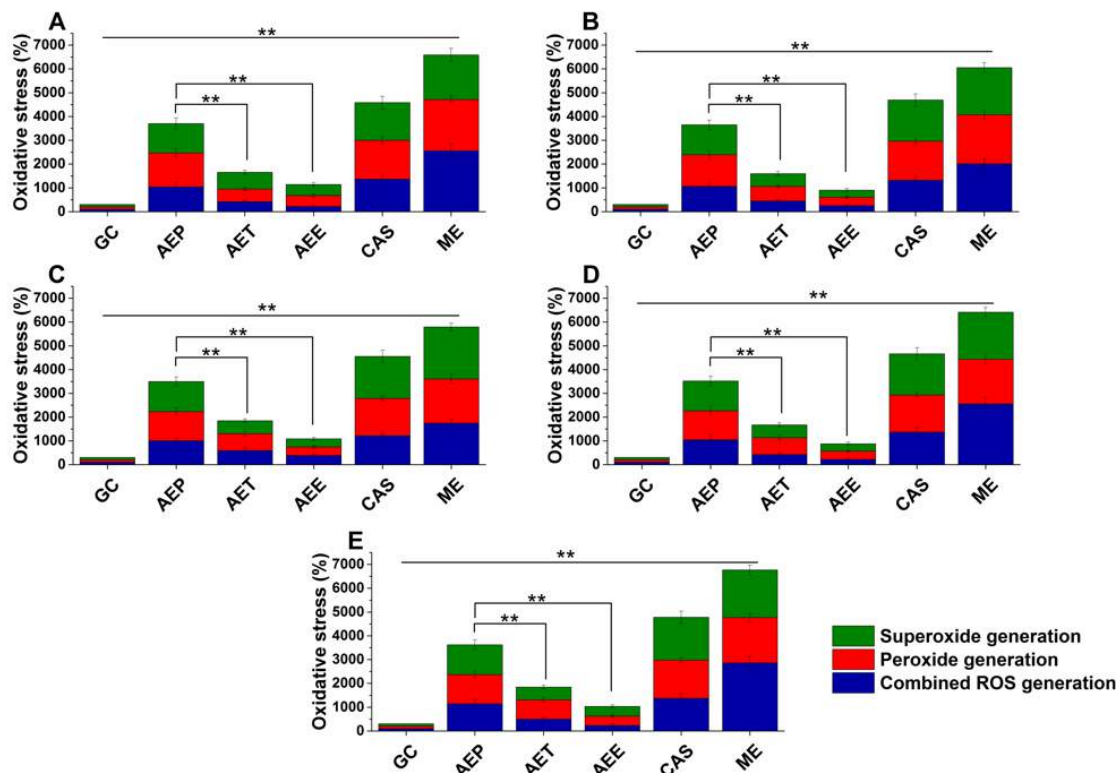


Figure 31. Percentage oxidative stress generation by AEP, AET, AEE, and CAS on *S. pombe* (A), *C. albicans* (B), *C. tropicalis* (C), *C. dubliniensis* (D) and *C. krusei* (E) at their respective MEC₁₀ concentrations and after a one-hour treatment. All results were compared to those for menadione (ME) and growth control (GC). The three formulations were evaluated separately as well. Six independent experiments, each with three technical replicates (** $P < 0.01$).

11.8. Effects on the microbial planktonics' behavior

11.8.1. Colony formation changes

The changes in the colony formation of the microbial cells were followed using a time-related (kinetic) means of investigating the quantity of the living population after a definite time interval under different samples' MEC₁₀ concentrations (Figures 32 and 33). A significant 50% reduction in the bacterial and fungal cell survivability after 6 and 18 h, respectively, was observed in the case of the AEP exposure when compared to that of AET and AEE ($P < 0.01$). AEE was the least effective among all other treatments.

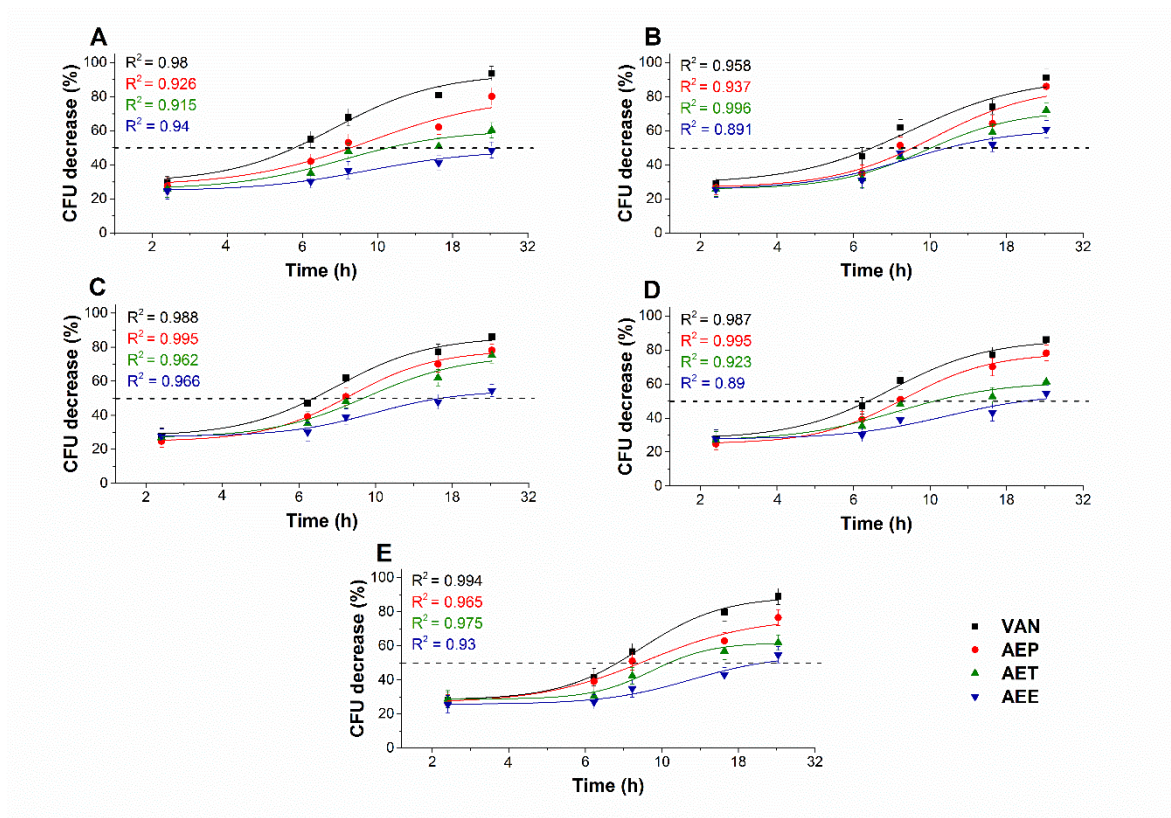


Figure 32. Effects of AEP, AET, and AEE at their MEC₁₀ concentrations on the mean percentage colony-forming unit (CFU/mL) decrement of the planktonic *E. coli* (A), *S. aureus* (B), *B. subtilis* (C), *P. aeruginosa* (D), and *S. pyogenes* (E) compared to their respective 0 h samples and vancomycin (VAN) standard antimicrobial controls after 2, 6, 8, 16 and 24 h of treatment (mean ± SD, *n* = 6 independent experiments each with three technical replicates).

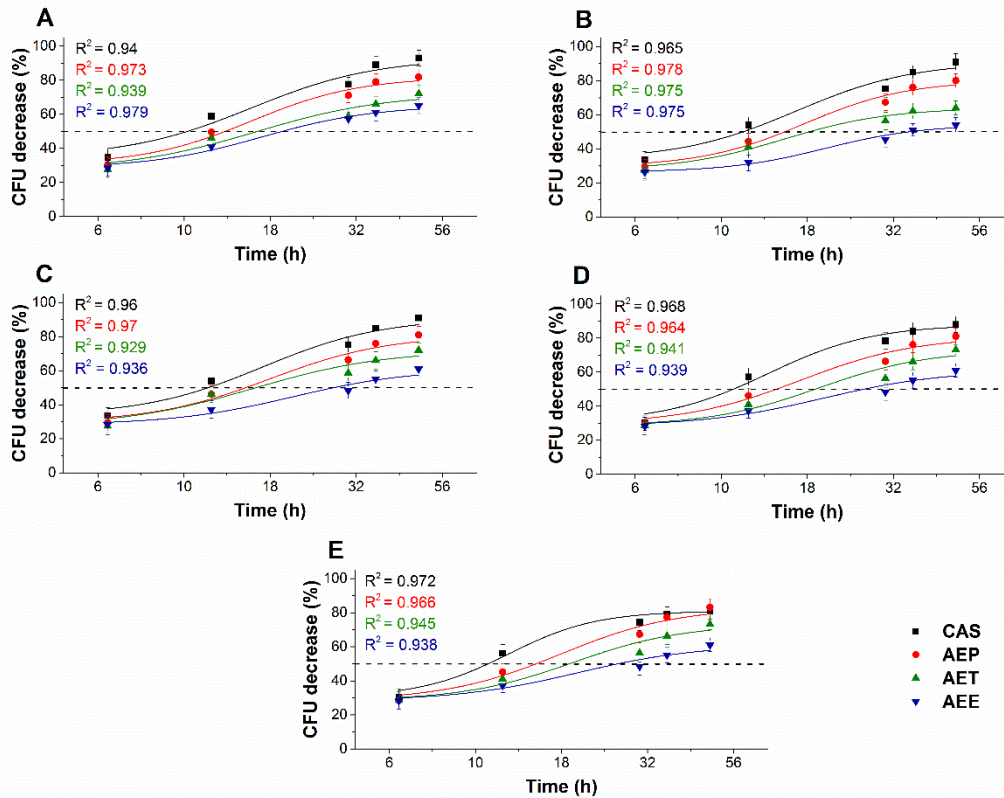


Figure 33. Effects of AEP, AET, and AEE at their MEC₁₀ concentrations on the metabolic activities of the mean percentage colony-forming unit (CFU/mL) decrement of the planktonic *S. pombe* (A), *C. albicans* (B), *C. tropicalis* (C), *C. dubliniensis* (D) and *C. krusei* (E) compared to their respective 0 h samples and caspofungin (CAS) standard antimicrobial controls after 6, 12, 30, 36 and 48 h of treatment (mean ± SD, *n* = 6 independent experiments each with three technical replicates).

11.8.2. Variations in the intracellular ATP to total protein content ratios

The energy depletive effects of AEP, AET, and AEE at their MEC₁₀ concentrations on the selected Gram-positive and -negative bacteria, and fungi were studied (Figures 34 and 35). Although no significant change in the total protein content (TP) over time in the planktonic cells was observed, a significant $60.37 \pm 5.35\%$ decrement in the ATP/TP ratio was found in the case of the AEP treated samples when compared to the 0 h samples ($P < 0.01$). Both AET and AEE have shown a decrease up to an average of 40% in the ATP/TP ratio in the cases of bacteria and fungi when compared to the 0 h samples.

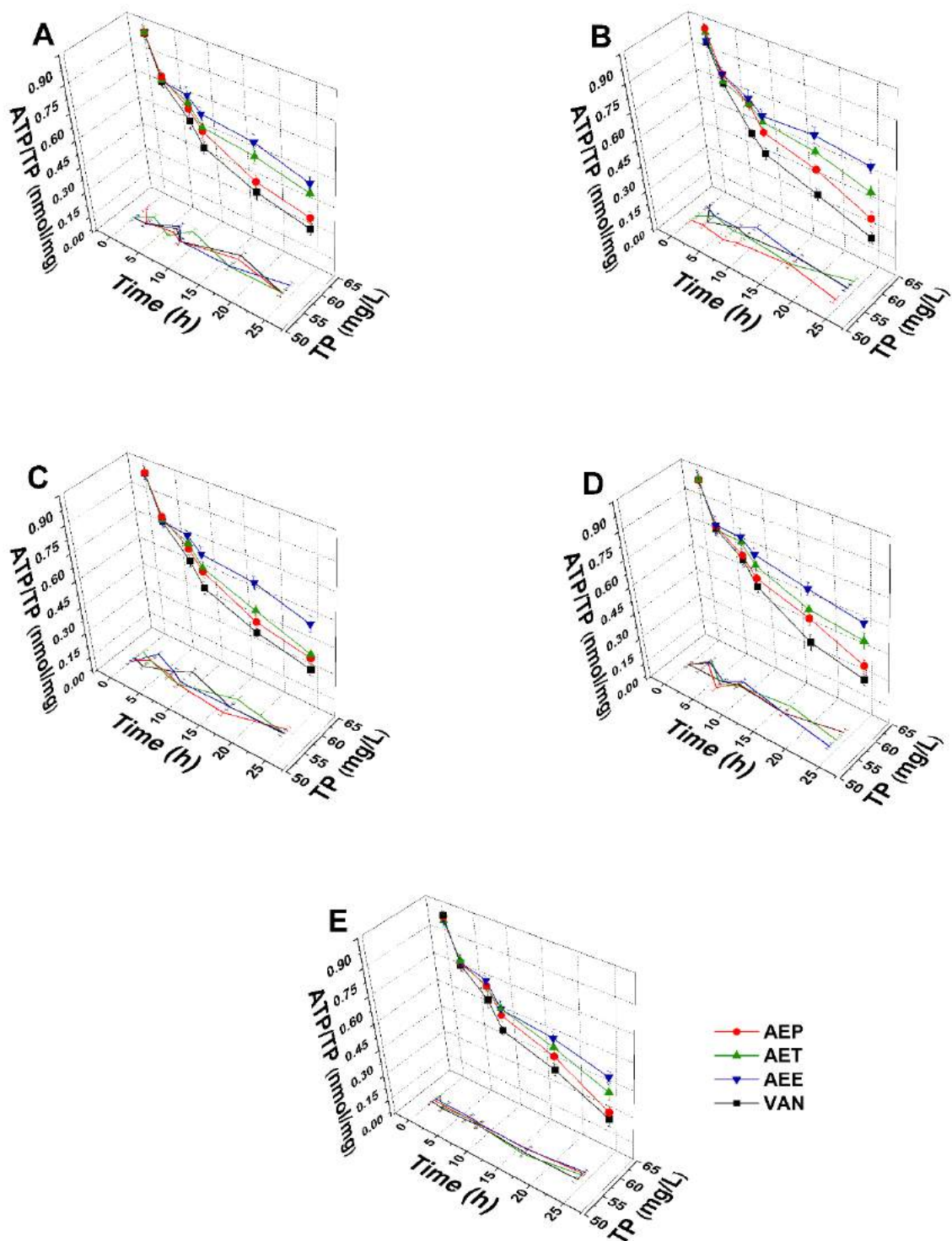


Figure 34. Effects of AEP, AET and AEE at their MEC₁₀ concentrations on the total protein content (TP) and intracellular ATP/TP ratio of the planktonic *E. coli* (A), *S. aureus* (B), *B. subtilis* (C), *P. aeruginosa* (D), and *S. pyogenes* (E) compared to their respective 0 h samples and vancomycin (VAN) standard antimicrobial controls after 2, 6, 8, 16 and 24 h of treatment (mean ± SD, *n* = 6 independent experiments each with three technical replicates).

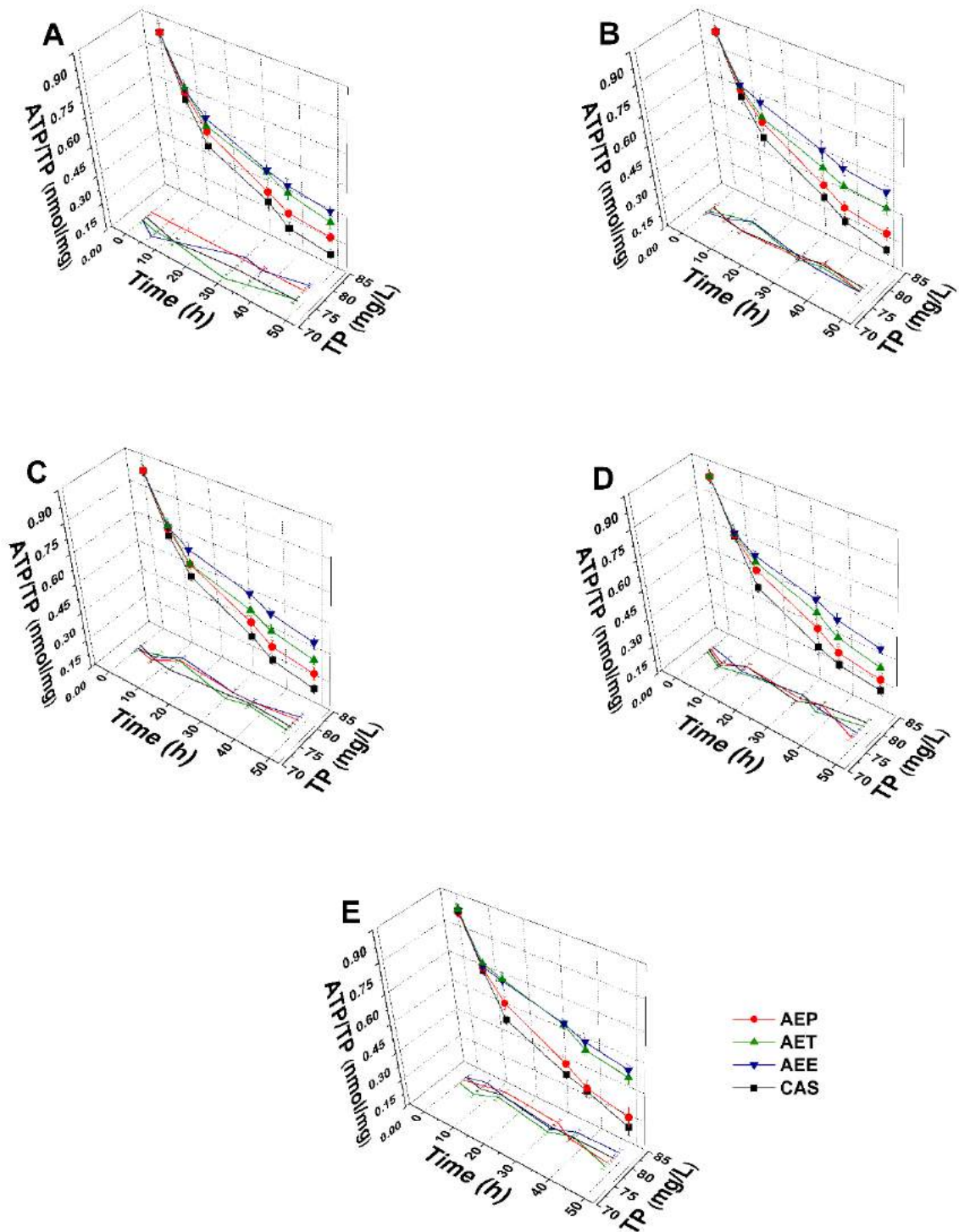


Figure 35. Effects of AEP, AET, and AEE at their MEC₁₀ concentrations on the total protein content (TP) and intracellular ATP/TP ratio of the planktonic *S. pombe* (A), *C. albicans* (B), *C. tropicalis* (C), *C. dubliniensis* (D) and *C. krusei* (E) compared to their respective 0 h samples and caspofungin (CAS) standard antimicrobial controls after 6, 12, 30, 36 and 48 h of treatment (mean ± SD, *n* = 6 independent experiments each with three technical replicates).

11.8.3. Effects on microbial cell viability and metabolic activity

The multi-parametric cytotoxicity assay has been performed to evaluate the viability of the microbial cells using SYBR Green I/PI live-dead cell technique while the resazurin fluorometric method was applied for reflecting the metabolic changes caused by the test samples. The cytotoxic effects of AEP, AET, and AEE on the viability (Figures 36 and 37) and the metabolic activity (Figures 43 and 44) of the selected bacteria and fungi were evaluated. The 50% reduction in the viable cell population was reached at an average of 9.9 ± 0.71 h and 17.09 ± 0.45 h in the case of the Gram-positive and -negative bacteria, and fungi under AEP exposure. A delayed effect at an average of 9.74 ± 1.65 h was observed in the case of AET to initiate a 50% mean non-viability in the microbial populations when compared to AEP ($P < 0.01$). The AEE has shown the slowest induction of microbial non-viability with a delay of 20.63 ± 3.73 h compared to AEP ($P < 0.01$). A significant 50% decrement in the metabolic activity was observed in the case AEP treated bacteria and fungi at an average of 10.63 ± 0.55 h and 26.35 ± 0.36 h, respectively (Figures 38 and 39). The AET treatment showed an average of 7.42 ± 2.63 h delay in reducing metabolic activity by 50% when compared to AEP treated samples ($P < 0.01$). No significant decrease in the metabolic activity was found in the case of the AEE treated fungal samples.

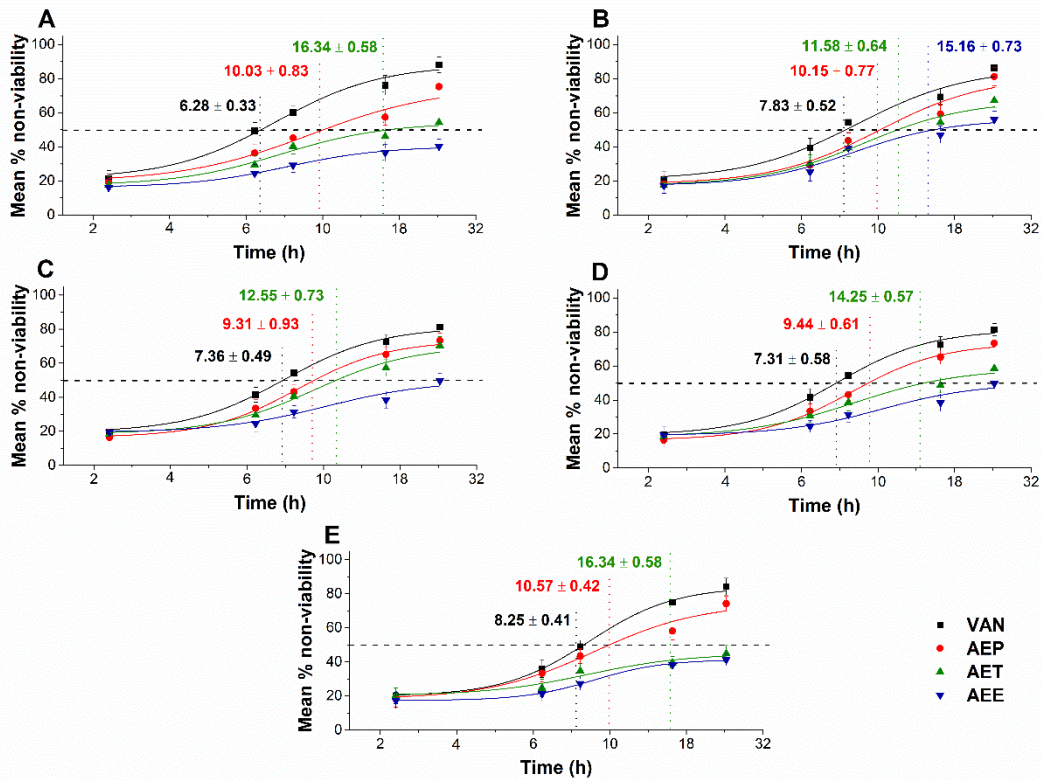


Figure 36. Mean percentage non-viability of AEP, AET and AEE at their MEC₁₀ concentrations on the metabolic activities of the planktonic *E. coli* (A), *S. aureus* (B), *B. subtilis* (C), *P. aeruginosa* (D), and *S. pyogenes* (E) compared to their respective 0 h samples and vancomycin (VAN) standard antimicrobial controls after 2, 6, 8, 16 and 24 h of treatment (mean ± SD, *n* = 6 independent experiments each with three technical replicates).

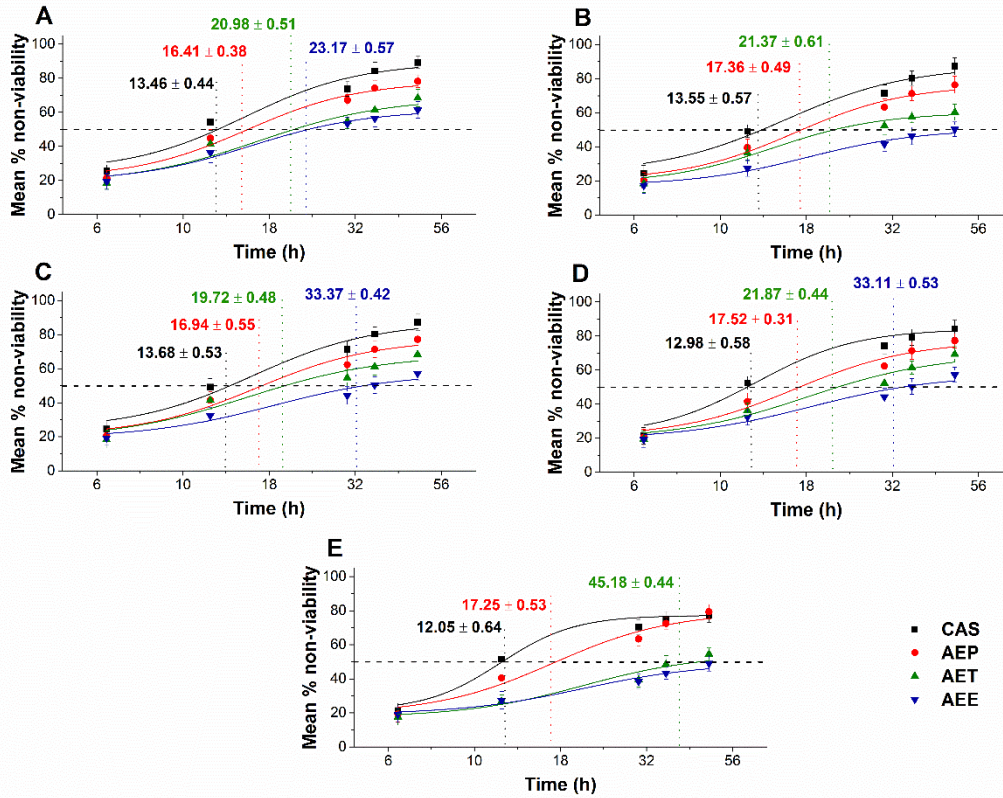


Figure 37. Mean percentage non-viability of AEP, AET, and AEE at their MEC₁₀ concentrations on the metabolic activities of the planktonic *S. pombe* (A), *C. albicans* (B), *C. tropicalis* (C), *C. dubliniensis* (D) and *C. krusei* (E) compared to their respective 0 h samples prior and caspofungin (CAS) standard antimicrobial controls after 6, 12, 30, 36 and 48 h of treatment (mean \pm SD, $n = 6$ independent experiments each with three technical replicates).

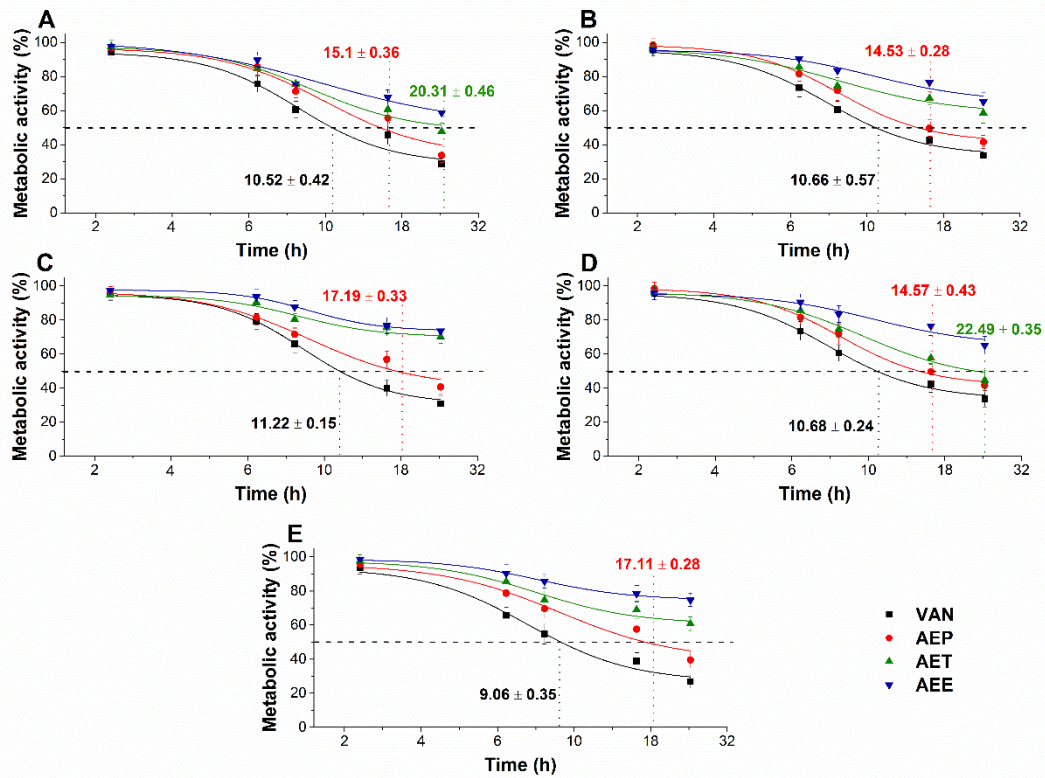


Figure 38. Effects of AEP, AET and AEE at their MEC₁₀ concentrations on the metabolic activities of the planktonic *E. coli* (A), *S. aureus* (B), *B. subtilis* (C), *P. aeruginosa* (D), and *S. pyogenes* (E) compared to their respective 0 h samples and vancomycin (VAN) standard antimicrobial controls after 2, 6, 8, 16 and 24 h of treatment (mean \pm SD, $n = 6$ independent experiments each with three technical replicates).

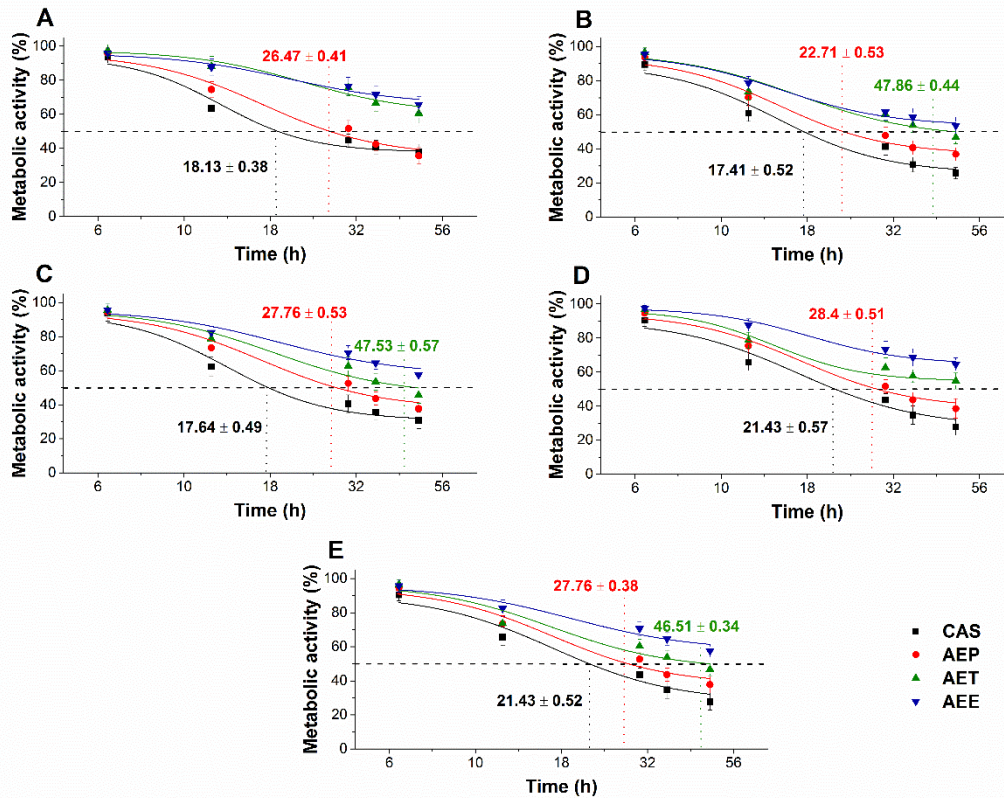


Figure 39. Effects of AEP, AET and AEE at their MEC₁₀ concentrations on the metabolic activities of the planktonic *S. pombe* (A), *C. albicans* (B), *C. tropicalis* (C), *C. dubliniensis* (D) and *C. krusei* (E) compared to their respective 0 h samples and caspofungin (CAS) standard antimicrobial controls after 6, 12, 30, 36 and 48 h of treatment (mean ± SD, *n* = 6 independent experiments, each with three technical replicates).

11.9. Effects on mature *Candida* spp. biofilms

The changes in the metabolic activity, fungal cell viability, total biofilm biomass, total protein content (TP) of the biofilm-attached *Candida* cells, and their ATP content in terms of ATP/TP ratio are shown in Figures 40 and 41. Variable response to the AEP, AET, and AEE treatments at their respective MEC₁₀ concentrations was observed when compared to the growth control (GC). Although no changes were found in the total biofilm biomass, a significant 40% reduction in the metabolic activity of the AEP treated mature biofilm-attached *Candida* species after 24 h was observed compared to GC. Whereas, AET and AEE treated samples have shown an average of 20% to 30% metabolic activity reduction compared to the AEP treatment ($P < 0.01$). The reduction of the 50% viable biofilm-attached *Candida* cells was also observed compared to the GC after 24 h of the treatment. The killing activity of the AEE treatments was found to be the lowest compared to the AEP treatments ($P < 0.01$). Total protein (reflecting the number of cells, TP) did not change significantly during the treatments, but a

significant 60% reduction of the ATP/TP ratio was found in the case of the AEP treated mature biofilm-attached *Candida* samples when compared to the GC ($P < 0.01$). An average of $28.57 \pm 5.26\%$ and $15.34 \pm 4.64\%$ reduction in the ATP/TP ratio for the AET and AEE were recorded, resulting in the AEE treatments to be the least effective among the treatment groups. Several experiments have been conducted previously; however, the mechanism of action at the sub-inhibitory concentrations has not been studied at all [98,146,160]. Our data suggest an effective microbial killing activity of AEP on selected bacteria and fungi. Previous studies believe that the killing action of the essential oils happens due to the leakage in the cells' cytoplasmic membrane and induction of oxidative stress [94,99,159]. We have introduced several staining methods to visualize and to understand the mechanism of action of the AEP, AET, and AEE. The AEP was able to induce higher oxidative stress compared to AET and AEE followed by metabolic interference, cell wall disruption, ATP depletion, and finally cell death in the case of planktonic bacterial and fungal cells as well as in mature biofilm-attached *Candida* cells at their respective sub-inhibitory concentrations.

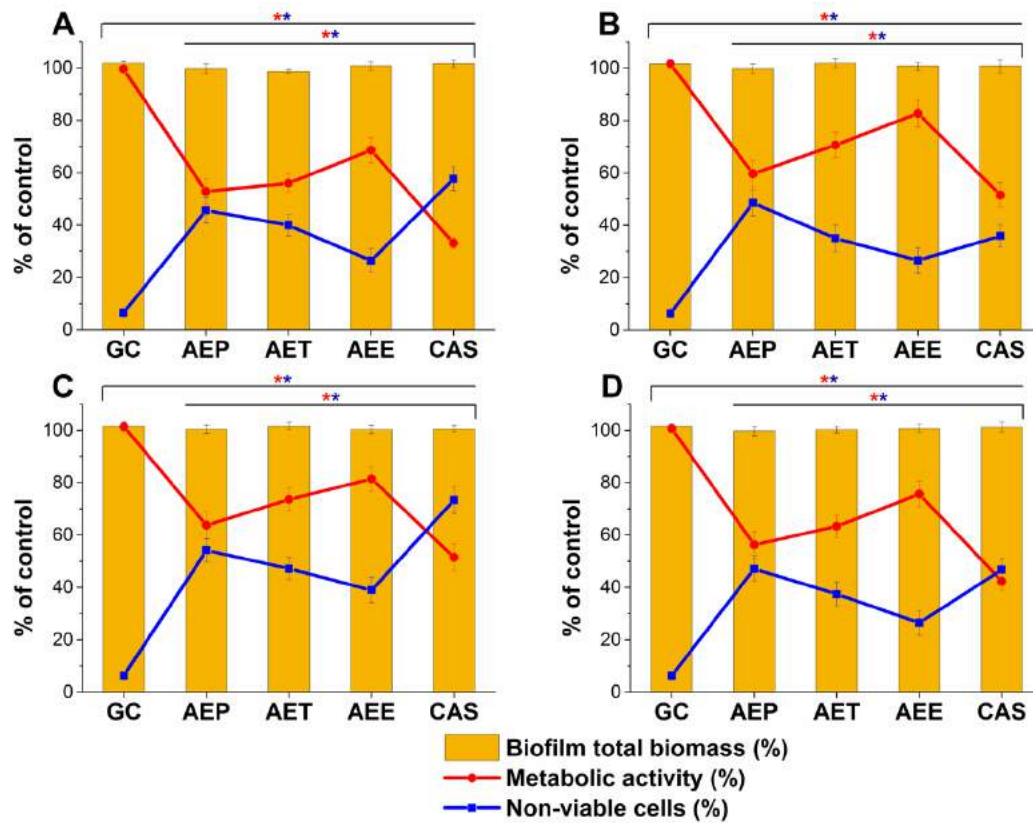


Figure 40. Effects of AEP, AET and AEE after 24 h of treatments at their respective MEC₁₀ concentrations on the metabolic activity, amount of biofilm biomass, and viability of *C. albicans* (A), *C. tropicalis* (B), *C. dubliniensis* (C) and *C. krusei* (D) cell populations (mean \pm SD, $n = 6$ independent experiments each with three technical replicates, data were compared with untreated controls (GC) and with caspofungin (CAS)-treated positive controls. The red (*) and blue (*) asterisks represent a significance value of $P < 0.01$ for the metabolic activity and viability measurements, respectively.

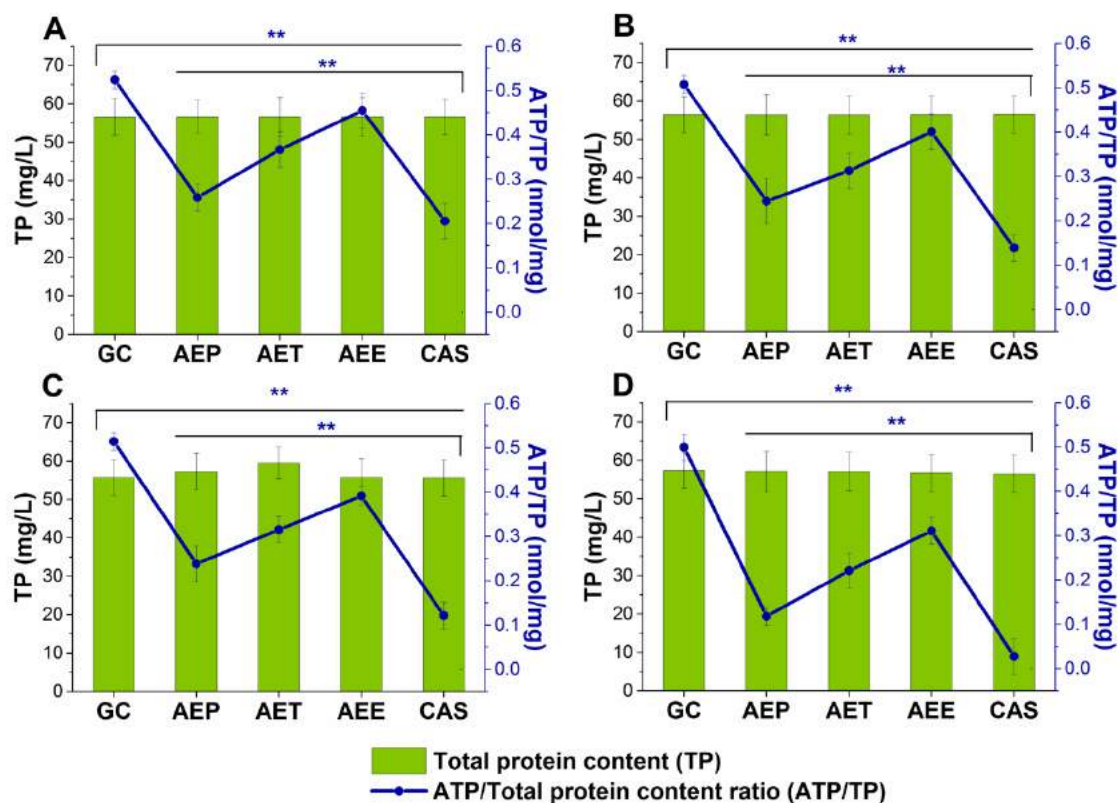


Figure 41. Effects of AEP, AET, and AEE after 24 h of treatments at their respective MEC_{10} concentrations on the ATP and the total protein content (TP) of *C. albicans* (A), *C. tropicalis* (B), *C. dubliniensis* (C) and *C. krusei* (D) cell populations in the mature biofilms (mean \pm SD, $n = 6$ independent experiments each with three technical replicates, data were compared with untreated controls (GC) and with caspofungin (CAS)-treated positive controls. The blue double asterisks (**) represent a significance value of $P < 0.01$ for the intracellular ATP/Total protein content (ATP/TP), respectively.

12. Conclusions

In this study, we have analyzed the total antioxidant capacity and antimicrobial activity of various plants' secondary metabolites including their extracted essential oils. We worked out novel formulations for the essential oils in order to enable their examination in aqueous test systems. In case of randomly methylated cyclodextrin (RAMEB) encapsulation, the RAMEB captured essential oils (EOs) and their components showed significantly higher antioxidant and antimicrobial activities than the previously reported data on conventional formulations of essential oils/components. This suggests that the encapsulation with RAMEB may provide some protection to the EOs and their components from the variable oxidative environment. Also, the cyclodextrin captured essential oil system may provide protection against different environmental conditions and the enhanced aqueous solubility and functional capabilities of the EOs may be utilized as additives in the food packaging industry.

Furthermore, we have established a novel, sensitive, and rapid fluorescent SYBR Green I/PI double-stain live/dead microbial discrimination technique as a methodological development with optimization and validation of the method by flow cytometric analyses. The introduction of the term of live/dead population ratio proved to have promising predictive capacity regarding the antimicrobial action of the test drugs.

We observed combined antifungal effects of two well-known plant-derived secondary metabolites, artemisinin, and scopoletin, at their MEC₁₀ (minimum effective concentration) by quantitation of the sub-inhibitory dose-response curves of the tested drugs on several *Candida* species, using our novel rapid fluorescent techniques. At the sub-inhibitory concentrations, the synergistic antifungal activities of artemisinin and scopoletin on mature *Candida* biofilms and planktonic cells were significantly higher than their activities alone on those species. These promising results might be useful for further detailed research for their potential usage as alternative antimicrobial agents for the treatment of *Candida* infections using cyclodextrins, Pickering emulsions, and other targeted drug delivery systems resulting in improved systemic absorption and reduced toxicity.

Our Pickering emulsion stabilized essential oils and lipophilic plant active component formulations have been successfully tested for antimicrobial activities on Gram-positive and -negative bacteria, as well as on fungi. We have also developed quantitative, fast, and reliable multi-parametric fluorescent techniques to evaluate the fungal cytotoxicity including metabolic activities, microbial live/dead ratio, ROS, peroxide, and superoxide anion radical generation of the test drugs on biofilm-attached and planktonic *Candida* fungal cell populations. The formulated oil in water Pickering essential oil nanemulsions have shown better antimicrobial and biofilm degradation activities when compared to the detergent and apolar solvent based formulations at their sub-inhibitory concentrations.

These findings suggest the potential usage of cyclodextrins and surface stabilized silica Pickering nanoemulsions as the targeted and sustained-release systems for the active plant metabolites, EOs and their components in the field of food industry and pharmaceuticals. Furthermore, our data also encourages the usage of the multiparametric fluorescent assay techniques, along with the conventional microbial assays for a fast, reliable and high throughput *in-vitro* data production. These data and test systems may serve as a starting point for obtaining more detailed information for future researches in the fight against pathogenic microbes.

13. Future perspectives

Over the years, many scientists have performed research on different plant families to be able to identify antimicrobial activities and other actions of secondary metabolites. Therefore, in the future, high throughput and sensitive experimental studies should be developed and applied to test the biological activities of different plant families. Future research should be able to identify and decipher the mechanisms these secondary metabolites undergo. Also, future researchers should focus on the selective isolation of plant compounds, to be able to determine exactly which one is contributing to the antimicrobial activity and how. Our results regarding the applied new drug formulations (encapsulation and nanoemulsion techniques) proved that the antioxidant and antimicrobial efficiency of secondary plant metabolites can be significantly increased when compared to the present “classical” formulations. These findings may be used in the future in food industry and in healthcare as well. Lastly, the future of ethnopharmacology seems very fascinating, there is hope to eradicate these antibiotic-resistant microorganisms by eliminating them with phytochemicals.

14. Acknowledgements

First of all, I would like to express my gratitude to Prof. Dr. Tamás Kőszegi who introduced me to medical research and has tutored me throughout many years. He inspired and raised me through his critical thinking, expertise in laboratory medicine, and fascinating personality.

I am grateful to Prof. Dr. Attila Miseta for his generous support and for allowing me to perform research at the Department of Laboratory Medicine and the János Szentágothai Research Center.

I would like to thank Prof. Dr. Lajos Botz for allowing me to get enrolled in his doctoral program to pursue my research studies.

I wish to thank Prof. Dr. Csaba Fekete for allowing me to continue my research at the Department of General and Environmental Microbiology, University of Pécs.

I thank Prof. Dr. Sándor Kunsági-Máté, Dr. Beáta Lemli, Dr. Zoltán Gazdag, Dr. Gábor Papp, Dr. Nóra Papp and Dr. Györgyi Horváth for their methodological and technical support.

I sincerely thank Dr. Aleksandar Széchenyi for his pioneer findings regarding the Pickering emulsions and their applications which created the basis of many of our research ideas.

I am very grateful to Barbara Horváth for her technical, methodological and analytical supports to my research.

I am indebted to Dr. Mónika Kuzma, Prof. Dr. Luigi Mondello, and Dr. Giuseppe Micalizzi for their invaluable technical guidance and research support regarding GC-MS analyses.

I would like to thank Dr. Tímea Bencsik for introducing me to the exciting field of natural product isolation methodologies.

I am thankful to my colleagues, Viktória Das-Báló, Viktória Temesfői, Rita Csepregi, Lilla Czuni and, Mátyás Meggyes, for their encouraging creative ideas and friendship.

Finally, I am grateful to my family and friends, for their critical insights and loving care, which helped me to complete this work.

15. Novel findings of the Ph.D. research

- We have developed thermodynamically stable novel cyclodextrin based essential oils/component complexes with high encapsulation efficiency. As a result, we could produce more reliable and sustainable data for the antioxidant and antimicrobial analyses of encapsulated various essential oils/pure components.
- We have developed and optimized a rapid microplate live/dead microbial viability assay technique using a fluorescent double-staining method. The assay was validated by flow-cytometry, and we successfully established the protocol for a fast, reliable, and high throughput antimicrobial analysis.
- We were able to increase the antioxidant and antimicrobial potentials of various essential oils/components with the cyclodextrin encapsulation, when compared to their un-complexed forms. The total antioxidant capacity and the antimicrobial properties of the RAMEB encapsulated EOs and their components showed 5-6 times higher efficiency than other (classical) EOs' formulations.
- We have successfully created surface-modified silica nanoemulsion based delivery systems of the essential oil(s) along with their components and plant's secondary metabolites for their enhanced aqueous solubility and better characterization of their biological properties.
- We were able to characterize the antimicrobial effects of essential oils and pure plant extracts at their Minimum Effective Concentrations (MEC_{10}) by various methods (metabolic activity, oxidative stress, live/dead discrimination assay, killing activity vs. exposure time). Based on our results, the Pickering EO nanoemulsions have shown higher growth inhibitory actions at lower MIC compared to the apolar solvent and conventional detergent based formulations. Furthermore, at the minimum effective concentrations (MEC_{10}), the Pickering EO nanoemulsions were able to generate 3-5

times higher cellular oxidative stress followed by metabolic interference and consequent cell damage.

- We have investigated the antimicrobial and anti-biofilm actions of artemisinin and scopoletin (secondary metabolites of *Artemisia annua* L.) and have revealed their effects on cellular viability, metabolic activity, and oxidative stress balance of microbial biofilms and planktonic cells, as well. Our data suggest, that both artemisinin and scopoletin, even at their MEC₁₀ concentrations were able to initiate oxidative imbalance and reducing metabolic activities followed by induction of cellular damage in the tested *Candida* species.
- We have introduced several multi-parametric fluorescent techniques to overcome the challenges associated with the measurements of the antimicrobial assay of the *Artemisia annua* L. Pickering EO nanoemulsions (AEP) on biofilms and on planktonic cells, and have investigated the possible mode of action (metabolic activity, oxidative stress, live/dead discrimination assay and intracellular ATP/total protein content). An effective microbial killing activity has been observed in case of AEP, when compared to the conventional detergent and apolar solvent based formulations. Overall, our observations demonstrated that the Pickering nanoemulsions facilitated the penetration of *Artemisia annua* L. essential oil through the biofilm and the cells, inducing oxidative imbalance and disruption of the cell wall integrity.

16. References

1. Manion, C.R.; Widder, R.M. Essentials of essential oils. *American Journal of Health-System Pharmacy* **2017**, *74*, e153–e162.
2. Omonijo, F.A.; Ni, L.; Gong, J.; Wang, Q.; Lahaye, L.; Yang, C. Essential oils as alternatives to antibiotics in swine production. *Animal Nutrition* **2018**, *4*, 126–136.
3. McKay, D.L.; Blumberg, J.B. A Review of the bioactivity and potential health benefits of chamomile tea (*Matricaria recutita* L.). *Phytotherapy Research* **2006**, *20*, 519–530.
4. Lis-Balchin, M. *Aromatherapy science: a guide for healthcare professionals*; Pharmaceutical Press: London ; Chicago, **2006**; ISBN 978-0-85369-578-3.
5. Bhargava, K.; Conti, D.S.; da Rocha, S.R.P.; Zhang, Y. Application of an oregano oil nanoemulsion to the control of foodborne bacteria on fresh lettuce. *Food Microbiology* **2015**, *47*, 69–73.
6. Oussalah, M.; Caillet, S.; Salmiéri, S.; Saucier, L.; Lacroix, M. Antimicrobial Effects of Alginate-Based Films Containing Essential Oils on *Listeria monocytogenes* and

- Salmonella Typhimurium* Present in Bologna and Ham. *Journal of Food Protection* **2007**, *70*, 901–908.
7. Perricone, M.; Arace, E.; Corbo, M.R.; Sinigaglia, M.; Bevilacqua, A. Bioactivity of essential oils: a review on their interaction with food components. *Frontiers in Microbiology* **2015**, *6*, 76.
 8. Guo, J.; Gao, Z.; Li, G.; Fu, F.; Liang, Z.; Zhu, H.; Shan, Y. Antimicrobial and antibiofilm efficacy and mechanism of essential oil from Citrus Changshan-huyou Y. B. chang against *Listeria monocytogenes*. *Food Control* **2019**, *105*, 256–264.
 9. Ju, J.; Chen, X.; Xie, Y.; Yu, H.; Guo, Y.; Cheng, Y.; Qian, H.; Yao, W. Application of essential oil as a sustained release preparation in food packaging. *Trends in Food Science & Technology* **2019**, *92*, 22–32.
 10. Wang, T.; Li, B.; Si, H.; Lin, L.; Chen, L. Release characteristics and antibacterial activity of solid state eugenol/ β -cyclodextrin inclusion complex. *Journal of Inclusion Phenomena and Macrocyclic Chemistry* **2011**, *71*, 207–213.
 11. He, J.; Wu, D.; Zhang, Q.; Chen, H.; Li, H.; Han, Q.; Lai, X.; Wang, H.; Wu, Y.; Yuan, J.; et al. Efficacy and Mechanism of Cinnamon Essential Oil on Inhibition of *Colletotrichum acutatum* Isolated From ‘Hongyang’ Kiwifruit. *Frontiers in Microbiology* **2018**, *9*, 1288.
 12. Nazzaro, F.; Fratianni, F.; De Martino, L.; Coppola, R.; De Feo, V. Effect of Essential Oils on Pathogenic Bacteria. *Pharmaceuticals* **2013**, *6*, 1451–1474.
 13. Silhavy, T.J.; Kahne, D.; Walker, S. The Bacterial Cell Envelope. *Cold Spring Harbor Perspectives in Biology* **2010**, *2*, a000414–a000414.
 14. Hyldgaard, M.; Mygind, T.; Meyer, R.L. Essential Oils in Food Preservation: Mode of Action, Synergies, and Interactions with Food Matrix Components. *Frontiers in Microbiology* **2012**, *3*, 12.
 15. Efferth, T. From ancient herb to modern drug: *Artemisia annua* and artemisinin for cancer therapy. *Seminars in Cancer Biology* **2017**, *46*, 65–83.
 16. Ho, W.E.; Peh, H.Y.; Chan, T.K.; Wong, W.S.F. Artemisinins: Pharmacological actions beyond anti-malarial. *Pharmacology & Therapeutics* **2014**, *142*, 126–139.
 17. Das, S.; Czuni, L.; Báló, V.; Papp, G.; Gazdag, Z.; Papp, N.; Kőszegi, T. Cytotoxic Action of Artemisinin and Scopoletin on Planktonic Forms and on Biofilms of *Candida* Species. *Molecules* **2020**, *18*, 476.
 18. Radulović, N.S.; Randjelović, P.J.; Stojanović, N.M.; Blagojević, P.D.; Stojanović-Radić, Z.Z.; Ilić, I.R.; Djordjević, V.B. Toxic essential oils. Part II: Chemical,

- toxicological, pharmacological and microbiological profiles of *Artemisia annua* L. volatiles. *Food and Chemical Toxicology* **2013**, *58*, 37–49.
19. Bilia, A.R.; Santomauro, F.; Sacco, C.; Bergonzi, M.C.; Donato, R. Essential Oil of *Artemisia annua* L.: An Extraordinary Component with Numerous Antimicrobial Properties. *Evidence-Based Complementary and Alternative Medicine* **2014**, *2014*, 1–7.
 20. Čavar, S.; Maksimović, M.; Vidic, D.; Parić, A. Chemical composition and antioxidant and antimicrobial activity of essential oil of *Artemisia annua* L. from Bosnia. *Industrial Crops and Products* **2012**, *37*, 479–485.
 21. Das, S.; Vörös-Horváth, B.; Bencsik, T.; Micalizzi, G.; Mondello, L.; Horváth, G.; Kőszegi, T.; Széchenyi, A. Antimicrobial Activity of Different Artemisia Essential Oil Formulations. *Molecules* **2020**, *25*, 2390.
 22. Tzeng, T.; Lin, Y.; Jong, T.; Chang, C. Ethanol modified supercritical fluids extraction of scopoletin and artemisinin from *Artemisia annua* L. *Separation and Purification Technology* **2007**, *56*, 18–24.
 23. Gnonlonfin, G.J.B.; Sanni, A.; Brimer, L. Review Scopoletin – A Coumarin Phytoalexin with Medicinal Properties. *Critical Reviews in Plant Sciences* **2012**, *31*, 47–56.
 24. Moon, P.-D.; Lee, B.-H.; Jeong, H.-J.; An, H.-J.; Park, S.-J.; Kim, H.-R.; Ko, S.-G.; Um, J.-Y.; Hong, S.-H.; Kim, H.-M. Use of scopoletin to inhibit the production of inflammatory cytokines through inhibition of the I κ B/NF- κ B signal cascade in the human mast cell line HMC-1. *European Journal of Pharmacology* **2007**, *555*, 218–225.
 25. Galal, A.M.; Ross, S.A.; Jacob, M.; ElSohly, M.A. Antifungal Activity of Artemisinin Derivatives. *Journal of Natural Products* **2005**, *68*, 1274–1276.
 26. Cai, X.; Yang, J.; Zhou, J.; Lu, W.; Hu, C.; Gu, Z.; Huo, J.; Wang, X.; Cao, P. Synthesis and biological evaluation of scopoletin derivatives. *Bioorganic & Medicinal Chemistry* **2013**, *21*, 84–92.
 27. Dhiman, R.; Kumar Aggarwal, N. Efficacy of Plant Antimicrobials as Preservative in Food. In *Food Preservation - From Basics to Advanced Technologies*; IntechOpen, **2019**. DOI: 10.5772/intechopen.83440.
 28. Gottardi, D.; Bukvicki, D.; Prasad, S.; Tyagi, A.K. Beneficial Effects of Spices in Food Preservation and Safety. *Frontiers in Microbiology* **2016**, *7*, 1394.
 29. Govari (M. Γκοβαρη), M.; Pexara (A. Πεξαρα), A. Nitrates and Nitrites in meat products. *Journal of the Hellenic Veterinary Medical Society* **2018**, *66*, 127.
 30. Fewtrell, L. Drinking-Water Nitrate, Methemoglobinemia, and Global Burden of Disease: A Discussion. *Environmental Health Perspectives* **2004**, *112*, 1371–1374.

31. Piper, P. Potential Safety Issues Surrounding the Use of Benzoate Preservatives. *Beverages* **2018**, *4*, 33.
32. Stratford, M.; Plumridge, A.; Archer, D.B. Decarboxylation of Sorbic Acid by Spoilage Yeasts Is Associated with the PAD1 Gene. *Applied and Environmental Microbiology* **2007**, *73*, 6534–6542.
33. Panche, A.N.; Diwan, A.D.; Chandra, S.R. Flavonoids: an overview. *Journal of Nutritional Science* **2016**, *5*, e47.
34. Al-Fattani, M.A.; Douglas, L.J. Penetration of Candida Biofilms by Antifungal Agents. *Antimicrobial Agents and Chemotherapy* **2004**, *48*, 3291–3297.
35. Bonhomme, J.; d'Enfert, C. Candida albicans biofilms: building a heterogeneous, drug-tolerant environment. *Current Opinion in Microbiology* **2013**, *16*, 398–403.
36. Høiby, N.; Bjarnsholt, T.; Givskov, M.; Molin, S.; Ciofu, O. Antibiotic resistance of bacterial biofilms. *International Journal of Antimicrobial Agents* **2010**, *35*, 322–332.
37. Gugnani, H.C.; Denning, D.W. Burden of serious fungal infections in the Dominican Republic. *Journal of Infection and Public Health* **2016**, *9*, 7–12.
38. Cordeiro, R. de A.; Sales, J.A.; Castelo-Branco, D. de S.C.M.; Brilhante, R.S.N.; Ponte, Y.B. de; dos Santos Araújo, G.; Mendes, P.B.L.; Pereira, V.S.; Alencar, L.P. de; Pinheiro, A. de Q.; et al. *Candida parapsilosis* complex in veterinary practice: A historical overview, biology, virulence attributes and antifungal susceptibility traits. *Veterinary Microbiology* **2017**, *212*, 22–30.
39. Álvarez-Pérez, S.; García, M.E.; Cutuli, M.T.; Fermín, M.L.; Daza, M.Á.; Peláez, T.; Blanco, J.L. Acquired multi-azole resistance in *Candida tropicalis* during persistent urinary tract infection in a dog. *Medical Mycology Case Reports* **2016**, *11*, 9–12.
40. Ostrosky-Zeichner, L.; Sobel, J.D. Fungal Infections. *Infectious Disease Clinics of North America* **2016**, *30*, 13–14.
41. Wang, X.; van de Veerdonk, F.L.; Netea, M.G. Basic Genetics and Immunology of Candida Infections. *Infectious Disease Clinics of North America* **2016**, *30*, 85–102.
42. Brilhante, R.S.N.; Oliveira, J.S. de; Evangelista, A.J. de J.; Serpa, R.; Silva, A.L. da; Aguiar, F.R.M. de; Pereira, V.S.; Castelo-Branco, D. de S.C.M.; Pereira-Neto, W.A.; Cordeiro, R. de A.; et al. *Candida tropicalis* from veterinary and human sources shows similar in vitro hemolytic activity, antifungal biofilm susceptibility and pathogenesis against *Caenorhabditis elegans*. *Veterinary Microbiology* **2016**, *192*, 213–219.
43. Ksiezopolska, E.; Gabaldón, T. Evolutionary Emergence of Drug Resistance in Candida Opportunistic Pathogens. *Genes (Basel)* **2018**, *9*, 461.

44. Jothiprakasam, V.; Sambantham, M.; Chinnathambi, S.; Vijayaboopathi, S. *Candida tropicalis* biofilm inhibition by ZnO nanoparticles and EDTA. *Archives of Oral Biology* **2017**, *73*, 21–24.
45. Armstrong-James, D.; Meintjes, G.; Brown, G.D. A neglected epidemic: fungal infections in HIV/AIDS. *Trends in Microbiology* **2014**, *22*, 120–127.
46. Turek, C.; Stintzing, F.C. Stability of Essential Oils: A Review: Stability of essential oils.... *Comprehensive Reviews in Food Science and Food Safety* **2013**, *12*, 40–53.
47. Tao, F.; Hill, L.E.; Peng, Y.; Gomes, C.L. Synthesis and characterization of β -cyclodextrin inclusion complexes of thymol and thyme oil for antimicrobial delivery applications. *LWT - Food Science and Technology* **2014**, *59*, 247–255.
48. Jiang, Z.; Kempinski, C.; Chappell, J. Extraction and Analysis of Terpenes/Terpenoids. *Current Protocols in Plant Biology* **2016**, *1*, 345–358.
49. Dhifi, W.; Bellili, S.; Jazi, S.; Bahloul, N.; Mnif, W. Essential Oils' Chemical Characterization and Investigation of Some Biological Activities: A Critical Review. *Medicines* **2016**, *3*, 25.
50. Pfaller, M.A.; Sheehan, D.J.; Rex, J.H. Determination of Fungicidal Activities against Yeasts and Molds: Lessons Learned from Bactericidal Testing and the Need for Standardization. *Clinical Microbiology Reviews* **2004**, *17*, 268–280.
51. Donsì, F.; Ferrari, G. Essential oil nanoemulsions as antimicrobial agents in food. *Journal of Biotechnology* **2016**, *233*, 106–120.
52. Singh, O.; Khanam, Z.; Misra, N.; Srivastava, M. Chamomile (*Matricaria chamomilla* L.): An overview. *Pharmacognosy Reviews* **2011**, *5*, 82.
53. Alastruey-Izquierdo, A.; Gomez-Lopez, A.; Arendrup, M.C.; Lass-Flörl, C.; Hope, W.W.; Perlin, D.S.; Rodriguez-Tudela, J.L.; Cuenca-Estrella, M. Comparison of Dimethyl Sulfoxide and Water as Solvents for Echinocandin Susceptibility Testing by the EUCAST Methodology. *Journal of Clinical Microbiology* **2012**, *50*, 2509–2512.
54. Inouye, S.; Tsuruoka, T.; Uchida, K.; Yamaguchi, H. Effect of Sealing and Tween 80 on the Antifungal Susceptibility Testing of Essential Oils. *Microbiology and Immunology* **2001**, *45*, 201–208.
55. Thielmann, J.; Muranyi, P.; Kazman, P. Screening essential oils for their antimicrobial activities against the foodborne pathogenic bacteria *Escherichia coli* and *Staphylococcus aureus*. *Heliyon* **2019**, *5*, e01860.
56. Pina-Barrera, A.M.; Alvarez-Roman, R.; Baez-Gonzalez, J.G.; Amaya-Guerra, C.A.; Rivas-Morales, C.; Gallardo-Rivera, C.T.; Galindo-Rodriguez, S.A. Application of a

- multisystem coating based on polymeric nanocapsules containing essential oil of *Thymus vulgaris* L. to increase the shelf life of table grapes (*Vitis vinifera* L.). *IEEE Transactions on NanoBioscience* **2019**, 1–1.
57. Zhou, Y.; Sun, S.; Bei, W.; Zahi, M.R.; Yuan, Q.; Liang, H. Preparation and antimicrobial activity of oregano essential oil Pickering emulsion stabilized by cellulose nanocrystals. *International Journal of Biological Macromolecules* **2018**, *112*, 7–13.
 58. Fasihi, H.; Noshirvani, N.; Hashemi, M.; Fazilati, M.; Salavati, H.; Coma, V. Antioxidant and antimicrobial properties of carbohydrate-based films enriched with cinnamon essential oil by Pickering emulsion method. *Food Packaging and Shelf Life* **2019**, *19*, 147–154.
 59. Abarca, R.L.; Rodríguez, F.J.; Guarda, A.; Galotto, M.J.; Bruna, J.E. Characterization of beta-cyclodextrin inclusion complexes containing an essential oil component. *Food Chemistry* **2016**, *196*, 968–975.
 60. Ciobanu, A.; Landy, D.; Fourmentin, S. Complexation efficiency of cyclodextrins for volatile flavor compounds. *Food Research International* **2013**, *53*, 110–114.
 61. Feng, J.; Wang, T.; Zhang, S.; Shi, W.; Zhang, Y. An Optimized SYBR Green I/PI Assay for Rapid Viability Assessment and Antibiotic Susceptibility Testing for *Borrelia burgdorferi*. *PLoS One* **2014**, *9*, e111809.
 62. Sun, Z.; Zhang, Y. Spent Culture Supernatant of Mycobacterium tuberculosis H37Ra Improves Viability of Aged Cultures of This Strain and Allows Small Inocula To Initiate Growth. *Journal of Bacteriology* **1999**, *181*, 7626–7628.
 63. Taylor, J.P.; Wilson, B.; Mills, M.S.; Burns, R.G. Comparison of microbial numbers and enzymatic activities in surface soils and subsoils using various techniques. *Soil Biology and Biochemistry* **2002**, *34*, 387–401.
 64. Gabrielson, J.; Hart, M.; Jarelöv, A.; Kühn, I.; McKenzie, D.; Möllby, R. Evaluation of redox indicators and the use of digital scanners and spectrophotometer for quantification of microbial growth in microplates. *Journal of Microbiological Methods* **2002**, *50*, 63–73.
 65. Mshana, R.N.; Tadesse, G.; Abate, G.; Rner, H.M. Mycobacterium tuberculosis. *Journal of Clinical Microbiology* **1998**, *36*, 6.
 66. Wang, H.; Cheng, H.; Wang, F.; Wei, D.; Wang, X. An improved 3-(4,5-dimethylthiazol-2-yl)-2,5-diphenyl tetrazolium bromide (MTT) reduction assay for evaluating the viability of Escherichia coli cells. *Journal of Microbiological Methods* **2010**, *82*, 330–333.

67. Boulos, L.; Prevost, M.; Barbeau, B.; Coallier, J.; Desjardins, R. LIVE/DEAD BacLight: application of a new rapid staining method for direct enumeration of viable and total bacteria in drinking water. *Journal of Microbiological Methods* **1999**, *37*, 77–86.
68. Peeters, E.; Nelis, H.J.; Coenye, T. Comparison of multiple methods for quantification of microbial biofilms grown in microtiter plates. *Journal of Microbiological Methods* **2008**, *72*, 157–165.
69. Cornell, K.A.; Primus, S.; Martinez, J.A.; Parveen, N. Assessment of methylthioadenosine/S-adenosylhomocysteine nucleosidases of *Borrelia burgdorferi* as targets for novel antimicrobials using a novel high-throughput method. *Journal of Antimicrobial Chemotherapy* **2009**, *63*, 1163–1172.
70. Barbesti, S.; Citterio, S.; Labra, M.; Baroni, M.D.; Neri, M.G.; Sgorbati, S. Two and three-color fluorescence flow cytometric analysis of immunoidentified viable bacteria. *Cytometry* **2000**, *40*, 214–218.
71. Cerca, F.; Trigo, G.; Correia, A.; Cerca, N.; Azeredo, J.; Vilanova, M. SYBR green as a fluorescent probe to evaluate the biofilm physiological state of *Staphylococcus epidermidis*, using flow cytometry. *Canadian Journal of Microbiology* **2011**, *57*, 850–856.
72. Bankier, C.; Cheong, Y.; Mahalingam, S.; Edirisinghe, M.; Ren, G.; Cloutman-Green, E.; Ciric, L. A comparison of methods to assess the antimicrobial activity of nanoparticle combinations on bacterial cells. *PLOS ONE* **2018**, *13*, e0192093.
73. Fenyvesi, É.; Vikmon, M.; Szente, L. Cyclodextrins in Food Technology and Human Nutrition: Benefits and Limitations. *Critical Reviews in Food Science and Nutrition* **2016**, *56*, 1981–2004.
74. Anaya-Castro, M.A.; Ayala-Zavala, J.F.; Muñoz-Castellanos, L.; Hernández-Ochoa, L.; Peydecastaing, J.; Durrieu, V. β -Cyclodextrin inclusion complexes containing clove (*Eugenia caryophyllata*) and Mexican oregano (*Lippia berlandieri*) essential oils: Preparation, physicochemical and antimicrobial characterization. *Food Packaging and Shelf Life* **2017**, *14*, 96–101.
75. Mahjoubin-Tehran, M.; Kovanen, P.T.; Xu, S.; Jamialahmadi, T.; Sahebkar, A. Cyclodextrins: Potential therapeutics against atherosclerosis. *Pharmacology & Therapeutics* **2020**, *214*, 107620.
76. Cossu, A.; Wang, M.S.; Chaudhari, A.; Nitin, N. Antifungal activity against *Candida albicans* of starch Pickering emulsion with thymol or amphotericin B in suspension and calcium alginate films. *International Journal of Pharmaceutics* **2015**, *493*, 233–242.

77. Wang, J.; Li, Y.; Gao, Y.; Xie, Z.; Zhou, M.; He, Y.; Wu, H.; Zhou, W.; Dong, X.; Yang, Z.; et al. Cinnamon oil-loaded composite emulsion hydrogels with antibacterial activity prepared using concentrated emulsion templates. *Industrial Crops and Products* **2018**, *112*, 281–289.
78. Chevalier, Y.; Bolzinger, M.-A. Emulsions stabilized with solid nanoparticles: Pickering emulsions. *Colloids and Surfaces A: Physicochemical and Engineering Aspects* **2013**, *439*, 23–34.
79. Liu, H.; Yang, G.; Tang, Y.; Cao, D.; Qi, T.; Qi, Y.; Fan, G. Physicochemical characterization and pharmacokinetics evaluation of β -caryophyllene/ β -cyclodextrin inclusion complex. *International Journal of Pharmaceutics* **2013**, *450*, 304–310.
80. Poór, M.; Kunsági-Máté, S.; Sali, N.; Kőszegi, T.; Szente, L.; Peles-Lemli, B. Interactions of zearalenone with native and chemically modified cyclodextrins and their potential utilization. *Journal of Photochemistry and Photobiology B: Biology* **2015**, *151*, 63–68.
81. Poór, M.; Zand, A.; Szente, L.; Lemli, B.; Kunsági-Máté, S. Interaction of α - and β -zearalenols with β -cyclodextrins. *Molecules* **2017**, *22*, 1910.
82. Nicolescu, C.; Aram, C.; Nsedelcu, A.; Monciu, C.-M. Phase solubility studies of the inclusion complexes of rapaglinide with β -cyclodextrin and β -cyclodextrin derivatives, *Pharmacia* **2010**, *58*(5), 620–628.
83. Kfoury, M.; Auezova, L.; Greige-Gerges, H.; Fourmentin, S. Promising applications of cyclodextrins in food: Improvement of essential oils retention, controlled release and antiradical activity. *Carbohydrate Polymers* **2015**, *131*, 264–272.
84. Prevc, T.; Šegatin, N.; Poklar Ulrih, N.; Cigić, B. DPPH assay of vegetable oils and model antioxidants in protic and aprotic solvents. *Talanta* **2013**, *109*, 13–19.
85. Sharma, O.P.; Bhat, T.K. DPPH antioxidant assay revisited. *Food Chemistry* **2009**, *113*, 1202–1205.
86. Wollinger, A.; Perrin, É.; Chahboun, J.; Jeannot, V.; Touraud, D.; Kunz, W. Antioxidant activity of hydro distillation water residues from *Rosmarinus officinalis* L. leaves determined by DPPH assays. *Comptes Rendus Chimie* **2016**, *19*, 754–765.
87. Deng, J.; Cheng, W.; Yang, G. A novel antioxidant activity index (AAU) for natural products using the DPPH assay. *Food Chemistry* **2011**, *125*, 1430–1435.
88. Mishra, K.; Ojha, H.; Chaudhury, N.K. Estimation of antiradical properties of antioxidants using DPPH assay: A critical review and results. *Food Chemistry* **2012**, *130*, 1036–1043.

89. Kőszegi, T.; Sali, N.; Raknić, M.; Horváth-Szalai, Z.; Csepregi, R.; Končić, M.Z.; Papp, N.; Poór, M. A novel luminol-based enhanced chemiluminescence antioxidant capacity microplate assay for use in different biological matrices. *Journal of Pharmacological and Toxicological Methods* **2017**, *88*, 153–159.
90. Llop, C.; Pujol, I.; Aguilar, C.; Sala, J.; Riba, D.; Guarro, J. Comparison of three methods of determining MICs for filamentous fungi using different end point criteria and incubation periods. *Antimicrobial agents and chemotherapy* **2000**, *44*, 239–242.
91. Das, S.; Horváth, B.; Šafranko, S.; Jokić, S.; Széchenyi, A.; Kőszegi, T. Antimicrobial Activity of Chamomile Essential Oil: Effect of Different Formulations. *Molecules* **2019**, *24*, 4321.
92. Balázs, V.L.; Horváth, B.; Kerekes, E.; Ács, K.; Kocsis, B.; Varga, A.; Böszörményi, A.; Nagy, D.U.; Krisch, J.; Széchenyi, A.; et al. Anti-Haemophilus Activity of Selected Essential Oils Detected by TLC-Direct Bioautography and Biofilm Inhibition. *Molecules* **2019**, *24*, 3301.
93. Horváth, B.; Balázs, V.L.; Horváth, G.; Széchenyi, A. Preparation and in vitro diffusion study of essential oil Pickering emulsions stabilized by silica nanoparticles for *Streptococcus mutans* biofilm inhibition. *Flavour and Fragrance Journal* **2018**, *33*, 385–396.
94. Fujs, S.; Gazdag, Z.; Poljčak, B.; Stibilj, V.; Milacic, R.; Pesti, M.; Raspor, P.; Batic, M. The oxidative stress response of the yeast *Candida intermedia* to copper, zinc, and selenium exposure. *Journal of Basic Microbiology* **2005**, *45*, 125–135.
95. Das, S.; Gazdag, Z.; Szenté, L.; Meggyes, M.; Horváth, G.; Lemli, B.; Kunsági-Máté, S.; Kuzma, M.; Kőszegi, T. Antioxidant and antimicrobial properties of randomly methylated β cyclodextrin – captured essential oils. *Food Chemistry* **2019**, *278*, 305–313.
96. Eruslanov, E.; Kusmartsev, S. Identification of ROS Using Oxidized DCFDA and Flow-Cytometry. In *Advanced Protocols in Oxidative Stress II*; Armstrong, D., Ed.; Humana Press: Totowa, NJ, **2010**; Vol. 594, pp. 57–72 ISBN 978-1-60761-410-4.
97. Dong, T.G.; Dong, S.; Catalano, C.; Moore, R.; Liang, X.; Mekalanos, J.J. Generation of reactive oxygen species by lethal attacks from competing microbes. *Proceedings of the National Academy of Sciences of the United States of America* **2015**, *112*, 2181–2186.

98. Stromájer-Rácz, T.; Gazdag, Z.; Belágyi, J.; Vágvölgyi, C.; Zhao, R.Y.; Pesti, M. Oxidative stress induced by HIV-1 F34IVpr in *Schizosaccharomyces pombe* is one of its multiple functions. *Experimental and Molecular Pathology* **2010**, *88*, 38–44.
99. Gazdag, Z.; Máté, G.; Čertík, M.; Türmer, K.; Virág, E.; Pócsi, I.; Pesti, M. *tert*-Butyl hydroperoxide-induced differing plasma membrane and oxidative stress processes in yeast strains BY4741 and *erg5Δ*: *t*-BuOOH-induced cytotoxic processes in yeast. *Journal of Basic Microbiology* **2014**, *54*, S50–S62.
100. Henderson, L.M.; Chappell, J.B. Dihydrorhodamine 123: a fluorescent probe for superoxide generation? *European Journal of Biochemistry* **1993**, *217*, 973–980.
101. Appiah, T.; Boakye, Y.D.; Agyare, C. Antimicrobial Activities and Time-Kill Kinetics of Extracts of Selected Ghanaian Mushrooms. *Evidence-Based Complementary and Alternative Medicine* **2017**, *2017*, 1–15.
102. Gazdag, Z.; Fujs, S.; Kőszegi, B.; Kálmán, N.; Papp, G.; Emri, T.; Belágyi, J.; Pócsi, I.; Raspor, P.; Pesti, M. The *abc1 - /coq8 -* respiratory-deficient mutant of *Schizosaccharomyces pombe* suffers from glutathione underproduction and hyperaccumulates Cd²⁺. *Folia Microbiologica* **2011**, *56*, 353–359.
103. Lee, J.; Dawes, I.W.; Roe, J.-H. Adaptive response of *Schizosaccharomyces pombe* to hydrogen peroxide and menadione. *Microbiology* **1995**, *141*, 3127–3132.
104. Pesti, M.; Gazdag, Z.; Belágyi, J. In vivo interaction of trivalent chromium with yeast plasma membrane, as revealed by EPR spectroscopy. *FEMS Microbiology Letters* **2000**, *182*, 375–380.
105. Rajendran, R.; Sherry, L.; Nile, C.J.; Sherriff, A.; Johnson, E.M.; Hanson, M.F.; Williams, C.; Munro, C.A.; Jones, B.J.; Ramage, G. Biofilm formation is a risk factor for mortality in patients with *Candida albicans* bloodstream infection-Scotland, 2012-2013. *Clinical Microbiology and Infection* **2016**, *22*, 87–93.
106. Kerekes, E.-B.; Deák, É.; Takó, M.; Tserennadmid, R.; Petkovits, T.; Vágvölgyi, C.; Krisch, J. Anti-biofilm forming and anti-quorum sensing activity of selected essential oils and their main components on food-related micro-organisms. *Journal of Applied Microbiology* **2013**, *115*, 933–942.
107. Fai, P.B.; Grant, A. A rapid resazurin bioassay for assessing the toxicity of fungicides. *Chemosphere* **2009**, *74*, 1165–1170.
108. Van den Driessche, F.; Rigole, P.; Brackman, G.; Coenye, T. Optimization of resazurin-based viability staining for quantification of microbial biofilms. *Journal of Microbiological Methods* **2014**, *98*, 31–34.

109. Csepregi, R.; Bencsik, T.; Papp, N. Examination of secondary metabolites and antioxidant capacity of *Anthyllis vulneraria*, *Fuchsia sp.*, *Galium mollugo* and *Veronica beccabunga*. *Acta Biologica Hungarica* **2016**, *67*, 442–446.
110. Rahman, M.M.; Ichihyanagi, T.; Komiyama, T.; Hatano, Y.; Konishi, T. Superoxide radical- and peroxynitrite scavenging activity of anthocyanins; structure-activity relationship and their synergism. *Free Radical Research* **2006**, *40*, 993–1002.
111. Bradford, M.M. A Rapid and Sensitive Method for the Quantitation of Microgram Quantities of Protein Utilizing the Principle of Protein-Dye Binding. *Analytical Biochemistry* **1976**, *72*, 248–254.
112. Roscetto, E.; Contursi, P.; Vollaro, A.; Fusco, S.; Notomista, E.; Catania, M.R. Antifungal and anti-biofilm activity of the first cryptic antimicrobial peptide from an archaeal protein against *Candida* spp. clinical isolates. *Scientific Reports* **2018**, *8*, 17570.
113. Nasr Bouzaiene, N.; Kilani Jaziri, S.; Kovacic, H.; Chekir-Ghedira, L.; Ghedira, K.; Luis, J. The effects of caffeic, coumaric and ferulic acids on proliferation, superoxide production, adhesion and migration of human tumor cells in vitro. *European Journal of Pharmacology* **2015**, *766*, 99–105.
114. Szejtli, J.; Szente, L. Elimination of bitter, disgusting tastes of drugs and foods by cyclodextrins. *European Journal of Pharmaceutics and Biopharmaceutics* **2005**, *61*, 115–125.
115. Hill, L.E.; Gomes, C.; Taylor, T.M. Characterization of beta-cyclodextrin inclusion complexes containing essential oils (trans-cinnamaldehyde, eugenol, cinnamon bark, and clove bud extracts) for antimicrobial delivery applications. *LWT - Food Science and Technology* **2013**, *51*, 86–93.
116. Ponce Cevallos, P.A.; Buera, M.P.; Elizalde, B.E. Encapsulation of cinnamon and thyme essential oils components (cinnamaldehyde and thymol) in β -cyclodextrin: Effect of interactions with water on complex stability. *Journal of Food Engineering* **2010**, *99*, 70–75.
117. Kunsági-Máté, S.; Csók, Z.; Tuzi, A.; Kollár, L. Permittivity-Dependent Entropy Driven Complexation Ability of Cone and Paco Tetranitro-calix[4]arene toward *para* - Substituted Phenols. *The Journal of Physical Chemistry B* **2008**, *112*, 11743–11749.
118. Roberts, W.J.; Day, A.R. A Study of the Polymerization of α - and β -Pinene with Friedel—Crafts Type Catalysts. **1950**, *72*, 5.
119. García-Padial, M.; Martínez-Ohárriz, M.C.; Navarro-Blasco, I.; Zornoza, A. The Role of Cyclodextrins in ORAC-Fluorescence Assays. Antioxidant Capacity of Tyrosol and

- Caffeic Acid with Hydroxypropyl- β -Cyclodextrin. *Journal of Agricultural and Food Chemistry* **2013**, *61*, 12260–12264.
120. Abdelli, M.; Moghrani, H.; Aboun, A.; Maachi, R. Algerian *Mentha pulegium* L. leaves essential oil: Chemical composition, antimicrobial, insecticidal and antioxidant activities. *Industrial Crops and Products* **2016**, *94*, 197–205.
 121. Anastasaki, E.; Zoumpopoulou, G.; Astraka, K.; Kampoli, E.; Skoumpi, G.; Papadimitriou, K.; Tsakalidou, E.; Polissiou, M. Phytochemical analysis and evaluation of the antioxidant and antimicrobial properties of selected herbs cultivated in Greece. *Industrial Crops and Products* **2017**, *108*, 616–628.
 122. Cutillas, A.-B.; Carrasco, A.; Martinez-Gutierrez, R.; Tomas, V.; Tudela, J. Thyme essential oils from Spain: Aromatic profile ascertained by GC–MS, and their antioxidant, anti-lipoxygenase and antimicrobial activities. *Journal of Food and Drug Analysis* **2018**, *26*, 529–544.
 123. Queiroga, C.L.; Teixeira Duarte, M.C.; Baesa Ribeiro, B.; de Magalhães, P.M. Linalool production from the leaves of *Bursera aloexylon* and its antimicrobial activity. *Fitoterapia* **2007**, *78*, 327–328.
 124. Hamoud, R.; Sporer, F.; Reichling, J.; Wink, M. Antimicrobial activity of a traditionally used complex essential oil distillate (Olbas[®] Tropfen) in comparison to its individual essential oil ingredients. *Phytomedicine* **2012**, *19*, 969–976.
 125. Srivastava, J.K.; Shankar, E.; Gupta, S. Chamomile: A herbal medicine of the past with bright future. *Molecular Medicine Reports* **2010**, *3*, 895–901.
 126. Stanojevic, L.P.; Marjanovic-Balaban, Z.R.; Kalaba, V.D.; Stanojevic, J.S.; Cvetkovic, D.J. Chemical Composition, Antioxidant and Antimicrobial Activity of Chamomile Flowers Essential Oil (*Matricaria chamomilla* L.). *Journal of Essential Oil Bearing Plants* **2016**, *19*, 2017–2028.
 127. Göger, G.; Demirci, B.; Ilgın, S.; Demirci, F. Antimicrobial and toxicity profiles evaluation of the Chamomile (*Matricaria recutita* L.) essential oil combination with standard antimicrobial agents. *Industrial Crops and Products* **2018**, *120*, 279–285.
 128. Memar, M.Y.; Ghotaslou, R.; Samiei, M.; Adibkia, K. Antimicrobial use of reactive oxygen therapy: current insights. *Infect Drug Resist* **2018**, *11*, 567–576.
 129. Máté, G.; Gazdag, Z.; Mike, N.; Papp, G.; Pócsi, I.; Pesti, M. Regulation of oxidative stress-induced cytotoxic processes of citrinin in the fission yeast *Schizosaccharomyces pombe*. *Toxicon* **2014**, *90*, 155–166.

130. Dohare, S.; Dubey, S.D.; Kalia, M.; Verma, P.; Pandey, H.; Singh, K.; Agarwal, V. Anti-biofilm activity of *Eucalyptus globulus* oil encapsulated silica nanoparticles against *E. coli* biofilm. *International Journal of Pharmaceutical Sciences and Research* **2014**, *5*, 5013–5018.
131. Saad, N.Y.; Muller, C.D.; Lobstein, A. Major bioactivities and mechanism of action of essential oils and their components: Essential oils and their bioactive components. *Flavour and Fragrance Journal* **2013**, *28*, 269–279.
132. Bravo Cadena, M.; Preston, G.M.; Van der Hoorn, R.A.L.; Townley, H.E.; Thompson, I.P. Species-specific antimicrobial activity of essential oils and enhancement by encapsulation in mesoporous silica nanoparticles. *Industrial Crops and Products* **2018**, *122*, 582–590.
133. Zorić, N.; Kosalec, I.; Tomić, S.; Bobnjarić, I.; Jug, M.; Vlainić, T.; Vlainić, J. Membrane of *Candida albicans* as a target of berberine. *BMC Complementary and Alternative Medicine* **2017**, *17*, 268.
134. Romero, D.; Sanabria-Valentín, E.; Vlamakis, H.; Kolter, R. Biofilm Inhibitors that Target Amyloid Proteins. *Chemistry & Biology* **2013**, *20*, 102–110.
135. Rukayadi, Y.; Hwang, J.-K. *In Vitro* Activity of Xanthorrhizol Isolated from the Rhizome of Javanese Turmeric (*Curcuma xanthorrhiza* Roxb.) Against *Candida albicans* Biofilms: Anti-Candida Biofilm Activity of Xanthorrhizol. *Phytotherapy Research* **2013**, *27*, 1061–1066.
136. Wu, H.; Moser, C.; Wang, H.-Z.; Høiby, N.; Song, Z.-J. Strategies for combating bacterial biofilm infections. *International Journal of Oral Science* **2015**, *7*, 1–7.
137. Girardot, M.; Imbert, C. Natural Sources as Innovative Solutions Against Fungal Biofilms. In *Fungal Biofilms and related infections: Advances in Microbiology, Infectious Diseases and Public Health Volume 3*; Imbert, C., Ed.; Advances in Experimental Medicine and Biology; Springer International Publishing: Cham, **2016**; pp. 105–125 ISBN 978-3-319-42360-9.
138. Oppenheimer-Shaanan, Y.; Steinberg, N.; Kolodkin-Gal, I. Small molecules are natural triggers for the disassembly of biofilms. *Trends in Microbiology* **2013**, *21*, 594–601.
139. Reen, F.J.; Gutiérrez-Barranquero, J.A.; Parages, M.L.; O’Gara, F. Coumarin: a novel player in microbial quorum sensing and biofilm formation inhibition. *Applied Microbiology and Biotechnology* **2018**, *102*, 2063–2073.
140. Sardi, J. de C.O.; Freires, I.A.; Lazarini, J.G.; Infante, J.; de Alencar, S.M.; Rosalen, P.L. Unexplored endemic fruit species from Brazil: Antibiofilm properties, insights into

- mode of action, and systemic toxicity of four *Eugenia* spp. *Microbial Pathogenesis* **2017**, *105*, 280–287.
141. Verderosa, A.D.; Totsika, M.; Fairfull-Smith, K.E. Bacterial Biofilm Eradication Agents: A Current Review. *Frontiers in Chemistry* **2019**, *7*, 824.
 142. Prasad, R.; Kapoor, K. Multidrug Resistance in Yeast *Candida*. In *International Review of Cytology*; Elsevier, 2004; Vol. 242, pp. 215–248 ISBN 978-0-12-364646-0.
 143. Sharma, D.; Misba, L.; Khan, A.U. Antibiotics versus biofilm: an emerging battleground in microbial communities. *Antimicrobial Resistance & Infection Control* **2019**, *8*, 76.
 144. Tsui, C.; Kong, E.F.; Jabra-Rizk, M.A. Pathogenesis of *Candida albicans* biofilm. *Pathogens and Disease* **2016**, *74*, ftw018.
 145. Brown, A.J.P.; Brown, G.D.; Netea, M.G.; Gow, N.A.R. Metabolism impacts upon *Candida* immunogenicity and pathogenicity at multiple levels. *Trends in Microbiology* **2014**, *22*, 614–622.
 146. Papp, G.; Horváth, E.; Mike, N.; Gazdag, Z.; Belágyi, J.; Gyöngyi, Z.; Bánfalvi, G.; Hornok, L.; Pesti, M. Regulation of patulin-induced oxidative stress processes in the fission yeast *Schizosaccharomyces pombe*. *Food and Chemical Toxicology* **2012**, *50*, 3792–3798.
 147. Brown, A.J.P.; Budge, S.; Kaloriti, D.; Tillmann, A.; Jacobsen, M.D.; Yin, Z.; Ene, I.V.; Bohovych, I.; Sandai, D.; Kastora, S.; et al. Stress adaptation in a pathogenic fungus. *Journal of Experimental Biology* **2014**, *217*, 144–155.
 148. Stepanović, S.; Vuković, D.; Hola, V.; Di Bonaventura, G.; Djukić, S.; Cirković, I.; Ruzicka, F. Quantification of biofilm in microtiter plates: overview of testing conditions and practical recommendations for assessment of biofilm production by staphylococci. *APMIS* **2007**, *115*, 891–899.
 149. Dowd, S.E.; Sun, Y.; Smith, E.; Kennedy, J.P.; Jones, C.E.; Wolcott, R. Effects of biofilm treatments on the multi-species Lubbock chronic wound biofilm model. *Journal of Wound Care* **2009**, *18*, 508, 510–512.
 150. Alves, F.R.F.; Silva, M.G.; Rôças, I.N.; Siqueira Jr, J.F. Biofilm biomass disruption by natural substances with potential for endodontic use. *Brazilian Oral Research* **2013**, *27*, 20–25.
 151. Kirmusaoğlu, S. The Methods for Detection of Biofilm and Screening Antibiofilm Activity of Agents. In *Antimicrobials, Antibiotic Resistance, Antibiofilm Strategies and Activity Methods*; Kirmusaoğlu, S., Ed.; IntechOpen, **2019** ISBN 978-1-78985-789-4.

152. Salari, S.; Sadat Seddighi, N.; Ghasemi Nejad Almani, P. Evaluation of biofilm formation ability in different *Candida* strains and anti-biofilm effects of Fe₃O₄-NPs compared with Fluconazole: an in vitro study. *Journal de Mycologie Médicale* **2018**, *28*, 23–28.
153. Alonso, B.; Cruces, R.; Pérez, A.; Sánchez-Carrillo, C.; Guembe, M. Comparison of the XTT and resazurin assays for quantification of the metabolic activity of *Staphylococcus aureus* biofilm. *Journal of Microbiological Methods* **2017**, *139*, 135–137.
154. Azeredo, J.; Azevedo, N.F.; Briandet, R.; Cerca, N.; Coenye, T.; Costa, A.R.; Desvaux, M.; Di Bonaventura, G.; Hébraud, M.; Jaglic, Z.; et al. Critical review on biofilm methods. *Critical Reviews in Microbiology* **2017**, *43*, 313–351.
155. Kuhn, D.M.; Balkis, M.; Chandra, J.; Mukherjee, P.K.; Ghannoum, M.A. Uses and Limitations of the XTT Assay in Studies of *Candida* Growth and Metabolism. *Journal of Clinical Microbiology* **2003**, *41*, 506–508.
156. Nett, J.E.; Cain, M.T.; Crawford, K.; Andes, D.R. Optimizing a *Candida* biofilm microtiter plate model for measurement of antifungal susceptibility by tetrazolium salt assay. *Journal of Clinical Microbiology* **2011**, *49*, 1426–1433.
157. Kainz, K.; Tadic, J.; Zimmermann, A.; Pendl, T.; Carmona-Gutierrez, D.; Ruckstuhl, C.; Eisenberg, T.; Madeo, F. Methods to Assess Autophagy and Chronological Aging in Yeast. In *Methods in Enzymology*; Elsevier, **2017**; Vol. 588, pp. 367–394 ISBN 978-0-12-809674-1.
158. Sali, N.; Nagy, S.; Poór, M.; Kőszegi, T. Multiparametric luminescent cell viability assay in toxicology models: A critical evaluation. *Journal of Pharmacological and Toxicological Methods* **2016**, *79*, 45–54.
159. Poljšak, B.; Gazdag, Z.; Pesti, M.; Jenko-Brinovec, Š.; Belagyi, J.; Plesničar, S.; Raspor, P. Pro-oxidative versus antioxidative reactions between Trolox and Cr(VI): The role of H₂O₂. *Environmental Toxicology and Pharmacology* **2006**, *22*, 15–19.
160. Tafforeau, L.; Le Blastier, S.; Bamps, S.; Dewez, M.; Vandenhaute, J.; Hermand, D. Repression of ergosterol level during oxidative stress by fission yeast F-box protein Pof14 independently of SCF. *The EMBO Journal* **2006**, *25*, 4547–4556.
161. Khan, H.; Saeed, M.; Muhammad, N.; Tariq, S.A.; Ghaffar, R.; Gul, F. Antimalarial and free radical scavenging activities of aerial parts of *Polygonatum verticillatum* (L.) all. and identification of chemical constituents by GC-MS. *Pakistan Journal of Botany* **2013**, *45*, 497–500.

162. Virág, E.; Pesti, M.; Kunsági-Máté, S. Complex formation between primycin and ergosterol: entropy-driven initiation of modification of the fungal plasma membrane structure. *The Journal of Antibiotics* **2012**, *65*, 193–196.
163. De Cremer, K.; Lanckacker, E.; Cools, T.L.; Bax, M.; De Brucker, K.; Cos, P.; Cammue, B.P.A.; Thevissen, K. Artemisinins, New Miconazole Potentiators Resulting in Increased Activity against *Candida albicans* Biofilms. *Antimicrobial Agents and Chemotherapy* **2015**, *59*, 421–426.
164. Li, W.; Mo, W.; Shen, D.; Sun, L.; Wang, J.; Lu, S.; Gitschier, J.M.; Zhou, B. Yeast Model Uncovers Dual Roles of Mitochondria in the Action of Artemisinin. *PLoS Genetics* **2005**, *1*, e36.
165. Marcos-Zambrano, L.J.; Escribano, P.; Bouza, E.; Guinea, J. Production of biofilm by *Candida* and non-*Candida* spp. isolates causing fungemia: Comparison of biomass production and metabolic activity and development of cut-off points. *International Journal of Medical Microbiology* **2014**, *304*, 1192–1198.
166. Munusamy, K.; Vadivelu, J.; Tay, S.T. A study on *Candida* biofilm growth characteristics and its susceptibility to aureobasidin A. *Revista Iberoamericana de Micología* **2018**, *35*, 68–72.
167. Blankenship, J.R.; Mitchell, A.P. How to build a biofilm: a fungal perspective. *Current Opinion in Microbiology* **2006**, *9*, 588–594.
168. Mowat, E.; Lang, S.; Williams, C.; McCulloch, E.; Jones, B.; Ramage, G. Phase-dependent antifungal activity against *Aspergillus fumigatus* developing multicellular filamentous biofilms. *Journal of Antimicrobial Chemotherapy*. **2008**, *62*, 1281–1284.
169. Mukherjee, P.K.; Chandra, J.; Kuhn, D.M.; Ghannoum, M.A. Mechanism of fluconazole resistance in *Candida albicans* biofilms: phase-specific role of efflux pumps and membrane sterols. *Infection and Immunity* **2003**, *71*, 4333–4340.
170. Ramage, G.; Rajendran, R.; Sherry, L.; Williams, C. Fungal Biofilm Resistance. *International Journal of Microbiology* **2012**, *2012*, doi:10.1155/2012/528521.
171. Raspor, P.; Plesnicar, S.; Gazdag, Z.; Pesti, M.; Miklavcic, M.; Lah, B.; Logarmansek, R.; Poljsak, B. Prevention of intracellular oxidation in yeast: the role of vitamin E analogue, Trolox (6-hydroxy-2,5,7,8-tetramethylkroman-2-carboxyl acid). *Cell Biology International* **2005**, *29*, 57–63.

Supplementary materials

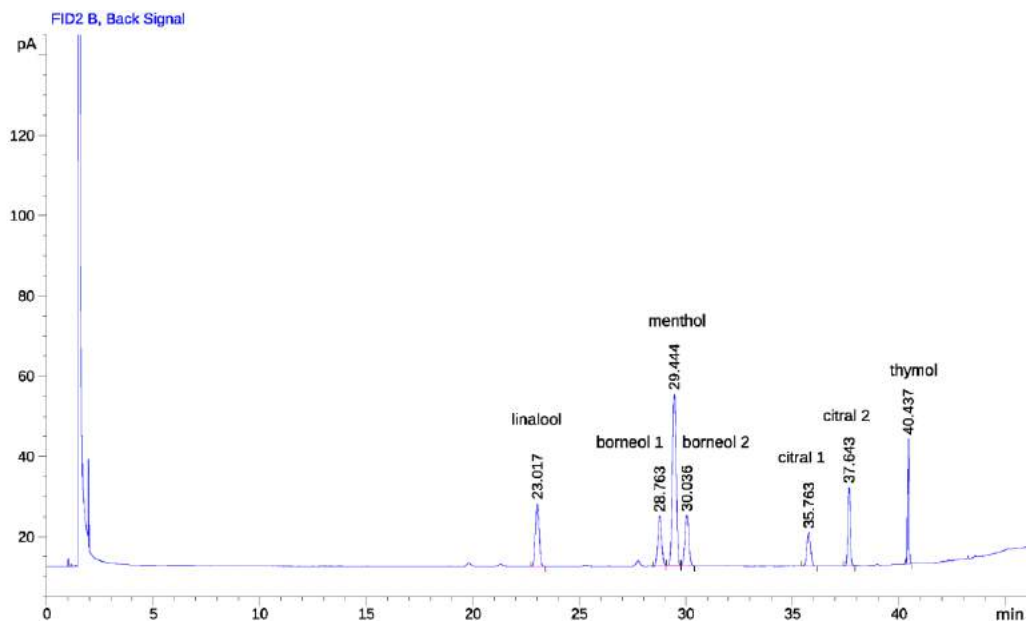


Figure S1. Mixture of EO pure components: GC chromatogram of the solution containing linalool, borneol, menthol, citral and thymol at the concentration of 0.5 mg/mL (each), diluted with acetonitrile.

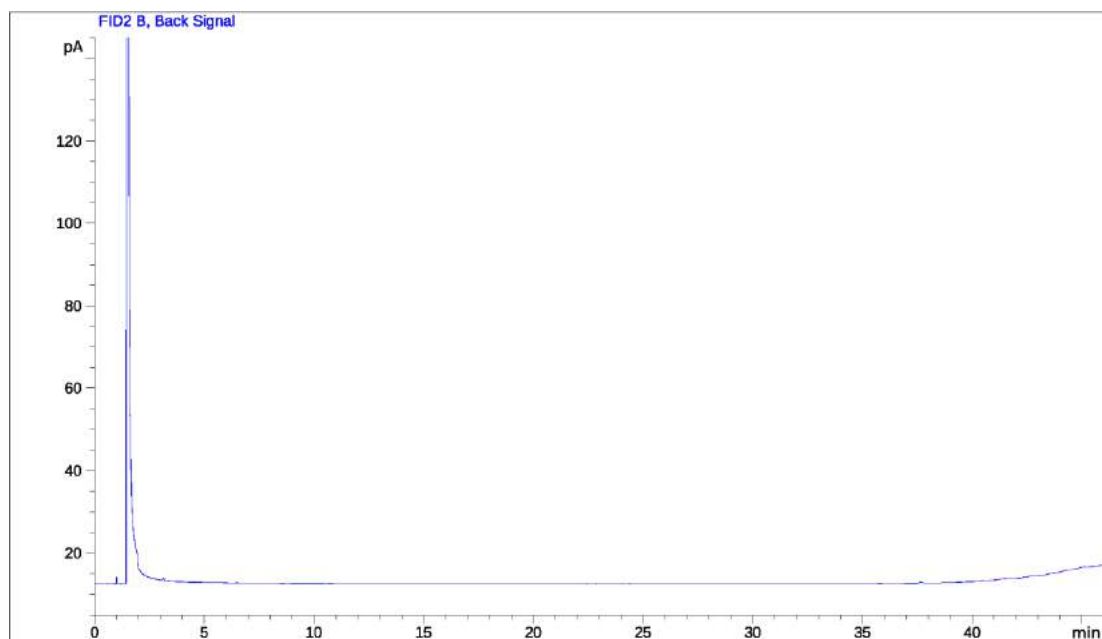


Figure S2. RAMEB only: GC chromatogram of the mixture made by 50 mg RAMEB mixed with acetonitrile at 50 mg/mL, shaken for 10 minutes and the supernatant was used after centrifugation.

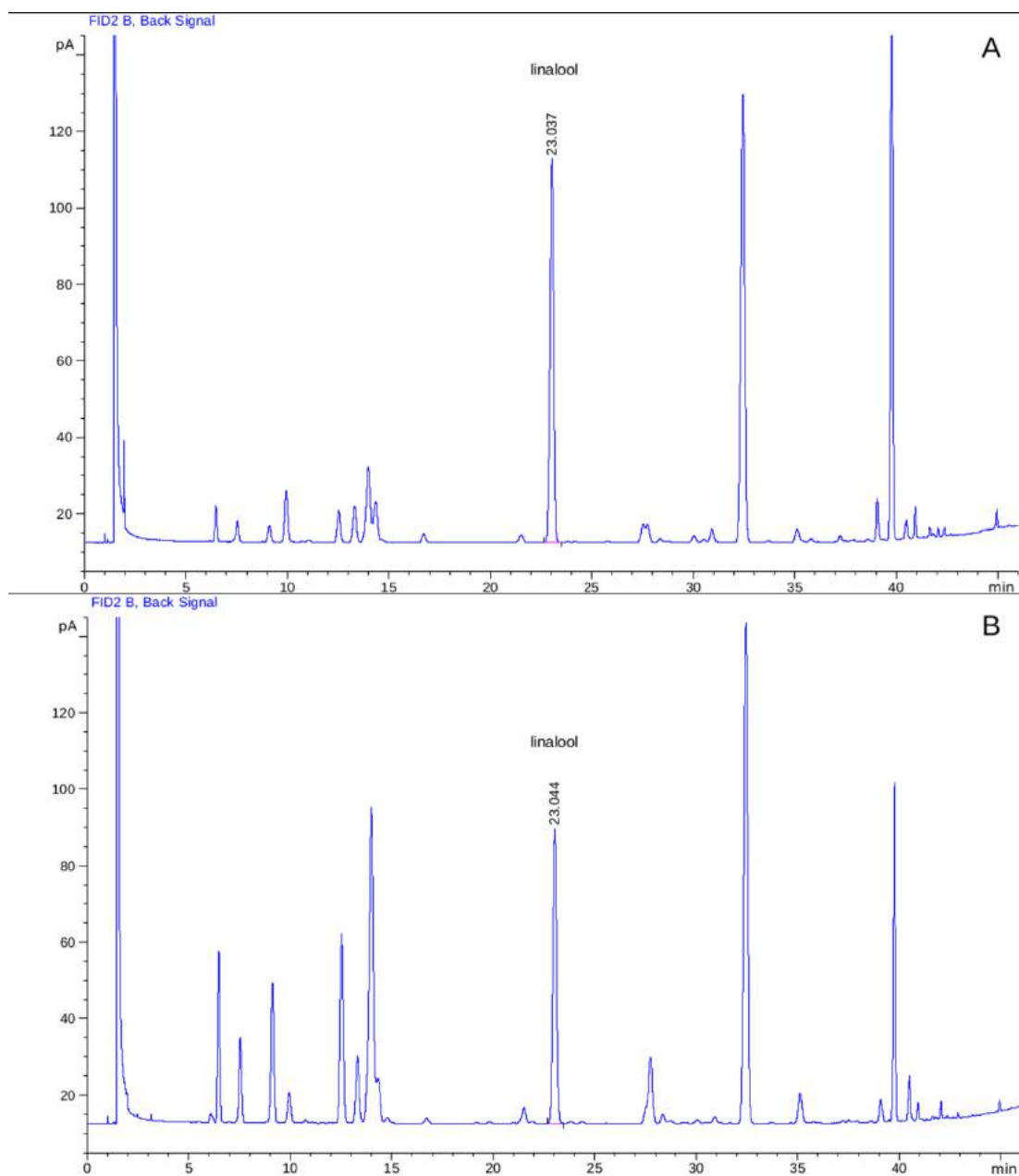


Figure S3. Lavender: GC chromatogram of the solution containing lavender oil (2.5 mg/mL) diluted with acetonitrile (A) and the chromatogram of the mixture prepared by 50 mg RAMEB-lavender oil complex mixed with acetonitrile at 50 mg/mL (B).

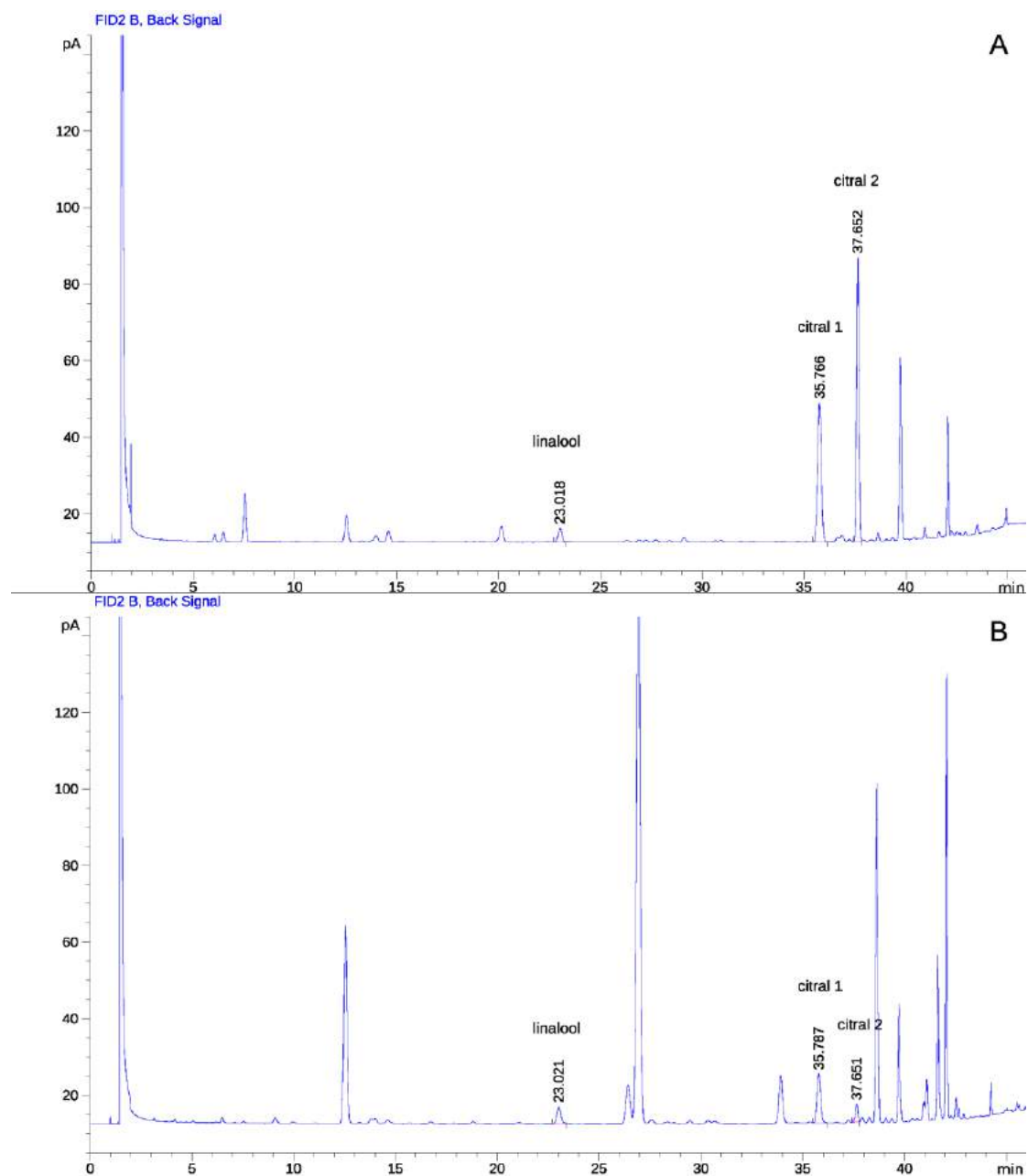


Figure S4. Lemon balm: GC chromatogram of the solution containing lemon balm oil (2.5 mg/mL) diluted with acetonitrile (A) and the chromatogram of the mixture prepared by 50 mg RAMEB-lemon balm oil complex mixed with acetonitrile at 50 mg/mL (B).

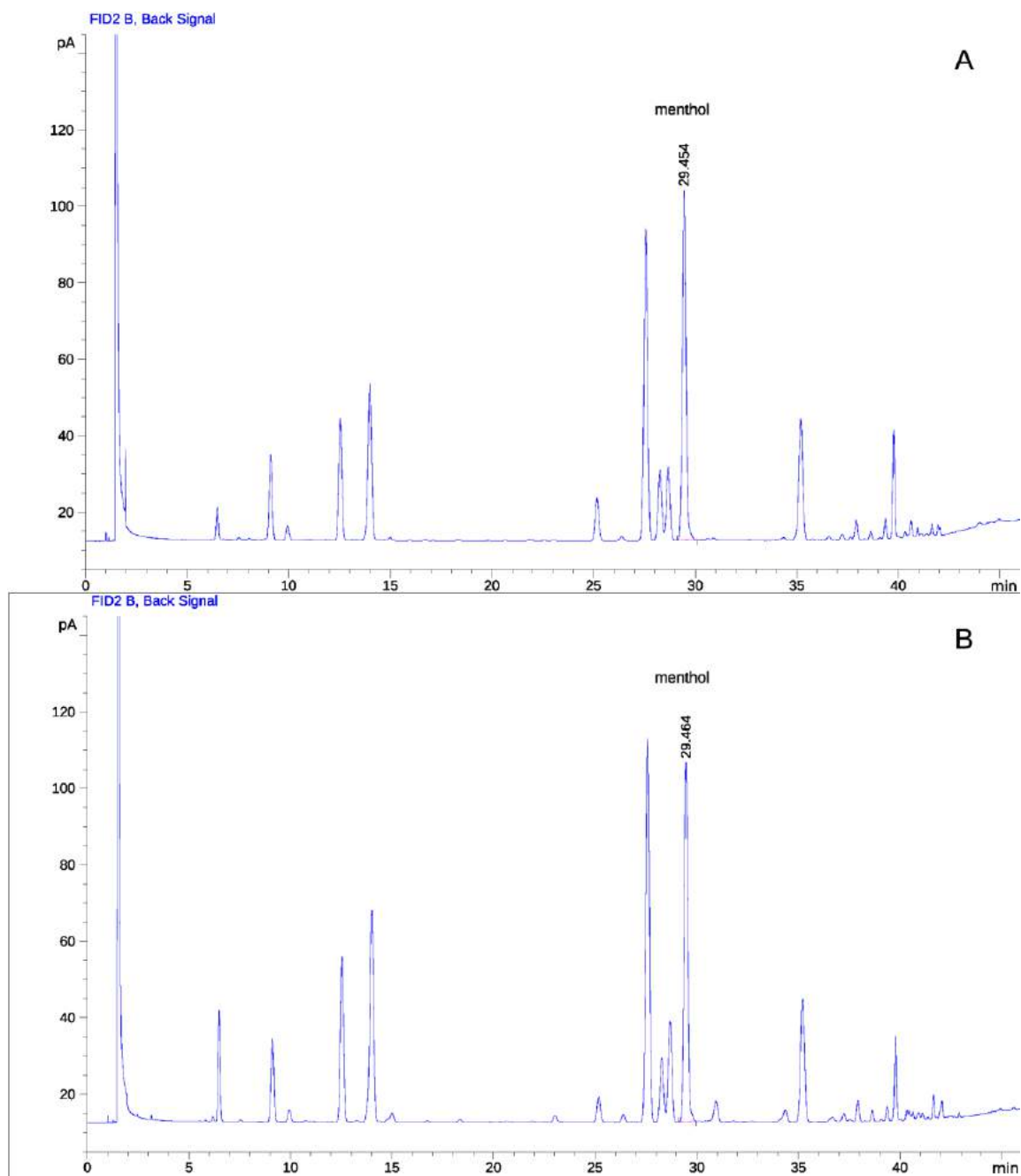


Figure S5. Peppermint: GC chromatogram of the solution containing peppermint oil (2.5 mg/mL) diluted with acetonitrile (A) and the chromatogram of the mixture prepared by 50 mg RAMEB-peppermint oil complex mixed with acetonitrile at 50 mg/mL (B).

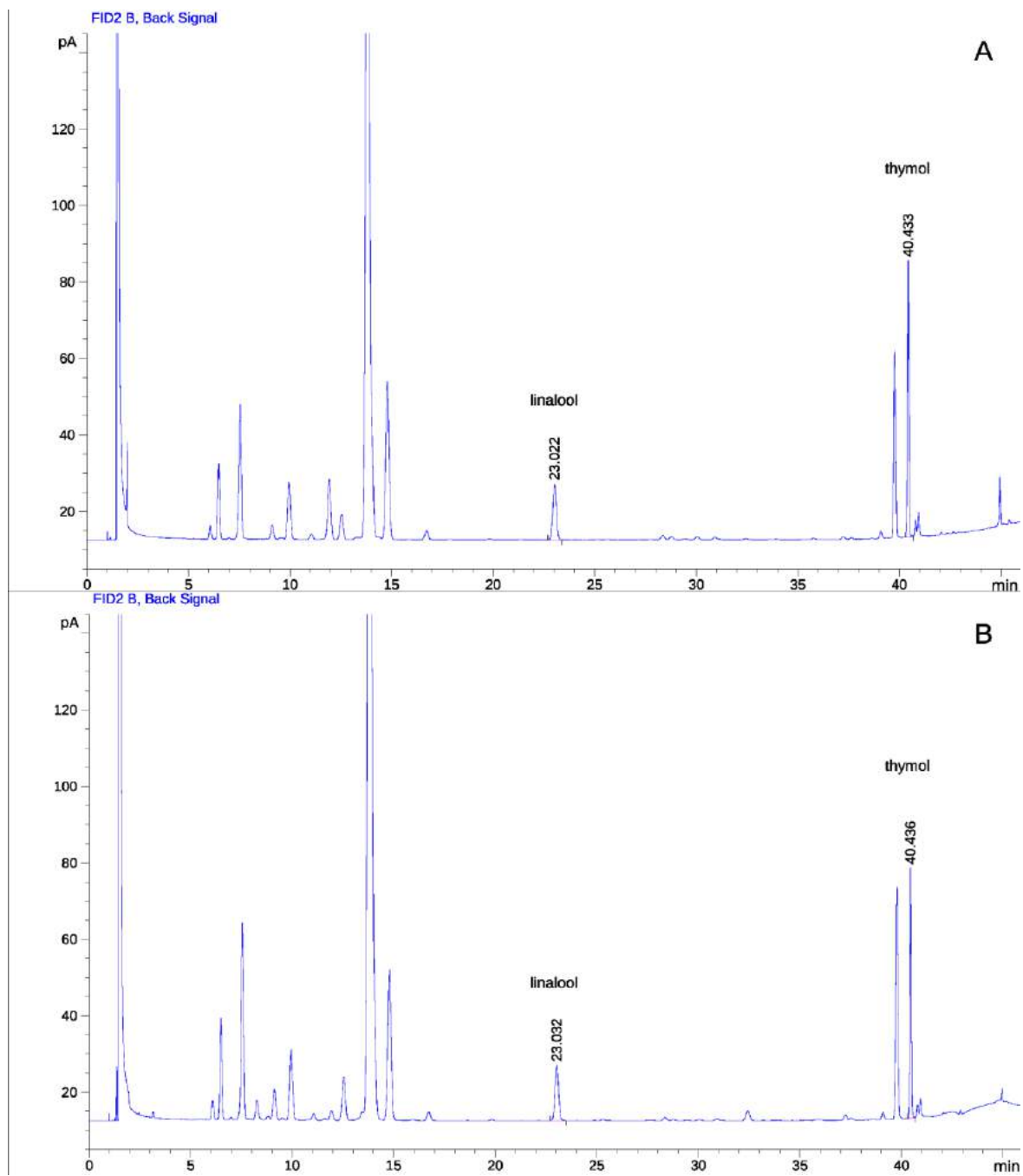
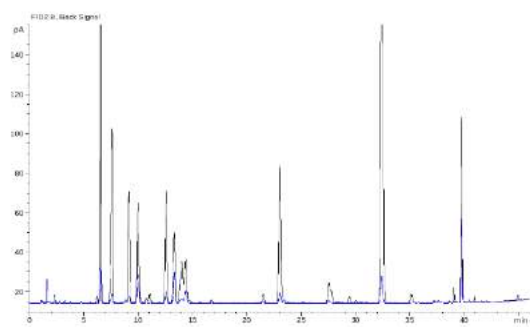
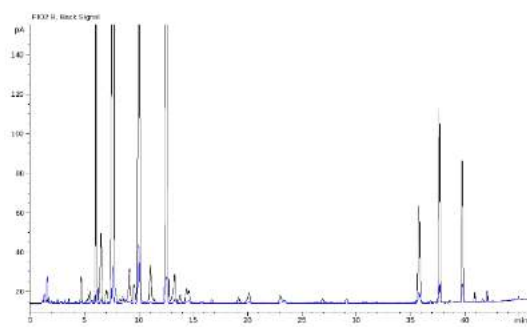


Figure S6. Thyme: GC chromatogram of the solution containing thyme oil (2.5 mg/mL) diluted with acetonitrile (A) and the chromatogram of the mixture prepared by 50 mg RAMEB-thyme oil complex mixed with acetonitrile at 50 mg/mL (B).

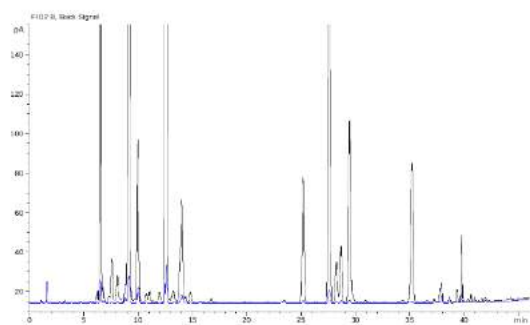
A



B



C



D

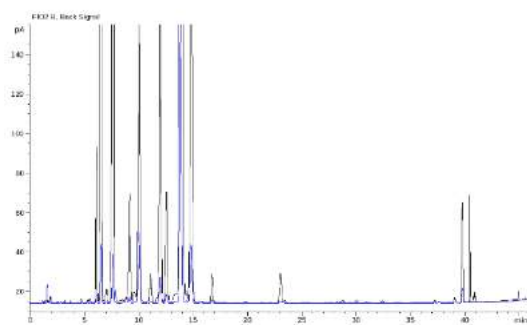


Figure S7. GC chromatograms for studying the encapsulation efficiency of RAMEB complexed lavender oil (A), lemon balm oil (B), peppermint oil (C) and thyme oil (D) based on GC analyses. Black lines: free EOs/components, blue lines: RAMEB complexed EOs/components.

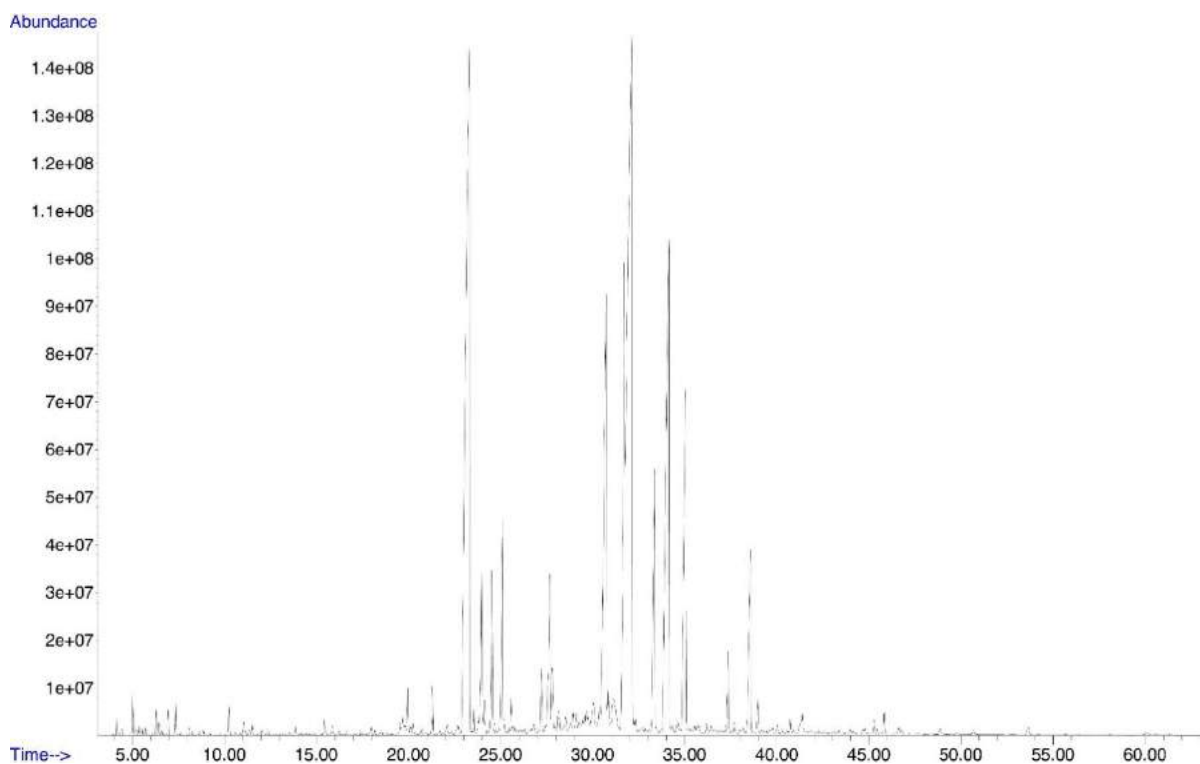


Figure S8. Chromatogram of chamomile essential oil obtained by GC-MS.

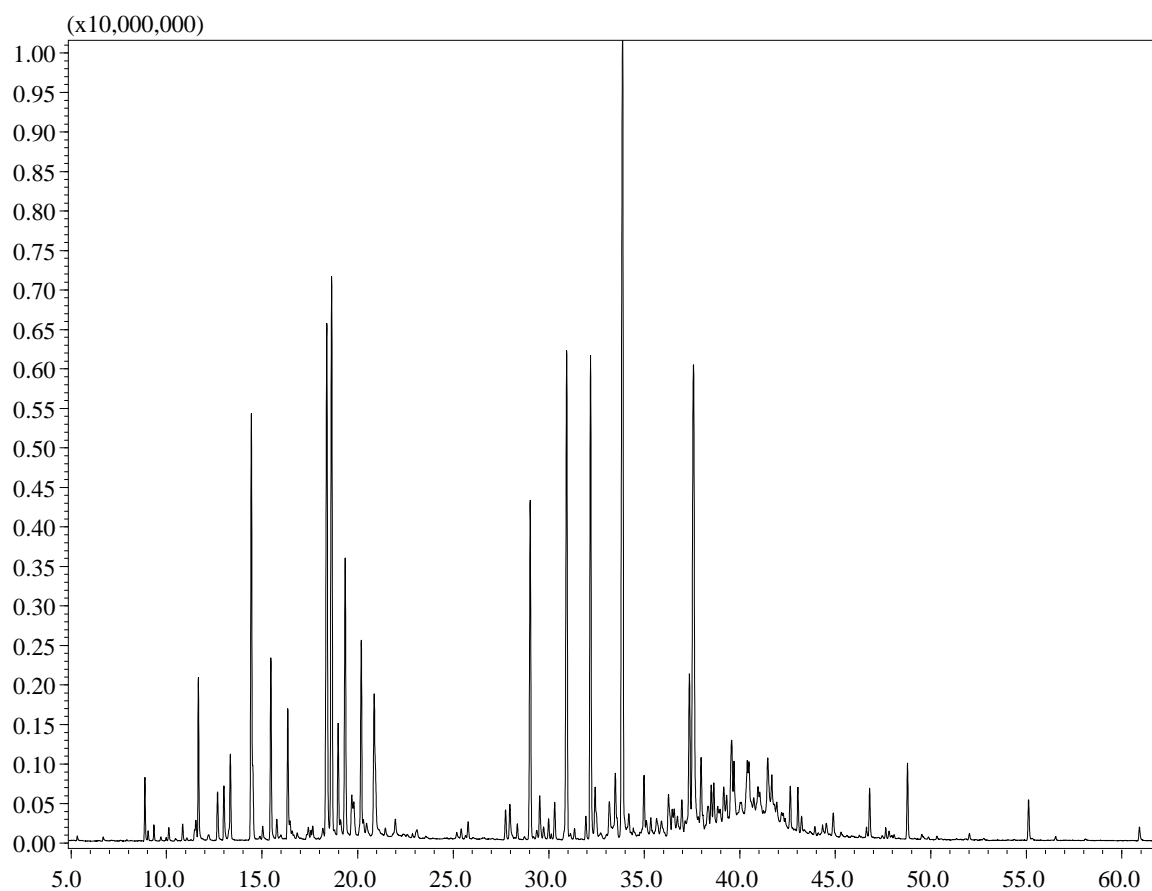


Figure S9. GC-MS chromatogram relative to the analysis of *Artemisia annua* L. essential oil on SLB-5ms column.

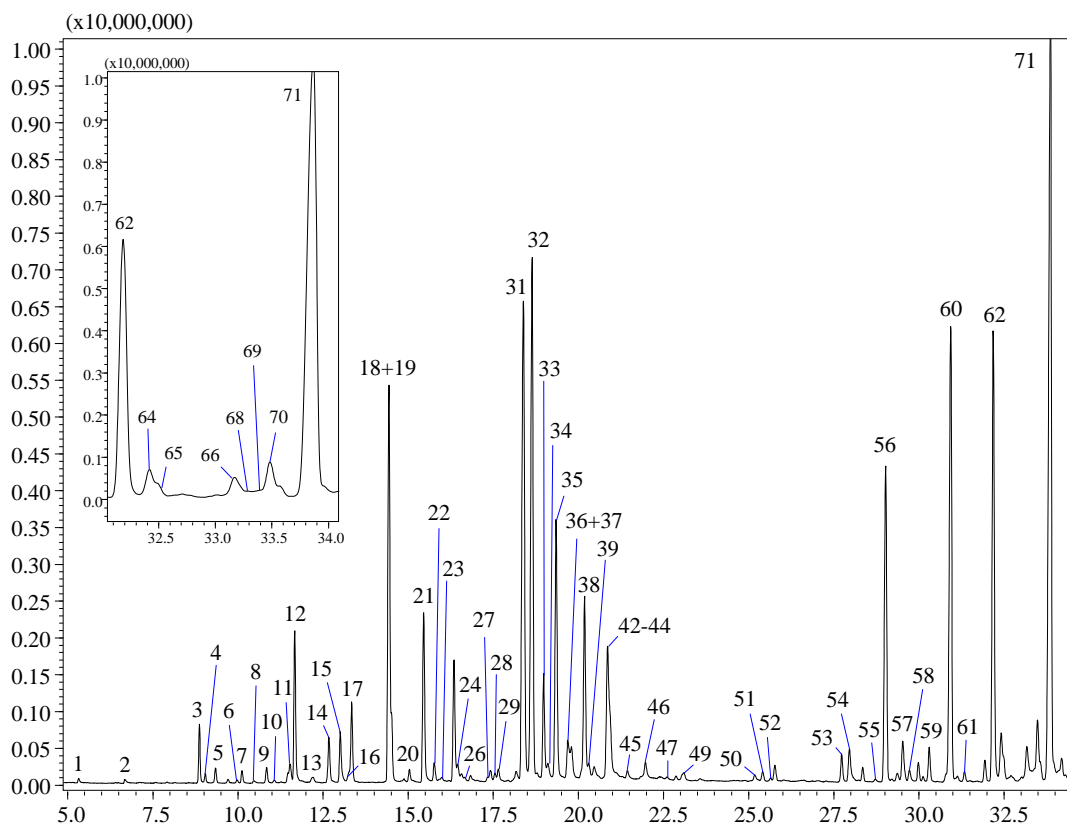


Figure S10. Expansion (5-35min) of the GC-MS chromatogram relative to the analysis of *Artemisia annua* L. essential oil on SLB-5ms column.

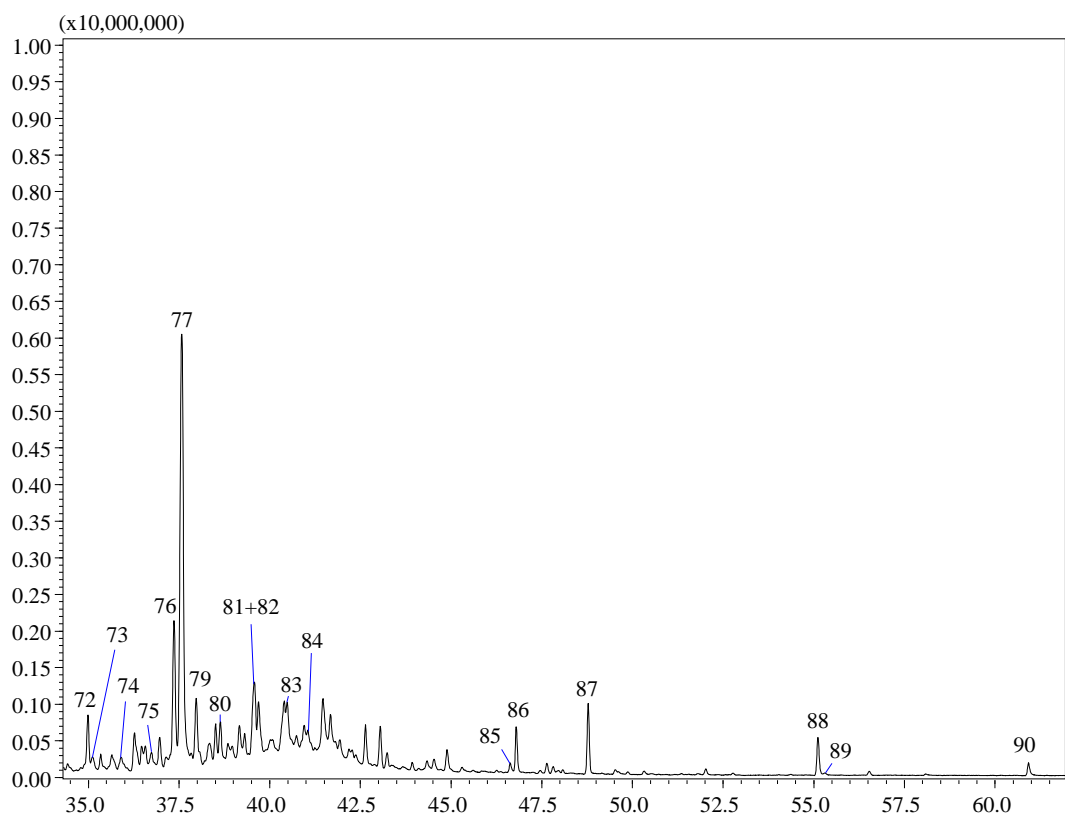


Figure S11. Expansion (35-63min) of the GC-MS chromatogram relative to the analysis of *Artemisia annua* L. essential oil on SLB-5ms column.

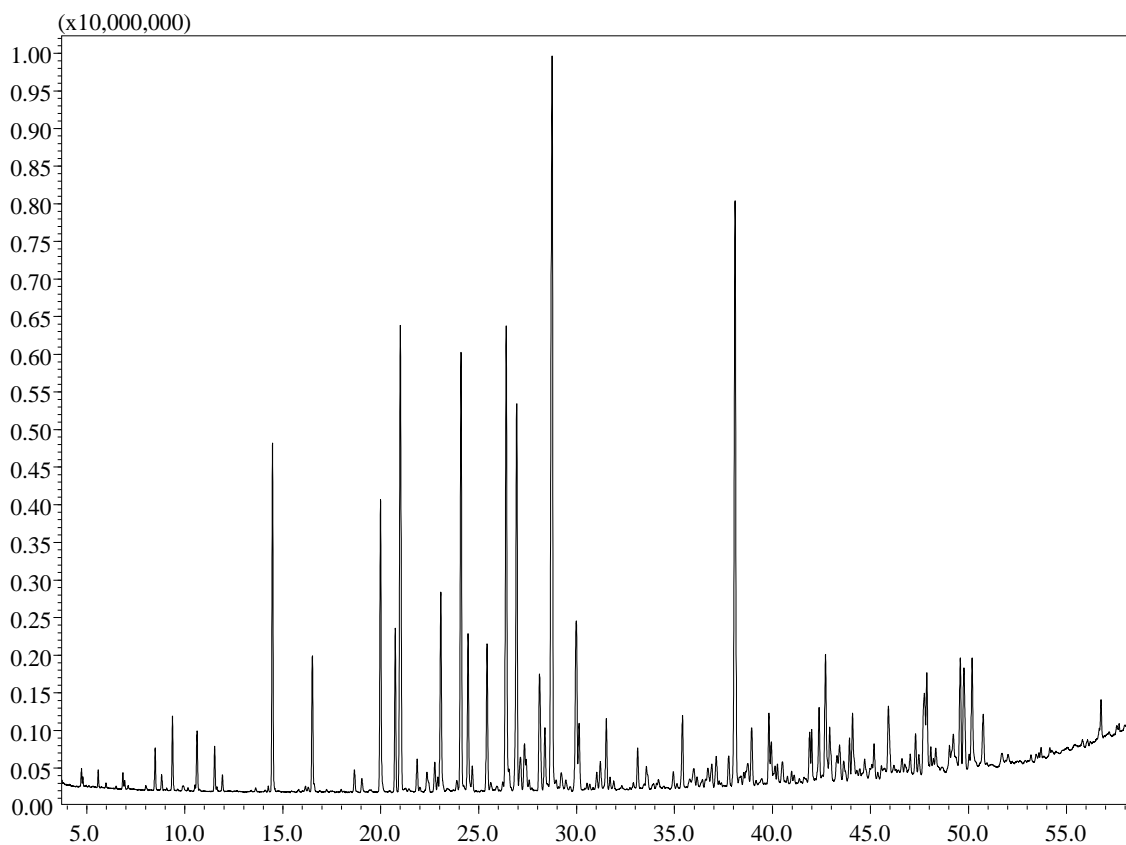


Figure S12. GC-MS chromatogram relative to the analysis of *Artemisia annua* L. essential oil on Supelcowax-10 column.

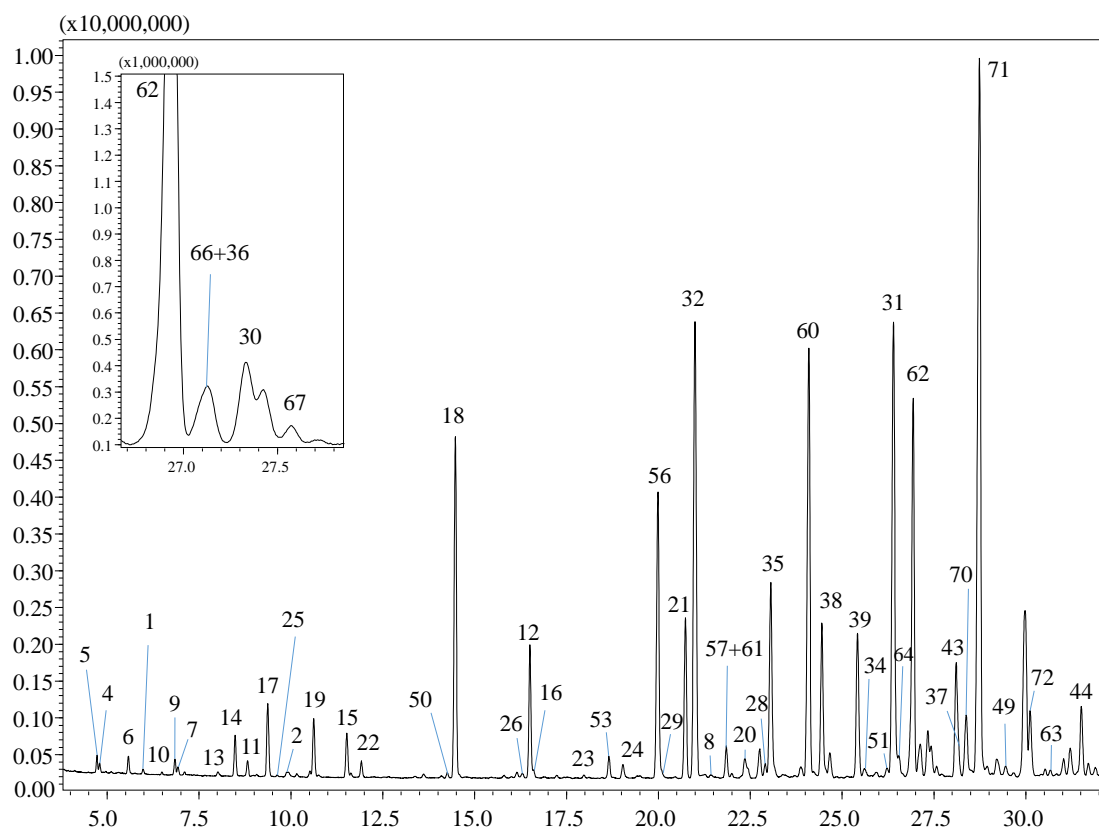


Figure S13. Expansion (4-32min) of GC-MS chromatogram relative to the analysis of *Artemisia annua* L. essential oil on Supelcowax-10 column.

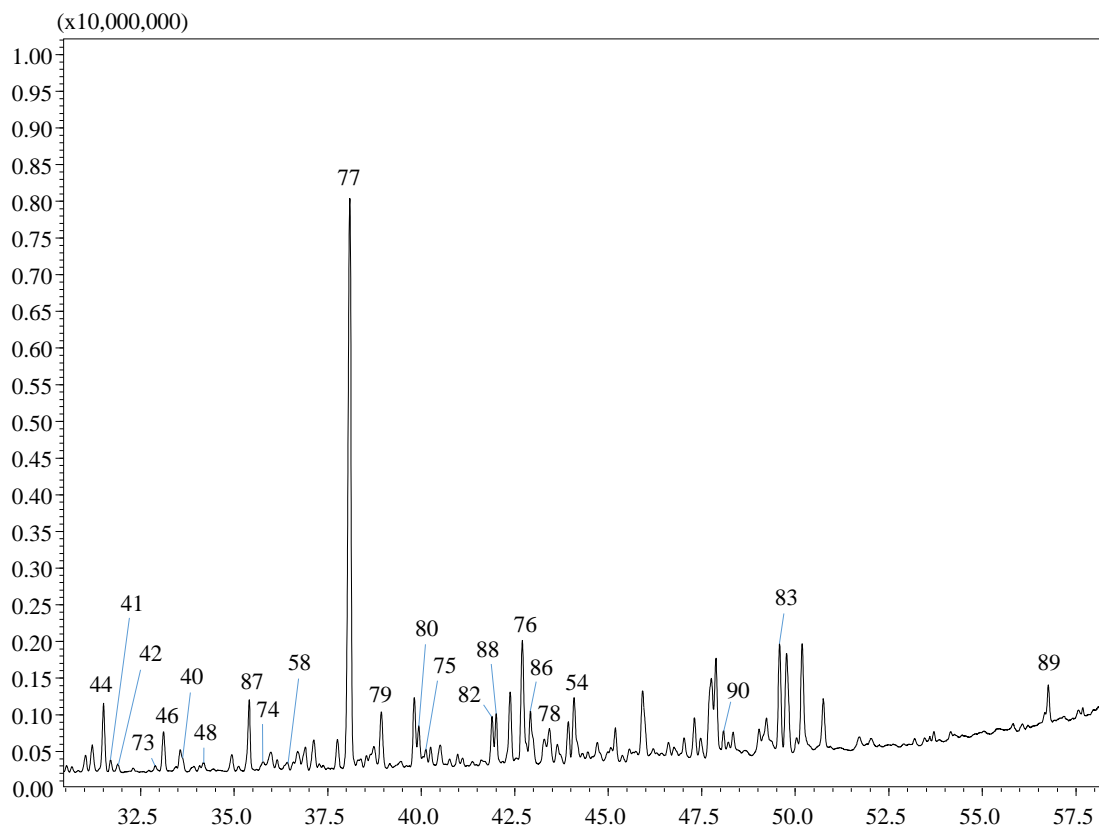


Figure S14. Expansion (32-58min) of the GC-MS chromatogram relative to the analysis of *Artemisia annua* L. essential oil on Supelcowax-10 column.

Table S1. Results of GC-MS analysis of chamomile EO. In the table the major components can be seen, the compounds that were present significantly under 1% were not indicated or identified.

No.	Compound	t _R (min)	Area percentage (%)
1	trans β -Farnesene	23.304	17.93
2	Germacrene D	23.971	1.54
3	bicyclogermacrene	24.526	1.39
4	(E,E)- α -Farnesene	25.100	2.08
5	spathulenol	27.676	1.88
6	Bisabolol oxide B	30.732	7.57
7	Bisabolone	32.133	21.83
8.	Chamazulen	33.375	3.19
9.	Bisabolol oxide A	34.127	10.48
10.	Vetivazulene	35.048	4.94

Table S2. Identification of chemical composition of *Artemisia annua* L. essential oil by using LRI (Linear Retention Index). LRI lib are values reported in FFNSC 3.01 library; LRI exp are obtained experimentally on SLB-5ms and Supelcowax-10 columns. % MS Sim. represents the similarity between experimental and library spectra. Quantification of chemical composition of *Artemisia annua* L. essential oil is expressed by GC % area.

ID	Compounds	% MS Sim.	SLB-5ms			Supelcowax-10			
			LRI Lib	LRI exp	Sample Area %	% MS Sim.	LRI Lib	LRI exp	Sample Area %
1	Hexanal	91	802	801	0.05	92	480	477	0.05
2	2-Hexenal, (E)	92	850	850	0.07	92	631	628	0.06
3	Artemisia triene	95	922	923	0.40	-	-	-	nd
4	Thujene <alpha->	97	926	927	0.05	96	428	427	0.05
5	Pinene <alpha->	96	934	933	0.10	95	425	427	0.11
6	Camphene	97	951	953	0.02	91	462	459	0.23
7	Thuja-2,4(10)-diene	96	955	953	0.06	97	521	519	0.06
8	Benzaldehyde	98	963	960	0.05	95	925	931	0.03
9	Sabinene	97	974	972	0.12	97	517	518	0.11
10	Pinene <beta->	97	980	978	0.03	93	502	505	0.02
11	1,8-cineol <2,3-Dehydro->	87	992	991	0.17	95	602	-	0.14
12	Yomogi alcohol	97	995	996	1.29	95	810	812	1.32
13	Phellandrene <alpha->	92	1008	1007	0.03	89	570	574	0.04
14	Terpinene <alpha->	96	1019	1018	0.31	97	589	586	0.28
15	Cymene <para->	95	1026	1025	0.38	97	676	678	0.35
16	Santolina alcohol	86	1031	1033	0.07	96	812	814	0.05
17	Eucalyptol	98	1033	1032	0.55	96	617	614	0.57
18	Artemisia ketone	92	1058	1056	4.43	91	756	754	3.98
19	Terpinene <gamma->	91	1060	1058	*	95	651	654	0.47
20	Sabinene hydrate <cis->	91	1071	1069	0.13	92	964	-	0.21
21	Artemisia alcohol	94	1081	1079	1.68	94	914	913	1.74
22	Terpinolene	93	1088	1086	0.15	95	686	681	0.13
23	Cymenene <para->	94	1093	1093	0.05	89	846	847	0.02
24	Sabinene hydrate <trans->	86	1099	1103	0.15	92	872	873	0.15
25	Menthatriene <1,3,8-para->	-	-	-	nd	88	624	626	0.01
26	Nonanal <n->	86	1106	1107	0.08	91	805	807	0.04
27	Sabina ketone <dehydro->	89	1122	1122	0.03	-	-	-	nd
28	Menth-2-en-1-ol <cis-, para->	95	1127	1124	0.10	85	968	968	0.09
29	Campholenal <alpha->	92	1129	1125	0.10	91	898	899	0.09
30	Verbenol <trans->	-	-	-	nd	91	1080	1079	0.70
31	Pinocarveol <trans->	93	1145	1141	7.55	94	1056	1055	7.60
32	Camphor	95	1151	1149	7.06	96	920	918	6.82
33	Pinene oxide <beta->	87	1158	1156	1.25	-	-	-	nd
34	Sabina ketone	93	1160	1157	0.16	90	1035	1035	0.13
35	Pinocarvone	95	1166	1164	3.22	95	971	971	2.91

36	Terpineol <delta->	94	1173	1170	0.43	95	1075	1076	0.35 ^B
37	Borneol	96	1175	1173	0.40	94	1102	-	1.71 ^C
38	Terpinen-4-ol	91	1184	1184	1.75	90	1005	1002	1.66
39	Myrtenal	95	1186	1196	0.11	87	1030	1034	1.51
40	Cymen-8-ol <para->	91	1189	1189	0.15	91	1247	1243	0.18
41	Isocarveol <trans->	85	1191	1189	0.12	90	1193	1192	0.15
42	Mentha-1,5-dien-7-ol <para->	85	1195	1194	0.06	91	1198	1191	0.08
43	Terpineol <alpha->	92	1198	1195	2.19	95	1099	1099	1.71 ^C
44	Myrtenol	95	1201	1202	*	96	1188	1191	0.85
45	Verbenone	94	1211	1208	0.12	-	-	-	nd
46	Carveol <trans->	93	1222	1223	0.39	91	1232	1232	0.40
47	Butanoate <hex-(3Z)- enyl, 2-methyl->	86	1231	1231	0.08	-	-	-	nd
48	Carveol <cis->	86	1236	1232	0.11	90	1262	1262	0.11
49	Carvone	94	1247	1246	0.11	92	1135	1133	0.05
50	Tridec-1-ene <n->	95	1293	1292	0.13	95	750	-	0.01
51	Pinocarvyl acetate <trans->	92	1298	1296	0.07	85	1051	1052	0.07
52	Thymol	87	1293	1293	0.09	-	-	-	nd
53	Cubebene <alpha->	90	1345	1350	0.16	98	863	864	0.19
54	Eugenol	85	1356	1357	0.42	87	1554	1552	0.61
55	Cyclosativene	93	1372	1367	0.02	-	-	-	nd
56	Copaene <alpha->	93	1380	1375	2.75	95	896	898	2.87
57	Cubebene <beta->	95	1391	1392	0.32	96	941	942	0.36 ^A
58	Jasmone <(Z)->	93	1396	1394	0.12	86	1326	1330	0.10
59	Ylanga-2,4(15)-diene	89	1410	1411	0.16	-	-	-	nd
60	Caryophyllene <(E)->	95	1425	1424	5.26	96	996	996	5.55
61	Copaene <beta->	90	1434	1432	0.07	93	942	944	0.36 ^A
62	Farnesene <(E)-, beta->	91	1455	1452	4.80	96	1070	1070	4.07
63	Sesquisabinene	-	-	-	nd	92	1166	1170	0.05
64	Humulene <alpha->	91	1459	1460	0.34	95	1067	1067	0.40
65	Cadina-4,11-diene	88	1462	1458	0.15	-	-	-	nd
66	Selina-4,11-diene	91	1478	1476	0.29	86	1074	1076	0.35 ^B
67	Muurolene <gamma->	-	-	-	nd	95	1086	1086	0.13
68	Amorpha-4,7(11)-diene	90	1481	1480	0.06	-	-	-	nd
69	Ionone <(E)-, beta->	92	1483	1482	0.08	-	-	-	nd
70	Germacrene D	89	1485	1480	0.52	92	1107	-	0.59
71	Selinene <beta->	97	1497	1492	12.27	94	1116	1117	12.75
72	Cadinene <delta->	94	1523	1518	0.42	93	1152	1152	0.47
73	Calamenene <trans->	89	1526	1527	0.12	88	1226	1229	0.05
74	Calacorene <alpha->	90	1546	1544	0.10	87	1306	1310	0.12
75	Nerolidol <(E)->	87	1563	1561	0.15	93	1431	1431	0.15
76	Spathulenol	84	1581	1576	1.75	89	1510	1512	1.15
77	Caryophyllene oxide	91	1589	1587	8.64	93	1371	1364	8.71
78	Copaen-4-alfa-ol <beta->	-	-	-	nd	87	1532	1534	0.39
79	Salvial-4(14)-en-1-one	88	1599	1596	0.62	94	1395	1397	0.57
80	Humulene epoxide II	86	1616	1613	0.73	90	1425	1431	0.43

81	Eudesma-4(15),11-dien-5-ol	85	1639	-	1.06	-	-	-	nd
82	Cadin-4en-7-ol <cis->	88	1642	1638	*	89	1485	1486	0.40
83	Eudesma-4(15),7-dien-1-beta-ol	88	1665	1670	0.75	87	1730	-	1.06
84	Mustakone	89	1681	1681	1.27	-	-	-	nd
85	Neophytadiene	94	1837	1836	0.33	-	-	-	nd
86	Phytone	90	1842	1841	0.25	89	1516	1514	0.54
87	Nonadecane	95	1901	1900	0.29	88	1295	1296	0.41
88	Heneicosane <n->	95	2101	2100	0.12	88	1488	1488	0.27
89	Phytol	92	2107	2111	0.17	95	1982	1983	0.22
90	Tricosane <n->	96	2301	2300	0.24	94	1681	1678	0.29
	Not identified				18.99				21.43
	TOTAL				100.00				100.00

nd: not detected

*: coelution

*A: coelution between Cubebene <beta-> and Copaene <beta-> on Supelcowax-10 column

*B: coelution between Terpeneol <delta-> and Selina-4,11-diene on Supelcowax-10 column

*C: coelution between Terpeneol <alpha-> and Borneol on Supelcowax-10 column

List of publications and conferences

Articles related to this thesis

1. **Das Sourav**, Gazdag Zoltán, Sente Lajos, Meggyes Mátyás, Horváth Györgyi, Lemli Beáta, Kunsági-Máté Sándor, Kuzma Mónika, Kőszegi Tamás. Antioxidant and antimicrobial properties of randomly methylated β cyclodextrin – captured essential oils, FOOD CHEMISTRY 278 pp. 305-313., 9 p. (2019). **IF: 6.306**
2. **Das Sourav**, Horváth Barbara, Šafranko Silvija, Jokić Stela, Széchenyi Aleksandar, Kőszegi Tamás. Antimicrobial activity of chamomile essential oil: Effect of different formulations, MOLECULES 24: 23 Paper: 4321, 18 p. (2019). **IF: 3.267**
3. **Das Sourav**, Czuni Lilla, Báló Viktória, Papp Gábor, Gazdag Zoltán, Papp Nóra, Kőszegi Tamás. Cytotoxic action of artemisinin and scopoletin on planktonic forms and on biofilms of *Candida* species, MOLECULES 25: 3 Paper: 476, 18 p. (2020). **IF: 3.267**
4. **Das Sourav**, Vörös-Horváth Barbara, Bencsik Tímea, Micalizzi Giuseppe, Mondello Luigi, Horváth Györgyi, Kőszegi Tamás, Széchenyi Aleksandar, Antimicrobial activity of different Artemisia essential oil formulations, MOLECULES 25: 10 Paper 2390, 27p. (2020). **IF: 3.267**

Article not related to this thesis

1. Csepregi Rita, Temesfői Viktória, **Das Sourav**, Alberti Ágnes, Tóth Csenge Anna, Herczeg Róbert, Papp Nóra, Kőszegi Tamás, Cytotoxic, Antimicrobial, Antioxidant Properties and Effects on Cell Migration of Phenolic Compounds of Selected Transylvanian Medicinal Plants, ANTIOXIDANTS 9: 2 Paper 166. 29p. (2020). **IF: 5.014**

Cumulative impact factor: 21.121

Conference presentations related to this thesis

1. **Das Sourav**, Gazdag Zoltán, Sente Lajos, Meggyes Mátyás, Horváth Györgyi, Kőszegi Tamás. Antioxidant and antimicrobial properties of randomly methylated β cyclodextrin complexed Essential Oils. International Conference on Analytical

and Nanoanalytical Methods for Biomedical and Environmental Sciences. IC-ANMBES (2018) pp. 112-112. , 1 p.

2. **Das Sourav**, Czuni Lilla, Balo Viktoria, Papp Gabor, Gazdag Zoltan, Koszegi Tamás. Anti-biofilm and cytotoxic activities of artemisinin and scopoletin on *Candida* spp. in combination with caspofungin. 46th Annual Conference on Yeasts May 7-10 2019 Slovakia Programme and Abstracts (2019) pp. 60-60. , 1 p.

Conference presentations not related to this thesis

1. Kócsó József Dániel, **Das Sourav**, Kovács Melinda, Gazdag Zoltán, Kőszegi Tamás, Papp Gábor. Cytotoxic effect and peroxides generation of deoxynivalenol and zearalenone alone or in combination on fission yeast. XVI. János Szentágothai Multidisciplinary Conference and Student Competition – Abstracts Pécs, Hungary: János Szentágothai Scholastic Honorary Society, Faculty of Sciences, University of Pécs, (2019) pp. 244-244. , 1 p.
2. Bouchelaghem Sarra, **Das Sourav**, Gazdag Zoltán, Fekete Csaba, Kőszegi, Tamás, Naorem Romen, Papp Gábor. Antimicrobial activities of Hungarian propolis alone and in combination with antibiotics and its antibiofilm activity on *Staphylococcus aureus*. XVI. János Szentágothai Multidisciplinary Conference and Student Competition – Abstracts Pécs, Hungary : János Szentágothai Scholastic Honorary Society, Faculty of Sciences, University of Pécs, (2019) pp. 16-16. , 1 p.
3. Balo Viktoria, Czuni Lilla, **Das Sourav**, Fekete Csaba, Papp Gábor, , Peter Urbán, Kőszegi, Tamás, Gazdag Zoltán. Examination of the antibiotic sensitivity and biofilm forming ability of various *Candida* strains. 46th Annual Conference on Yeasts May 7-10 2019 Slovakia Programme and Abstracts (2019) pp. 58-58. , 1 p.

Figure and table legends

Figure 1. Characteristics of synthetic cyclodextrins. Shapes, dimensions, chemical structures, and complexation of natural cyclodextrins.

Figure 2. Sketch of a Pickering emulsion and a classical (surfactant-based) emulsion.

Figure 3. The UV absorption spectra of the physical mixture of essential oil-RAMEB (1), physical mixture of component-RAMEB (2), essential oil (3), active component (4), encapsulated essential oil-RAMEB (5), encapsulated component-RAMEB (6), RAMEB (7) and chemicals extracted from encapsulated essential oils.

Figure 4. The A, B, C, and D represents slope, stability constant (K_s , L/mol), enthalpy (ΔH , kJ/mol), and entropy (ΔS , J/Kmol) changes of encapsulated essential oils and active components at specified temperatures.

Figure 5. Antioxidant activities of investigated EO-RAMEB (A) and EO components RAMEB (B) complexes. The effects of selected RAMEB packed EOs and their components on ORAC, ECL, and DPPH assays.

Figure 6. Anti-fungal and anti-microbial activity of investigated EO-RAMEB and EO component-RAMEB complexes and on *S. pombe*, *E. coli* and *S. aureus*.

Figure 7. Comparison of the live/dead discrimination results between the plate reader assay and the flow cytometric assay using SYBR Green I/propidium iodide double staining on *S. pombe*.

Figure 8. Percentage death of cells using SYBR Green I/PI double-stained plate reader method for live/dead discrimination of the test microbes.

Figure 9. Minimum inhibitory concentration (MIC_{90}) of C_{Pe} , C_{T80} , C_{Et} , and vancomycin (Van, $\mu\text{g/mL}$) on *E. coli* (A), *S. aureus* (B), *B. subtilis* (C), *P. aeruginosa* (D), and *S. pyogenes* (E).

Figure 10. Minimum inhibitory concentration (MIC_{90}) of C_{Pe} , C_{T80} , C_{Et} , and caspofungin (Cas, $\mu\text{g/mL}$) on *S. pombe* (A), *C. albicans* (B), and *C. tropicalis* (C).

Figure 11. Minimum effective concentration (MEC_{10}) of C_{Pe} , C_{T80} , C_{Et} , and Van ($\mu\text{g/mL}$) on *E. coli* (A), *S. aureus* (B), *B. subtilis* (C), *P. aeruginosa* (D), and *S. pyogenes* (E).

Figure 12. Minimum effective concentration (MEC_{10}) of C_{Pe} , C_{T80} , C_{Et} , and Cas ($\mu\text{g/mL}$) on *S. pombe* (A), *C. albicans* (B), and *C. tropicalis* (C).

Figure 13. Percentage oxidative stress generation by C_{Pe} , C_{T80} , C_{Et} , and Van on *E. coli* (A), *S. aureus* (B), *B. subtilis* (C), *P. aeruginosa* (D), and *S. pyogenes* (E).

Figure 14. Percentage oxidative stress generation by C_{Pe} , C_{T80} , C_{Et} , and Cas on *S. pombe* (A), *C. albicans* (B), and *C. tropicalis* (C).

Figure 15. Colony-forming unit (CFU/mL) of C_{Pe} , C_{T80} , and C_{Et} on *E. coli* (A), *S. aureus* (B), *B. subtilis* (C), *P. aeruginosa* (D), and *S. pyogenes* (E).

Figure 16. Colony-forming unit (CFU/mL) of C_{Pe}, C_{T80}, and C_{Et} on *S. pombe* (A), *C. albicans* (B), and *C. tropicalis* (C).

Figure 17. Mean percentage viability of C_{Pe}, C_{T80}, and C_{Et} on *E. coli* (A), *S. aureus* (B), *B. subtilis* (C), *P. aeruginosa* (D), and *S. pyogenes* (E).

Figure 18. Mean percentage viability of C_{Pe}, C_{T80}, and C_{Et} on *S. pombe* (A), *C. albicans* (B), and *C. tropicalis* (C).

Figure 19. Minimum inhibitory concentrations (MIC₉₀) (mean ± SD) of artemisinin (Ar) and scopoletin (Sc) on *C. albicans* (A), *C. dubliniensis* (B), *C. tropicalis* (C), *C. krusei* (D), *C. glabrata* (E), *C. guilliermondii* (F) and *C. parapsilosis* (G) species.

Figure 20. Minimum effective concentrations (MEC₁₀) (mean ± SD) of artemisinin (Ar) and scopoletin (Sc) on *C. albicans* (A), *C. dubliniensis* (B), *C. tropicalis* (C), *C. krusei* (D), *C. glabrata* (E), *C. guilliermondii* (F) and *C. parapsilosis* (G) species.

Figure 21. Effects of artemisinin (Ar) and scopoletin (Sc) at their MEC₁₀ concentrations on the metabolic activity, amount of biofilm biomass, and viability of *C. albicans* (A), *C. dubliniensis* (B), *C. tropicalis* (C), *C. krusei* (D), *C. glabrata* (E), *C. guilliermondii* (F), and *C. parapsilosis* (G) cell populations.

Figure 22. Effects of artemisinin (Ar) and scopoletin (Sc) at their MEC₁₀ concentrations on the viability of planktonic *C. albicans* (A), *C. dubliniensis* (B), *C. tropicalis* (C), *C. krusei* (D), *C. glabrata* (E), *C. guilliermondii* (F), and *C. parapsilosis* (G) species.

Figure 23. Effects of artemisinin (Ar) and scopoletin (Sc) at their MEC₁₀ concentrations on the metabolic activities of planktonic *C. albicans* (A), *C. dubliniensis* (B), *C. tropicalis* (C), *C. krusei* (D), *C. glabrata* (E), *C. guilliermondii* (F), and *C. parapsilosis* (G) species.

Figure 24. Effects of artemisinin (Ar) and scopoletin (Sc) at their MEC₁₀ concentrations on colony formation of planktonic *C. albicans* (A), *C. dubliniensis* (B), *C. tropicalis* (C), *C. krusei* (D), *C. glabrata* (E), *C. guilliermondii* (F) and *C. parapsilosis* (G) species.

Figure 25. Effects of artemisinin (Ar) and scopoletin (Sc) at their MEC₁₀ levels on peroxide (O₂²⁻) and superoxide anion (O₂⁻) generation in planktonic *C. albicans* (A), *C. dubliniensis* (B), *C. tropicalis* (C), *C. krusei* (D), *C. glabrata* (E), *C. guilliermondii* (F), and *C. parapsilosis* (G) species.

Figure 26. Minimum inhibitory concentration (MIC₉₀) of AEP, AET, AEE, and vancomycin (VAN) in µg/mL on *E. coli* (A), *S. aureus* (B), *B. subtilis* (C), *P. aeruginosa* (D), and *S. pyogenes* (E).

Figure 27. Minimum inhibitory concentration (MIC₉₀) of AEP, AET, AEE, and caspofungin (CAS) in µg/mL on *S. pombe* (A), *C. albicans* (B), *C. tropicalis* (C), *C. dubliniensis* (D) and *C. krusei* (E).

Figure 28. Minimum effective concentration (MEC₁₀) of AEP, AET, and AEE (µg/mL) on *E. coli* (A), *S. aureus* (B), *B. subtilis* (C), *P. aeruginosa* (D), and *S. pyogenes* (E).

Figure 29. Minimum effective concentration (MEC₁₀) of AEP, AET, and AEE (µg/mL) on *S. pombe* (A), *C. albicans* (B), *C. tropicalis* (C), *C. dubliniensis* (D) and *C. krusei* (E).

Figure 30. Percentage oxidative stress generation by AEP, AET, AEE, and VAN on *E. coli* (A), *S. aureus* (B), *B. subtilis* (C), *P. aeruginosa* (D), and *S. pyogenes* (E) at their respective MEC₁₀ concentrations after a one-hour treatment.

Figure 31. Percentage oxidative stress generation by AEP, AET, AEE, and CAS on *S. pombe* (A), *C. albicans* (B), *C. tropicalis* (C), *C. dubliniensis* (D) and *C. krusei* (E) at their respective MEC₁₀ concentrations and after a one-hour treatment.

Figure 32. Effects of AEP, AET, and AEE at their MEC₁₀ concentrations on the mean percentage colony-forming unit (CFU/mL) decrement of the planktonic *E. coli* (A), *S. aureus* (B), *B. subtilis* (C), *P. aeruginosa* (D), and *S. pyogenes* (E).

Figure 33. Effects of AEP, AET, and AEE at their MEC₁₀ concentrations on the metabolic activities of the mean percentage colony-forming unit (CFU/mL) decrement of the planktonic *S. pombe* (A), *C. albicans* (B), *C. tropicalis* (C), *C. dubliniensis* (D) and *C. krusei* (E).

Figure 34. Effects of AEP, AET and AEE at their MEC₁₀ concentrations on the total protein content (TP) and intracellular ATP/TP ratio of the planktonic *E. coli* (A), *S. aureus* (B), *B. subtilis* (C), *P. aeruginosa* (D), and *S. pyogenes* (E).

Figure 35. Effects of AEP, AET, and AEE at their MEC₁₀ concentrations on the total protein content (TP) and intracellular ATP/TP ratio of the planktonic *S. pombe* (A), *C. albicans* (B), *C. tropicalis* (C), *C. dubliniensis* (D) and *C. krusei* (E).

Figure 36. Mean percentage non-viability of AEP, AET and AEE at their MEC₁₀ concentrations on the metabolic activities of the planktonic *E. coli* (A), *S. aureus* (B), *B. subtilis* (C), *P. aeruginosa* (D), and *S. pyogenes* (E).

Figure 37. Mean percentage non-viability of AEP, AET, and AEE at their MEC₁₀ concentrations on the metabolic activities of the planktonic *S. pombe* (A), *C. albicans* (B), *C. tropicalis* (C), *C. dubliniensis* (D) and *C. krusei* (E).

Figure 38. Effects of AEP, AET and AEE at their MEC₁₀ concentrations on the metabolic activities of the planktonic *E. coli* (A), *S. aureus* (B), *B. subtilis* (C), *P. aeruginosa* (D), and *S. pyogenes* (E).

Figure 39. Effects of AEP, AET and AEE at their MEC₁₀ concentrations on the metabolic activities of the planktonic *S. pombe* (A), *C. albicans* (B), *C. tropicalis* (C), *C. dubliniensis* (D) and *C. krusei* (E).

Figure 40. Effects of AEP, AET and AEE after 24 h of treatments at their respective MEC₁₀ concentrations on the metabolic activity, amount of biofilm biomass, and

viability of *C. albicans* (A), *C. tropicalis* (B), *C. dubliniensis* (C) and *C. krusei* (D) cell populations.

Figure 41. Effects of AEP, AET, and AEE after 24 h of treatments at their respective MEC₁₀ concentrations on the ATP and the total protein content (TP) of *C. albicans* (A), *C. tropicalis* (B), *C. dubliniensis* (C) and *C. krusei* (D) cell populations in the mature biofilms.

Table 1. *Candida* species examined in the study.

Supplementary figure and table legends

Figure S1. Mixture of EO pure components: GC chromatogram of the solution containing linalool, borneol, menthol, citral and thymol at the concentration of 0.5 mg/mL (each), diluted with acetonitrile.

Figure S2. RAMEB only: GC chromatogram of the mixture made by 50 mg RAMEB mixed with acetonitrile at 50 mg/mL, shaken for 10 minutes and the supernatant was used after centrifugation.

Figure S3. Lavender: GC chromatogram of the solution containing lavender oil (2.5 mg/mL) diluted with acetonitrile (A) and the chromatogram of the mixture prepared by 50 mg RAMEB-lavender oil complex mixed with acetonitrile at 50 mg/mL (B).

Figure S4. Lemon balm: GC chromatogram of the solution containing lemon balm oil (2.5 mg/mL) diluted with acetonitrile (A) and the chromatogram of the mixture prepared by 50 mg RAMEB-lemon balm oil complex mixed with acetonitrile at 50 mg/mL (B).

Figure S5. Peppermint: GC chromatogram of the solution containing peppermint oil (2.5 mg/mL) diluted with acetonitrile (A) and the chromatogram of the mixture prepared by 50 mg RAMEB-peppermint oil complex mixed with acetonitrile at 50 mg/mL (B).

Figure S6. Thyme: GC chromatogram of the solution containing thyme oil (2.5 mg/mL) diluted with acetonitrile (A) and the chromatogram of the mixture prepared by 50 mg RAMEB-thyme oil complex mixed with acetonitrile at 50 mg/mL (B).

Figure S7. GC chromatograms for studying the encapsulation efficiency of RAMEB complexed lavender oil (A), lemon balm oil (B), peppermint oil (C) and thyme oil (D) based on GC analyses. Black lines: free EOs/components, blue lines: RAMEB complexed EOs/components.

Figure S8. Chromatogram of chamomile essential oil obtained by GC-MS.

Figure S9. GC-MS chromatogram relative to the analysis of *Artemisia annua* L. essential oil on SLB-5ms column.

Figure S10. Expansion (5-35min) of the GC-MS chromatogram relative to the analysis of *Artemisia annua* L. essential oil on SLB-5ms column.

Figure S11. Expansion (35-63min) of the GC-MS chromatogram relative to the analysis of *Artemisia annua* L. essential oil on SLB-5ms column.

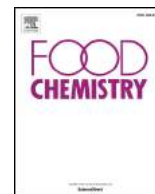
Figure S12. GC-MS chromatogram relative to the analysis of *Artemisia annua* L. essential oil on Supelcowax-10 column.

Figure S13. Expansion (4-32min) of GC-MS chromatogram relative to the analysis of *Artemisia annua* L. essential oil on Supelcowax-10 column.

Figure S14. Expansion (32-58min) of the GC-MS chromatogram relative to the analysis of *Artemisia annua* L. essential oil on Supelcowax-10 column.

Table S1. Results of GC-MS analysis of chamomile EO. In the table the major components can be seen, the compounds that were present significantly under 1% were not indicated or identified.

Table S2. Identification of chemical composition of *Artemisia annua* L. essential oil by using LRI (Linear Retention Index). LRI lib are values reported in FFNSC 3.01 library; LRI exp are obtained experimentally on SLB-5ms and Supelcowax-10 columns. % MS Sim. represents the similarity between experimental and library spectra. Quantification of chemical composition of *Artemisia annua* L. essential oil is expressed by GC % area.



Antioxidant and antimicrobial properties of randomly methylated β cyclodextrin – captured essential oils

Sourav Das^a, Zoltán Gazdag^{b,f}, Lajos Szente^c, Mátyás Meggyes^d, Györgyi Horváth^e, Beáta Lemli^{g,h}, Sándor Kunsági-Máté^{g,h}, Mónika Kuzmaⁱ, Tamás Kőszegi^{a,g,*}

^a Department of Laboratory Medicine, University of Pécs, Medical School, 7624 Pécs, Ifjúság u. 13., Hungary

^b Department of General and Environmental Microbiology, Institute of Biology, University of Pécs, 7624 Pécs, Ifjúság u. 6., Hungary

^c CycloLab Cyclodextrin Research & Development Laboratory, Ltd., 1097 Budapest, Illatos út 7., Hungary

^d Department of Medical Microbiology and Immunology, University of Pécs, Medical School, 7624 Pécs, Szigeti út 12., Hungary

^e Department of Pharmacognosy, University of Pécs, 7624 Pécs, Rókus u. 2., Hungary

^f Microbial Biotechnology Research Group, János Szentágotthai Research Center, University of Pécs, 7624 Pécs, Ifjúság u. 20., Hungary

^g János Szentágotthai Research Center, University of Pécs, 7624 Pécs, Ifjúság u. 20., Hungary

^h Department of Pharmaceutical Chemistry, University of Pécs, 7624 Pécs, Rókus u. 2., Hungary

ⁱ Department of Forensic Medicine, University of Pécs, Medical School, 7624 Pécs, Szigeti út 12., Hungary

ARTICLE INFO

Keywords:

Essential oils
Methylated β cyclodextrin
Antioxidant capacity
Fluorescence antimicrobial test
Microplate assay

ABSTRACT

Free essential oils and their active components have a low physicochemical stability and low aqueous solubility which limit their applications as food preservatives and in packaging industry. The aim of this study was to characterize the physicochemical properties, antioxidant activities and antimicrobial activity of randomly methylated β cyclodextrin (RAMEB) encapsulated thyme oil, lemon balm oil, lavender oil, peppermint oil and their active components that include thymol, citral, linalool, menthol and borneol. Inclusion complex formation of essential oils (EOs) and RAMEB were evaluated by several methods. Antioxidant capacities of RAMEB-EOs/components were reported to be more stable than free EOs/components ($P < 0.05$). Rapid SYBR green I/propidium iodide live/dead microbial cellular discrimination assay for *Schizosaccharomyces pombe*, *Escherichia coli* and *Staphylococcus aureus* showed similar results when compared with flow cytometry analysis ($P < 0.01$) suggesting that our novel microplate fluorescence method could be applied for the fast live/dead microbial discrimination in antimicrobial assays.

1. Introduction

Natural volatile aromatic oily plant extracts (essential oils, EOs) have been in focus for a long time because of their antioxidant and antimicrobial activity (Costa, Garcia-Diaz, Jimenez, & Silva, 2013) without exerting health hazards. On the other hand, recent studies consider synthetic antioxidants like butylated hydroxyanisole (BHA) and butylated hydroxytoluene (BHT) as potential carcinogenic agents (Kfoury, Auezova, Greige-Gerges, & Fourmentin, 2015). Opposite to synthetic antioxidants, several EOs are classified as “Generally Recognized as Safe” (GRAS) and the Environment Protection Agency does not require toxicity data. Therefore, these compounds are widely accepted by the consumers all over the world. EOs along with their purified components can be considered as alternative preservatives in food

and pharmaceutical industries and several studies highlight the effectiveness of the use of EOs and their components in the preservation of food products (Kfoury et al., 2016). EOs can be introduced into the packaging system because of their active biological potencies due to their insect repellent capacity and they might provide protection against the penetration of the insect pests and microorganisms (Kfoury, Pipkin, Antle, & Fourmentin, 2017). Therefore, packaging systems integrated with essential oils could be a solution for industrial high-level expectations (Cid et al., 2013; Cid et al., 2014). One of the major drawbacks of using EOs in food packaging is their interaction with the organoleptic features of foods causing alterations in the flavoring characteristics. Thus, designing proper controlled release of EOs inside the food packaging system should be done to optimize the preservation applications. Hence, the development of controlled release system for

* Corresponding author at: Department of Laboratory Medicine, University of Pécs, Medical School, 7624 Pécs, Ifjúság u. 13., Hungary.

E-mail addresses: pharma.souravdas@gmail.com (S. Das), gazdag@gamma.ttk.pte.hu (Z. Gazdag), szente@cyclolab.hu (L. Szente), meggyes.matyas@pte.hu (M. Meggyes), gyorgyi.horvath@aok.pte.hu (G. Horváth), lemli.beata@gytk.pte.hu (B. Lemli), kunsagi-mate.sandor@gytk.pte.hu (S. Kunsági-Máté), monika.kuzma@aok.pte.hu (M. Kuzma), tamas.koszegi@aok.pte.hu (T. Kőszegi).

<https://doi.org/10.1016/j.foodchem.2018.11.047>

Received 20 January 2018; Received in revised form 31 October 2018; Accepted 9 November 2018

Available online 09 November 2018

0308-8146/ © 2018 Elsevier Ltd. All rights reserved.

the essential oils inside packaging system is required for the optimization of their application.

Cyclodextrins (CDs) are also in a major research focus because of their potent encapsulating property (Astray, Gonzalez-Barreiro, Mejuto, Rial-Otero, & Simal-Gándara, 2009). EOs complexation with CDs may act as a potential reservoir for trapping volatile components and thus providing controlled release and formulation in hydrophilic environment can be achieved. It has been suggested that inclusion of EOs and their components into CDs can provide protection against harmful environmental conditions and allow the preservation of antioxidant and antimicrobial activity (Astray et al., 2009). CDs are cyclic oligosaccharides derived from the enzymatic conversion of starch. They are non-toxic with hydrophilic outer surface and a hydrophobic core allowing the hydrophobic guest molecule to enter and stay inside. This interaction among the guest molecules and CDs forms a non-covalent inclusion complex in polar medium. This inclusion complex is in dynamical equilibrium allowing the guest molecule to diffuse out from the CDs complex system (Ciobanu, Landy, & Fourmentin, 2013). Native CDs are composed of six, seven or eight glucosyl units and are known as α -cyclodextrin (α -CD), β -cyclodextrin (β -CD) and γ -cyclodextrin (γ -CD), respectively. The diameter of the CDs cavity is measured by the number of glucose units in the CD and this controls the size of the guest molecule for encapsulation. Many CD derivatives with enhanced solubility and increased encapsulation performance are of major interest at present.

Inclusion of EOs with CDs can act as a reservoir of volatile component encapsulation and eventually may allow controlled release of the oils. This enables the EOs to reach the desired concentration in the food without exceeding the organoleptically tolerated levels. Several research papers have documented that preservation of EOs with CDs might help in conserving the guest molecule's properties including antioxidant and antimicrobial activities by protecting them from the harmful environmental conditions. The combination of EOs and CD as a complex to be used as active food packaging material has been suggested because CDs are non-toxic cyclic oligosaccharides (Rakmai, Cheirsilp, & Mejuto et al., 2017).

Non-complexed EOs are suggested to have antioxidant and antimicrobial activity properties. Indeed, several papers have reported the antioxidant and antimicrobial activity of EOs dissolved in polar solvents like DMSO, and ethanol. Water miscible EOs have been found to possess antimicrobial and antioxidant activity. However, these solvents might cause interference with the EOs' micro-environment as they are composed of several active molecules which react with polar solvents differently (Rakmai, Cheirsilp, & Torrado-Agrasar et al., 2017; Rakmai, Cheirsilp, Mejuto, Torrado-Agrasar, & Simal-Gándara, 2018).

The aim of this work was to evaluate the total antioxidant capacity (TAC) and antimicrobial activities of four EOs namely, lemon balm oil (*Melissa officinalis* L.), lavender oil (*Lavandula angustifolia* Mill.), peppermint oil (*Mentha x piperita* L.), thyme oil (*Thymus vulgaris* L.) and their components such as, borneol, citral, linalool, menthol and thymol using their RAMEB complexes. We also established a novel fluorescence microplate viability assay using SYBR green I/propidium iodide double staining for the rapid live/dead discrimination of Gram-negative/positive test bacteria and *Schizosaccharomyces pombe* (*S. pombe*) treated with EOs-RAMEB compounds. These oils and their components are known for their antioxidant, antimicrobial, analgesic and anti-inflammatory properties (Chrysargyris, Panayiotou, & Tzortzakakis, 2016). To our best knowledge, it is the first time that effects of EOs-RAMEB and EOs components-RAMEB complexes have been evaluated by rapid live/dead discrimination of Gram-negative/positive test bacteria and *Schizosaccharomyces pombe* using SYBR green I/propidium iodide double stained fluorescent assay technique with simultaneous analysis of their antimicrobial and antioxidant properties.

2. Materials and methods

2.1. Reagents and materials

All chemicals used for the in vitro analysis were of analytical or spectroscopic grade and highly purified water ($< 1 \mu\text{S}$) was applied throughout the experiments. Horseradish peroxidase (POD from Sigma Aldrich), 1 mg/mL bovine serum albumin (BSA, Serva) in 50 mmol/L phosphate buffer pH 7.4, H_2O_2 (Molar Chemicals) diluted with 0.1% citric acid (Ph. Eur 8.0.), 6-hydroxy-2,5,7,8-tetramethylchroman-2-carboxylic acid (Trolox), luminol, para-iodophenol, diphenyl-2-2 picryl-hydroxyl (DPPH, stable free radical), fluorescein Na_2 salt, 2,2'-azobis (2-methylpropionamide) dihydrochloride (AAPH), SYBR green I and propidium iodide (PI) were all from Sigma Aldrich and used as received. Ethanol and methanol (Reanal, Hungary) were of spectroscopic grade. In the oxygen radical absorbance capacity (ORAC) assay, 75 mmol/L K-phosphate buffer of pH 7.4 was used. All the EOs/components – RAMEB namely lavender oil, lemon balm oil, peppermint oil, thyme oil, \pm borneol, cis/trans citral, linalool, menthol and thymol were obtained from CycloLab Cyclodextrin Research & Development Laboratory, Ltd. (Budapest, Hungary).

For the microbial culture media, trypsin soy broth from Biolab (Hungary), peptone (OXOID, UK), NaCl (VWR), yeast extract (Merck), dextrose (Sigma-Aldrich), adenine (Fluka Chemicals), histidine (VWR), leucine (Applichem, Germany), glycine (Reanal, Hungary) and uracil (Sigma-Aldrich) have been used throughout the whole experiments.

S. pombe (ATCC strain: 38366), *Escherichia coli* (*E. coli*, Microbial Collection of University of Pécs strain: 201) and *Staphylococcus aureus* (*S. aureus*, ATCC strain: 29213) were obtained from the Department of General and Environmental Microbiology, Institute of Biology, University of Pécs, Hungary.

2.2. Inclusion complex formation of RAMEB and selected essential oils/components

25 g (close to 0.02 mol) of statistically (Random) methylated beta-cyclodextrin (having an average degree of methylation of 1.8 methoxy-groups/glucopyranose unit) was dissolved in 30 mL of deionized water at room temperature under nitrogen stream protected from light. Then 1.5 g (close to 0.01 mol) of the essential oils or pure components were fed dropwise to the stirred cyclodextrin solution. The resulting emulsion was sonicated for 3 min and stirred for further 2 h protected from light. It was then chilled to -45°C in dry ice/ethanol mixture and lyophilized. The resulting light powder was homogenized and used for the further studies.

2.3. Characterization of encapsulated essential oils and their components

2.3.1. UV–VIS spectroscopy analysis

The formation of inclusion complexes of the selected essential oils, their components and RAMEB was evaluated by UV–VIS spectrophotometry (Hitachi U-3900). Essential oils were dissolved in acetonitrile (0.5 mg/mL). RAMEB, encapsulated essential oils, components and a 4:1 mixture of RAMEB-essential oils/components were mixed in acetonitrile at 5 mg/mL and shaken for 10 min. The supernatant was separated by centrifugation, diluted hundred times in acetonitrile and was scanned in the range of 200–400 nm to obtain UV–VIS absorption spectra (Liu et al., 2013).

2.3.1.1. Photometric titration. The photometric titration was performed in acetonitrile. In brief, the oil concentrations were kept constant (1 mmol/L) while the CD concentrations were varied from 1 mmol/L up to 8 mmol/L. Data evaluation was performed as described before (Poór et al., 2015; Poór, Zand, Szente, Lemli, & Kunsági-Máté, 2017).

2.3.2. Phase solubility studies

Phase solubility plots were obtained to identify and evaluate the stability of the inclusion complexes (Nicolescu, Aram, Nsedelcu, & Monciu, 2010). In brief, excess of essential oils were added to 10 mL aqueous solutions of RAMEB in a concentration range of 0–10 mmol/L, incubated at 25 °C and 35 °C, shaken at 200 rpm for 24 h and filtered through 0.45 µm syringe filter (Fisher Scientific). The quantity of essential oils remained in the solution was measured spectrophotometrically at 214.5 nm (Hitachi U-3900) and data were compared with the standard curve obtained for the components. The quantity of essential oils in the solution was plotted against RAMEB concentration. The stability constant K_s (L/mole) was calculated from slope and intercept of the plot from the equation:

$$K_s = \frac{\text{slope}}{\text{intercept} \times (1 - \text{slope})}$$

where K_s (L/mole) represents the stability constant and intercept (mmol/L) is the dissolved guest molecules (essential oil or their pure components) in aqueous complex medium when no cyclodextrin is present.

2.3.2.1. Thermodynamics of the formation of inclusion complexes of BCDs with essential oils. To get deeper insights into the processes associated to the complex formation, thermodynamic parameters were determined using the stability constants measured at different temperatures applying the van't Hoff equation:

$$\ln(K) = \frac{-\Delta G}{RT} = \frac{-\Delta H}{RT} + \frac{\Delta S}{R}$$

2.3.3. HS-GC-FID analysis

The formation of inclusion complexes of the selected essential oils, their components and RAMEB was examined by headspace gas chromatography with flame-ionization detection (Agilent 7890A GC system, G1888 Network Headspace Sampler). Encapsulation efficiency for the RAMEB-EO complexes and formation constant (K_f) values of RAMEB/aroma inclusion complexes were determined using the static headspace gas chromatography based on the publication of Kfoury et al., 2017. Essential oils (100 ppm) or their components (1 mmol/L) were added to 10 mL deionized water or RAMEB's aqueous solution (20 mmol/L) previously introduced into 20 mL headspace vial. The vial was crimp sealed and thermostated at 25 ± 0.1 °C. After the equilibrium was established (30 min), 100 µL of vapor was injected directly into the chromatographic column (DB-ALC2, Agilent J&W Scientific, 30 m × 0.32 mm i.d. and a 1.2 µm film thickness). The HS loop and transfer line temperatures were set at 80 °C and 150 °C, respectively. The injection port temperature was held at 230 °C and used in split mode with a split ratio of 1:2. The FID temperature was maintained at 250 °C. Nitrogen was used as carrier gas. The initial GC oven temperature was held at 76 °C for 10 min, then the temperature increased at 2 °C/min to 128 °C and then ramped at 10 °C/min to 218 °C which was kept for 1 min.

To determine the formation constant (K_f) and the encapsulation efficiency (EE) 3-3 parallel measurements were performed. K_f values (L/mole) and EE (%) were calculated using the following equations:

$$K_f = \frac{\left(\frac{A_0}{A_{RAMEB}}\right) - 1}{C_{RAMEB}}$$

where A_0 and A_{RAMEB} are the peak areas of aroma components in the absence and in the presence of RAMEB, respectively; C_{RAMEB} is the initial concentration of RAMEB.

$$EE = \left(\frac{\sum A_0 - \sum A_{RAMEB}}{\sum A_0}\right) \times 100$$

where $\sum A_0$ and $\sum A_{RAMEB}$ are the sum of the peak areas of aroma

components in the absence and in the presence of RAMEB, respectively.

2.3.4. Determination of average molecular weight of the essential oils

In brief, the average molecular weight of the experimented essential oils was examined by determining the cryoscopic constants of dimethyl sulfoxide (DMSO, 4.484 K kg/mole) using 1.003654 kg/mole naphthalene. DMSO was used as the media. All measurements were repeated three times.

2.4. Determination of Total antioxidant capacity (TAC)

2.4.1. DPPH assay

DPPH assay has been performed following the procedure described previously (Prevc, Šegatin, Poklar Ulrih, & Gigić, 2013; Sharma & Bhat, 2009; Wollinger et al., 2016) with modifications. 2.94 mg DPPH in 25 mL of 96% ethanol (300 µM) was prepared and stored in the refrigerator being stable for one week. Acetate buffer (100 mmol/L, pH 5.5) was used throughout the experiments. Trolox standard of 1 mmol/L was prepared in 50% ethanol. Serial dilutions of Trolox standards ranging from 0 to 180 µM and EOs – RAMEB dilutions of 1 mg/mL – 0.01 mg/mL (w/v %) were prepared in PBS, pH 7.4. 50 µL of acetate buffer (100 mmol/L, pH 5.5) followed by 50 µL standard/sample dilutions and 95 µL DPPH (300 µM) were pipetted into 96-well general microplates (Sarstedt). The absorbance changes in the wells were measured at 517 nm by a Perkin Elmer EnSpire Multimode reader at 25 °C after 90 min of incubation in the dark, at room temperature. Measurements were performed in triplicates or more. Antioxidant capacities were calculated in the form of inhibitory concentration at 50% TAC activity (IC_{50}) which was obtained from the equation derived from % scavenger activity vs. serial sample dilution concentration graph (Deng, Cheng, & Yang, 2011; Mishra, Ojha, & Chaudhury, 2012; Sharma & Bhat, 2009). IC_{50} values were referred to gram dry mass of the samples.

2.4.2. Enhanced chemiluminescence (ECL) assay

We followed the method previously published (Kőszegi et al., 2017). The enhanced chemiluminescence reaction was performed in 96-well white optical plates (Perkin-Elmer). Ice-cold premixed ECL reagent and POD working solution (200 µL POD + 70 µL ECL reagent) was prepared freshly. Trolox standards were used in the concentration range of 0–100 µM. 20 µL Trolox/blank/sample and 270 µL of POD-ECL reagent were pipetted into each well. For initiation of the ECL reaction, 20 µL ice-cold H_2O_2 in citric acid was injected into the wells by the automated dispenser of a Biotek Synergy HT Gen5 microplate reader. The chemiluminescence signal was followed for 10 min. For the ECL assay, total light output (area under curve, AUC) data were taken. TAC of the samples was obtained by using the regression equation obtained for the standards, results multiplied by the dilution factor and expressed as µM Trolox equivalent (TE). TE for each sample was further referred to 1 g of initial essential oil content. Measurements were performed at least in triplicates or more.

2.4.3. ORAC assay

We used a standard procedure described by Kőszegi et al. (2017) with modifications. The working fluorescein (FL) concentration was elevated to 400 nmol/L in 75 µmol/L phosphate buffer, pH 7.4 while the AAPH oxidant concentration was also increased to 400 mmol/L. Trolox standards were prepared as described above within the concentration range of 0–160 µmol/L. 25 µL of blank/standard/sample and 150 µL of working fluorescein solution were pipetted into the wells of 96-well general plates (Sarstedt). The outer wells were filled with 200 µL phosphate buffer only in order to have better temperature stabilization. Before the measurements, plates were preheated to 37 °C for 30 min in the dark. The reaction was started by automated injection of 25 µL AAPH solution into each well by the injector of the Biotek plate reader. Fluorescence intensities were monitored for 80 min using 490/

520 nm filter settings. Total light outputs as AUC were calculated. The AUC of the blank was subtracted from that of the standards/samples (net AUC) and was further used in the antioxidant capacity calculations. Total antioxidant capacity (TAC) of the samples was obtained by using the regression equation data obtained for the Trolox standards. TE was multiplied by the dilution factor and was finally expressed as $\mu\text{mol/L}$ Trolox equivalent. TE of the samples was referred to 1 g of initial essential oils content.

2.5. Determination of minimum inhibitory concentration (MIC)

2.5.1. Anti-fungal activity

The antifungal activity was carried out according to the standard protocol suggested by CLSI (Clinical & Laboratory Standards Institute) guidelines (Llop et al., 2000). Briefly, *S. pombe* slant agar inoculum stock was prepared from the main stock and was incubated for 16 h at 30 °C in YES media (Yeast extract-glucose media, pH 4.5, supplemented with amino acids and Wickerham solution). On the second day, EO-RAMEB and EO component-RAMEB complexes with concentrations ranging from 5 mg/mL to 0.039 mg/mL in square dilution format were added to the yeast population and incubated at 30 °C for 48 h in Yeast-Glucose media supplemented with appropriate amino acids and Wickerham solution. 96-well general plates (SPL Life Sciences) were used for all experiments. The final population of *S. pombe* per well was 10^3 cells/mL. The absorbance per well was measured by the Perkin Elmer EnSpire Multimode reader at 595 nm.

2.5.2. Anti-microbial activity against *E. coli* and *S. aureus*

The antimicrobial activity of the samples was evaluated on *E. coli* and *S. aureus* strains according to the protocol described by the CLSI (Clinical & Laboratory Standards Institute) guidelines (Barchiesi, Colombo, McGough, & Rinaldi, 1994; Llop et al., 2000). Briefly, the working population of the bacteria was prepared on day 1 from the stock. For *E. coli* and *S. aureus* we used LB (Lauria-Bertani) liquid medium and TSA (Tryptic Soy Broth), respectively throughout the experiments. On the second day, the desired population was obtained (0.5 McFarland standards mentioned in NCCLS protocols). The bacterial populations were reduced to 5×10^5 cells/mL and were kept as the final population per well throughout the whole experiment. EO-RAMEB and EO component-RAMEB complexes concentrations ranging from 5 mg/mL to 0.0312 mg/mL were introduced to the inoculated media. The absorbance was measured by the Perkin Elmer EnSpire Multimode reader at 600 nm after 12–16 h of incubation at 35 ± 2 °C.

2.6. Rapid viability assessment for *S. pombe*, *E. coli* and *S. aureus* with SYBR green I/PI double staining method

2.6.1. Validation of SYBR green I/propidium iodide microbial viability assay

Care has been taken to remove any traces of growth medium before staining the experimented microbial samples with the fluorescent dyes. The nucleic acids and other media components may bind SYBR green I and propidium iodide in an unpredictable manner, which may result in unacceptable imprecision in the staining procedure. A single wash step with PBS (pH 7.4) was sufficient to remove traces of interfering media components from the microbial suspension. Briefly, 15 mL cultures of either *S. pombe*, *E. coli* or *S. aureus* were grown to log phase in nutrient broth (YES media, LB media and TSA). 10 mL of microbial suspension in each tube was pelleted by centrifugation at $1000 \times g$ for 5 min. The supernatant was removed, and the pellet was re-suspended in 10 mL media (for living microbes) and in 2.5–25% (v/v) of 2-propanol in respective centrifuge tubes for obtaining different ratios of dead/live microbes. All samples were incubated at room temperature for 15 min then were centrifuged at $1000 \times g$. The supernatants were removed, and the pellets were re-suspended and washed with 5 mL PBS (pH 7.4) followed by centrifugation again. The pellets were finally suspended in

10 mL of PBS (pH 7.4).

2.6.1.1. Optimization of staining. The staining concentration of the two fluorescent dyes has been balanced so that the applied mixture should provide good live/dead cell discrimination in our experimental conditions. For thorough optimization of the staining protocol, we have experimented a wide range of concentrations (5.5–5500 times dilution in logarithmic dilution format) of SYBR green I dye (10,000 \times stock, Sigma-Aldrich) each in combination with a concentration range (500–5 times in logarithmic dilution format) of propidium iodide (20 mmol/L stock in DMSO).

2.6.1.2. Staining microbial suspensions with SYBR green I/propidium iodide for fluorescence microplate reader and flow cytometry testing. The microbial suspensions (live and killed) were adjusted to $\sim 10^6$ cells/mL. 100 μL of the above mentioned treated and untreated samples were pipetted into 96-well transparent flat bottom general plates. 100 μL of premixed dye was pipetted into the wells containing the samples and mixed thoroughly. The plates were incubated in the dark for 10 min. The outer wells (row A and H and columns 1 and 12) were kept filled with PBS (pH 7.4) to maintain even temperature distribution during the incubation process.

For the evaluation of microbial viability, fluorescence intensities of the samples in the 96-well plates were measured at two monochromator settings. First, fluorescence intensity was recorded at 490 nm/525 nm excitation/emission wavelengths (emission 1, green). Then the samples were re-measured at 530 nm/620 nm (emission 2, red). Data were analyzed by dividing the fluorescence intensity of the stained microbial suspensions (F_{cell1}) at emission 1 by fluorescence intensity at emission 2:

$$\text{Ratio}_{G/R} = \frac{F_{\text{cell,em1}}}{F_{\text{cell,em2}}}$$

Dose dependent % of dead cells in the microbial suspension was then calculated from the respective $\text{Ratio}_{G/R}$ using the following formula:

$$\% \text{Dead cells}_{\text{Dose}} = 100 - \left(\frac{\text{Dose}_{G/R}}{\text{Control}_{G/R}} \times 100 \right)$$

where, $\text{Dose}_{G/R}$ is the green to red ratio ($\text{Ratio}_{G/R}$) of a specific dose and $\text{Control}_{G/R}$ is the green to red ratio of the living control.

In our flow cytometric analysis, we assessed the ratio of living and dead cells using SYBR green I and propidium iodide double staining as in the case of the plate reader experiments. Flow cytometric measurements were performed on a FACS Canto II instrument (BD Biosciences) using FACS Diva V6.0 software (BD Biosciences). Before sample analysis, the flow cytometer settings were checked using Cytometer Setup and Tracking beads (CS&T beads, BD Biosciences) according to the manufacturer's instructions. Doublets were discriminated by a side scatter (SSC)-H vs. SSC-W plot, and forward scatter (FSC)-H vs. FSC-W plot. For data analyses we used FCS express V4.0 software.

2.6.2. Rapid viability assay on *S. pombe*, *E. coli* and *S. aureus* strains

The viability assay was performed according to the method reported by Feng, Wang, Zhang, Shi, and Zhang (2014) with modifications. For the discrimination of live and dead cells in 96-well plates, SYBR green I and PI were used for staining the nucleic acids of the test microbes. $100 \times$ dilutions of SYBR green I (10,000 \times stock, Sigma-Aldrich) in DMSO were prepared in aliquots and were stored at -20 °C for future use. In brief, 10 mL microbes with a population of 10^5 cells/mL were incubated (30 °C for *S. pombe* in YES medium, 37 °C for *E. coli* and *S. aureus* in LB broth and TS broth, respectively) for 16 h, treated by different EOs – RAMEB dilutions ranging from 2 mg/mL to 0.06 mg/mL. The treated microbes were centrifuged at $1000 \times g$ for 5 min, washed in PBS (pH 7.4) and were re-suspended in PBS (pH 7.4). Working dye solution was prepared by mixing 18 μL of SYBR green I from the

aliquots and 2 μ L of propidium iodide (20 mmol/L in DMSO) with 1000 μ L of PBS, pH 7.4. 100 μ L of re-suspended treated microbes were pipetted into each well of 96-well general plates (Sarstedt). Then 100 μ L of working dye solution was pipetted into each well containing the microbes and the plate was incubated at room temperature in the dark with mild shaking, for 15 min. Considering the excitation wavelength of 490 nm for SYBR green I and 530 nm for PI, fluorescence intensities at 525 nm (green emission) and 620 nm (red emission) were measured for each well by the Perkin Elmer EnSpire Multimode reader. Green to red ratios of every sample and for every dose were achieved. Percentage of dead cells with response to the dose was calculated using the formula described earlier and the percentage of dead cells were plotted against EOs-RAMEB/components-RAMEB doses applied to the cells.

2.7. Statistical analysis

Statistical analysis was conducted using a one-way ANOVA test (Origin 2016, OriginLab Corp., US). Significance was set at $P < 0.05$.

3. Results and discussion

3.1. UV–VIS spectroscopy analysis

The UV absorption spectra of investigated essential oils, active components and RAMEB are shown in [Supplementary Fig. 1 \(Fig. S1\)](#). The maximum absorption of the essential oils was found to be in the range of 210–220 nm which is attributed to the active components. The absorption peak of essential oils at 250 nm corresponded to 1,8-cineole. The spectral analysis of physical mixture of RAMEB with essential oils and with components prior to complexation were found to be harmonious with the essential oils and components. The absorbance spectra of physical mixture of essential oils with RAMEB with components were in symmetry with the essential oil spectra and components. In case of complexation, the absorption peaks disappear in RAMEB complexation spectra. The active compounds from the encapsulation were recovered by dissolving the complexes in 95% acetonitrile (Liu et al., 2013). The compounds were released from the RAMEB cavity and were separated by centrifugation. The solutions were diluted to hundred times in acetonitrile and the absorbance was measured. In this line, beside the active compounds, 1,8 cineole, cis- β -ocimene, α -pinene, α -terpineol, *p*-cymene and β -caryophyllene were also observed at 210 nm and 240 nm respectively. We are aware of the complexity of EOs which makes our absorbance spectroscopic analysis to be an approximation only however, it indicates the successful formation of complexation of essential oils and their components with RAMEB.

3.2. Phase solubility studies

The y-intercept is referred as the concentration of solubilized guests without host in the solution medium. The plot indicates the type of the inclusion complex. Positive slopes < 1 with a linear relationship among the concentration of dissolved essential oil or active components and RAMEB were obtained in every case (Table 1). The complexes thus maybe classified as A_L type (1:1 M ratio of guest to host) (Nicolescu et al., 2010). Major entrapped compounds are mono- and sesquiterpenoids and phenylpropane derivatives (average molecular weight: 120–160 g/mole), thus a 1:1 complex formation can be expected (Szejtli & Szente, 2005). K_s (stability constant) is an important parameter to measure the difference in the equilibrium between free and complex formulation. Low K_s were obtained in case of essential oils while for the active components they are in the order for those of RAMEB complexes (Table 1). This maybe because of competition or affinity of other compounds with the active components used in the study to form RAMEB complexes. The decrease in K_s with increase of temperature reflects an exothermic process (Hill, Gomes, & Taylor, 2013). The phase solubility study (Table 1) shows that the aqueous solubility of essential

Table 1

Stability constant (K_s), enthalpy (H) and entropy (S) changes of encapsulated essential oils and active components at specified temperatures. Data in parentheses reflect stability constants determined in acetonitrile. R^2 is higher than 0.86 for all components.

Inclusion compound	Temperature °C	Slope	K_s (L/mol)	delta H kJ/mol	delta S J/Kmol
Lavender oil	25	0.296	16.1	−3.8	21.5
Lavender oil	35	0.355	15.3		
Linalool	25	0.945	630.7 (74.1)	−1.8	52.8
Linalool	35	0.984	615.4		
Peppermint oil	25	0.312	16.9	−3.7	22.0
Peppermint oil	35	0.373	16.1		
Menthol	25	0.827	641.6 (38.0)	−3.6	52.2
Menthol	35	0.933	611.7		
Borneol	25	0.862	638.5	−4.0	52.0
Borneol	35	0.915	605.4		
Thyme oil	25	0.241	13.2	−4.7	19.5
Thyme oil	35	0.287	12.4		
Thymol	25	0.869	628.7 (77.6)	−2.3	52.61
Thymol	35	0.914	609.5		
Lemon balm oil	25	0.311	16.9	−3.7	22.0
Lemon balm oil	35	0.372	16.1		
Citral	25	0.896	632.4 (72.4)	−3.5	52.1
Citral	35	0.947	603.5		

oils used in the study can be increased with increasing RAMEB concentration. The complex stabilities for thymol with cyclodextrins vary from 152 L/mole (Fenyvesi, Zemlényi, Orgoványi, Oláh, & Szente, 2016) to 3337 L/mole (Kfoury et al., 2016). One possible reason for this variation of the complex stability constants is the encapsulation of water molecules by the host cyclodextrins and also the microsolvation of guest molecules by water (Peggy, Maria, & Beatriz, 2010). This property highly affects the complex formation due to the modified structure of the solvation shell of guest and the exit of the solvent water molecules from the CD cavity prior the formation of the complexes. Studies performed previously on the host-guest interactions of calixarenes with similar sized aromatic guests, the protic character of water should be considered, as the entropy change associated to the complex formation is also highly affected by the processes (Kunsági-Máté, Csók, Tuzi, & Kollár, 2008). Furthermore, the large difference of complex stabilities obtained in protic aqueous and non-protic acetonitrile media (brackets in Table 1) for the main components of essential oils also highlights the role of microsolvation during the complex formation.

The thermodynamic data show clearly that the complex formation is an entropy-driven process. The enthalpy changes associated to the complex formation are about 2–4 kJ/mole which value is just the average kinetic energy associated according to the equipartition theorem. This stabilization energy is far to be responsible for complex formation. In contrast, the entropy gain plays determinant role to improve the complex stability. It is doubled in some cases (for main components) resulting in huge increase of the calculated stabilities compared to those of related to the essential oils. Comparing the complex stabilities derived from the measurements performed in aqueous or acetonitrile media the probable determinant process responsible for the complex formation is the leave of solvent molecules from the CD cavity prior the complex formation. The hydrophobic interior of the cavity supports exchange of water molecules with the guest essential oils while this process is just blocked when the essential oils want to replace the acetonitrile molecules in the CDs cavity. As a result, the enhanced freedom of water molecules after formation of complexes manifest the entropy gain while no similar process can be obtained in acetonitrile media. As a result, much lower stabilities can be obtained in acetonitrile. It is worth to mention here the much larger stability derived for the main component compared with the appropriate oil: the components of oil other than the main component only weakly can replace the water molecules in the CD interior resulting

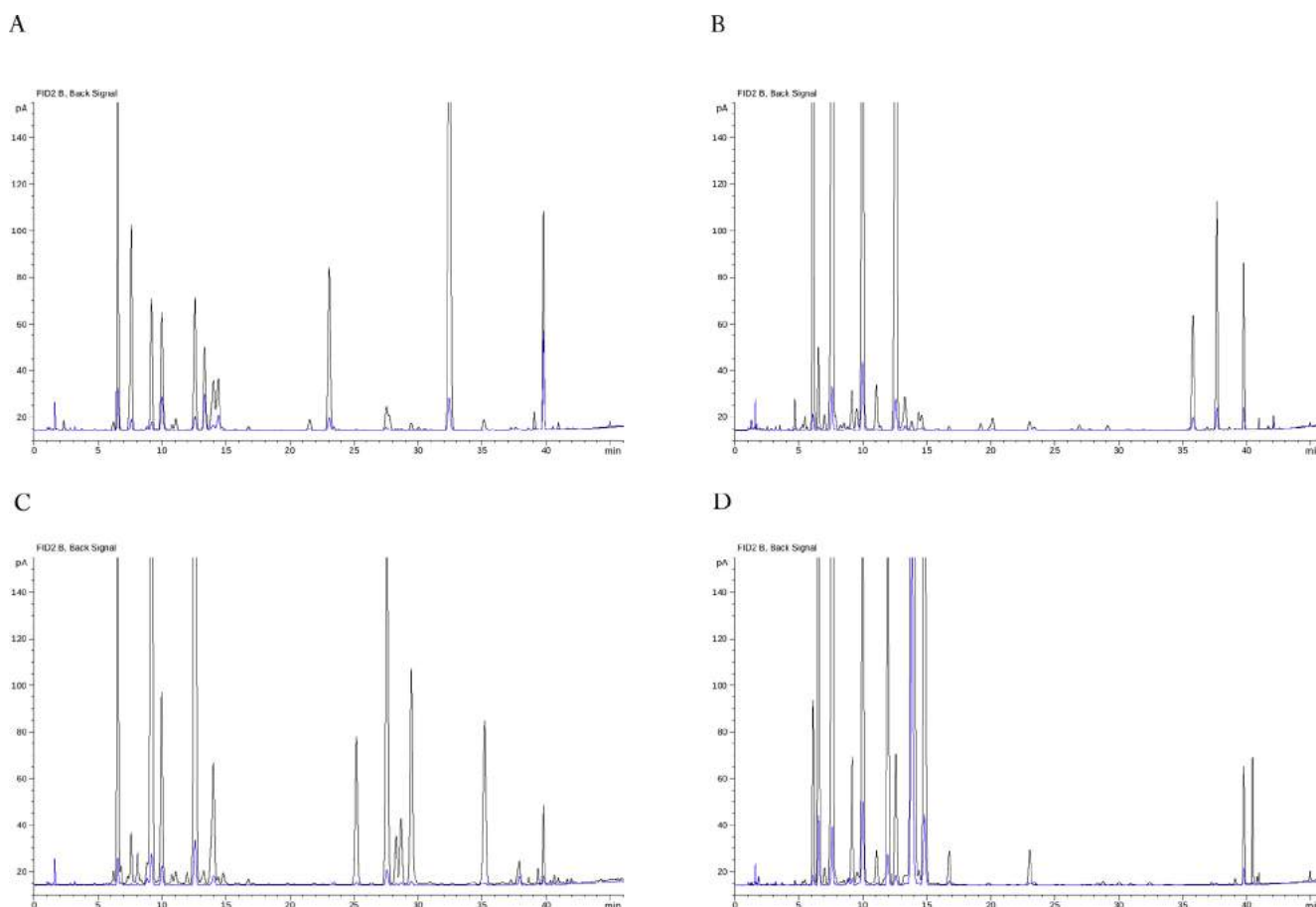


Fig. 1. Chromatograms for studying the encapsulation efficiency of RAMEB complexed lavender oil (A), lemon balm oil (B), peppermint oil (C) and thyme oil (D) based on GC analyses. Black lines: free EOs/components, blue lines: RAMEB complexed EOs/components. (For interpretation of the references to colour in this figure legend, the reader is referred to the web version of this article.)

much lower entropy gain during complex formation.

3.3. Determination of average molecular weight of the essential oils

The evaluated average molecular weight of the examined essential oils are as follows in decreasing order: peppermint oil (237.19), lemon balm oil (236.64), lavender oil (225.44) and thyme oil (182.84). All measurements were repeated three times showing less than 1% inaccuracy.

3.4. Encapsulation efficiency

Encapsulation efficiency (EE) expressed in % of RAMEB-EO complexes is based on GC analyses (Fig. 1). Peppermint oil showed the highest encapsulation efficiency ($94.95 \pm 0.57\%$) followed by thyme oil ($93.30 \pm 1.58\%$), lemon balm oil ($93.13 \pm 1.04\%$) and lavender oil ($87.38 \pm 2.28\%$) respectively. Several EO components, including pinene are able to polymerize in low-permittivity solutions (Roberts & Day, 1950). In such cases, the large polymer adducts are not able to form complexes with the RAMEB molecules. As a result, the concentration of the components which are active in the complex formation are much lower than it can be assumed from the physical amount of EO used in the experiments.

Formation constant (K_f) values of RAMEB/aroma inclusion complexes are as follows (L/mole): linalool 688, neral (Z-citral) 399, geranial (E-citral) 416, menthol 1464, isoborneol 1689, borneol 1784 and thymol 1206 (SD < 10%).

3.5. Antioxidant activity (DPPH, ECL and ORAC assay)

We have quantified the antioxidant properties of EOs – RAMEB and their components by DPPH, ORAC and ECL assay methods. As reported previously (García-Padial, Martínez-Ohárriz, Navarro-Blasco, & Zornoza, 2013) cyclodextrin may have influence on the ORAC fluorescence assay for antioxidant activity evaluation. However, we could not find any interference of RAMEB at the applied concentrations (1–100 mg/mL) on the emission intensity of fluorescein used in the ORAC assay. Also, EOs are strongly lipophilic molecules with limited effect in aqueous antioxidant tests therefore, entrapment by RAMEB was essential for our TAC assays. Consequently, it was postulated that EOs – RAMEB complexes being water miscible, enable the use of less amounts of entrapped EOs than the free oils alone. The antioxidant activity obtained by thyme oil and its component thymol was found to be the highest followed by lemon balm oil, lavender oil and peppermint oil (Table 2). Previous data (Abdelli, Moghrani, Aboun, & Maachi, 2016; Anastasaki et al., 2017; Prevc et al., 2013; Wollinger et al., 2016) reported higher concentration of EOs than were used in our experiments to produce suitable antioxidant activity. We found, that when EOs are captured by RAMEB, a remarkable antioxidant activity is achieved despite the use of smaller amounts of them.

3.6. Antifungal and antimicrobial activity

Different EOs-RAMEB inclusions were tested against *S. pombe* cultured for 48 h at 30 °C, *E. coli* and *S. aureus* cultured for 24 h at 37 °C. Antifungal and antimicrobial effectiveness were expressed as minimum inhibitory concentration 80 (MIC₈₀) which is the first concentration

Table 2

Total antioxidant capacity (TAC) and inhibitory activity of four EO-RAMEB and five EO component-RAMEB complexes measured by three different spectroscopic methods (mean \pm SD). IC₅₀: μ g complex at 50% inhibition (6 independent experiments, each in 3 replicates).

Investigated oils and their main components	DPPH assay	Chemiluminescence assay	ORAC assay
	IC ₅₀ (μ g)	TAC (μ mol/g of EO)	TAC (μ mol/g of EO)
Thyme oil	0.01 \pm 0.01	1417.67 \pm 103.42	3292.50 \pm 93.64
Lemon balm oil	0.12 \pm 0.01	469.59 \pm 84.98	933.09 \pm 75.35
Lavender oil	0.39 \pm 0.02	329.77 \pm 52.76	362.36 \pm 53.22
Peppermint oil	0.41 \pm 0.03	326.80 \pm 74.23	89.69 \pm 15.76
Thymol	0.09 \pm 0.01	9049.05 \pm 105.75	11601.11 \pm 233.38
Menthol	0.68 \pm 0.05	397.28 \pm 92.58	23.05 \pm 10.26
Linalool	0.65 \pm 0.05	86.99 \pm 25.35	748.60 \pm 82.12
Citral	0.15 \pm 0.06	144.02 \pm 43.68	1136.63 \pm 103.54
Borneol	0.51 \pm 0.03	340.46 \pm 64.25	12.86 \pm 5.68

Table 3

Minimum inhibitory concentration (MIC₈₀) of investigated EO-RAMEB and EO component-RAMEB complexes on *S. pombe*, *E. coli* and *S. aureus*; (6 independent experiments, each in 3 replicates).

EO-RAMEB and EO component-RAMEB (mg/mL)	<i>S. pombe</i> 38366	<i>E. coli</i> 201	<i>S. aureus</i> 29213
Thyme oil	0.125–0.25	0.15–0.31	0.5–1.0
Lemon balm oil	0.5–1.0	0.62–1.25	0.5–1.0
Peppermint oil	1.25–2.5	0.62–1.25	1.25–2.5
Lavender oil	1.25–2.5	1.25–2.5	1.25–2.5
Linalool	0.07–0.15	1.25–2.5	1.25–2.5
Menthol	0.62–1.25	0.5–1.0	1.25–2.5
Citral	0.07–0.15	0.12–0.25	0.07–0.15
Thymol	0.07–0.15	0.12–0.5	0.25–0.5
Borneol	1.25–2.5	1.25–2.5	1.25–2.5

where 80% of microorganisms are inhibited. All the inclusion complexes showed antifungal and antimicrobial activity. However, RAMEB-thyme oil was found to have the best MIC (MIC₈₀ = 0.125–0.25 mg/mL, 0.156–0.312 mg/mL, 0.5–1 mg/mL) against *S. pombe*, *E. coli* and *S. aureus* respectively, followed by lemon balm oil, peppermint oil and lavender oil, in this order (Table 3). RAMEB-EO components also showed antifungal and antimicrobial activity. Antimicrobial and antifungal effect of RAMEB-citral (MIC₈₀ = 0.0078–0.156 mg/mL, 0.125–0.25 mg/mL, 0.078–0.156 mg/mL) was close to RAMEB-thymol (MIC₈₀ = 0.078–0.156 mg/mL, 0.125–0.5 mg/mL, 0.25–0.5 mg/mL) under our test conditions.

Free thyme oil and thymol with MIC of 0.64 mg/mL and 0.73 mg/mL have been reported by several authors (Cutillas, Carrasco, Martinez-Gutierrez, Tomas, & Tudela, 2017; Queiroga, Teixeira Duarte, Baesa Ribeiro, & de Magalhães, 2007). Our study shows MIC of 0.156 mg/mL and 0.125 mg/mL against *E. coli*. When applied against both *E. coli* and *S. aureus*, free peppermint oil showed MIC at 0.6 mg/mL (Ciobanu et al., 2013). Both free linalool and lavender oil have MIC at higher concentrations (Hamoud, Sporer, Reichling, & Wink, 2012). Our data suggests that RAMEB encapsulated lavender oil and linalool have MIC at lower concentration 1.25 mg/mL and 0.078 mg/mL, respectively. It has been reported that inclusion complexes with RAMEB may elevate aqueous solubility of the encapsulated guests resulting in better antimicrobial efficiency of the essential oils and their components at lower concentration (Hill et al., 2013; Wang, Li, Si, Lin, & Chen, 2011). Our evaluated MIC results are different from those of previously published results by other authors that maybe due to differences in media composition, methodology and strains of bacteria and fungus used in the studies (Hill et al., 2013).

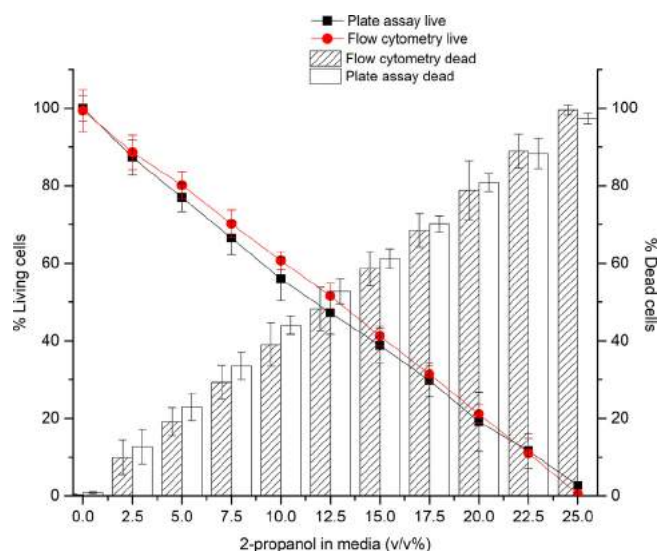


Fig. 2. Comparison of the live/dead discrimination results between the plate reader assay and the flow cytometric assay using SYBR green I/propidium iodide double staining on *S. pombe* (6 independent experiments). (For interpretation of the references to colour in this figure legend, the reader is referred to the web version of this article.)

3.7. Rapid SYBR green/propidium iodide live-dead discrimination assay

3.7.1. Validation of the plate reader and the flow cytometry SYBR green I and propidium iodide double stained live/dead cells discrimination assays

To evaluate if the SYBR green I/propidium iodide staining can be used for rapid plate reader viability assay, *S. pombe* was subjected to treatment with different concentrations of 2-propanol (see Methods). In addition, we also assessed the ability of SYBR green I/propidium iodide assay to determine the viability of *S. pombe* by flow cytometry. In summary, we have evaluated the microbial viability to compare the percentage of dead cells by both plate reader and flow cytometry methods. We found the optimized SYBR green I/propidium iodide assay to be reliable for rapid estimation of the viability of microbes using the plate reader technique (Fig. 2).

3.7.2. Rapid microbial cell live/dead discrimination plate reader assay of *S. pombe*, *E. coli* and *S. aureus*

This viability assay was attempted for the fast evaluation of the susceptibility of different concentrations of EOs – RAMEB on *S. pombe*, *E. coli* and *S. aureus*. Our findings suggest that complexed peppermint oil is less effective in killing *S. pombe* at 2 mg/mL when compared to the percentage of dead/compromised cells of *E. coli* and *S. aureus* at the same concentration (Table 4). Thyme oil was found to be more potent at 0.5 mg/mL, killing 90% of cells in all three cases followed by citral which showed 90% inhibition at 0.25 mg/mL. Lavender oil, although expressing less killing property at 2 mg/mL, was more effective towards *E. coli* and *S. aureus* at more than 90% efficiency at the same concentration. Thymol being the active constituent of thyme oil showed high (80% and above) killing/compromising ability at low concentrations starting from 0.25 mg/mL. On the other hand, menthol showed more effectiveness in killing *E. coli* and *S. aureus* at 2 mg/mL. Borneol had no killing or inhibiting properties at all towards both microbes.

The validity of our plate reader assay was verified by testing the microbial samples using flow cytometry as well. The two methods can be considered to be equivalent and the plate reader assay offers the advantage of high throughput determinations.

All essential oils and their components were complexed with RAMEB. The above mentioned results support the idea to test the usage of RAMEB complexed EOs in the food and pharmaceutical industries in the future, as efficient natural antioxidants and preservatives.

Table 4

Percentage death of cells using SYBR green I/PI double stained plate reader method for live/dead discrimination of the test microbes (mean \pm SD, n = 6 independent experiments).

Test microbes	Dose of EO-RAMEB and EO component-RAMEB complexes						
	Dose (mg/mL)	0.06	0.12	0.25	0.5	1	2
<i>S. pombe</i>	Peppermint oil	4.52 \pm 0.23	9.34 \pm 1.34	14.25 \pm 0.43	18.93 \pm 0.43	37.18 \pm 1.85	49.93 \pm 0.75
	Thyme oil	16.47 \pm 0.67	40.19 \pm 0.77	85.21 \pm 1.68	92.05 \pm 1.86	92.11 \pm 0.99	95.07 \pm 0.92
	Lavender oil	0.00 \pm NA	0.00 \pm NA	1.99 \pm 0.54	4.34 \pm 0.66	6.58 \pm 0.47	15.07 \pm 1.22
	Lemon balm oil	2.64 \pm 0.57	10.15 \pm 0.79	16.79 \pm 1.24	39.48 \pm 1.57	62.14 \pm 0.76	77.92 \pm 0.75
	Citral	45.73 \pm 1.34	78.31 \pm 0.56	95.23 \pm 0.87	96.98 \pm 1.55	97.53 \pm 0.62	97.87 \pm 0.88
	Borneol	0.00 \pm NA	0.00 \pm NA	2.24 \pm 1.44	2.86 \pm 1.38	2.42 \pm 1.70	0.00 \pm NA
	Menthol	0.00 \pm NA	0.00 \pm NA	1.27 \pm 0.97	6.96 \pm 1.64	27.95 \pm 1.98	45.99 \pm 0.66
	Linalool	0.00 \pm NA	0.00 \pm NA	1.91 \pm 1.15	6.89 \pm 1.74	18.99 \pm 0.63	28.02 \pm 0.45
	Thymol	2.05 \pm 0.42	34.26 \pm 0.75	73.26 \pm 1.54	93.51 \pm 1.74	92.72 \pm 1.85	99.77 \pm 0.63
<i>S. aureus</i>	Peppermint oil	4.86 \pm 1.36	9.47 \pm 1.88	18.36 \pm 0.65	36.36 \pm 0.77	71.85 \pm 0.63	96.14 \pm 0.73
	Thyme oil	31.01 \pm 0.56	57.39 \pm 0.77	87.48 \pm 1.64	87.51 \pm 1.88	87.96 \pm 1.92	87.65 \pm 0.67
	Lavender oil	5.17 \pm 0.83	7.46 \pm 0.99	11.89 \pm 1.64	20.76 \pm 1.77	38.47 \pm 1.66	73.92 \pm 0.74
	Lemon balm oil	9.87 \pm 1.77	13.69 \pm 0.76	21.07 \pm 1.32	35.82 \pm 1.66	65.32 \pm 1.71	93.32 \pm 0.73
	Citral	15.45 \pm 1.77	34.56 \pm 1.34	65.64 \pm 1.99	86.58 \pm 0.83	86.87 \pm 0.83	86.76 \pm 1.61
	Borneol	5.72 \pm 1.66	8.72 \pm 1.94	15.56 \pm 1.74	21.52 \pm 0.78	33.65 \pm 0.67	57.74 \pm 0.89
	Menthol	14.44 \pm 0.65	19.41 \pm 1.74	29.09 \pm 1.89	48.22 \pm 1.67	86.64 \pm 1.94	98.88 \pm 0.24
	Linalool	7.64 \pm 1.64	13.96 \pm 1.63	19.16 \pm 1.89	28.17 \pm 0.98	37.74 \pm 0.84	54.12 \pm 1.74
	Thymol	27.95 \pm 1.66	45.04 \pm 1.88	77.91 \pm 0.83	88.17 \pm 0.76	92.58 \pm 0.24	98.71 \pm 0.31
<i>E. coli</i>	Peppermint oil	16.99 \pm 1.66	18.89 \pm 1.85	22.57 \pm 2.63	29.83 \pm 2.83	44.67 \pm 1.83	73.56 \pm 0.53
	Thyme oil	10.93 \pm 2.68	16.68 \pm 1.67	27.75 \pm 1.88	49.88 \pm 1.77	94.08 \pm 0.55	97.67 \pm 0.64
	Lavender oil	8.51 \pm 1.54	10.28 \pm 1.64	13.71 \pm 1.77	20.57 \pm 0.77	33.66 \pm 0.87	61.72 \pm 0.77
	Lemon balm oil	10.16 \pm 1.22	15.61 \pm 2.24	26.11 \pm 1.58	47.18 \pm 1.44	89.09 \pm 0.65	96.05 \pm 1.38
	Citral	31.23 \pm 2.54	65.11 \pm 0.44	86.48 \pm 0.77	91.57 \pm 1.83	95.25 \pm 1.88	98.36 \pm 0.82
	Borneol	1.89 \pm 1.77	3.39 \pm 1.92	6.28 \pm 0.83	11.72 \pm 2.82	23.59 \pm 2.37	46.68 \pm 1.98
	Menthol	8.67 \pm 1.88	16.34 \pm 1.11	20.76 \pm 0.76	29.55 \pm 0.73	47.26 \pm 1.87	82.56 \pm 1.21
	Linalool	6.25 \pm 1.65	11.22 \pm 2.89	15.96 \pm 2.66	25.33 \pm 1.93	44.06 \pm 0.73	72.66 \pm 0.78
	Thymol	19.24 \pm 2.85	34.07 \pm 1.77	62.64 \pm 2.77	86.75 \pm 2.19	92.29 \pm 1.83	92.76 \pm 1.93

4. Conclusions

Encapsulation of essential oils and their active components with RAMEB may provide protection from the variable environmental conditions and enhances their aqueous solubility, thus increasing their functional capabilities as additives in food packaging industry. The characteristic UV bands of the essential oils disappeared from the inclusion complex spectra, as the essential oils entered the RAMEB cavity. The TAC activity of the essential oils and their components encapsulated in RAMEB showed 35–40% higher stability than the previously reported data, which suggests that the inclusion complex with RAMEB may protect the active components of the essential oils against the effect of reactive oxidative environments. Encapsulation also elevated the antimicrobial and antifungal activities of essential oils and their components by 2–4 times compared with those of the free oils. Live/dead SYBR green I/PI plate reader microbial discrimination assay of the encapsulated essential oils was also performed. The validity of the plate reader method was verified by flow cytometry using the same double fluorescence staining conditions. Our results suggest, that RAMEB inclusion complexes could overcome the limitations of essential oils application in food industry by reducing their volatility and losses during food processing or storage and enhancing their radical scavenging activity, antimicrobial activity and microbial termination ability. Thus, they could generate a controlled release system or environment for food packaging as well as improving their aroma burst.

Acknowledgements

Funding: The work was financially supported by “KA-2016-04 (University of Pécs, Medical School, Hungary) and GINOP-2.3.2-15-2016-00021 “The use of chip-technology in increasing the effectiveness of human in vitro fertilization”; NKFI-EPR K/115394/2015 “Early biochemical indicators of embryo viability” grants.

Appendix A. Supplementary data

Supplementary data to this article can be found online at <https://doi.org/10.1016/j.foodchem.2018.11.047>.






References

- Abdelli, M., Moghrani, H., Aboun, A., & Maachi, R. (2016). Algerian *Mentha pulegium* L. leaves essential oil: Chemical composition, antimicrobial, insecticidal and antioxidant activities. *Industrial Crops and Products*, *94*, 197–205.
- Anastasaki, E., Zoumpoulou, G., Astraka, K., Kampoli, E., Skoumpi, G., Papadimitriou, K., ... Polissiou, M. (2017). Phytochemical analysis and evaluation of the antioxidant and antimicrobial properties of selected herbs cultivated in Greece. *Industrial Crops and Products*, *108*, 616–628.
- Astray, G., Gonzalez-Barreiro, C., Mejuto, J. C., Rial-Otero, R., & Simal-Gándara, J. (2009). A review on the use of cyclodextrins in foods. *Food Hydrocolloids*, *23*(7), 1631–1640.
- Barchiesi, F., Colombo, A. L., McGough, D. A., & Rinaldi, M. G. (1994). Comparative study of broth macrodilution and microdilution techniques for in vitro antifungal susceptibility testing of yeasts by using the National Committee for Clinical Laboratory Standards' proposed standard. *Journal of Clinical Microbiology*, *32*(10), 2494–2500.
- Chrysargyris, A., Panayiotou, C., & Tzortzakis, N. (2016). Nitrogen and phosphorus levels affected plant growth, essential oil composition and antioxidant status of lavender plant (*Lavandula angustifolia* Mill.). *Industrial Crops and Products*, *83*, 577–586.
- Cid, A., Mejuto, J. C., Orellana, P. G., López-Fernández, O., Rial-Otero, R., & Simal-Gándara, J. (2013). Effects of ascorbic acid on the microstructure and properties of SDS micellar aggregates for potential food applications. *Food Research International*, *50*(1), 143–148.
- Cid, A., Morales, J., Mejuto, J. C., Briz-Cid, N., Rial-Otero, R., & Simal-Gándara, J. (2014). Thermodynamics of sodium dodecyl sulphate-salicylic acid based micellar systems and their potential use in fruits postharvest. *Food Chemistry*, *151*, 358–363.
- Ciobanu, A., Landy, D., & Fourmentin, S. (2013). Complexation efficiency of cyclodextrins for volatile flavor compounds. *Food Research International*, *53*(1), 110–114.
- Costa, A. G. V., Garcia-Diaz, D. F., Jimenez, P., & Silva, P. I. (2013). Bioactive compounds and health benefits of exotic tropical red–black berries. *Journal of Functional Foods*, *5*(2), 539–549.
- Cutillas, A.-B., Carrasco, A., Martinez-Gutierrez, R., Tomas, V., & Tudela, J. (2017). Thyme essential oils from Spain: Aromatic profile ascertained by GC–MS, and their antioxidant, anti-lipoxygenase and antimicrobial activities. *Journal of Food and Drug Analysis*.
- Deng, J., Cheng, W., & Yang, G. (2011). A novel antioxidant activity index (AAU) for natural products using the DPPH assay. *Food Chemistry*, *125*(4), 1430–1435.

- Feng, J., Wang, T., Zhang, S., Shi, W., & Zhang, Y. (2014). An optimized SYBR green I/PI assay for rapid viability assessment and antibiotic susceptibility testing for *Borrelia burgdorferi*. *PLoS One*, *9*(11), e111809.
- Fenyvesi, E., Zemlényi, C. S., Orgoványi, J., Oláh, E., & Szente, L. (2016). Can conversion mixture substitute beta-cyclodextrin in encapsulation of essential oils and their components? *Journal of Inclusion Phenomena and Macroscopic Chemistry*, *86*, 55–66.
- García-Padial, M., Martínez-Ohárriz, M. C., Navarro-Blasco, I., & Zornoza, A. (2013). The role of cyclodextrins in ORAC-fluorescence assays. Antioxidant capacity of tyrosol and caffeic acid with hydroxypropyl- β -cyclodextrin. *Journal of Agricultural and Food Chemistry*, *61*(50), 12260–12264.
- Hamoud, R., Sporer, F., Reichling, J., & Wink, M. (2012). Antimicrobial activity of a traditionally used complex essential oil distillate (Olbas® Tropfen) in comparison to its individual essential oil ingredients. *Phytomedicine*, *19*(11), 969–976.
- Hill, L. E., Gomes, C., & Taylor, T. M. (2013). Characterization of beta-cyclodextrin inclusion complexes containing essential oils (*trans*-cinnamaldehyde, eugenol, cinnamon bark, and clove bud extracts) for antimicrobial delivery applications. *LTW-Food Science and Technology*, *51*(1), 86–93.
- Kfoury, M., Auezova, L., Greige-Gerges, H., & Fourmentin, S. (2015). Promising applications of cyclodextrins in food: Improvement of essential oils retention, controlled release and antiradical activity. *Carbohydrate Polymers*, *131*, 264–272.
- Kfoury, M., Landy, D., Ruellan, S., Auezova, L., Greige-Gerges, H., & Fourmentin, S. (2016). Determination of formation constants and structural characterization of cyclodextrin inclusion complexes with two phenolic isomers: Carvacrol and thymol. *Beilstein Journal of Organic Chemistry*, *12*, 29–42.
- Kfoury, M., Pipkin, D. J., Antle, V., & Fourmentin, S. (2017). Captisol®: An efficient carrier and solubilizing agent for essential oils and their components. *Flavour Fragrance Journal*, *32*, 340–346.
- Kószegi, T., Sali, N., Raknić, M., Horváth-Szalai, Z., Csepregi, R., Končić, M. Z., ... Poór, M. (2017). A novel luminol-based enhanced chemiluminescence antioxidant capacity microplate assay for use in different biological matrices. *Journal of Pharmacological and Toxicological Methods*, *88*, 153–159.
- Kunsági-Máté, S., Csók, Z., Tuzi, A., & Kollár, L. (2008). Permittivity-dependent entropy driven complexation ability of cone and paco tetranitro-calix(4)arene toward para substituted phenols. *L. Phys. Chem. B*, *112*, 1743–1749.
- Liu, H., Yang, G., Tang, Y., Cao, D., Qi, T., Qi, Y., & Fan, G. (2013). Physicochemical characterization and pharmacokinetics evaluation of β -caryophyllene/ β -cyclodextrin inclusion complex. *International Journal of Pharmaceutics*, *450*, 304–310.
- Llop, C., Pujol, I., Aguilar, C., Sala, J., Riba, D., & Guarro, J. (2000). Comparison of three methods of determining MICs for filamentous fungi using different end point criteria and incubation periods. *Antimicrobial Agents and Chemotherapy*, *44*(2), 239–242.
- Mishra, K., Ojha, H., & Chaudhury, N. K. (2012). Estimation of antiradical properties of antioxidants using DPPH assay: A critical review and results. *Food Chemistry*, *130*(4), 1036–1043.
- Nicolescu, C., Aram, C., Nsedelcu, A., & Monciu, C.-M. (2010). Phase solubility studies of the inclusion complexes of rapaglinide with β -cyclodextrin and β -cyclodextrin derivatives. *Pharmacia*, *58*(5), 620–628.
- Peggy, A. P. C., Maria, P. B., & Beatriz, E. E. (2010). Encapsulation of cinnamon and thyme essential oils components (Cinnamaldehyde and Thymol) in β -cyclodextrin. Effect of interactions with water on complex stability. *J. Food. Eng.* *99*, 70–75.
- Poór, M., Kunsági-Máté, S., Sali, N., Kószegi, T., Szente, L., & Peles-Lemli, B. (2015). Interactions of zearalenone with native and chemically modified cyclodextrins and their potential utilization. *Journal Photochemistry and Photobiology B – Biology*, *151*, 63–68.
- Poór, M., Zand, A., Szente, L., Lemli, B., & Kunsági-Máté, S. (2017). Interaction of α - and β -zearalenols with β -cyclodextrins. *Molecules*, *22*, 1910.
- Prevc, T., Šegatin, N., Poklar Ulrih, N., & Cigić, B. (2013). DPPH assay of vegetable oils and model antioxidants in protic and aprotic solvents. *Talanta*, *109*, 13–19.
- Queiroga, C. L., Teixeira Duarte, M. C., Baesa Ribeiro, B., & de Magalhães, P. M. (2007). Linalool production from the leaves of *Bursera aloexylon* and its antimicrobial activity. *Fitoterapia*, *78*(4), 327–328.
- Rakmai, J., Cheirsilp, B., Mejuto, J. C., Torrado-Agrasar, A., & Simal-Gándara, J. (2017). Physico-chemical characterization and evaluation of bio-efficacies of black pepper essential oil encapsulated in hydroxypropyl-beta-cyclodextrin. *Food Hydrocolloids*, *65*, 157–164.
- Rakmai, J., Cheirsilp, B., Torrado-Agrasar, A., Simal-Gándara, J., & Mejuto, J. C. (2017). Encapsulation of yarrow essential oils in hydroxypropyl-beta-cyclodextrin: Physicochemical characterization and evaluation of bio-efficacies. *CYTA – Journal of Food*, *15*(3), 1–9.
- Rakmai, J., Cheirsilp, B., Mejuto, J. C., Torrado-Agrasar, A., & Simal-Gándara, J. (2018). Antioxidant and antimicrobial properties of encapsulated guava leaf oil in hydroxypropyl-beta-cyclodextrin. *Industrial Crops & Products*, *111*, 219–222.
- Roberts, W. J., & Day, A. R. (1950). A study of the polymerization of α - and β -pinene with friedel-crafts type catalysts. *Journal of the American Chemical Society*, *72*(3), 1226–1230.
- Sharma, O. P., & Bhat, T. K. (2009). DPPH antioxidant assay revisited. *Food Chemistry*, *113*(4), 1202–1205.
- Szejtli, J., & Szente, L. (2005). Elimination of bitter, disgusting tastes of drugs and foods by cyclodextrins. *European Journal of Pharmaceutics and Biopharmaceutics*, *61*(3), 115–125.
- Wang, T., Li, B., Si, H., Lin, L., & Chen, L. (2011). Release characteristics and antibacterial activity of solid state eugenol/ β -cyclodextrin inclusion complex. *Journal of Inclusion Phenomena and Macroscopic Chemistry*, *71*(1–2), 207–213.
- Wollinger, A., Perrin, É., Chahboun, J., Jeannot, V., Touraud, D., & Kunz, W. (2016). Antioxidant activity of hydro distillation water residues from *Rosmarinus officinalis* L. leaves determined by DPPH assays. *Comptes Rendus Chimie*, *19*(6), 754–765.

Article

Antimicrobial Activity of Chamomile Essential Oil: Effect of Different Formulations

Sourav Das ^{1,4,†}, Barbara Horváth ^{2,†}, Silviya Šafranko ³, Stela Jokić ³, Aleksandar Széchenyi ² and Tamás Kőszegi ^{1,4,*}

¹ Department of Laboratory Medicine, Faculty of Medicine, University of Pécs, H-7624 Pécs, Hungary; pharma.souravdas@gmail.com

² Institute of Pharmaceutical Technology and Biopharmacy, Faculty of Pharmacy, University of Pécs, H-7624 Pécs, Hungary; barbara.horvath@aok.pte.hu (B.H.); szechenyi.aleksandar@gytk.pte.hu (A.S.)

³ Faculty of Food Technology Osijek, University of Osijek, Franje Kuhaca 20, 31000 Osijek, Croatia; silviya.safranko@ptfos.hr (S.Š.); stela.jokic@ptfos.hr (S.J.)

⁴ János Szentágothai Research Center, University of Pécs, H-7624 Pécs, Hungary

* Correspondence: koszegi.tamas@pte.hu; Tel.: +36-72-501-500 (ext. 29249)

† These authors contributed equally to this work.

Academic Editor: Igor Jerković

Received: 31 October 2019; Accepted: 21 November 2019; Published: 26 November 2019



Abstract: Essential oils (EOs) are highly lipophilic, which makes the measurement of their biological action difficult in an aqueous environment. We formulated a Pickering nanoemulsion of chamomile EO (C_{Pe}). Surface-modified Stöber silica nanoparticles (20 nm) were prepared and used as a stabilizing agent of C_{Pe} . The antimicrobial activity of C_{Pe} was compared with that of emulsion stabilized with Tween 80 (C_{T80}) and ethanolic solution (C_{Et}). The antimicrobial effects were assessed by their minimum inhibitory concentration (MIC_{90}) and minimum effective (MEC_{10}) concentrations. Besides growth inhibition (CFU/mL), the metabolic activity and viability of Gram-positive and Gram-negative bacteria as well as *Candida* species, in addition to the generation of oxygen free radical species (ROS), were studied. We followed the killing activity of C_{Pe} and analyzed the efficiency of the EO delivery for examined formulations by using unilamellar liposomes as a cellular model. C_{Pe} showed significantly higher antibacterial and antifungal activities than C_{T80} and C_{Et} . Chamomile EOs generated superoxide anion and peroxide related oxidative stress which might be the major mode of action of Ch essential oil. We could also demonstrate that C_{Pe} was the most effective in donation of the active EO components when compared with C_{T80} and C_{Et} . Our data suggest that C_{Pe} formulation is useful in the fight against microbial infections.

Keywords: chamomile essential oil; Pickering emulsion; antimicrobial activity; free radical generation

1. Introduction

Essential oils (EOs) have been widely used in folk medicine throughout the history of humankind. The application of EOs covers a wide range from therapeutic, hygienic, and spiritual to ritualistic purposes. EOs are aromatic, volatile, lipophilic liquids extracted from different parts of plant materials such as barks, buds, flowers, fruits, seeds, and roots [1]. EOs are mixtures of complex compounds with variable individual chemical composition and concentrations that includes primarily terpenoids, like monoterpenes (C₁₀), sesquiterpenes (C₁₅), diterpenes (C₂₀), acids, alcohols, aldehydes, aliphatic hydrocarbons, acyclic esters or lactones, rare nitrogen- and sulfur-containing compounds, coumarin, and homologues of phenylpropanoids [1,2]. The biological effects of EOs cover a wide range of effects, including antioxidant, antimicrobial, antitumor, anti-inflammatory, and antiviral activity [3].

The increase in demand for the use of aromatherapy as complementary and alternative medicine has led people to believe in the myth that EOs are harmless because they are natural and have been used for a long time [4]. However, there might be several side effects of EOs even if topical administration is applied and, among these, allergic reactions are the most frequent (many EOs can cause, e.g., rashes on the skin). Some of them can be poisonous if absorbed through the skin, breathed, or swallowed. Previous studies also report the interaction of EOs with other drugs [5]. The continuous production of new aroma chemicals and their widespread and uncontrolled usage as alternative therapies together with many carrier diluents have brought serious problems, especially among children. In this regard, it is of utmost importance to study the mode of action of essential oils and to find a proper, unharmed formulation. Another serious problem is the highly lipophilic nature of EOs, which makes it impossible to measure their biological effects in an aqueous environment [1,6,7].

One major characteristic and application of EOs are their strong antimicrobial activity, including antibacterial and antifungal effects without the development of microbial resistance. Numerous studies are found in the literature describing the antimicrobial activities of a large variety of EOs [8–13]. Most of these assays include conventional broth dilution method, disk diffusion method, and bioautography assay to measure the antimicrobial activity of EOs. Efforts have been made to overcome the lipophilic nature of the oils usually by application of EOs diluted in seemingly suitable solvents/detergents. In the case of natural lipophilic volatile compounds like EOs, solvents of varying polarity, e.g., DMSO, ethanol, and methanol, are most commonly used. However, previous studies have reported the antimicrobial effects of the solvents themselves (DMSO, ethanol, and other solvents in various microbial assays) or their influence on the true antimicrobial effects of EOs [14]. The usage of solubilizing agents limits the precise determination of the antimicrobial activities of EOs. Also, a major problem might arise in the classical assays due to the evaporation of EOs during the assay or the inability of the test microbes to reach the lipophilic range of the tested EOs (in bioautography, as an example) [15,16].

Therefore, new formulations have been determined to increase the solubility or to emulsify the EOs in an aqueous environment. These efforts help to stabilize the oils, to produce an even release of the active components into the required environment, and to maintain their antioxidant and antimicrobial activities [6,11,17,18]. Detergents and organic solvents are not welcome in this regard. Attempts have been made to entrap EOs by modified cyclodextrins for the exact determination of their antimicrobial characteristics [19,20].

The application of Pickering nanoemulsion is a quite novel approach to stabilize oil-in-water (O/W) and water-in-oil (W/O) emulsions by solid particles instead of surfactants. The mechanism involves the adsorption of solid particles on the oil–water interface, causing a significant decrease in the interfacial surface tension that results in high emulsion stability [18]. Previous studies have reported decreased evaporation of EOs from O/W emulsion of nanoparticle-stabilized formulations versus EO–surfactant systems to be a beneficial factor [21,22].

Despite the numerous existing studies on EO–Pickering emulsion, we could not find any literature data on chamomile volatile oil–nanoparticle formulation [7,23]. The main aim of the present work is to use Pickering emulsion of chamomile EO stabilized with modified Stöber silica nanoparticles and characterize its antimicrobial effect using Gram-positive and Gram-negative bacteria as well as *Candida* fungal species. We could demonstrate the strong antimicrobial effects of the chamomile EO–Pickering emulsion and suggest a plausible mode of action of this formulation. Experimental efforts were made to support the suggested mode of action.

2. Results

2.1. Characteristics of Stöber Silica Nanoparticles

The mean diameter, PDI value (polydispersity index), and zeta potential of modified Stöber silica nanoparticles (SNPs) were determined by dynamic light scattering (DLS), and these values were 20 nm, 0.01, and -21.3 mV, respectively. The size and morphology of SNPs were examined by TEM (see

Figure 1). The size distribution obtained by DLS was confirmed by TEM, which showed that the mean diameter of silica samples was 20 nm; they are highly monodisperse and have a spherical shape.

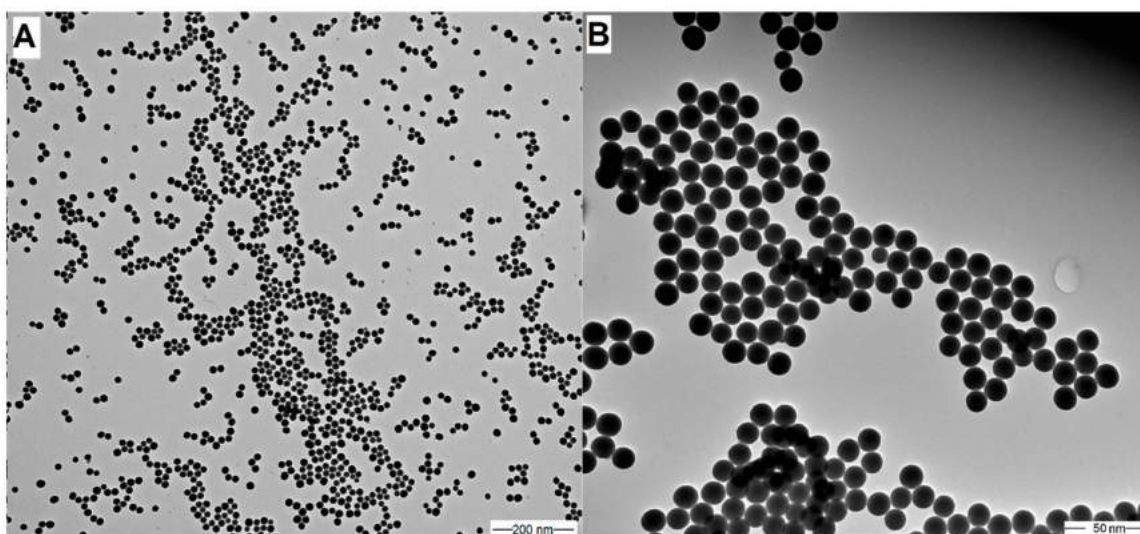


Figure 1. TEM images of silica nanoparticles (SNPs) with different resolutions: 100,000 \times magnification (A) and 500,000 \times magnification (B), accelerating voltage: 80 kV; $d_{\text{TEM}} = 20$ nm. PDI = 0.015.

2.2. Nanoemulsion Stability

We have prepared a Pickering nanoemulsion with surface-modified silica nanoparticles as a stabilizing agent; the particle concentration was 1 mg/mL in every case. The chamomile EO concentration was 100 $\mu\text{g/mL}$. To compare properties of chamomile EO–Pickering nanoemulsion (C_{Pe}) with the conventional, surfactant-stabilized nanoemulsions, and an emulsion with the Tween 80 stabilizing agent was also prepared. The concentration of surfactant was the same as nanoparticles, 1 mg/mL. The emulsions were stored at room temperature (25 $^{\circ}\text{C}$).

We considered the emulsion to be stable when its droplet size does not change and sedimentation, aggregation of particles, or phase separation cannot be observed. The results show that the prepared Pickering emulsion is more stable than conventional emulsion (see Table 1). When the volume fraction of chamomile EO was very low, we assumed that all emulsions were of O/W type and this was confirmed by filter paper tests with CoCl_2 and dye test with Sudan Red G.

Table 1. Parameters of Pickering nanoemulsion and conventional emulsion.

Stabilizing Agent	D_{droplet} (nm)	Stability
SNP	290 ± 4.5	3 months
Tw80	210 ± 10.5	1 month

2.3. Antibacterial and Antifungal Activities (MIC_{90}) of Prepared Emulsions

The effect of chamomile Pickering nanoemulsion, conventional emulsion, and essential oil in ethanol on the growth of some foodborne microbes and opportunistic fungi have been evaluated. The C_{Pe} has been shown to have good antibacterial and antifungal activities (MIC_{90}) on *Escherichia coli* (*E. coli*) (2.19 $\mu\text{g/mL}$), *Pseudomonas aeruginosa* (*P. aeruginosa*) (1.02 $\mu\text{g/mL}$), *Bacillus subtilis* (*B. subtilis*) (1.13 $\mu\text{g/mL}$), *Staphylococcus aureus* (*S. aureus*) (1.06 $\mu\text{g/mL}$), *Streptococcus pyogenes* (*S. pyogenes*) (2.45 $\mu\text{g/mL}$), *Schizosaccharomyces pombe* (*S. pombe*) (1.28 $\mu\text{g/mL}$), *Candida albicans* (*C. albicans*) (2.65 $\mu\text{g/mL}$), and *Candida tropicalis* (*C. tropicalis*) (1.69 $\mu\text{g/mL}$), respectively when compared to C_{T80} counterpart ($P < 0.01$). C_{Pe} showed antimicrobial activity on the selected microbes at an average of fourteen-fold less concentration compared with free essential oil in ethanol (C_{Et}). Simultaneously, C_{Pe} showed a similar antifungal

effect as caspofungin (Cas) on *Candida tropicalis*. The comparative dose–response curves are shown in Figures 2 and 3 for bacteria and fungi, respectively.

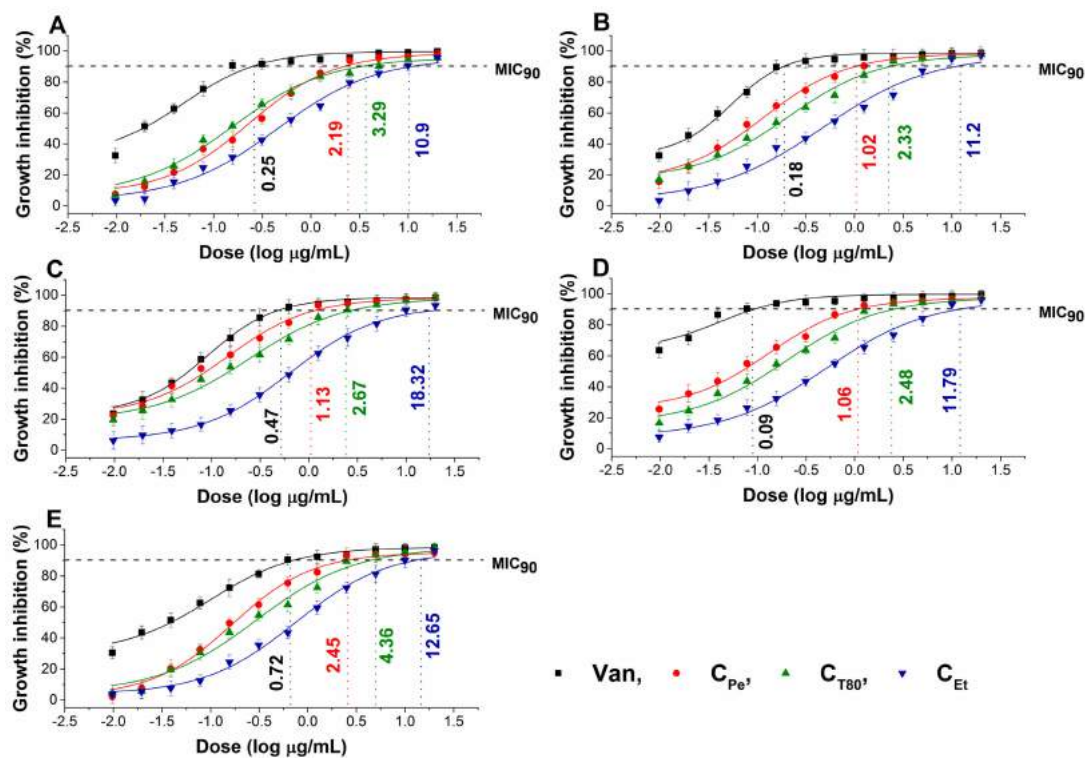


Figure 2. Minimum inhibitory concentration (MIC₉₀) of C_{Pe}, C_{T80}, C_{Et}, and vancomycin (Van, μg/mL) on *E. coli* (A), *S. aureus* (B), *B. subtilis* (C), *P. aeruginosa* (D), and *S. pyogenes* (E).

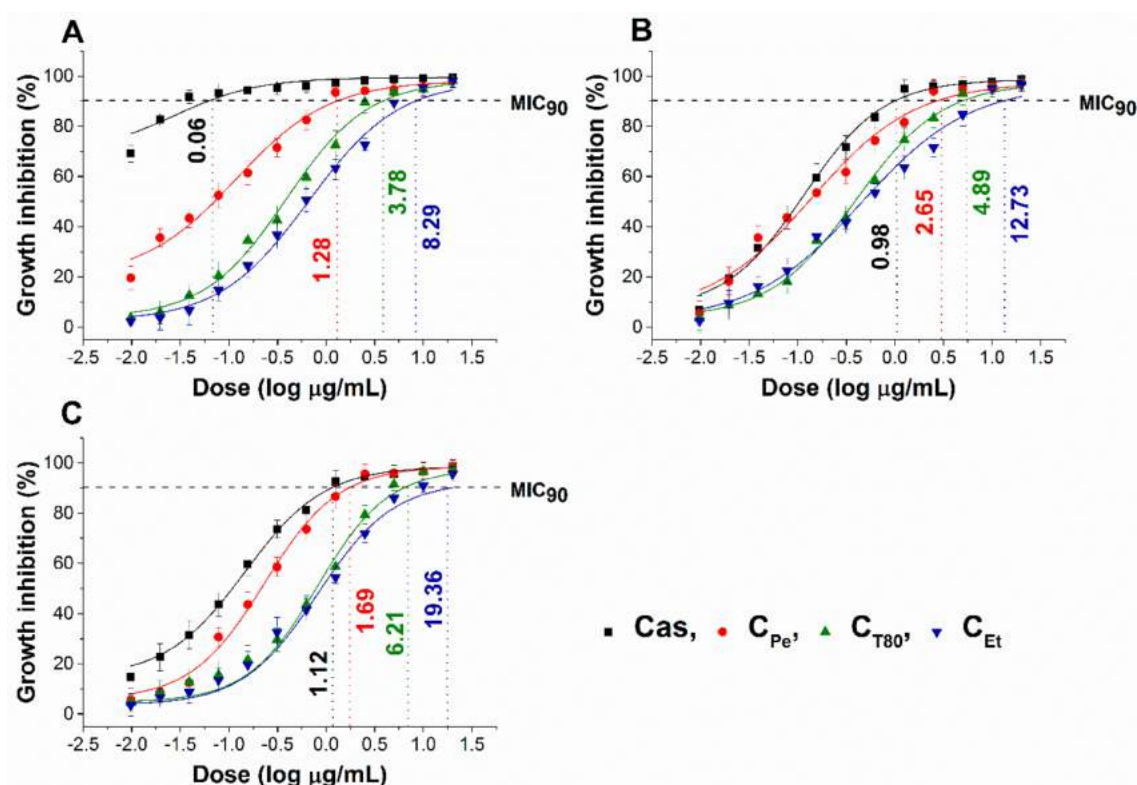


Figure 3. Minimum inhibitory concentration (MIC₉₀) of C_{Pe}, C_{T80}, C_{Et}, and caspofungin (Cas, μg/mL) on *S. pombe* (A), *C. albicans* (B), and *C. tropicalis* (C).

2.4. Minimum Effective Concentrations (MEC₁₀) for Tested Bacteria and Fungi

The minimum effective concentration (MEC₁₀) of C_{Pe}, C_{T80}, and C_{Et} on foodborne Gram-positive and Gram-negative bacteria as well as fungi have been determined. The dose–response curve shows a slow killing effect ($\leq 10\%$ of the population) of C_{Pe} after 1 h of treatment at a two-fold higher concentration compared with MIC₉₀ data. The MEC₁₀ also highlights the effective killing effect of C_{Pe} when compared to C_{T80} and C_{Et} (Figures 4 and 5) ($P < 0.01$).

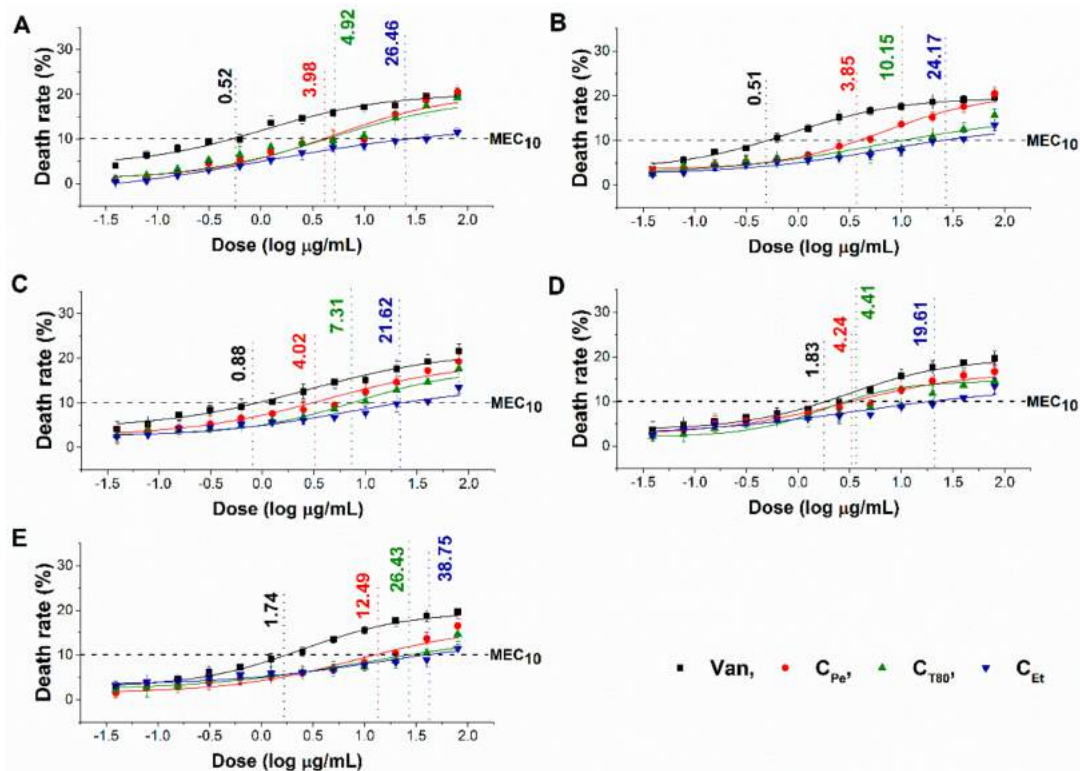


Figure 4. Minimum effective concentration (MEC₁₀) of C_{Pe}, C_{T80}, C_{Et}, and Van (µg/mL) on *E. coli* (A), *S. aureus* (B), *B. subtilis* (C), *P. aeruginosa* (D), and *S. pyogenes* (E).

2.5. Effect on Microbial Oxidative Balance

Reactive oxygen species (ROS) production and accumulation in the cells initiates oxidative stress, leading to cellular structural damage followed by induced apoptosis [6]. We have investigated the relationship between oxidative stress generation after 1 h of treatment and microbial killing activity. The results are demonstrated in Figures 6 and 7 for bacteria and fungi, respectively. Data expressed as % of the control are as follows: the ROS (1085.86 ± 126.36), peroxide (1229.86 ± 164.52) and superoxide (1276.86 ± 165.42) generation were the highest in case of *S. aureus*. The C_{Pe} showed an effective increment of ROS, peroxide, and superoxide generation in both Gram-positive and -negative bacteria when compared to C_{T80} and C_{Et} ($P < 0.01$). C_{Pe} showed increased oxidative stress in both bacteria and fungi at least seven-fold higher than the negative control whereas the positive control (menadione) produced an eight- to nine-fold increase in 1 h. The C_{Et} has generated a two to four-fold increment in oxidative stress which is the lowest among all tested compounds.

2.6. Time–Kill Kinetics Study

The time–kill kinetics curve was performed to quantify living populations after a definite time interval under different sample MEC₁₀ concentrations. A significant reduction (four log-fold) in the cell survivability has been observed in case of C_{Pe} when compared to Gc ($P < 0.01$) (Figures 8 and 9). Fifty percent of cell death occurred by C_{Pe} at 16 and 36 h in the case of bacteria and fungi, and was most

effective in reducing living colonies in case of *C. albicans* (1.73 ± 0.15 CFU/mL) after 48 h of treatment. At an average of a two-fold higher concentration, C_{Et} was able to show a killing effect compared to C_{Pe} ($P < 0.01$).

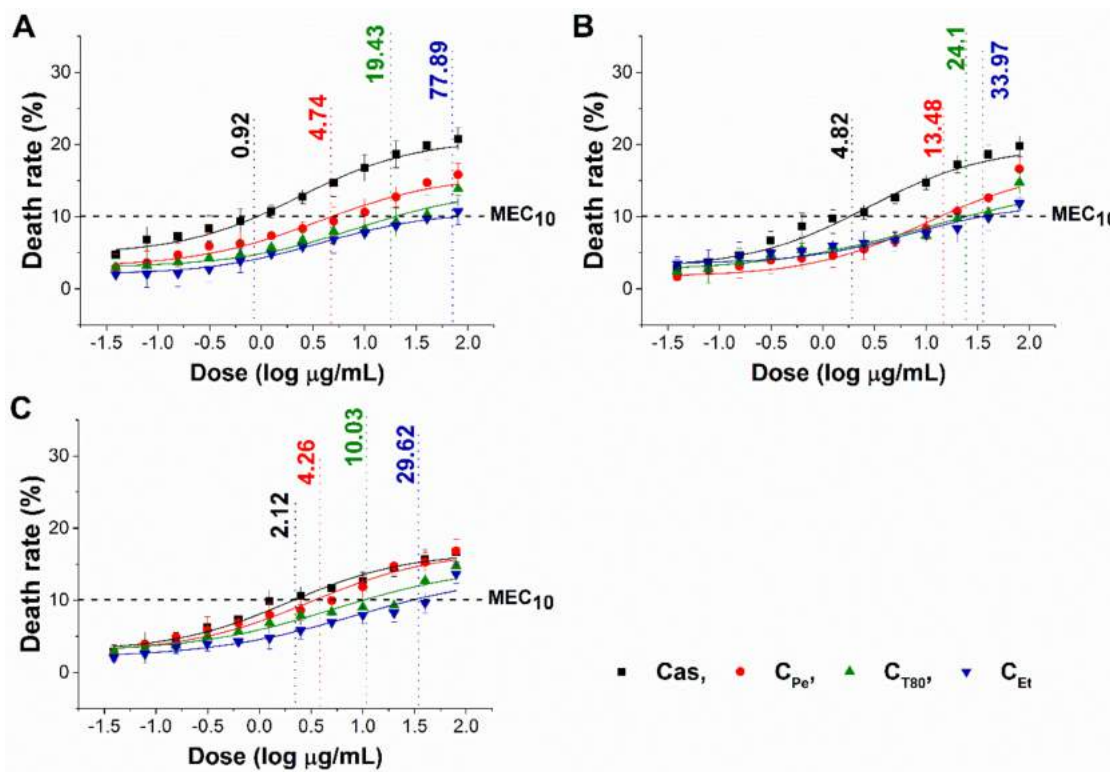


Figure 5. Minimum effective concentration (MEC₁₀) of C_{Pe} , C_{T80} , C_{Et} , and Cas ($\mu\text{g/mL}$) on *S. pombe* (A), *C. albicans* (B), and *C. tropicalis* (C).

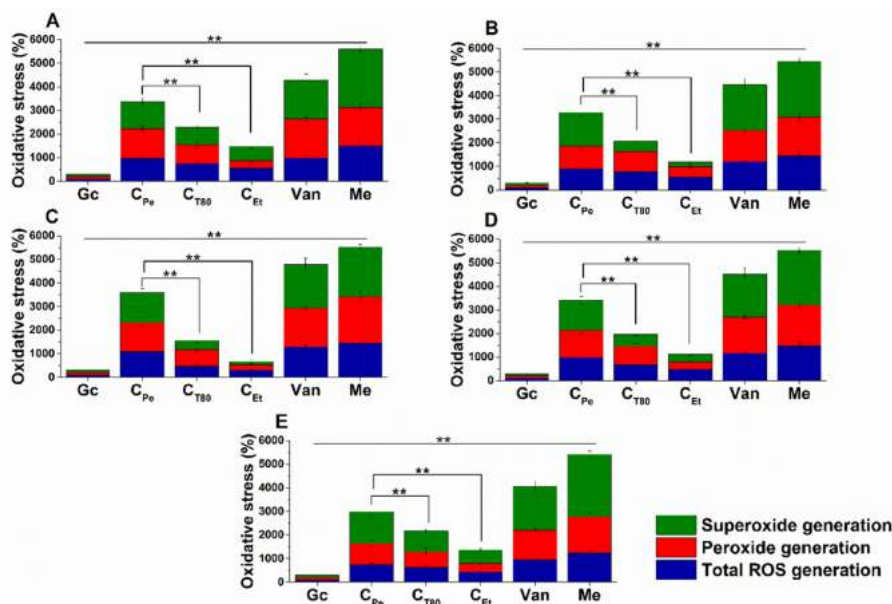


Figure 6. Percentage oxidative stress generation by C_{Pe} , C_{T80} , C_{Et} , and Van on *E. coli* (A), *S. aureus* (B), *B. subtilis* (C), *P. aeruginosa* (D), and *S. pyogenes* (E). Six independent experiments, each with 3 replicates, compared with menadione (Me) and growth control (Gc) as controls after 1 h of treatment (** $P < 0.01$).

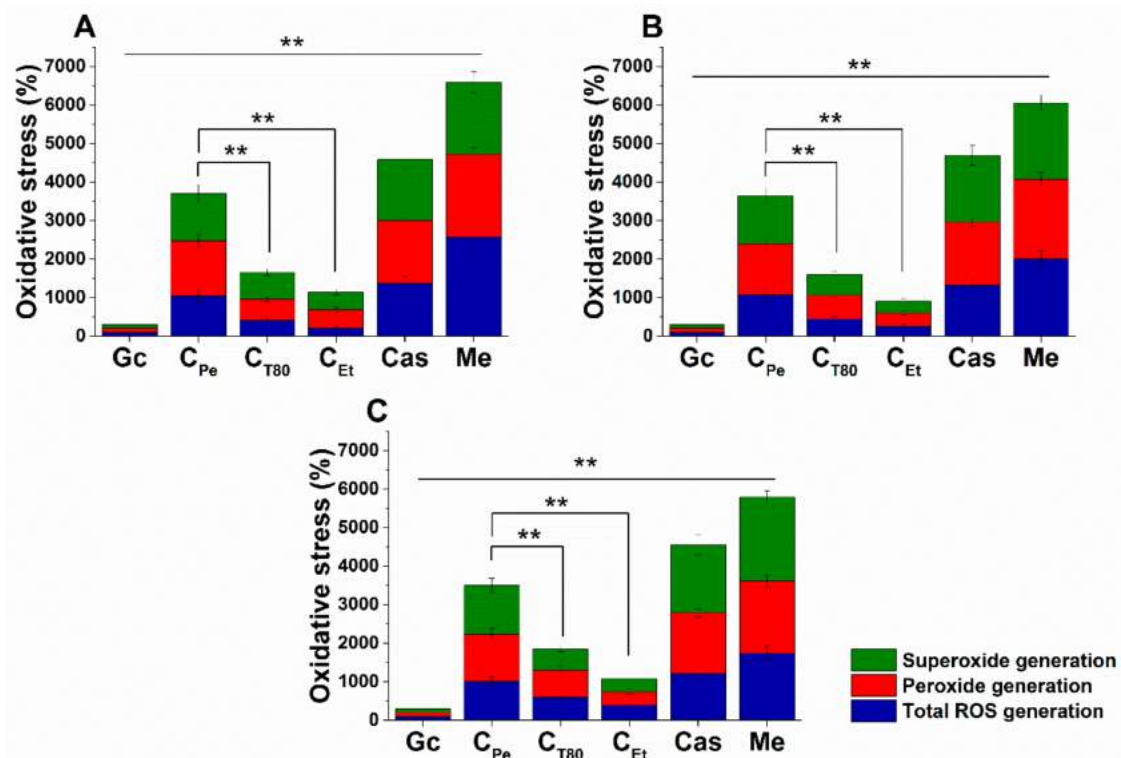


Figure 7. Percentage oxidative stress generation by C_{Pe} , C_{T80} , C_{Et} , and Cas on *S. pombe* (A), *C. albicans* (B), and *C. tropicalis* (C). Six independent experiments, each with 3 replicates, compared with Me and Gc as positive and growth controls after 1 h of treatment (** $P < 0.01$).

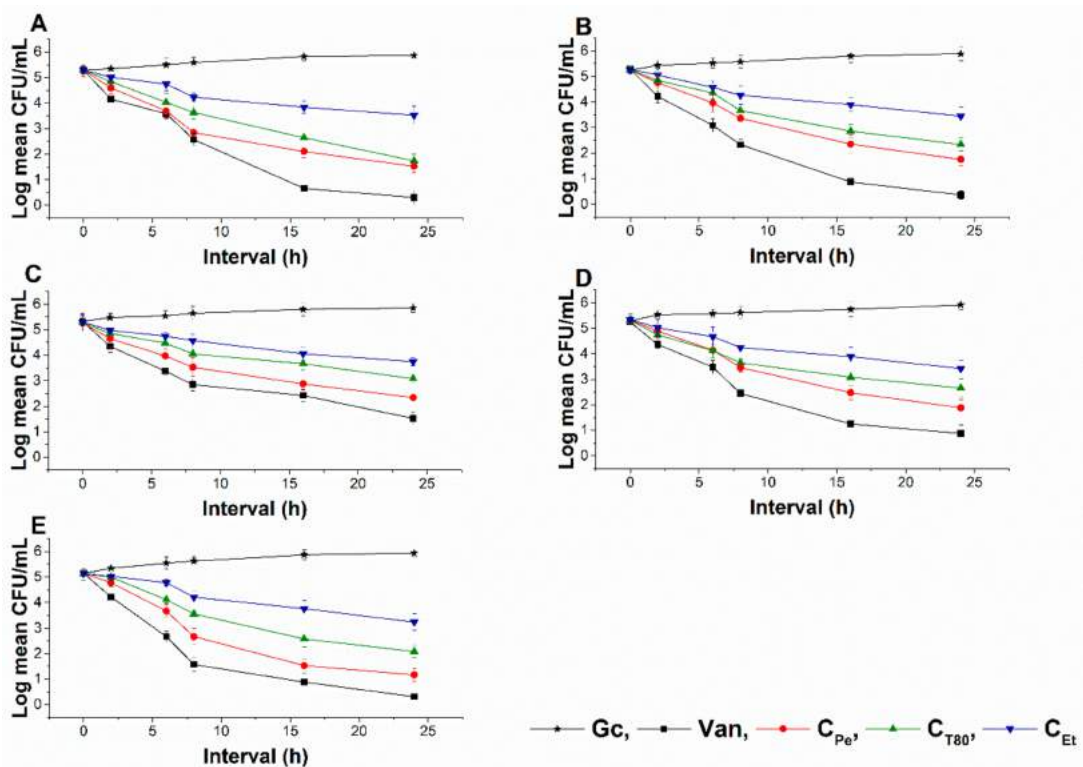


Figure 8. Colony-forming unit (CFU/mL) of C_{Pe} , C_{T80} , and C_{Et} on *E. coli* (A), *S. aureus* (B), *B. subtilis* (C), *P. aeruginosa* (D), and *S. pyogenes* (E). Six independent experiments, each with 3 replicates, compared with Van and Gc as positive and growth controls.

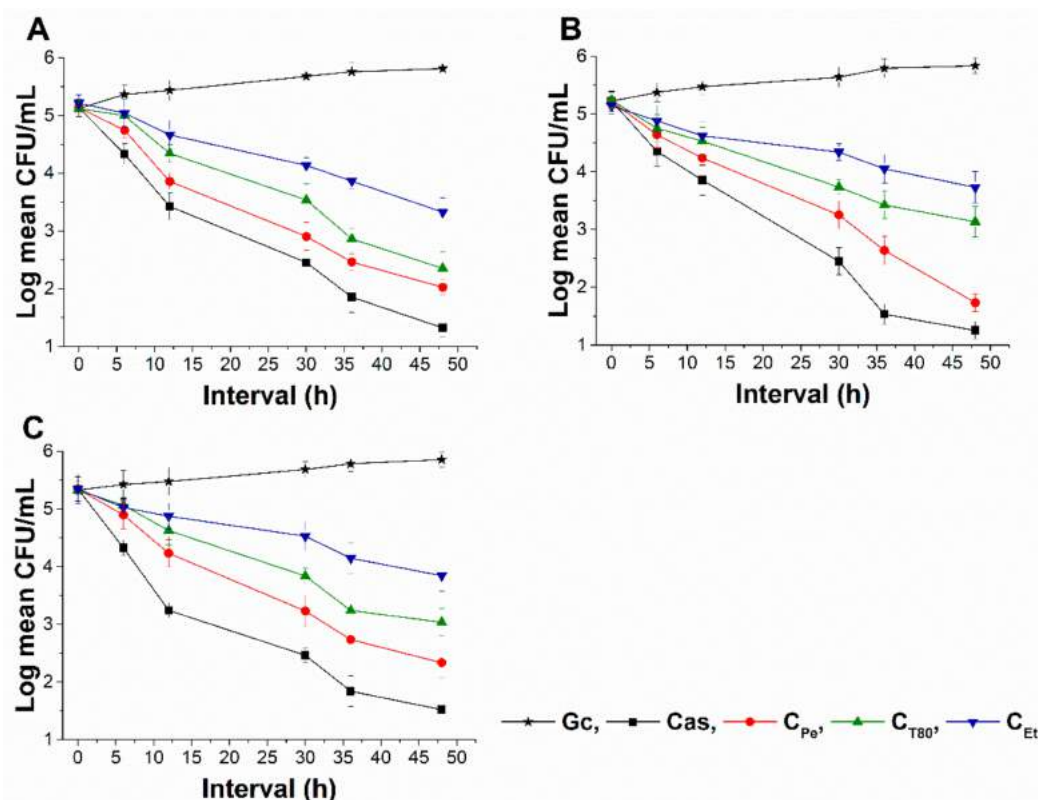


Figure 9. Colony-forming unit (CFU/mL) of C_{Pe} , C_{T80} , and C_{Et} on *S. pombe* (A), *C. albicans* (B), and *C. tropicalis* (C). Six independent experiments, each with 3 replicates, compared with Cas and Gc as positive and growth controls.

2.7. Live/dead Cell Viability Discrimination

The effect of C_{Pe} , C_{T80} , and C_{Et} on the viability of selected bacteria and fungi were tested (Figures 10 and 11). C_{Pe} decreases the viability of the tested bacteria and fungi with an average viability reduction to $42.36\% \pm 3.74\%$ and $49.62\% \pm 5.25\%$ of mean percentage viability compared to Gc after 16 and 36 h of treatments in bacteria and fungi respectively ($P < 0.01$), whereas C_{T80} and C_{Et} were less effective than C_{Pe} with mean percentage viabilities of $\geq 60\%$ and 70% , respectively.

2.8. Interaction Study between Cell Model and Different Formulations of Chamomile EO

The unilamellar liposomes (ULs), consisting of a single phospholipid, can be used as artificial cells or biological membrane model for studying the interactions between cells or cell membranes and drugs or biologically active components [24]. This study was conducted to determine the intracellular delivery ability of active components from chamomile EO for different formulations.

We have studied the interaction of ULs and different forms of chamomile EO for 24 h at 35°C . After 1 h of interaction, 27.2% of EO have penetrated the liposomes from Pickering nanoemulsion, while conventional emulsion and the ethanolic solution did not provide a measurable amount. The next sampling was after 2 h, where Pickering emulsion has delivered 48.3% of EO, conventional emulsion 0.5%, while the amount of EO delivered by the ethanolic solution was not measurable. Final sampling was after 24 h, with 82.2% of chamomile EO found in the ULs when it was introduced in Pickering nanoemulsion form, and this value was 66.8% for conventional emulsion and 32.5% for the ethanolic solution (see Table 2).

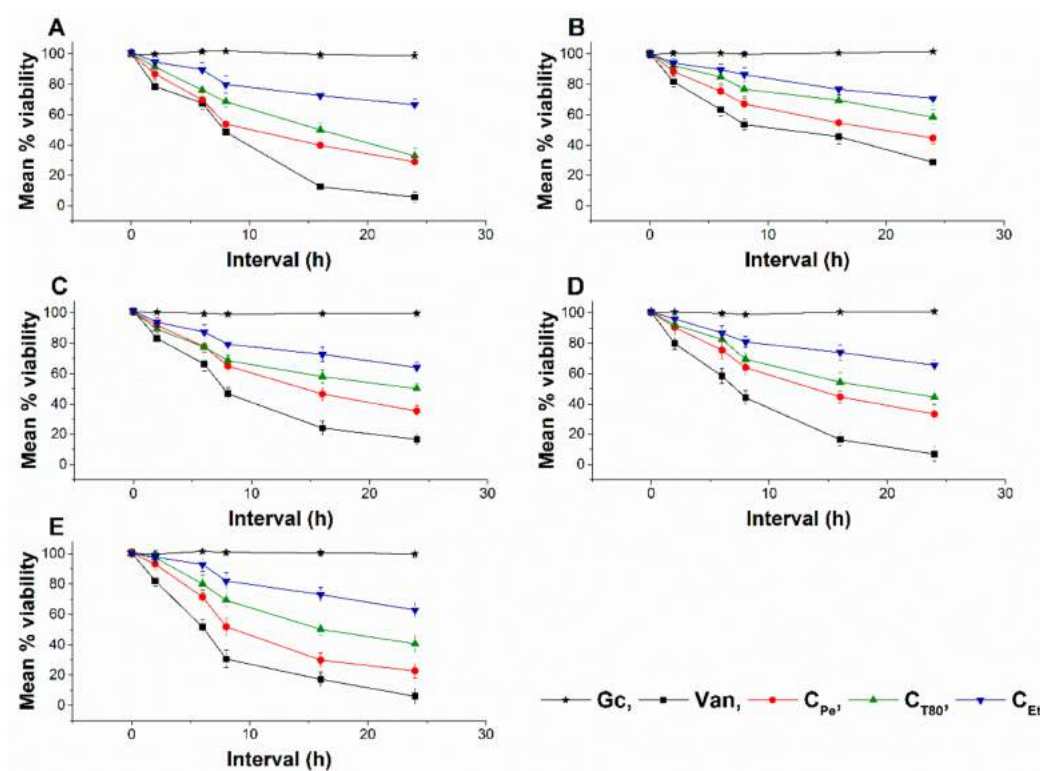


Figure 10. Mean percentage viability of C_{Pe}, C_{T80}, and C_{Et} on *E. coli* (A), *S. aureus* (B), *B. subtilis* (C), *P. aeruginosa* (D), and *S. pyogenes* (E). Six independent experiments, each with 3 replicates, compared with Van and Gc as positive and growth controls.

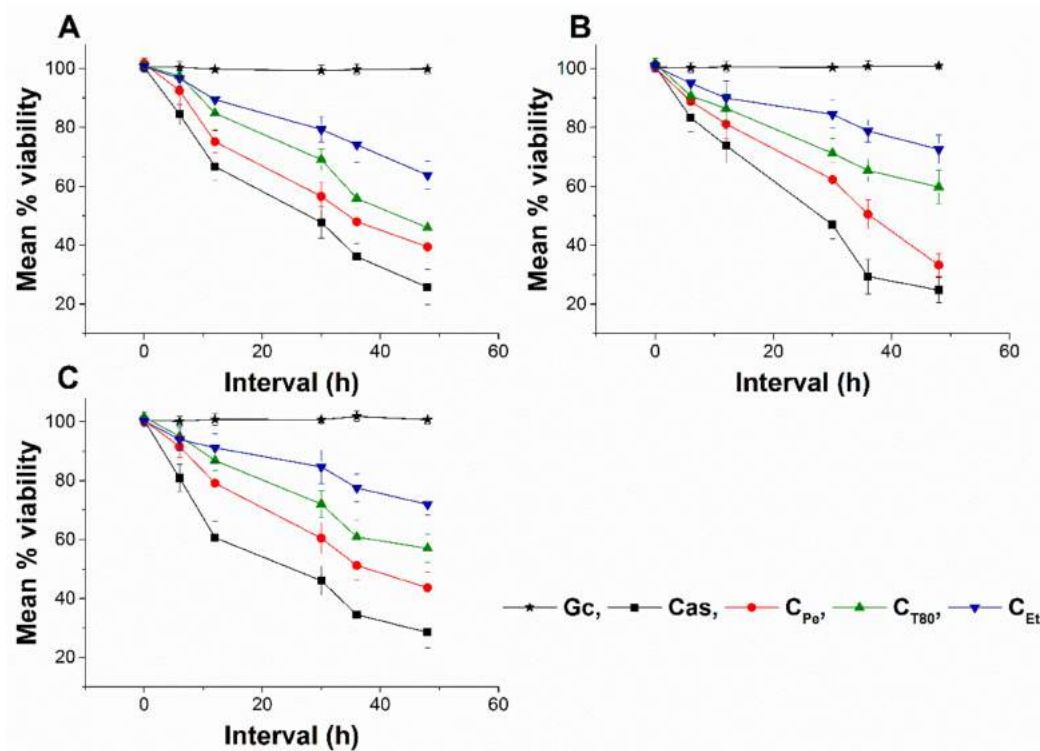


Figure 11. Mean percentage viability of C_{Pe}, C_{T80}, and C_{Et} on *S. pombe* (A), *C. albicans* (B) and *C. tropicalis* (C). Six independent experiments, each with 3 replicates, compared with Cas and Gc as positive and growth controls.

Table 2. Results of the interaction study between unilamellar liposomes (ULs) and different formulations of chamomile EO. PA means the amount in the percentage of penetrated chamomile EO. Standard deviations were calculated from 3 independent experiments.

Formulation	PA _{1h}	PA _{2h}	PA _{24h}
C _{Pe}	27.2 ± 3.7	48.3 ± 5.1	82.2 ± 4.9
C _{T80}	-	0.5 ± 0.1	66.8 ± 3.6
C _{Et}	-	-	35.5 ± 1.0

3. Discussion

The effect of three different formulations on antimicrobial activity of chamomile essential oil has been examined. We have successfully prepared stable Pickering nanoemulsion using silica nanoparticles with appropriate lipophilicity. The emulsion was stable for three months. The effectiveness of Pickering emulsion was compared with conventional emulsion and ethanolic solution.

Based on our antimicrobial activity analyses, C_{Pe} shows higher growth inhibitory action and consequently lower MICs compared to C_{T80} and C_{Et}. Many researchers have studied the antimicrobial activity of chamomile oil [3,7,13,23,25], however, the mechanism of action at subinhibitory concentrations has not previously been studied. Our data suggest an effective killing activity of C_{Pe} on selected bacteria and fungi. It is believed that EOs act against cell cytoplasmic membrane and induce stress in microorganisms [26–29]. To visualize the effects of C_{Pe}, C_{T80}, and C_{Et}, we introduced different staining methods to understand their mechanism. C_{Pe} was able to generate higher oxidative stress compared to the conventional emulsion and ethanolic solution followed by metabolic interference and cell wall disruption and finally caused cell death at subinhibitory concentration [21,30–33].

The results obtained in the model experiment show that C_{Pe} is the most effective form for the intracellular delivery of chamomile EO. Based on these results it can be established that the different antibacterial and antifungal effects may be caused by the difference of adsorption properties of EO forms to the microbial cells. The mechanism of delivery has not been revealed in this study, but evidence for the adsorption of Pickering emulsion droplets on the cell membrane has been previously reported [18]. Assuming the adsorption of C_{Pe} droplets on the cell membrane of investigated microbes, intracellular delivery of active components from EO is feasible in two ways. Passive diffusion is caused by the higher local concentration gradient of EO on the cell membrane, or fusion of C_{Pe} droplets with microbial cells. Overall, our observations demonstrate that C_{Pe} facilitates chamomile oil to permeate cells, inducing oxidative stress and disrupting the membrane integrity because of higher adsorption efficacy of chamomile EO. SNP acts as a stabilizer, inhibiting the easy escape of EOs from the emulsion system compared to the conventional emulsion and free oils.

4. Materials and Methods

4.1. Synthesis, Surface Modification, and Characterization of Stöber Silica Nanoparticles

We have performed the synthesis of 20 nm hydrophilic silica nanoparticles with the previously reported modified Stöber method [9]. Briefly, a solution of tetraethoxysilane (TEOS) and ultrapure water in ethanol was prepared by using tetraethoxysilane, (Thermo Fisher GmbH, Kandel, Germany, pur. 98%); absolute ethanol AnalaR Normapur ≥99.8% purity (VWR Chemicals, Debrecen, Hungary) and water (membraPure Astacus Analytical with UV, VWR Chemicals, Debrecen, Hungary). The solution was stirred for 20 min and sonicated for another 20 min (Bandelin Sonorex RK 52H, BANDELIN electronic GmbH & Co. KG, Berlin, Germany). An appropriate amount of NH₃ solution (28% (w/w) ammonium solution, VWR Chemicals, Debrecen, Hungary) was added to the reaction mixture and was stirred at 1000 rpm for 24 h at room temperature (25 °C). The molar ratio of components was water/ethanol/TEOS/NH₃ = 100:300:5.2:1. The surface of hydrophilic silica nanoparticles was modified with propyltriethoxysilane (PTES Alfa Aesar, Haverhill, MA, USA, pur. 99%) in a post-synthesis modification reaction [32]. The ethanolic solution of the modifying agent was added to the freshly

prepared hydrophilic silica nanoparticle suspensions; the mixtures were stirred for 6 h with 1000 rpm at room temperature. Before further use of the SNPs, the ammonium hydroxide and ethanol were always removed from the reaction mixture by distillation (Heidolph Laborota 4000, Heidolph Instruments GmbH & CO. KG, Germany). The water content was supplemented three times. The concentration of silica nanoparticle water-based suspension was finally adjusted to 1 mg/cm³.

The size distribution and zeta potential of silica nanoparticles were determined by dynamic light scattering (DLS) using Malvern Zetasizer NanoS and NanoZ instruments (Malvern Instruments-Malvern Panalytical, Worcester, UK). The morphology and size distribution were also examined with transmission electron microscopy (TEM), (JEOL JEM-1200 EX II and JEM-1400, JEOL Ltd., Tokyo, Japan). The samples were dropped onto 200 mesh copper grids coated with carbon film (EMR Carbon support grids, Micro to Nano Ltd, Haarlem, The Netherlands) from diluted suspensions.

4.2. Preparation and Characterization of Pickering Nanoemulsion

As stabilizing agents, surface-modified silica nanoparticles or Tween 80 surfactant (Polysorbate80, Acros Organics, New Jersey, NJ, USA) were used. The concentration of stabilizing agents and chamomile essential oil (bluish *Matricaria chamomilla* oil, Aromax Ltd., Budapest, Hungary) was kept constant for all experiments, the values were 1 mg/mL and 100 µg/mL, respectively. The first step of the emulsification process was sonication for 2 minutes (Bandelin Sonorex RK 52H, BANDELIN electronic GmbH & Co. KG, Germany), then emulsification using UltraTurrax (IKA Werke T-25 basic, IKA®-Werke GmbH & Co. KG, Germany) for 5 min at 21,000 rpm. To compare the different formulations, an ethanolic solution was also prepared; chamomile essential oil was added to absolute ethanol at 100 µg/mL concentration, and the solution was sonicated for 5 min.

The stability of Pickering emulsion was studied from periodical droplet size determination using DLS measurements (Malvern Zetasizer Nano S, Malvern Panalytical Ltd, Worcester, UK).

4.3. Materials for Biological Experiments

In these experiments, the sterile 96-well microtiter plates were from Greiner Bio-One (Kremsmünster, Austria), potassium phosphate monobasic, glucose, adenine, 96% ethanol (Et), peptone, yeast extract, agar-agar, and Mueller Hinton agar were from Reanal Labor (Budapest, Hungary), modified RPMI 1640 (contains 3.4% MOPS, 1.8% glucose, and 0.002% adenine), SYBR green I 10,000×, propidium iodide, dihydrorhodamine 123 (DHR 123), 2',7'-dichlorofluorescein diacetate (DCFDA), dihydroethidine (DHE) and menadione (Me) were from Sigma-Aldrich Chemie GmbH (Steinheim, Germany), disodium phosphate and dimethyl sulfoxide (DMSO) were from Chemolab Ltd. (Budapest, Hungary), sodium chloride from VWR Chemicals (Debrecen, Hungary), potassium chloride was from Scharlau Chemie S.A (Barcelona, Spain), 3-(*N*-morpholino) propanesulfonic acid (MOPS) was from Serva Electrophoresis GmbH (Heidelberg, Germany), caspofungin (Cas) from Merck Sharp & Dohme Ltd (Hertfordshire, UK), vancomycin (Van) from Fresenius Kabi Ltd. (Budapest, Hungary), 0.22 µm vacuum filters from Millipore (Molsheim, France) and the cell spreader was from Sarstedt AG & Co. KG (Numbrecht, Germany). All other chemicals used in the study were of analytical or spectroscopic grade. For fungi, we used an in-house nutrient agar medium [34] while phosphate-buffered saline (PBS, pH 7.4) was from Life Technologies Ltd. (Budapest, Hungary). Highly purified water (<1.0 µS) was applied throughout the studies.

4.4. Determination of Minimum Inhibitory Concentration (MIC₉₀)

4.4.1. Microorganisms

Escherichia coli (*E. coli*) PMC 201, *Pseudomonas aeruginosa* (*P. aeruginosa*) PMC 103, *Bacillus subtilis* (*B. subtilis*) SZMC 0209, *Staphylococcus aureus* (*S. aureus*) ATCC 29213, *Streptococcus pyogenes* (*S. pyogenes*) SZMC 0119, *Schizosaccharomyces pombe* (*S. pombe*) ATCC 38366, *Candida albicans* (*C. albicans*) ATCC 1001, and *Candida tropicalis* (*C. tropicalis*) SZMC 1368 were obtained from Szeged Microbial Collection,

Department of Microbiology, University of Szeged, Hungary (SZMC) and Department of General and Environmental Microbiology, Institute of Biology, University of Pecs, Hungary (PMC).

4.4.2. Antimicrobial Activity Tests

The antibacterial activity of the tested drugs was separately evaluated on *E. coli*, *P. aeruginosa*, *B. subtilis*, *S. aureus*, and *S. pyogenes* according to our previously published protocol [35]. In brief, bacterial populations of $\sim 10^5$ CFU/mL were inoculated into RPMI media and incubated for 16 h at 35 ± 2 °C with test compounds (C_{Pe} , C_{T80} , C_{Et} , and Van) over a wide concentration range (0.3–0.01 $\mu\text{g/mL}$). The absorbance was measured by a Thermo Scientific Multiskan EX 355 plate reader (InterLabsystems, Budapest, Hungary) at 600 nm.

The antifungal activity against *S. pombe*, *C. albicans*, and *C. tropicalis* species were also carried out according to our previously published method [35]. Briefly, $\sim 10^3$ cells/mL were incubated for 48 h at 30 ± 2 °C with test compounds (C_{Pe} , C_{T80} , C_{Et} and Cas) at wide concentration range (20–0.01 $\mu\text{g/mL}$) in modified RPMI media. The absorbance was measured by a Thermo Scientific Multiskan EX 355 plate reader (InterLabsystems, Budapest, Hungary) at 595 nm. Absorbance values were converted to percentages compared to growth control ($\sim 100\%$) and data were fitted by nonlinear dose–response curve method to calculate the dose producing $\geq 90\%$ growth inhibition (MIC_{90}). All the measurements were performed by applying three technical replicates in six independent experiments. Van and Cas were used as a standard antibacterial and antifungal drug, respectively, throughout the experiments.

4.5. Determination of Minimum Effective Concentration (MEC_{10})

The assay has been designed to determine the killing effects of the test compounds for a certain period of time. In brief, a wide concentration range (0.03–80 $\mu\text{g/mL}$) of the test samples were used to treat $\sim 10^6$ cells/mL for one hour. One milliliter of treated and untreated samples were taken and were diluted 10^5 times followed by spreading 50 μL samples onto 20 mL nutrient agar media and incubated for 24 h at 35 °C (bacteria) and 30 °C (fungi) for colony-forming unit (CFU/mL) quantification. The data were compared with growth control and positive control (Van for bacteria and Cas for fungi) for percentage mortality ($\sim 10\%$ death) determination. It is noteworthy that in the MEC_{10} experiments, the inoculated microbial cell number was 10^3 times higher than was used in the MIC_{90} determinations (10^6 vs. 10^3). However, in both cases, the same formula was used (see Section 4.7). All the measurements were performed by applying three technical replicates in six independent experiments.

4.6. Determination of Microbial Oxidative Generation and Killing Activity

4.6.1. Quantification of Total ROS Generation

Total ROS generation was assayed according to previously published protocols [27,28,34,36]. Briefly, $\sim 10^6$ cells/mL were collected and centrifuged at 1500 g for 5 min and were suspended in PBS. The cells were stained with a 20 mM stock solution of DCFDA in PBS (pH 7.4) to achieve an end concentration of 25 μM , and were incubated at 35 °C (for bacteria) and 30 °C (for fungi) for 30 min in the dark with mild shaking. The cells were centrifuged (Hettich Rotina 420R, Auro-Science Consulting Ltd., Budapest, Hungary) and suspended in RPMI media. The cells were treated with C_{Pe} , C_{T80} , C_{Et} , Van (bacteria), and Cas (fungi) at their respective MEC_{10} concentrations for one hour. The fluorescence signals were recorded at Ex/Em = 485/535 nm wavelengths by a Hitachi F-7000 fluorescence spectrophotometer/plate reader (Auro-Science Consulting Ltd., Budapest, Hungary). The percentage increase in oxidative balance was measured by comparing the signals to those of the growth controls (Gc). Six independent experiments were done with three technical replicates for each treatment.

4.6.2. Detection of Peroxide (O_2^{2-}) and Superoxide Anion ($O_2^{\bullet-}$) Generation

The previously described protocol was adapted for peroxide [36,37] and superoxide anion radicals [34,38] with modifications. A positive control, Me (0.5 mmol/L as end concentration), C_{Pe} , C_{T80} , C_{Et} , Van (bacteria), and Cas (fungi) at their respective MEC_{10} concentrations were used to treat the cell suspensions ($\sim 10^6$ cells/mL) for an hour at 35 °C (bacteria) and 30 °C (fungi) in RPMI media. Thereafter, the cells were centrifuged at 1500 g for 5 min at room temperature followed by resuspension of pellets in PBS of the same volume. DHR 123 (10 μ mol/L, end concentration) and DHE (15 μ mol/L, end concentration) were added separately to the cell samples for peroxide and superoxide determination. The stained cells were further incubated at 35 °C (bacteria) and 30 °C (fungi) in the dark with mild shaking. The samples were centrifuged and resuspended in PBS followed by the distribution of the samples into the wells of 96-well microplates. The fluorescence was measured at excitation/emission wavelengths of 500/536 nm for peroxides and 473/521 nm for superoxide detection by a Hitachi F-7000 fluorescence spectrophotometer/plate reader (Auro-Science Consulting Ltd., Budapest, Hungary). The percentage increase in oxidative stress was measured by comparing the signals to those of the growth controls (Gc). Six independent experiments were done with three technical replicates for each treatment.

4.6.3. Time–Kill Kinetics Assay

We followed a protocol previously published by T. Appiah et. al., with modifications [39]. In brief, C_{Pe} , C_{T80} , C_{Et} , Van (bacteria), and Cas (fungi) at their respective MEC_{10} concentrations were used to treat the microbial population of $\sim 10^6$ CFU/mL and were incubated at 35 °C (bacteria) and 30 °C (fungi). One milliliter of the treated and untreated samples was pipetted at time intervals of 0, 2, 6, 8, 16, and 24 h for bacteria, and 0, 6, 12, 30, 36, and 48 h for fungi, and were diluted 10^5 times followed by spreading 50 μ L onto 20 mL nutrient agar media using a cell spreader and incubated at 35 °C (bacteria) and 30 °C (fungi) for 24 h. Van and Cas were used as reference controls for bacteria and fungi. Control without treatment was considered as growth control (Gc). The colony-forming unit (CFU/mL) of the microorganisms were determined, performed in triplicate and was plotted against time (h). Six independent experiments were done with three technical replicates for each treatment.

4.6.4. Live/dead Discrimination of Microbial Cells

For live/dead cell discrimination, we followed the protocol published previously [35]. In brief, the cell population of $\sim 10^6$ cells/mL were treated with C_{Pe} , C_{T80} , C_{Et} , Van (bacteria), and Cas (fungi) at their respective MEC_{10} concentrations and were incubated at 35 °C (bacteria) and 30 °C (fungi). Treated and untreated samples were pipetted at time intervals of 0, 2, 6, 8, 16, and 24 h for bacteria, and 0, 6, 12, 30, 36 and 48 h for fungi followed by centrifugation at 1000 g for 5 min, washed, and resuspended in PBS (100 μ L/well). One hundred microliters of freshly prepared working dye solution in PBS (using 20 μ L SYBR green I and 4 μ L propidium iodide diluted solutions as described earlier) were added to the samples. The plate was incubated at room temperature for 15 min in the dark with mild shaking. A Hitachi F-7000 fluorescence spectrophotometer/plate reader (Auro-Science, Consulting Ltd., Budapest, Hungary) was used to measure the fluorescence intensities of SYBR green I (excitation/emission wavelengths: 490/525 nm) and propidium iodide (excitation/emission wavelengths: 530/620 nm), respectively. A green to red fluorescence ratio for each sample and for each dose was achieved and the % of dead cells with the response to the applied dose was plotted against the applied test compound doses using a previously published formula [35]. All treatments were done in triplicates and six independent experiments were performed.

4.7. Statistical Analysis of Microbiological Experiments

All data were given as mean \pm SD. Graphs and statistical analyses were conducted using OriginPro 2016 (OriginLab Corp., Northampton, MA, USA). All experiments were performed independently six

times and data were analyzed by one-way ANOVA test. $P < 0.01$ was considered statistically significant. The growth inhibition concentration (MIC_{90}) and minimum effective concentration (MEC_{10}) were calculated using a nonlinear dose–response sigmoidal curve function as follows:

$$y = A_1 + \frac{A_2 - A_1}{1 + 10^{(\log_x 0 - x)p}}$$

where A_1 , A_2 , $LOG_x 0$ and p as the bottom asymptote, top asymptote, center, and hill slope of the curve have been considered.

4.8. Interaction Study between the Cell Model (Unilamellar Liposomes) and Different Formulations of Chamomile EO

Unilamellar liposomes (ULs) have been prepared from phosphatidylcholine (Phospolipon 90G, Phospholipid GmbH, Berlin, Germany) by the modified method described before by Alexander Moscho et al. [40]. Phosphatidylcholine was dissolved in chloroform ($\geq 98\%$ stabilized, VWR Chemicals, Debrecen, Hungary) in 0.1 M concentration, and 150 μ L of this solution was diluted in a mixture of 6 mL chloroform and 1 mL of methanol. This solution was added dropwise to 40 mL of PBS buffer while stirring on a magnetic stirrer at 600 rpm (VELP Scientifica Microstirrer, Magnetic Stirrer, Usmate Velate MB, Italy). The solvents were removed on a rotational evaporator at 40 °C (Heidolph Laborota 4000, Heidolph Instruments GmbH & CO. KG, Germany). The resulting suspension volume was set to 25 mL with PBS buffer and stored in the refrigerator at 8 °C until further use. A 5 mL suspension of ULs was mixed with 3 mL Pickering nanoemulsion, conventional emulsion, or ethanolic solution, and the chamomile EO concentration was 100 μ g/mL for the different formulations. The mixture was stirred at 600 rpm for 24 h at 35 °C, and 1 mL aliquots were taken after 1, 2, and 24 h. The samples were centrifuged at 3000 rpm and 20 °C for 5 min, and the ULs were collected and dissolved in absolute ethanol. The chamomile–EO content of samples was determined with UV/VIS Spectroscopy at 290 nm (Jasco V-550 UV/VIS Spectrophotometer; Jasco Inc., Easton, MD, USA). For UV/VIS measurements we have prepared samples without chamomile–EOs, i.e., ULs with SNP suspension, Tween 80 solution, or ethanol were also mixed and centrifuged and were used as blanks.

4.9. GC-MS Analysis of Chamomile EO

Gas chromatography and mass spectrometry (GC–MS) analyses were carried out on an Agilent Technologies (Palo Alto, CA, USA) gas chromatograph model 7890A with 5975C mass detector. Operating conditions were as follows: column HP-5MS (5% phenylmethyl polysiloxane), 30 m \times 0.25 mm i.d., 0.25 μ m coating thickness. Helium was used as the carrier gas at 1 mL/min, injector temperature was 250 °C. HP-5MS column temperature was programmed at 70 °C isothermal for 2 min, and then increased to 200 °C at a rate of 3 °C/min and held isothermal for 18 min. The split ratio was 1:50, ionization voltage 70 eV; ion source temperature 230 °C; mass scan range: 45–450 mass units. The percentage composition was calculated from the GC peak areas using the normalization method (without correction factors). The component percentages were calculated as mean values from duplicate GC–MS analyses of the oil sample. The results of GC–MS analysis can be seen in Supplementary Materials.

Supplementary Materials: The followings are available online: Composition of chamomile essential oil analyzed by GC-MS method. Results can be seen in Supplementary Table S1 and Figure S1.

Author Contributions: Conceptualization T.K., and A.S.; methodology S.D., B.H., T.K. and A.S.; software, S.D.; formal analysis, S.D. and B.H.; investigation, S.D. and B.H.; GC analysis S.Š. and S.J. resources, A.S.; data curation, S.D., B.H.; writing—original draft preparation, S.D. and B.H.; writing—review and editing, T.K. and A.S.; visualization, S.D. and B.H.; supervision, T.K. and A.S.; funding acquisition A.S. and T.K.

Funding: This work was supported by EFOP 3.6.1-16-2016-00004 project (Comprehensive Development for Implementing Smart Specialization Strategies at the University of Pécs), University of Pécs, Medical School, KA-2018-17 and NKFI-EPR K/115394/2015 grants.

Conflicts of Interest: The authors declare no conflict of interest.

References

1. Manion, C.R.; Widder, R.M. Essentials of essential oils. *Am. J. Health-Syst. Pharm.* **2017**, *74*, e153–e162. [[CrossRef](#)]
2. Omonijo, F.A.; Ni, L.; Gong, J.; Wang, Q.; Lahaye, L.; Yang, C. Essential oils as alternatives to antibiotics in swine production. *Anim. Nutr.* **2018**, *4*, 126–136. [[CrossRef](#)]
3. McKay, D.L.; Blumberg, J.B. A Review of the bioactivity and potential health benefits of chamomile tea (*Matricaria recutita* L.). *Phytother. Res.* **2006**, *20*, 519–530. [[CrossRef](#)]
4. Lis-Balchin, M. *Aromatherapy Science: A Guide for Healthcare Professionals*; Pharmaceutical Press: London, UK, 2006; ISBN 978-0-85369-578-3.
5. Pfaller, M.A.; Sheehan, D.J.; Rex, J.H. Determination of Fungicidal Activities against Yeasts and Molds: Lessons Learned from Bactericidal Testing and the Need for Standardization. *Clin. Microbiol. Rev.* **2004**, *17*, 268–280. [[CrossRef](#)]
6. Donsì, F.; Ferrari, G. Essential oil nanoemulsions as antimicrobial agents in food. *J. Biotechnol.* **2016**, *233*, 106–120. [[CrossRef](#)] [[PubMed](#)]
7. Singh, O.; Khanam, Z.; Misra, N.; Srivastava, M. Chamomile (*Matricaria chamomilla* L.): An overview. *Pharmacogn. Rev.* **2011**, *5*, 82. [[CrossRef](#)] [[PubMed](#)]
8. Alizadeh Behbahani, B.; Tabatabaei Yazdi, F.; Vasiee, A.; Mortazavi, S.A. Oliveria decumbens essential oil: Chemical compositions and antimicrobial activity against the growth of some clinical and standard strains causing infection. *Microb. Pathog.* **2018**, *114*, 449–452. [[CrossRef](#)]
9. Balázs, V.L.; Horváth, B.; Kerekes, E.; Ács, K.; Kocsis, B.; Varga, A.; Böszörményi, A.; Nagy, D.U.; Krisch, J.; Széchenyi, A.; et al. Anti-Haemophilus Activity of Selected Essential Oils Detected by TLC-Direct Bioautography and Biofilm Inhibition. *Molecules* **2019**, *24*, 3301. [[CrossRef](#)] [[PubMed](#)]
10. Ćavar, S.; Maksimović, M.; Vidic, D.; Parić, A. Chemical composition and antioxidant and antimicrobial activity of essential oil of *Artemisia annua* L. from Bosnia. *Ind. Crop. Prod.* **2012**, *37*, 479–485.
11. Fasihi, H.; Noshirvani, N.; Hashemi, M.; Fazilati, M.; Salavati, H.; Coma, V. Antioxidant and antimicrobial properties of carbohydrate-based films enriched with cinnamon essential oil by Pickering emulsion method. *Food Packag. Shelf Life* **2019**, *19*, 147–154. [[CrossRef](#)]
12. Tang, X.; Shao, Y.-L.; Tang, Y.-J.; Zhou, W.-W. Antifungal Activity of Essential Oil Compounds (Geraniol and Citral) and Inhibitory Mechanisms on Grain Pathogens (*Aspergillus flavus* and *Aspergillus ochraceus*). *Molecules* **2018**, *23*, 2108. [[CrossRef](#)] [[PubMed](#)]
13. Stanojevic, L.P.; Marjanovic-Balaban, Z.R.; Kalaba, V.D.; Stanojevic, J.S.; Cvetkovic, D.J. Chemical Composition, Antioxidant and Antimicrobial Activity of Chamomile Flowers Essential Oil (*Matricaria chamomilla* L.). *J. Essent. Oil Bear. Plants* **2016**, *19*, 2017–2028. [[CrossRef](#)]
14. Alastruey-Izquierdo, A.; Gomez-Lopez, A.; Arendrup, M.C.; Lass-Flörl, C.; Hope, W.W.; Perlin, D.S.; Rodriguez-Tudela, J.L.; Cuenca-Estrella, M. Comparison of Dimethyl Sulfoxide and Water as Solvents for Echinocandin Susceptibility Testing by the EUCAST Methodology. *J. Clin. Microbiol.* **2012**, *50*, 2509–2512. [[CrossRef](#)] [[PubMed](#)]
15. Inouye, S.; Tsuruoka, T.; Uchida, K.; Yamaguchi, H. Effect of Sealing and Tween 80 on the Antifungal Susceptibility Testing of Essential Oils. *Microbiol. Immunol.* **2001**, *45*, 201–208. [[CrossRef](#)] [[PubMed](#)]
16. Thielmann, J.; Muranyi, P.; Kazman, P. Screening essential oils for their antimicrobial activities against the foodborne pathogenic bacteria *Escherichia coli* and *Staphylococcus aureus*. *Heliyon* **2019**, *5*, e01860. [[CrossRef](#)]
17. Pina-Barrera, A.M.; Alvarez-Roman, R.; Baez-Gonzalez, J.G.; Amaya-Guerra, C.A.; Rivas-Morales, C.; Gallardo-Rivera, C.T.; Galindo-Rodriguez, S.A. Application of a multisystem coating based on polymeric nanocapsules containing essential oil of *Thymus vulgaris* L. to increase the shelf life of table grapes (*Vitis vinifera* L.). *IEEE Trans. NanoBiosci.* **2019**, 549–557. [[CrossRef](#)]
18. Zhou, Y.; Sun, S.; Bei, W.; Zahi, M.R.; Yuan, Q.; Liang, H. Preparation and antimicrobial activity of oregano essential oil Pickering emulsion stabilized by cellulose nanocrystals. *Int. J. Biol. Macromol.* **2018**, *112*, 7–13. [[CrossRef](#)]
19. Abarca, R.L.; Rodríguez, F.J.; Guarda, A.; Galotto, M.J.; Bruna, J.E. Characterization of beta-cyclodextrin inclusion complexes containing an essential oil component. *Food Chem.* **2016**, *196*, 968–975. [[CrossRef](#)]

20. Ciobanu, A.; Landy, D.; Fourmentin, S. Complexation efficiency of cyclodextrins for volatile flavor compounds. *Food Res. Int.* **2013**, *53*, 110–114. [[CrossRef](#)]
21. Cossu, A.; Wang, M.S.; Chaudhari, A.; Nitin, N. Antifungal activity against *Candida albicans* of starch Pickering emulsion with thymol or amphotericin B in suspension and calcium alginate films. *Int. J. Pharm.* **2015**, *493*, 233–242. [[CrossRef](#)]
22. Wang, J.; Li, Y.; Gao, Y.; Xie, Z.; Zhou, M.; He, Y.; Wu, H.; Zhou, W.; Dong, X.; Yang, Z.; et al. Cinnamon oil-loaded composite emulsion hydrogels with antibacterial activity prepared using concentrated emulsion templates. *Ind. Crop. Prod.* **2018**, *112*, 281–289. [[CrossRef](#)]
23. Srivastava, J.K.; Shankar, E.; Gupta, S. Chamomile: A herbal medicine of the past with bright future. *Mol. Med. Rep.* **2010**, *3*, 895–901. [[PubMed](#)]
24. Rideau, E.; Dimova, R.; Schwille, P.; Wurm, F.R.; Landfester, K. Liposomes and polymersomes: A comparative review towards cell mimicking. *Chem. Soc. Rev.* **2018**, *47*, 8572–8610. [[CrossRef](#)] [[PubMed](#)]
25. Göger, G.; Demirci, B.; Ilgin, S.; Demirci, F. Antimicrobial and toxicity profiles evaluation of the Chamomile (*Matricaria recutita* L.) essential oil combination with standard antimicrobial agents. *Ind. Crop. Prod.* **2018**, *120*, 279–285.
26. Memar, M.Y.; Ghotaslou, R.; Samiei, M.; Adibkia, K. Antimicrobial use of reactive oxygen therapy: Current insights. *Infect. Drug Resist.* **2018**, *11*, 567–576. [[CrossRef](#)] [[PubMed](#)]
27. Eruslanov, E.; Kusmartsev, S. Identification of ROS Using Oxidized DCFDA and Flow-Cytometry. In *Advanced Protocols in Oxidative Stress II*; Armstrong, D., Ed.; Humana Press: Totowa, NJ, USA, 2010; Volume 594, pp. 57–72. ISBN 978-1-60761-410-4.
28. Dong, T.G.; Dong, S.; Catalano, C.; Moore, R.; Liang, X.; Mekalanos, J.J. Generation of reactive oxygen species by lethal attacks from competing microbes. *Proc. Natl. Acad. Sci. USA* **2015**, *112*, 2181–2186. [[CrossRef](#)] [[PubMed](#)]
29. Máté, G.; Gazdag, Z.; Mike, N.; Papp, G.; Pócsi, I.; Pesti, M. Regulation of oxidative stress-induced cytotoxic processes of citrinin in the fission yeast *Schizosaccharomyces pombe*. *Toxicon* **2014**, *90*, 155–166. [[CrossRef](#)]
30. Dohare, S.; Dubey, S.D.; Kalia, M.; Verma, P.; Pandey, H.; Singh, K.; Agarwal, V. Anti-biofilm activity of *Eucalyptus globulus* oil encapsulated silica nanoparticles against *E. coli* biofilm. *Int. J. Pharm. Sci. Res.* **2014**, *5*, 5013–5018.
31. Saad, N.Y.; Muller, C.D.; Lobstein, A. Major bioactivities and mechanism of action of essential oils and their components: Essential oils and their bioactive components. *Flavour Fragr. J.* **2013**, *28*, 269–279. [[CrossRef](#)]
32. Horváth, B.; Balázs, V.L.; Horváth, G.; Széchenyi, A. Preparation and in vitro diffusion study of essential oil Pickering emulsions stabilized by silica nanoparticles for *Streptococcus mutans* biofilm inhibition. *Flavour Fragr. J.* **2018**, *33*, 385–396. [[CrossRef](#)]
33. Bravo Cadena, M.; Preston, G.M.; Van der Hoorn, R.A.L.; Townley, H.E.; Thompson, I.P. Species-specific antimicrobial activity of essential oils and enhancement by encapsulation in mesoporous silica nanoparticles. *Ind. Crop. Prod.* **2018**, *122*, 582–590. [[CrossRef](#)]
34. Fujs, S.; Gazdag, Z.; Poljsak, B.; Stibilj, V.; Milacic, R.; Pesti, M.; Raspor, P.; Batic, M. The oxidative stress response of the yeast *Candida intermedia* to copper, zinc, and selenium exposure. *J. Basic Microbiol.* **2005**, *45*, 125–135. [[CrossRef](#)] [[PubMed](#)]
35. Das, S.; Gazdag, Z.; Szente, L.; Meggyes, M.; Horváth, G.; Lemli, B.; Kunsági-Máté, S.; Kuzma, M.; Kőszegi, T. Antioxidant and antimicrobial properties of randomly methylated β cyclodextrin—Captured essential oils. *Food Chem.* **2019**, *278*, 305–313. [[CrossRef](#)] [[PubMed](#)]
36. Stromájer-Rácz, T.; Gazdag, Z.; Belágyi, J.; Vágvölgyi, C.; Zhao, R.Y.; Pesti, M. Oxidative stress induced by HIV-1 F34IVpr in *Schizosaccharomyces pombe* is one of its multiple functions. *Exp. Mol. Pathol.* **2010**, *88*, 38–44. [[CrossRef](#)]
37. Gazdag, Z.; Máté, G.; Čertik, M.; Türmer, K.; Virág, E.; Pócsi, I.; Pesti, M. *tert*-Butyl hydroperoxide-induced differing plasma membrane and oxidative stress processes in yeast strains BY4741 and *erg5* Δ : *t*-BuOOH-induced cytotoxic processes in yeast. *J. Basic Microbiol.* **2014**, *54*, S50–S62. [[CrossRef](#)]
38. Henderson, L.M.; Chappell, J.B. Dihydrorhodamine 123: A fluorescent probe for superoxide generation? *Eur. J. Biochem.* **1993**, *217*, 973–980. [[CrossRef](#)]
39. Appiah, T.; Boakye, Y.D.; Agyare, C. Antimicrobial Activities and Time-Kill Kinetics of Extracts of Selected Ghanaian Mushrooms. *Evid. Based Complement. Altern. Med.* **2017**, *2017*, 1–15. [[CrossRef](#)]

40. Moscho, A.; Orwar, O.; Chiu, D.T.; Modi, B.P.; Zare, R.N. Rapid preparation of giant unilamellar vesicles. *Proc. Natl. Acad. Sci.* **1996**, *93*, 11443–11447. [[CrossRef](#)]



Sample Availability: Samples of the compounds chamomile EO and SNPs are available from the authors.



© 2019 by the authors. Licensee MDPI, Basel, Switzerland. This article is an open access article distributed under the terms and conditions of the Creative Commons Attribution (CC BY) license (<http://creativecommons.org/licenses/by/4.0/>).

Article

Cytotoxic Action of Artemisinin and Scopoletin on Planktonic Forms and on Biofilms of *Candida* Species

Sourav Das ^{1,2}, Lilla Czuni ^{3,4}, Viktória Báló ³, Gábor Papp ^{3,4}, Zoltán Gazdag ^{3,4}, Nóra Papp ⁵ and Tamás Kőszegi ^{1,2,*}

¹ Department of Laboratory Medicine, University of Pécs, Medical School, 7624 Pécs, Ifjúság u. 13., Hungary; pharma.souravdas@gmail.com

² János Szentágothai Research Center, University of Pécs, 7624 Pécs, Ifjúság u. 20., Hungary

³ Department of General and Environmental Microbiology, Institute of Biology, University of Pécs, 7624 Pécs, Ifjúság u. 6., Hungary; czuni.lilla@gmail.com (L.C.); balo.viktoria@gmail.com (V.B.); pappgab@gamma.ttk.pte.hu (G.P.); gazdag@gamma.ttk.pte.hu (Z.G.)

⁴ Microbial Biotechnology Research Group, János Szentágothai Research Center, University of Pécs, 7624 Pécs, Ifjúság u. 20., Hungary

⁵ Department of Pharmacognosy, University of Pécs, Faculty of Pharmacy, 7624 Pécs, Rókus u. 2, Hungary; nora4595@gamma.ttk.pte.hu

* Correspondence: tamas.koszegi@aok.pte.hu or koszegi.tamas@pte.hu; Tel.: +36-30-4917719

Received: 18 December 2019; Accepted: 20 January 2020; Published: 22 January 2020



Abstract: We investigated the antifungal activities of purified plant metabolites artemisinin (Ar) and scopoletin (Sc) including inhibition, effects on metabolic activities, viability, and oxidative stress on planktonic forms and on preformed biofilms of seven *Candida* species. The characteristic minimum inhibitory concentration (MIC₉₀) of Ar and Sc against *Candida* species ranged from 21.83–142.1 µg/mL and 67.22–119.4 µg/mL, respectively. Drug concentrations causing ≈10% CFU decrease within 60 min of treatments were also determined (minimum effective concentration, MEC₁₀) using 100-fold higher CFUs than in the case of MIC₉₀ studies. Cytotoxic effects on planktonic and on mature biofilms of *Candida* species at MEC₁₀ concentrations were further evaluated with fluorescent live/dead discrimination techniques. *Candida glabrata*, *Candida guilliermondii*, and *Candida parapsilosis* were the species most sensitive to Ar and Sc. Ar and Sc were also found to promote the accumulation of intracellular reactive oxygen species (ROS) by increasing oxidative stress at their respective MEC₁₀ concentrations against the tested planktonic *Candida* species. Ar and Sc possess dose-dependent antifungal action but the underlying mechanism type (fungistatic and fungicidal) is not clear yet. Our data suggest that Ar and Sc found in herbal plants might have potential usage in the fight against *Candida* biofilms.

Keywords: *Candida* species; artemisinin; scopoletin; oxidative stress; mature biofilm; antifungal effect

1. Introduction

Fungal biofilms play an important role in numerous infections. They are composed of structural microbial communities adhering to different surfaces and being enveloped by the exopolymeric matrix [1]. Development of biofilms hinders the action of the defense system of the host and increases the resistance to standard antifungal agents [2]. *Candida* species like *Candida albicans* (*C. albicans*), *Candida dubliniensis* (*C. dubliniensis*), *Candida tropicalis* (*C. tropicalis*), *Candida krusei* (*C. krusei*), *Candida glabrata* (*C. glabrata*), *Candida guilliermondii* (*C. guilliermondii*), and *Candida parapsilosis* (*C. parapsilosis*) are fungal species of major medical importance. *Candida* species, members of human microflora, are diploid polymorphic yeasts [3] that can be found in the human gastrointestinal, respiratory, and inside the genitourinary tracts; therefore, *C. albicans* is found in vaginal, mucosal, and deep tissue

infections [2,4,5]. In certain individuals with immune-compromised status, the *Candida* species might induce consequent infection. Also, *Candida* species can rapidly adapt to the host's micro-environmental circumstances caused by pH and nutritional changes in the gastrointestinal tract [1]. Environmental imbalance because of nutritional change or pH shifting facilitates the abnormal growth of *Candida* species which results in candidiasis [6]. *Candida* species attack the gut epithelium barriers to reach the bloodstream via micro-fold cells (M cells) that are found in the gut-associated lymphoid tissue (GALT) of Peyer's patches in the small intestine promoting intestinal infections [4]. Esophageal candidiasis is one of the major and common infections in people living with HIV/AIDS [1]. Symptoms of candidiasis in the mouth, throat, and esophagus generally include swallowing problems and pain [7,8]. Because of the increasing incidence of candidiasis and the difficulties in its treatment because of the limited options in the use of antifungal drugs with species-specific efficacy [9], there is an ultimate need for at least prevention of fungal infections.

Artemisinin (Ar), belonging to a family of sesquiterpene lactones originally derived from *Artemisia annua* L. is well-known for its anti-malarial actions by forming free radicals through cleavage of intra-parasitic iron-endoperoxide groups and by alkylation of specific malarial proteins mediating eradication of *Plasmodium* species [10]. Protection against cancers and inflammation by artemisinin has also been documented [11]. Ar has been reported to possess anti-infective activity against viruses (Human cytomegalovirus) and fungi (*Cryptococcus neoformans*) [12].

Scopoletin (Sc, 6-methoxy-7-hydroxycoumarin) is a phenolic compound isolated from several plants including *A. annua* L. [13]. Sc possesses anti-tumor and anti-angiogenesis properties by initiating cell cycle arrest and facilitating apoptosis in human prostate tumor cells and leukemia cell lines [14,15]. Although anti-fungal effects including anti-*Candida* activity of Ar and Sc were already studied, yet no detailed data are found in the literature on *Candida* species' viability and biofilm formation treated with Ar and Sc at their minimum effective concentration (MEC₁₀). Moreover, there are no experimental results obtained by using the double-stain rapid fluorescent assay for live/dead cellular discrimination along with metabolic activity determination for Ar- and Sc-exposed *Candida* species.

Because of the diverse biological activities including reactive oxygen species (ROS) generation [13,14,16,17], we hypothesized that both Ar and Sc having a wide range of biological actions might exert antimicrobial activity as well. Therefore, the aim of our present study is to contribute to the knowledge of the hypothesized anti-microbial and anti-biofilm activity of Ar and Sc regarding their effects on *C. albicans* and on non-*albicans* species. The effect of Ar and Sc on cellular viability, metabolic activity (enzymatic reducing ability) and oxidative stress balance of the *Candida* species was evaluated by SYBR green I-propidium iodide double staining method, resazurin assay, dihydroethidium (DHE) and dihydrorhodamine 123 (DHR 123) fluorescence assays, respectively. The biomass and metabolic activity of the living cells in the mature biofilms were assessed by colorimetric and double fluorescence staining techniques.

2. Results

2.1. Antifungal Activities (MIC₉₀) of Artemisinin and Scopoletin

Average MIC₉₀ data obtained after 48 h of treatment with Ar and Sc for seven *Candida* spp. are presented in Figure 1. Ar MIC₉₀ ranged from 21.83 to 142.1 µg/mL, while Sc MIC₉₀ was between 83.43 and 119 µg/mL taking all the tested *Candida* species. Ar MIC₉₀ values were significantly lower than those of Sc in the case of *C. dubliniensis*, *C. krusei*, and *C. parapsilosis* ($p < 0.01$). *C. glabrata* and *C. tropicalis* was more susceptible to Sc (67.22 and 119 µg/mL, respectively). However, in general Ar expressed higher fungicidal activity than Sc at concentrations in the range of 27 to 80%, less than was seen for Sc.

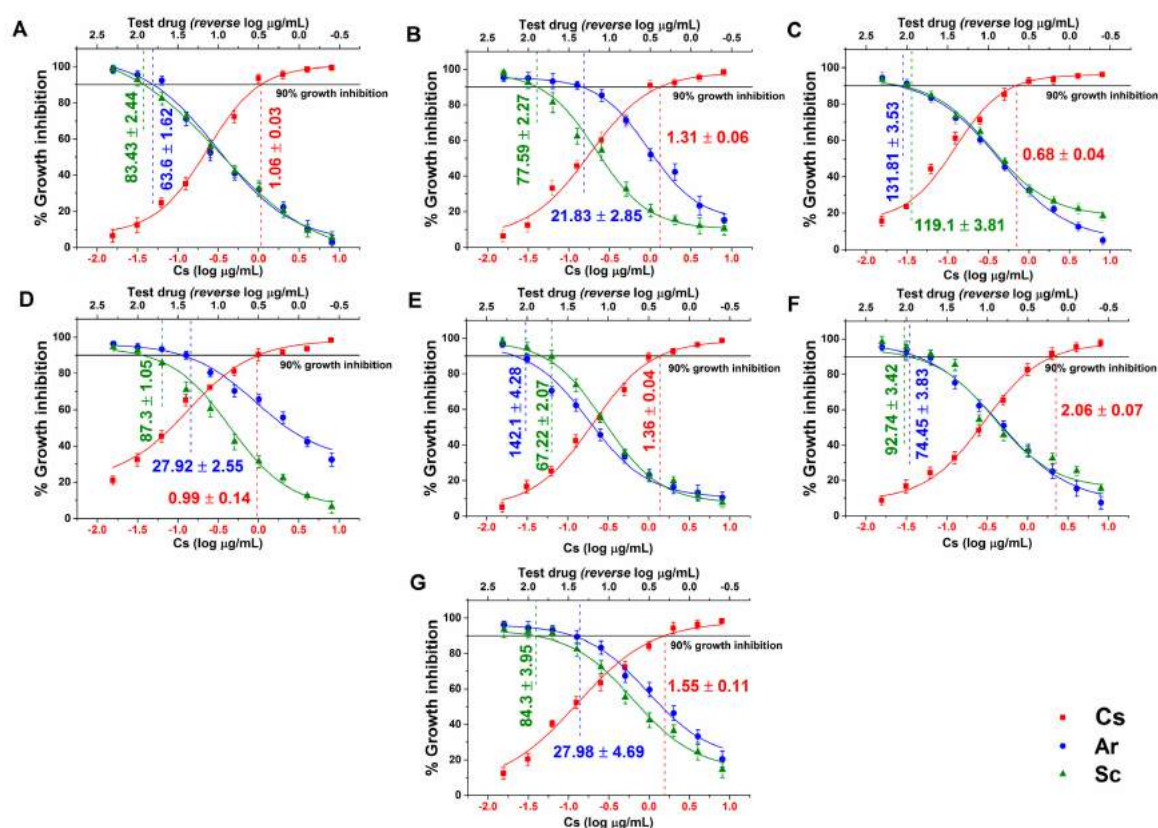


Figure 1. Minimum inhibitory concentrations (MIC₉₀) (mean ± SD) of artemisinin (Ar) and scopoletin (Sc) on *C. albicans* (A), *C. dubliniensis* (B), *C. tropicalis* (C), *C. krusei* (D), *C. glabrata* (E), *C. guilliermondii* (F) and *C. parapsilosis* (G) species. Six independent experiments, each in three replicates, compared with caspofungin (Cs) as positive control and comparison of Ar and Sc treatments (µg/mL).

2.2. Data of Minimum Effective Concentrations (MEC₁₀) for Planktonic *Candida* Species

Dose-response curves regarding the minimum effective concentrations (MEC₁₀) for Ar and Sc on the selected opportunistic *Candida* species are shown in Figure 2. For Ar the obtained MEC₁₀ concentrations are as follows: *C. albicans* 84.04 ± 2.92; *C. dubliniensis* 71.26 ± 3.81; *C. tropicalis* 89.95 ± 3.62; *C. krusei* 233.14 ± 4.72; *C. glabrata* 324.97 ± 4.42; *C. guilliermondii* 180.9 ± 3.36; and *C. parapsilosis* 171.86 ± 4.24 (in µg/mL). For Sc the MEC₁₀ values were: *C. albicans* 132.17 ± 4.19; *C. dubliniensis* 132.17 ± 5.08; *C. tropicalis* 134.27 ± 4.66; *C. krusei* 162.01 ± 5.03; *C. glabrata* 215.38.97 ± 5.41; *C. guilliermondii* 149.2 ± 5.32, and *C. parapsilosis* 164.7 ± 5.26 (in µg/mL). The curves have expressed a dose-dependent cell survival (CFU count) after 60 min exposure to Ar and Sc. The doses corresponding to MEC₁₀ (meaning an average 90% survival rate of mid-log phased populations, at ~10⁵ CFU/mL) were further used to evaluate their effects on planktonic cells and on mature biofilms. Cs, Ar, and Sc have shown an average MEC₁₀ of 6.66 ± 0.14 µg/mL, 165.16 ± 3.87 µg/mL, and 160.84 ± 4.99 µg/mL, respectively for the tested planktonic *Candida* spp. Ar appeared to have the lowest MEC₁₀ in the case of *C. dubliniensis* (21.83 ± 2.85 µg/mL), *C. krusei* (27.92 ± 2.55 µg/mL), and *C. parapsilosis* (27.98 ± 4.69 µg/mL), respectively.

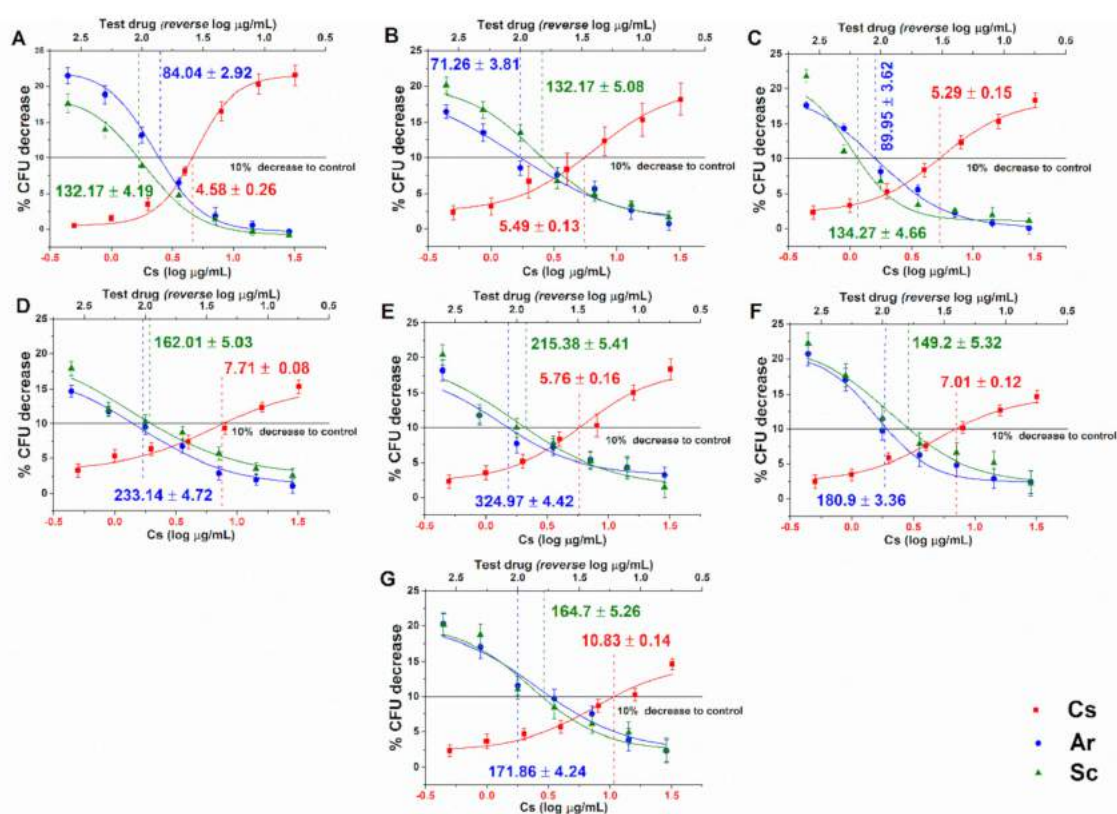


Figure 2. Minimum effective concentrations (MEC₁₀) (mean ± SD) of artemisinin (Ar) and scopoletin (Sc) on *C. albicans* (A), *C. dubliniensis* (B), *C. tropicalis* (C), *C. krusei* (D), *C. glabrata* (E), *C. guilliermondii* (F) and *C. parapsilosis* (G) species. Six independent experiments, each in three replicates, compared with caspofungin (Cs) as positive control and comparison of Ar and Sc treatments (µg/mL).

2.3. Effects on Mature Biofilms

A variable response to Ar, Sc, and Cs at MEC₁₀ doses have been found. Although no changes in the biomass have been observed in the case of Ar treatments, yet an average $55.04 \pm 9.46\%$ and $46.32 \pm 12.62\%$ reduction in metabolic activities and non-viable cells were seen in the case of *C. albicans*, *C. dubliniensis*, *C. tropicalis*, and *C. glabrata* when compared to growth control ($p < 0.01$). A significant reduction up to an average of 60% in the total biomass on Sc-treated *C. albicans*, *C. dubliniensis* and *C. glabrata* ($p < 0.01$) was found when compared with growth control (Gc) and Cs treatments. However, the data obtained from metabolic activity testing and non-viable cell numbers are invalid for the above species because of the significant biomass loss. *C. guilliermondii* has shown significantly higher resistance to Ar and Sc compared with the other species. The highest cell death (>60%) detected by the double fluorescence staining assay and the reduced metabolic activities (<50%) for *C. krusei*, and *C. parapsilosis* were found in the case of Sc treatment (Figure 3).

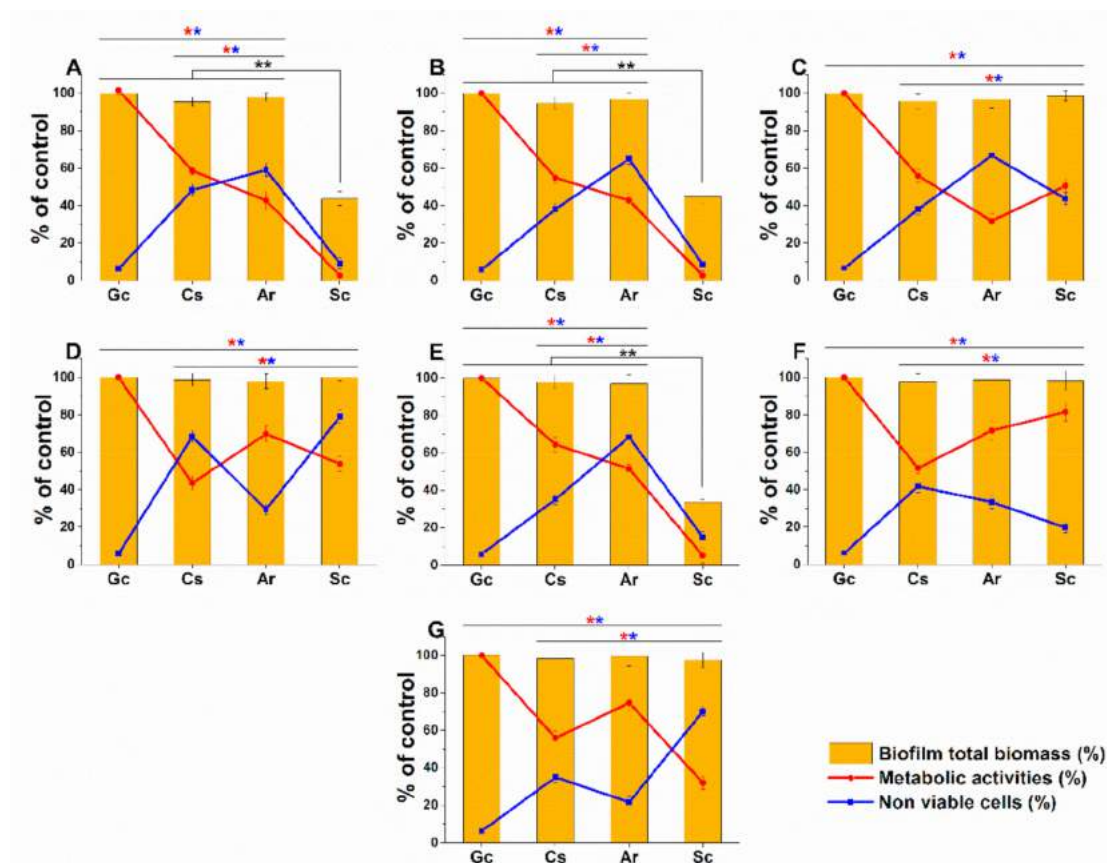


Figure 3. Effects of artemisinin (Ar) and scopoletin (Sc) at their MEC₁₀ concentrations on the metabolic activity, amount of biofilm biomass, and viability of *C. albicans* (A), *C. dubliniensis* (B), *C. tropicalis* (C), *C. krusei* (D), *C. glabrata* (E), *C. guilliermondii* (F), and *C. parapsilosis* (G) cell populations (mean \pm SD, n = 6 independent experiments, data were compared with untreated controls (Gc) and with caspofungin (Cs)-treated positive controls. The red (*) and blue (*) asterisks represent a significance value of $p < 0.01$ for the metabolic activity and viability measurements, respectively. Whereas, the black double asterisks (**) highlight the changes in the Sc-treated biofilm biomass when compared to Gc, Cs, and Ar treatments at $p < 0.01$ significance level.

2.4. Live/Dead Planktonic Cell Viability Discrimination

The long-term effects of Ar and Sc on the viability were tested on mid-log phased planktonic *Candida* spp. as well. Ar and Sc decreased the viability of the tested *Candida* spp. with an average viability reduction of $58.2 \pm 3.5\%$ and $58.6 \pm 4.2\%$ after 8 h, whereas $33.6 \pm 3.9\%$ and $32.2 \pm 3.6\%$ were seen after 16 h when compared with their respective controls. *C. glabrata*, *C. guilliermondii*, and *C. parapsilosis* were found to have less than 30% of viable cells in the presence of Ar and Sc for 16 h at their MEC₁₀ concentrations. Ar and Sc showed a reduction in viability $\leq 50\%$ after 8 h of treatment on *C. parapsilosis* and *C. krusei* compared with the controls (Figure 4).

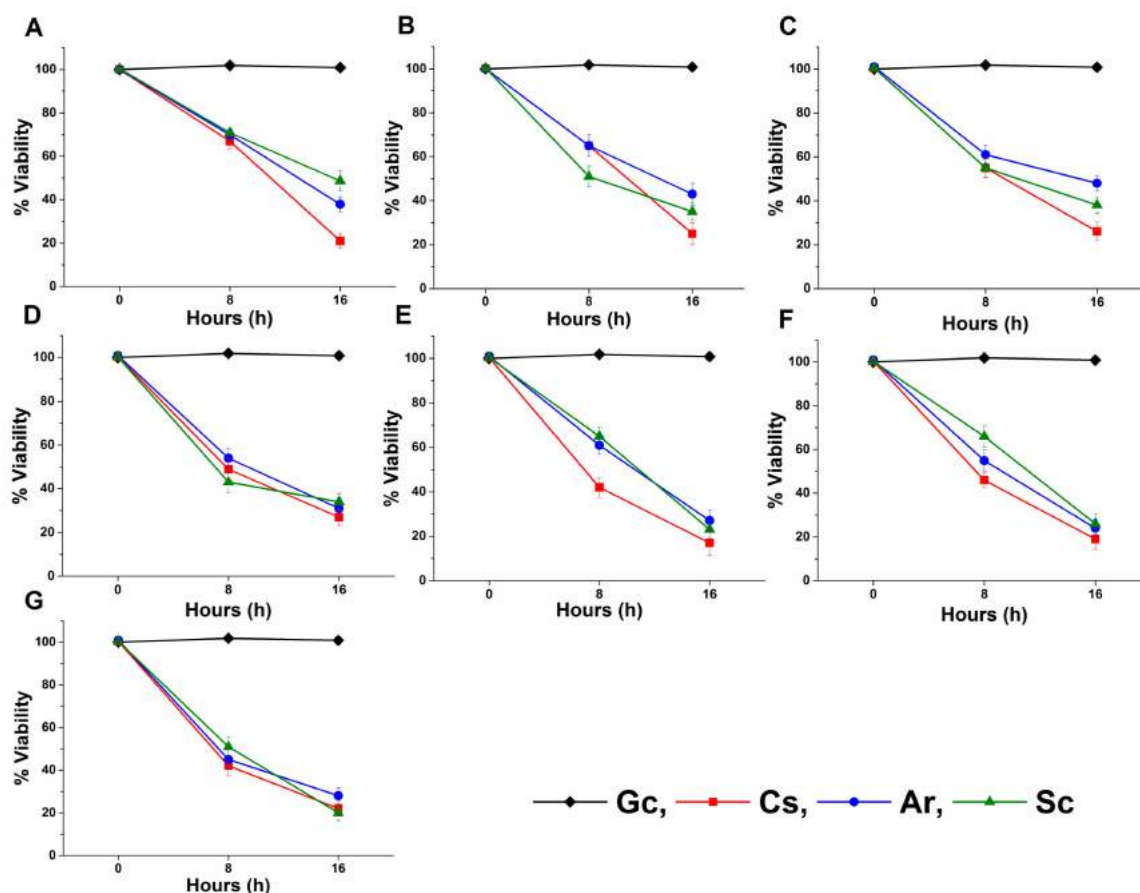


Figure 4. Effects of artemisinin (Ar) and scopoletin (Sc) at their MEC₁₀ concentrations on the viability of planktonic *C. albicans* (A), *C. dubliniensis* (B), *C. tropicalis* (C), *C. krusei* (D), *C. glabrata* (E), *C. guilliermondii* (F), and *C. parapsilosis* (G) species compared with untreated controls (Gc) after 8 and 16 h of treatment (mean \pm SD, n = 6 independent experiments, caspofungin (Cs) was used as positive control).

2.5. Effects on Metabolic Activity and on Colony Formation of Planktonic Cells

The metabolic activity of the mid-log phased planktonic *Candida* spp. in the presence of Ar and Sc at their MEC₁₀ concentrations was evaluated with resazurin at 0, 8, and 16 h time points (Figure 5). Ar and Sc showed an average reduction in the metabolic activities of tested *Candida* spp. to two-fold after 8 h of treatment followed by three-fold after 16 h of treatment when compared with their respective controls. A less than two-fold decrease of metabolic activity was found in *C. glabrata*, *C. guilliermondii*, and *C. parapsilosis* planktonic cells in the presence of Ar and Sc after 16 h of treatment.

A significant change in the planktonic cell number reduction compared with the control ($p < 0.01$) was also found after 8 and 16 h of treatment (Figure 6). A prominent reduction $\leq 50\%$ of planktonic cell population, when compared to the controls, was found in the case of *C. glabrata*, *C. guilliermondii* and *C. parapsilosis* after 16 h of Ar, Sc, and caspofungin (Cs) exposures.

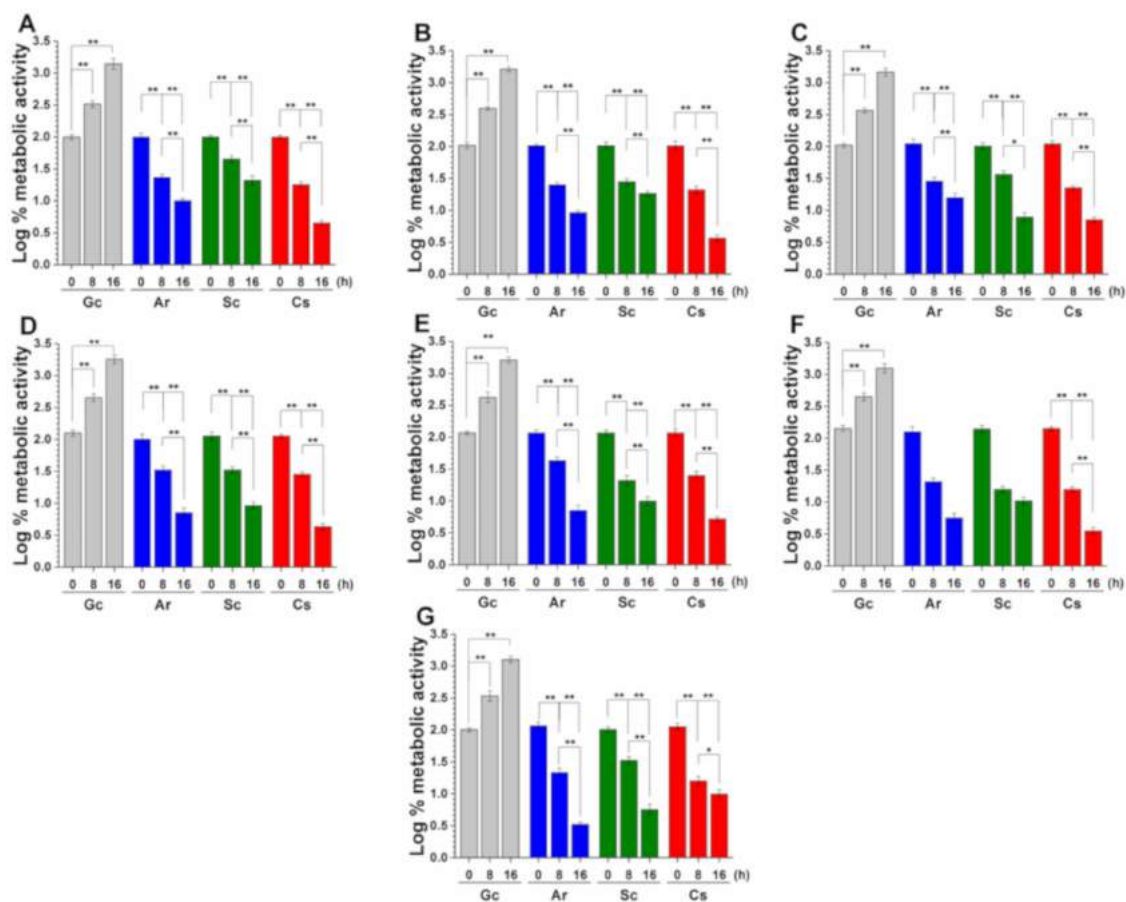


Figure 5. Effects of artemisinin (Ar) and scopoletin (Sc) at their MEC₁₀ concentrations on the metabolic activities of planktonic *C. albicans* (A), *C. dubliniensis* (B), *C. tropicalis* (C), *C. krusei* (D), *C. glabrata* (E), *C. guilliermondii* (F), and *C. parapsilosis* (G) species compared with untreated controls (Gc) and caspofungin (Cs) as positive control after 8 and 16 h of treatment (mean ± SD, n = 6 independent experiments, * $p < 0.05$ and ** $p < 0.01$).

2.6. Effects on Planktonics' Oxidative Balance

The effects of Ar and Sc on the induction of the oxidative stress at MEC₁₀ concentrations on respective mid-log phased *Candida* spp. planktonic cell populations are illustrated in Figure 7. Menadione (Me) was used as positive control. All the test drugs caused a significant oxidative stress in the planktonic cells compared with that of the controls ($p < 0.01$). More than 25% and 50% of O₂^{•-} generation was observed in *C. glabrata*, *C. guilliermondii*, and *C. parapsilosis* compared with other tested *Candida* spp. after the treatment with Ar and Sc for 16 h. The overall O₂^{•-} generation induced by Ar was found to be $13.4 \pm 1.8\%$ higher than that of Sc. Peroxide generation in *C. glabrata*, *C. guilliermondii*, and *C. parapsilosis* was also found to be higher (an average of 30.2% increment in Ar treatment and 8.4% increment in Sc treatment) compared with the other tested *Candida* spp. An average increment of $64.1 \pm 2.6\%$ was found in oxidative stress induction by Ar when compared to Sc in *Candida* species. In summary, we found that all the tested *Candida* species were susceptible to Ar and Sc treatments in favor of Ar vs. Sc.

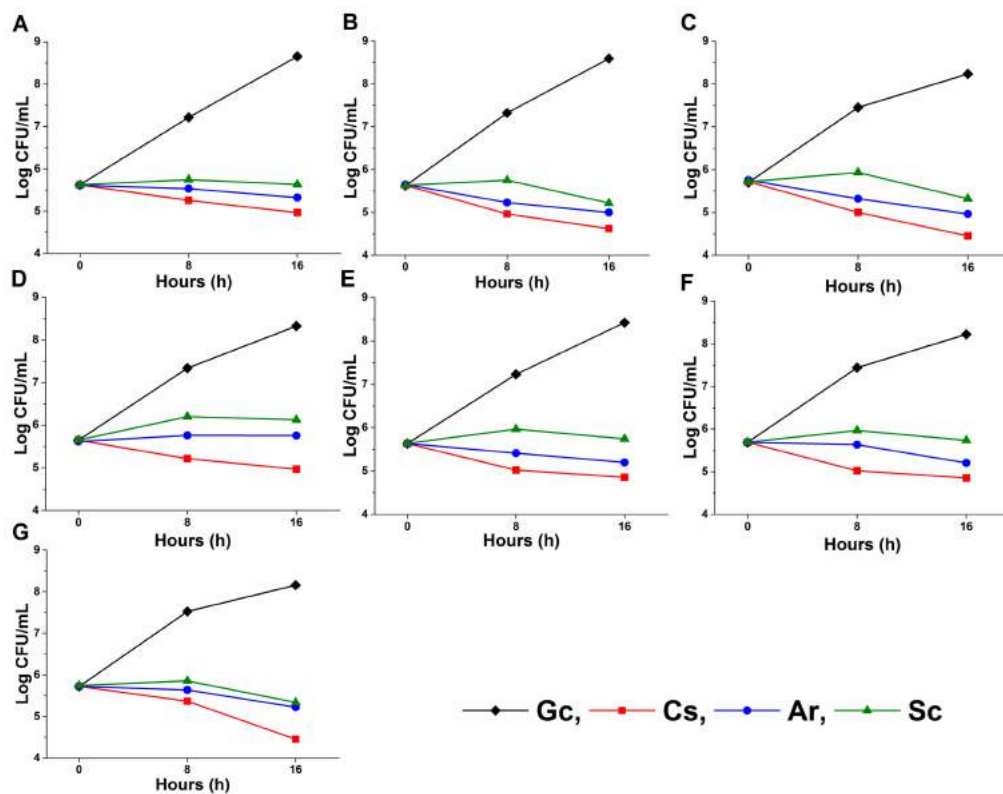


Figure 6. Effects of artemisinin (Ar) and scopoletin (Sc) at their MEC₁₀ concentrations on colony formation of planktonic *C. albicans* (A), *C. dubliniensis* (B), *C. tropicalis* (C), *C. krusei* (D), *C. glabrata* (E), *C. guilliermondii* (F) and *C. parapsilosis* (G) species compared with untreated controls (Gc) after 8 and 16 h of treatment (mean \pm SD, n = 6 independent experiments, caspofungin (Cs) was used as positive control).

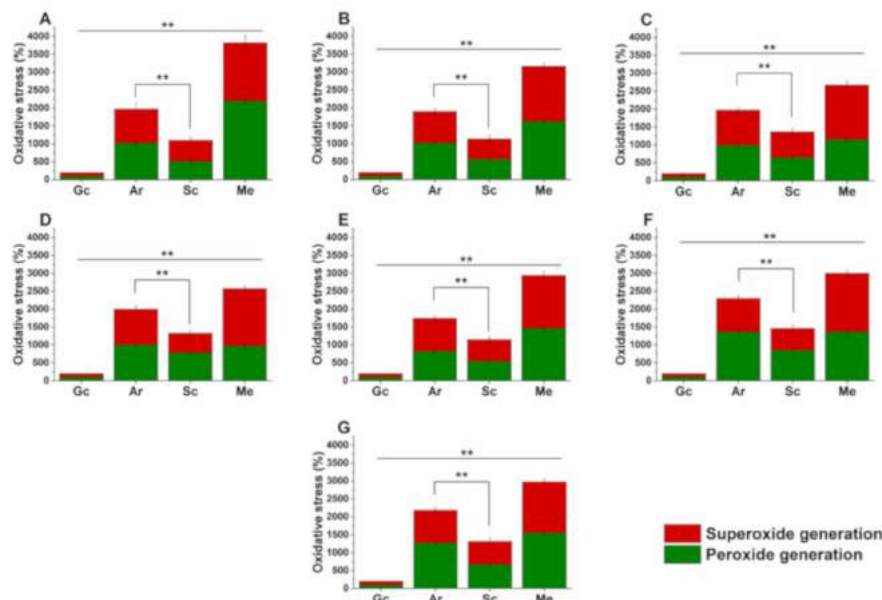


Figure 7. Effects of artemisinin (Ar) and scopoletin (Sc) at their MEC₁₀ concentrations on peroxides (O_2^{2-}) and superoxide anion ($O_2^{\bullet-}$) generation in planktonic *C. albicans* (A), *C. dubliniensis* (B), *C. tropicalis* (C), *C. krusei* (D), *C. glabrata* (E), *C. guilliermondii* (F), and *C. parapsilosis* (G) species compared with untreated (Gc), with menadione (Me)-treated controls and comparison of Ar and Sc treatments (mean \pm SD, n = 6 independent experiments, $**p < 0.01$).

3. Discussion

Ar and Sc were effective against the selected *Candida* spp. and their antifungal activities were comparable in every measured parameter to Cs even if the antifungal agent's MIC₉₀ value was much lower than that of our plant-derived test compounds. The susceptibility of selected *Candida* spp. to Ar and Sc has not been reported before. The antifungal activity of Ar and Sc may be attributed to the inhibition of efflux pumps as it was shown for berberine, a natural isoquinoline alkaloid [18]. The measured lower effects of Sc is not known, however, the presence of efflux pump proteins belonging to ABC (ATP Binding Cassette) and MFS (Major Facilitators) superfamily might also be the responsible factors [18,19].

The resazurin assay and SYBR green I-propidium iodide double-stain fluorescent method enabled us to characterize both the planktonic cell populations and biofilms after the treatment with Ar and Sc. As a limitation of our viability study, it should be mentioned that measuring a single parameter only (e.g., the resazurin assay) does not necessarily reflect total cell viability because cellular ATP levels may change rapidly without significant reduction in intracellular enzyme activities [20]. Based on literature data both Ar and Sc may induce time-dependent cell wall and membrane damage enabling propidium iodide to bind to fungal nucleic acids [21]. The double-stain fluorescence assay showed that the longer the exposure time is, the higher cellular death rate is found in the Ar and Sc-treated fungal populations. The difference in viability among the examined *Candida* species we think is due to the potential difference in the activity of multidrug efflux pumps among the *Candida* spp. The maintenance of metabolic activities at about 50% even in the presence of low planktonic cell populations indicates the adaptation of surviving planktonic cells [22].

Data presented in this study suggest the induction of apoptosis-like processes in the tested *Candida* spp. that may be due to the accumulation of reactive oxygen species (ROS) that induce or regulate the apoptosis in yeasts [23,24]. Using the superoxide and peroxide radicals' fluorescent assays, we showed the accumulation of reactive oxygen species, which are the indicators of lipid damage [25]. It has been postulated that Ar and Sc affect ergosterol synthesis [19,26]. Ergosterol, apart from maintenance and regulation of structural and functional integrity of the membrane, inhibits lipid peroxidation [27]. This can also facilitate the permeability of the cell membrane and incorporation of propidium iodide through the compromised membranes into the cells. Further characterization of the effects of Ar and Sc on the levels of superoxide dismutase and catalase at increased ROS level must be assessed [26,28]. Moreover, Ar also plays an important role in the electron transport chain by overexpressing nuclear distribution protein nude homolog 1 (*NDE1*) that is responsible for encoding mitochondrial NADH dehydrogenases causing sensitivity to Ar followed by membrane disruption resulting in mitochondrial dysfunction by the higher free radical generation when compared to Sc [29,30].

In this study, we have further investigated the effects of Ar and Sc on the preformed mature biofilms of different *Candida* spp. Our results demonstrated that Ar is more effective in disrupting the preformed complexed, extracellular matrix-covered biofilm structure and killing the sessile (surface-attached) cell population as well compared to Sc at their respective MEC₁₀ concentrations after 24 h exposure. This may be due to the abilities of the sesquiterpenoids to have action on amyloid proteins, which are one of the major building blocks of microbial biofilms [31–34]. On the other hand, Sc treatment showed a dramatic decrement in the total biomass including cell loss from the polystyrene surface in case of *C. albicans*, *C. dubliniensis*, and *C. glabrata*, which might be due to the action of coumarin derivatives on the chemical pathways such as quorum sensing resulting in biofilm dispersion [35–40]. However, the higher metabolic activities and the less cell death rate found in the case of *C. guilliermondii* indicates the presence of other drug resistance mechanism factors apart from poor drug penetration into *Candida* biofilms. The alternate mechanism might be related to the expression patterns of genes coding for multidrug efflux pumps [22,41,42]. Moreover, this might be the reason why the surviving cells can adapt to the stressful microenvironment by decreasing their metabolic activities [23,43]. Though the adapted cell populations with reduced metabolic activities might survive the toxicity of both test drugs, Ar exerts higher cell killing properties than those of Sc in the mature biofilm, whereas Sc might cause

changes in the biofilm adherence factors to the polystyrene surfaces. Adaptation of *Candida* species under various conditions has already been described [23,44].

Based on the results of the tested *Candida* planktonic cells, we found that the MEC₁₀ concentrations of our treating compounds are more effective to initiate oxidative imbalance and reducing metabolic activities followed by death of the planktonic cells when compared to the effects on preformed mature biofilms, which have shown variable results including cell death, biomass loss, and resistance. The reason behind the resistance to the MEC₁₀ concentrations maybe due to the extracellular matrix acting as a diffusion barrier [39,45,46] or the up-regulations of the genes coding the efflux pumps [47–49]. Previous studies also reported that the planktonic cells released from the biofilms express subtle genetic changes for producing resistant phenotypes. As a consequence, the resistant new population may form biofilms with altered phenotype that might be responsible for the hostility in some of the tested *Candida* species [50].

The widely accepted crystal violet assay was used to investigate the effects of the tested compounds on the changes of *Candida* biofilm biomass [51]. This chemically basic dye stains fungal cells including negatively charged surface molecules and polysaccharides in the biofilm extracellular matrix enabling a rapid quantification of biofilm mass prior to labor-intensive microscope analysis [52]. Although, the poor correlation between the biofilm biomass reduction, metabolic activities and cellular viability remains a major limitation of this method because of the non-selective staining of the biofilm matrix including viable and dead cells as well [53]. Therefore, results obtained from the crystal violet assay must be combined with other multi-parametric techniques such as intracellular ATP, ATP/protein ratio, live/dead cell discrimination and selective visualization of the biomass matrix [54–56].

Our novel multi-parametric evaluations have more precisely highlighted the planktonic fungal susceptibility, killing ability inside the mature biofilm than the classical proliferation assays [57–60]. The observed antifungal effects and combined actions on mature biofilms of Ar and Sc might be useful for further detailed research for their potential usage as alternative antimicrobial agents for the treatment of *Candida* infections.

4. Materials and Methods

4.1. Materials

For our experiments, sterile 96-well microtiter plates for antifungal activity, live/dead discrimination and metabolic assays (Catalog number: 30096, SPL Life Sciences Co. Ltd., Gyeonggi-do, Korea), and for biofilm assays (Catalog number: 83.3924.500, Sarstedt AG & Co. KG, Numbrecht, Germany), crystal violet, peptone, yeast extract, agar-agar, potassium phosphate monobasic, acetic acid (Reanal Labor, Budapest, Hungary), resazurin, modified RPMI 1640 medium (containing 3.4% (w/v) MOPS, 1.8% (w/v) dextrose and 0.002% (w/v) adenine) [61], menadione (Me), artemisinin (Ar), scopoletin (Sc), SYBR green I 10,000x, propidium iodide, dihydrorhodamine 123 (DHR 123) and dihydroethidine (DHE) (Sigma-Aldrich Chemie GmbH, Steinheim, Germany), disodium phosphate, dimethyl sulfoxide (DMSO) from Chemolab Ltd. (Budapest, Hungary), sodium chloride (VWR Chemicals, Debrecen, Hungary), dextrose, adenine, potassium chloride (Scharlau Chemie S.A, Barcelona, Spain), 3-(N-morpholino) propanesulfonic acid (MOPS) (Serva Electrophoresis GmbH, Heidelberg, Germany), 0.22 µm vacuum filters from Merck Millipore (Molsheim, France) were used. All other chemicals in the study were of analytical or spectroscopic grade. Highly purified water (<1.0 µS) was applied throughout the experiments. Caspofungin (Cs) was purchased from Merck Sharp & Dohme Ltd. (Hertfordshire, UK).

4.2. Instruments Used in the Experiments

A microbiological incubator (Thermo Scientific Heraeus B12, Auro-Science Consulting Kft., Budapest, Hungary), microtiter plate reader (PerkinElmer EnSpire Multimode plate reader,

Auro-Science Consulting Ltd., Budapest, Hungary), benchtop centrifuge (Hettich Rotina 420R, Auro-Science Consulting Kft., Budapest, Hungary) were used throughout the experiments.

4.3. Microorganisms and Culture Conditions

All the fungal species were obtained from Szeged Microbiology Collection, University of Szeged, Hungary (Table 1) and were maintained at the Department of General and Environmental Microbiology, Institute of Biology, University of Pécs, Hungary. *C. albicans* 1372, *C. dubliniensis* 1470, *C. tropicalis* 1368, *C. krusei* 779, *C. glabrata* 1374, *C. guilliermondii* 808, and *C. parapsilosis* 8006 were used to evaluate the MIC₉₀, the minimum effective concentration (MEC₁₀) for the planktonic cells and the inhibition of biofilm formation of the test samples. All the fungal species were cultured and maintained in yeast extract peptone dextrose agar medium (YPD: 1% (w/v) peptone, 0.5% (w/v) yeast extract, 2% (w/v) dextrose, 1.5% (w/v) agar-agar in distilled water [62]. Phosphate-buffered saline (PBS, pH 7.4) was from Life Technologies Ltd. (Budapest, Hungary), and highly purified water (<1.0 µS) was applied throughout the experiments.

Table 1. *Candida* species examined in the study.

Species	Collection Code	Origin
<i>C. albicans</i>	SZMC 1372	clinical sample/Debrecen, Hungary
<i>C. dubliniensis</i>	CBS 7987 SZMC 1470	oral cavity of HIV-infected patient/Melbourne, Australia
<i>C. tropicalis</i>	SZMC 1368	clinical sample/Debrecen, Hungary
<i>C. krusei</i>	SZMC 0779	clinical sample/National Institute of Environmental Health (NIEH), Hungary
<i>C. glabrata</i>	SZMC 1374	clinical sample/Debrecen, Hungary
<i>C. guilliermondii</i>	SZMC 0808	clinical sample/Pécs, Hungary
<i>C. parapsilosis</i>	SZMC 8006	clinical sample/Szeged, Hungary

Abbreviations: SZMC, Szeged Microbiological Collection, Szeged, Hungary (http://www.wfcc.info/ccinfo/collection/by_id/987); CBS, Westerdijk Fungal Biodiversity Institute, Utrecht, The Netherlands (<http://www.westerdijkinstitute.nl/>).

4.4. Determination of Minimum Inhibitory Concentration (MIC₉₀)

The MIC₉₀ was performed according to a previously published method [63] with modifications. Ar and Sc were prepared in DMSO at concentrations ranging from 0.39–200 µg/mL and 0.01–8 µg/mL for Cs. Total of 100 µL of fungal suspensions of 10³ colony forming units (CFU)/mL in modified RPMI 1640 medium was pipetted into each well of sterile 96-well microtiter plates and mixed with 100 µL of dilutions of Ar and Sc. The final solvent concentration for the dilution of the drugs was restricted up to 2.5% v/v in the wells. Inoculated growth medium without any treatment was considered as the growth control. The sterile medium was taken as the blank. After 48 h of incubation at 30 °C in a microbiological incubator, the absorbance was measured at 595 nm. Absorbance values were converted to percentages compared with those of the growth control (≈100%) and data were fitted by non-linear dose-response curve method to calculate the dose producing ≥90% growth inhibition (MIC₉₀). All the measurements were performed by applying three technical replicates in six independent experiments. Cs was used as a standard antifungal drug throughout the experiments.

4.5. Determination of Minimum Effective Concentration (MEC₁₀)

The MEC₁₀ measurement was performed according to our previously published protocol to estimate the dose-dependent survival rate of the cells [64–66] with modifications. Briefly, Ar and Sc were prepared in DMSO at concentrations ranging from 0.25–400 µg/mL and 0.5–32 µg/mL for Cs. Total of 100 µL of fungal suspensions of mid-log phased 10⁵ colony forming unit (CFU)/mL in modified RPMI 1640 medium were pipetted into each well of sterile 96-well microtiter plates and

mixed with 100 μ L of dilutions of Ar and Sc. The final solvent concentration for the dilutions of the drugs was restricted up to 2.5% (v/v) in the wells. Inoculated growth medium without any treatment was considered as the growth control. The sterile medium was taken as the blank. After 60 min of incubation at 30 °C in a microbiological incubator, 1 mL of treated and untreated samples was pipetted and were spread in nutrient agar media for 24 h at 30 °C for colony-forming unit (CFU/mL) quantification. CFU/mL values were converted to percentages and data were fitted with a non-linear dose-response curve to achieve drug concentrations producing an approximately 90% fungal cell growth (MEC_{10}) compared to the untreated culture after one hour treatment. All the measurements were performed by applying three technical replicates in six independent experiments. Cs was used as a standard antifungal drug throughout the experiments.

4.6. Determination of the Effects on Preformed Mature Biofilms

The protocol for the measurement of the effects on the mature biofilms and treatment was adapted from the literature [7,67] with modifications. Total of 200 μ L samples of 24 h old late-log phased *C. albicans* and non-*albicans* species in the modified RPMI 1640 medium (10^6 CFU/mL) were used to culture biofilms without treatments for 24 h at 30 °C. The microtiter plates were washed carefully with sterile PBS (pH. 7.4) and were re-incubated with 200 μ L culture medium containing Ar and Sc to be examined at MEC_{10} concentrations (μ g/mL) for further 24 h at 30 °C. Modified RPMI media as blank, inoculated growth media as growth control (Gc) and Cs-treated samples were considered as controls throughout the experiments. The percentage (%) of inhibition was measured based on the comparison of the values with those of Gc. Treatments were performed with three technical replicates in six independent experiments.

4.6.1. Evaluation of Total Fungal Biomass in the Biofilms

To determine the changes in the biofilms, a previously published crystal violet assay protocol was used [36] with modifications. After 24 h incubation, the crystal violet-stained and PBS-washed biofilms were treated with 200 μ L of 33% (v/v) acetic acid in double-distilled water. Finally, after 20 min the acetic acid-dissolved dye from the biofilm matrix was pipetted into the wells of a new microtiter plate and the absorbance was measured at 590 nm. Cs at MEC_{10} concentration was used as positive control. The % biofilm biomass reduction measurement was based on growth control (Gc) values which were assigned to be 100% fungal biofilm mass. Six independent experiments were done with three technical replicates for each treatment.

4.6.2. Resazurin-Derived Metabolism Assay in the Biofilms

A resazurin-based fluorescent assay published by Kerekes et al. was adapted [36] and was used to estimate the metabolically active (viable) cell number in the biofilm matrix treated with Ar and Sc at MEC_{10} concentrations. Briefly, after 24 h of treatment, the supernatants were removed and the wells were rinsed with PBS. Resazurin (12.5 μ mol/L) in 200 μ L of sterile PBS was added to each well containing the biofilm. After 40 min of incubation at 30 °C, the fluorescence was measured at excitation and emission wavelengths of 560/590 nm respectively. The % metabolic activity measurement was estimated based on the growth control (Gc) fluorescence values which were considered to be 100%. The PBS was taken as blank throughout the experiments. Six independent experiments were performed with three technical replicates for each treatment.

4.6.3. Viability Assay of the Biofilms and of Planktonic Candida Species

For determination of live/dead microbes in the preformed mature biofilms we followed the method previously published [63]. Briefly, after 24 h of treatment with Ar, Sc, and Cs (positive control) at MEC_{10} concentrations in the wells of a microplate, the modified RPMI 1640 medium and the non-attached planktonic cells were removed, and the wells were rinsed and filled with 100 μ L PBS. A working dye solution containing 20 μ L SYBR green I (from 10,000 \times stock in DMSO, diluted 100 times in PBS) and

4 μL propidium iodide (500-fold dilution of working stock in DMSO prepared from 20 mmol/L in DMSO) in 1000 μL of PBS was used. A total of 100 μL of this working solution was added into the wells of the microplate. The plates were incubated at room temperature in the dark with mild shaking for 15 min.

For the evaluation of the long-term effects of Ar, Sc, and Cs at their MEC_{10} on the tested *Candida* spp., a previously published live/dead planktonic cell discrimination [63] was optimized and used. A wide concentration range of SYBR green I (5.5–5500-fold logarithmic dilutions) and propidium iodide (5–500-fold logarithmic dilutions) was examined. For the discrimination of live/dead cells, mid-log phased cell populations of 10^5 CFU/mL were treated by Ar and Sc with a dose assigned for MEC_{10} concentrations and incubated at 30 °C for 16 h. Sampling was done at 0, 8, and 16 h time points for the measurements. The samples were centrifuged at 1000g for 5 min, washed in PBS and re-suspended in PBS (100 μL in each well). Then 100 μL of freshly prepared working dye solution in PBS (using 20 μL SYBR green I and 4 μL propidium iodide diluted solutions as described earlier) was added to the samples. The plate was incubated at room temperature for 15 min in the dark with mild shaking.

A PerkinElmer EnSpire multimode plate-reader was used to measure the fluorescence intensities of SYBR green I (excitation/emission wavelengths: 490/525 nm) and propidium iodide (excitation/emission wavelengths: 530/620 nm), respectively. A green to red fluorescence ratio for each sample and for each dose was achieved and the % of dead cells with the response to the applied dose was plotted against the applied Ar and Sc doses using the previously published formula [63]. In the case of biofilms, the measurements were done by area scan mode of the instrument. All treatments were done in triplicates and six independent experiments were performed.

4.7. Determination of the Metabolic Activity with Resazurin Assay and Colony Formation of Planktonic Fungal Cells

The metabolic activity of the cells under treatment conditions was performed by the widely accepted resazurin fluorescence method [68,69]. The experiments had to be optimized because the resazurin concentration, the cell number and the incubation time are crucial in order to increase the signal to noise ratio. Fluorescence data were corrected by subtracting background fluorescence (resazurin in PBS). The initial *Candida* cell density, resazurin levels, and duration of incubation time were varied by using resazurin concentrations ranging from 1.6 $\mu\text{mol/L}$ to 25 $\mu\text{mol/L}$ in the cell suspensions. The proper incubation time for resazurin exposure at an optimized concentration (12.5 $\mu\text{mol/L}$) was performed by 60 min incubation and sampling at intervals. The appropriate *Candida* species cell density was obtained by exposing a serial dilution of cells to 12.5 $\mu\text{mol/L}$ resazurin in PBS. PBS without resazurin but with identical cell density to the investigated samples was used as blank.

For fungal colony forming unit measurements, we followed a previously published protocol [70]. Briefly, 1 mL of untreated and Ar, Sc, and Cs-treated sample was pipetted at 0, 8, and 16 h time intervals and was diluted 10^5 times followed by spreading 50 μL onto 20 mL YPD agar medium using a cell spreader and incubated at 30 °C for 24 h. Cs was used as a reference control. Fungal colony forming units (CFU/mL) were determined, performed in triplicates and were plotted against time (h). Six independent experiments were done with three technical replicates for each treatment.

4.8. Detection of Peroxide (O_2^{2-}) and Superoxide Anion ($\text{O}_2^{\bullet-}$) Generation in Planktonic Fungal Cells

We adapted the protocols previously described [25] for peroxide anion radicals (O_2^{2-}) determination and for superoxide detection in the cells [62] with modifications. The final cell population for the experiment was set to mid-log phased 10^5 CFU/mL. An end concentration of 0.5 mmol/L of menadione (Me) in cell suspensions was added as the positive control. The cell suspensions were treated with MEC_{10} concentrations of test samples. The treatments were done for 60 min at 30 °C in the modified RPMI 1640 medium. Thereafter, the cells were centrifuged for 5 min at 1500g at room temperature. The pellets were re-suspended in PBS in the same volume. DHR 123 at a final concentration of 10 $\mu\text{mol/L}$ for peroxides determination and DHE at a final concentration of 15 $\mu\text{mol/L}$ for $\text{O}_2^{\bullet-}$ determination

were added separately to the cell samples. The stained cell samples were further incubated for 60 min at 30 °C in the dark condition with mild shaking. The samples were centrifuged and re-suspended in PBS followed by distribution of the samples into the wells of 96-well microplates. The fluorescence was measured at excitation/emission wavelengths of 500/536 nm for peroxides and 473/521 nm for O₂^{•−} detection, respectively by a PerkinElmer EnSpire multimode plate-reader. The percentage increase in oxidative stress was measured by comparing the signals to those of the growth controls. Six independent experiments were done with three technical replicates for each treatment.

4.9. Statistical Analysis

All data are given as mean ± SD. Graphs and statistical analyses were conducted using OriginPro 2016 (OriginLab Corp., Northampton, MA, USA). All experiments were performed independently six times in triplicates and data were analyzed by one-way ANOVA test. *P*-value of <0.05 was considered as statistically significant. The minimum inhibitory concentration (MIC₉₀) and the minimum effective concentration (MEC₁₀) were calculated using a non-linear dose-response curve function as follows:

$$y = A_1 + \frac{A_2 - A_1}{1 + 10^{(LOG_x 0 - x)p}} \quad (1)$$

where, *A*₁, *A*₂, LOG_{*x*}0, and *p* are the bottom asymptote, top asymptote, center and hill slope of the curve have been considered.

Author Contributions: Conceptualization T.K., S.D., and N.P.; methodology S.D., L.C., V.B., G.P., Z.G., and T.K.; software, S.D. and V.B.; formal analysis, S.D. and L.C.; investigation, S.D., L.C., and V.B.; resources, T.K. and N.P.; data curation, S.D., L.C., and V.B.; writing—original draft preparation, S.D.; writing—review and editing, T.K.; visualization, S.D., L.C., and V.B.; supervision, T.K.; funding acquisition T.K. All authors have read and agreed to the published version of the manuscript.

Funding: The work was financially supported by University of Pécs, Medical School, KA-2018-17, University of Pécs, Medical School EFOP-3.6.1.-16-2016-00004 and EFOP-3.6.3-VEKOP-16-2017-00009 and NKFI-EPR (Hungarian Scientific Research Fund. K 127944) grants.

Conflicts of Interest: The authors declare no conflict of interest.

References

1. Wang, X.; van de Veerdonk, F.L.; Netea, M.G. Basic Genetics and Immunology of Candida Infections. *Infect. Dis. Clin. N. Am.* **2016**, *30*, 85–102. [[CrossRef](#)] [[PubMed](#)]
2. De Aguiar Cordeiro, R.; Sales, J.A.; Castelo, D.D.S.C.M.; Brilhante, R.S.N.; de Ponte, Y.B.; dos Santos Araújo, G.; Mendes, P.B.L.; Pereira, V.S.; de Alencar, L.P.; de Queiroz Pinheiro, A.; et al. Candida parapsilosis complex in veterinary practice: A historical overview, biology, virulence attributes and antifungal susceptibility traits. *Vet. Microbiol.* **2017**, *212*, 22–30. [[CrossRef](#)] [[PubMed](#)]
3. Gugnani, H.C.; Denning, D.W. Burden of serious fungal infections in the Dominican Republic. *J. Infect. Public Health* **2016**, *9*, 7–12. [[CrossRef](#)] [[PubMed](#)]
4. Álvarez-Pérez, S.; García, M.E.; Cutuli, M.T.; Fermín, M.L.; Daza, M.Á.; Peláez, T.; Blanco, J.L. Acquired multi-azole resistance in *Candida tropicalis* during persistent urinary tract infection in a dog. *Med. Mycol. Case Rep.* **2016**, *11*, 9–12. [[CrossRef](#)] [[PubMed](#)]
5. Ostrosky-Zeichner, L.; Sobel, J.D. Fungal Infections. *Infect. Dis. Clin. N. Am.* **2016**, *30*, 13–14. [[CrossRef](#)]
6. Brilhante, R.S.N.; de Oliveira, J.S.; de Jesus Evangelista, A.J.; Serpa, R.; da Silva, A.L.; de Aguiar, F.R.M.; Pereira, V.S.; Castelo, D.D.S.C.M.; Pereira-Neto, W.A.; de Aguiar Cordeiro, R.; et al. Candida tropicalis from veterinary and human sources shows similar in vitro hemolytic activity, antifungal biofilm susceptibility and pathogenesis against *Caenorhabditis elegans*. *Vet. Microbiol.* **2016**, *192*, 213–219. [[CrossRef](#)]
7. Jothiprakasham, V.; Sambantham, M.; Chinnathambi, S.; Vijayaboopathi, S. *Candida tropicalis* biofilm inhibition by ZnO nanoparticles and EDTA. *Arch. Oral Biol.* **2017**, *73*, 21–24. [[CrossRef](#)]
8. Armstrong-James, D.; Meintjes, G.; Brown, G.D. A neglected epidemic: Fungal infections in HIV/AIDS. *Trends Microbiol.* **2014**, *22*, 120–127. [[CrossRef](#)]

9. Ksiezopolska, E.; Gabaldón, T. Evolutionary Emergence of Drug Resistance in *Candida* Opportunistic Pathogens. *Genes (Basel)* **2018**, *9*, 461. [[CrossRef](#)]
10. Efferth, T. From ancient herb to modern drug: *Artemisia annua* and artemisinin for cancer therapy. *Semin. Cancer Biol.* **2017**, *46*, 65–83. [[CrossRef](#)]
11. Radulović, N.S.; Randjelović, P.J.; Stojanović, N.M.; Blagojević, P.D.; Stojanović-Radić, Z.Z.; Ilić, I.R.; Djordjević, V.B. Toxic essential oils. Part II: Chemical, toxicological, pharmacological and microbiological profiles of *Artemisia annua* L. volatiles. *Food Chem. Toxicol.* **2013**, *58*, 37–49. [[CrossRef](#)] [[PubMed](#)]
12. Ho, W.E.; Peh, H.Y.; Chan, T.K.; Wong, W.S.F. Artemisinins: Pharmacological actions beyond anti-malarial. *Pharmacol. Ther.* **2014**, *142*, 126–139. [[CrossRef](#)]
13. Tzeng, T.; Lin, Y.; Jong, T.; Chang, C. Ethanol modified supercritical fluids extraction of scopoletin and artemisinin from *Artemisia annua* L. *Sep. Purif. Technol.* **2007**, *56*, 18–24. [[CrossRef](#)]
14. Liu, W.; Hua, J.; Zhou, J.; Zhang, H.; Zhu, H.; Cheng, Y.; Gust, R. Synthesis and in vitro antitumor activity of novel scopoletin derivatives. *Bioorg. Med. Chem. Lett.* **2012**, *22*, 5008–5012. [[CrossRef](#)]
15. Moon, P.-D.; Lee, B.-H.; Jeong, H.-J.; An, H.-J.; Park, S.-J.; Kim, H.-R.; Ko, S.-G.; Um, J.-Y.; Hong, S.-H.; Kim, H.-M. Use of scopoletin to inhibit the production of inflammatory cytokines through inhibition of the I κ B/NF- κ B signal cascade in the human mast cell line HMC-1. *Eur. J. Pharmacol.* **2007**, *555*, 218–225. [[CrossRef](#)] [[PubMed](#)]
16. Galal, A.M.; Ross, S.A.; Jacob, M.; ElSohly, M.A. Antifungal Activity of Artemisinin Derivatives. *J. Nat. Prod.* **2005**, *68*, 1274–1276. [[CrossRef](#)] [[PubMed](#)]
17. Gnonlonfin, G.J.B.; Sanni, A.; Brimer, L. Review Scopoletin—A Coumarin Phytoalexin with Medicinal Properties. *Crit. Rev. Plant Sci.* **2012**, *31*, 47–56. [[CrossRef](#)]
18. Zorić, N.; Kosalec, I.; Tomić, S.; Bobnjarić, I.; Jug, M.; Vlainić, T.; Vlainić, J. Membrane of *Candida albicans* as a target of berberine. *BMC Complement. Altern. Med.* **2017**, *17*, 268. [[CrossRef](#)]
19. Al-Fattani, M.A.; Douglas, L.J. Penetration of *Candida* Biofilms by Antifungal Agents. *Antimicrob. Agents Chemother.* **2004**, *48*, 3291–3297. [[CrossRef](#)]
20. Sali, N.; Nagy, S.; Poór, M.; Kőszegi, T. Multiparametric luminescent cell viability assay in toxicology models: A critical evaluation. *J. Pharmacol. Toxicol. Methods* **2016**, *79*, 45–54. [[CrossRef](#)]
21. Kainz, K.; Tadic, J.; Zimmermann, A.; Pendl, T.; Carmona-Gutierrez, D.; Ruckenstuhl, C.; Eisenberg, T.; Madeo, F. Methods to Assess Autophagy and Chronological Aging in Yeast. In *Methods in Enzymology*; Academic Press: Cambridge, MA, USA, 2017; Volume 588, pp. 367–394. ISBN 978-0-12-809674-1.
22. Prasad, R.; Kapoor, K. Multidrug Resistance in Yeast *Candida*. In *International Review of Cytology*; Academic Press: Cambridge, MA, USA, 2004; Volume 242, pp. 215–248. ISBN 978-0-12-364646-0.
23. Brown, A.J.P.; Brown, G.D.; Netea, M.G.; Gow, N.A.R. Metabolism impacts upon *Candida* immunogenicity and pathogenicity at multiple levels. *Trends Microbiol.* **2014**, *22*, 614–622. [[CrossRef](#)] [[PubMed](#)]
24. Poljšak, B.; Gazdag, Z.; Pesti, M.; Jenko-Brinovec, Š.; Belágyi, J.; Plesničar, S.; Raspor, P. Pro-oxidative versus antioxidative reactions between Trolox and Cr(VI): The role of H₂O₂. *Environ. Toxicol. Pharmacol.* **2006**, *22*, 15–19. [[CrossRef](#)] [[PubMed](#)]
25. Stromájer-Rácz, T.; Gazdag, Z.; Belágyi, J.; Vágvölgyi, C.; Zhao, R.Y.; Pesti, M. Oxidative stress induced by HIV-1 F34IVpr in *Schizosaccharomyces pombe* is one of its multiple functions. *Exp. Mol. Pathol.* **2010**, *88*, 38–44. [[CrossRef](#)]
26. Tafforeau, L.; Le Blastier, S.; Bamps, S.; Dewez, M.; Vandenhoute, J.; Hermand, D. Repression of ergosterol level during oxidative stress by fission yeast F-box protein Pof14 independently of SCF. *EMBO J.* **2006**, *25*, 4547–4556. [[CrossRef](#)] [[PubMed](#)]
27. Khan, H.; Saeed, M.; Muhammad, N.; Tariq, S.A.; Ghaffar, R.; Gul, F. Antimalarial and free radical scavenging activities of aerial parts of *Polygonatum verticillatum* (L.) all. and identification of chemical constituents by GC-MS. *Pak. J. Bot.* **2013**, *45*, 497–500.
28. Virág, E.; Pesti, M.; Kunsági-Máté, S. Complex formation between primycin and ergosterol: Entropy-driven initiation of modification of the fungal plasma membrane structure. *J. Antibiot.* **2012**, *65*, 193–196. [[CrossRef](#)] [[PubMed](#)]
29. De Cremer, K.; Lanckacker, E.; Cools, T.L.; Bax, M.; De Brucker, K.; Cos, P.; Cammue, B.P.A.; Thevissen, K. Artemisinins, New Miconazole Potentiators Resulting in Increased Activity against *Candida albicans* Biofilms. *Antimicrob. Agents Chemother.* **2015**, *59*, 421–426. [[CrossRef](#)]

30. Li, W.; Mo, W.; Shen, D.; Sun, L.; Wang, J.; Lu, S.; Gitschier, J.M.; Zhou, B. Yeast Model Uncovers Dual Roles of Mitochondria in the Action of Artemisinin. *PLoS Genet.* **2005**, *1*, e36. [[CrossRef](#)]
31. Romero, D.; Sanabria-Valentín, E.; Vlamakis, H.; Kolter, R. Biofilm Inhibitors that Target Amyloid Proteins. *Chem. Biol.* **2013**, *20*, 102–110. [[CrossRef](#)]
32. Romero, D.; Aguilar, C.; Losick, R.; Kolter, R. Amyloid fibers provide structural integrity to *Bacillus subtilis* biofilms. *PNAS* **2010**, *107*, 2230–2234. [[CrossRef](#)]
33. Rukayadi, Y.; Hwang, J.-K. In Vitro Activity of Xanthorrhizol Isolated from the Rhizome of Javanese Turmeric (*Curcuma xanthorrhiza* Roxb.) Against *Candida albicans* Biofilms: Anti-Candida Biofilm Activity of Xanthorrhizol. *Phytother. Res.* **2013**, *27*, 1061–1066. [[CrossRef](#)] [[PubMed](#)]
34. Wu, H.; Moser, C.; Wang, H.-Z.; Høiby, N.; Song, Z.-J. Strategies for combating bacterial biofilm infections. *Int. J. Oral Sci.* **2015**, *7*, 1–7. [[CrossRef](#)] [[PubMed](#)]
35. Girardot, M.; Imbert, C. Natural Sources as Innovative Solutions Against Fungal Biofilms. In *Fungal Biofilms and Related Infections: Advances in Microbiology, Infectious Diseases and Public Health Volume 3*; Imbert, C., Ed.; Advances in Experimental Medicine and Biology; Springer International Publishing: Cham, Switzerland, 2016; pp. 105–125. ISBN 978-3-319-42360-9.
36. Kerekes, E.-B.; Deák, É.; Takó, M.; Tserennadmid, R.; Petkovits, T.; Vágvölgyi, C.; Krisch, J. Anti-biofilm forming and anti-quorum sensing activity of selected essential oils and their main components on food-related micro-organisms. *J. Appl. Microbiol.* **2013**, *115*, 933–942. [[CrossRef](#)] [[PubMed](#)]
37. Oppenheimer-Shaanan, Y.; Steinberg, N.; Kolodkin-Gal, I. Small molecules are natural triggers for the disassembly of biofilms. *Trends Microbiol.* **2013**, *21*, 594–601. [[CrossRef](#)] [[PubMed](#)]
38. Reen, F.J.; Gutiérrez-Barranquero, J.A.; Parages, M.L.; O’Gara, F. Coumarin: A novel player in microbial quorum sensing and biofilm formation inhibition. *Appl. Microbiol. Biotechnol.* **2018**, *102*, 2063–2073. [[CrossRef](#)]
39. Sardi, J.D.C.O.; Freires, I.A.; Lazarini, J.G.; Infante, J.; de Alencar, S.M.; Rosalen, P.L. Unexplored endemic fruit species from Brazil: Antibiofilm properties, insights into mode of action, and systemic toxicity of four *Eugenia* spp. *Microb. Pathog.* **2017**, *105*, 280–287. [[CrossRef](#)] [[PubMed](#)]
40. Verderosa, A.D.; Totsika, M.; Fairfull-Smith, K.E. Bacterial Biofilm Eradication Agents: A Current Review. *Front. Chem.* **2019**, *7*, 824. [[CrossRef](#)]
41. Sharma, D.; Misba, L.; Khan, A.U. Antibiotics versus biofilm: An emerging battleground in microbial communities. *Antimicrob. Resist. Infect. Control* **2019**, *8*, 76. [[CrossRef](#)]
42. Tsui, C.; Kong, E.F.; Jabra-Rizk, M.A. Pathogenesis of *Candida albicans* biofilm. *Pathog. Dis.* **2016**, *74*, ftw018. [[CrossRef](#)]
43. Papp, G.; Horváth, E.; Mike, N.; Gazdag, Z.; Belágyi, J.; Gyöngyi, Z.; Bánfalvi, G.; Hornok, L.; Pesti, M. Regulation of patulin-induced oxidative stress processes in the fission yeast *Schizosaccharomyces pombe*. *Food Chem. Toxicol.* **2012**, *50*, 3792–3798. [[CrossRef](#)]
44. Brown, A.J.P.; Budge, S.; Kaloriti, D.; Tillmann, A.; Jacobsen, M.D.; Yin, Z.; Ene, I.V.; Bohovych, I.; Sandai, D.; Kastora, S.; et al. Stress adaptation in a pathogenic fungus. *J. Exp. Biol.* **2014**, *217*, 144–155. [[CrossRef](#)] [[PubMed](#)]
45. Marcos-Zambrano, L.J.; Escribano, P.; Bouza, E.; Guinea, J. Production of biofilm by *Candida* and non-*Candida* spp. isolates causing fungemia: Comparison of biomass production and metabolic activity and development of cut-off points. *Int. J. Med. Microbiol.* **2014**, *304*, 1192–1198. [[CrossRef](#)] [[PubMed](#)]
46. Munusamy, K.; Vadivelu, J.; Tay, S.T. A study on *Candida* biofilm growth characteristics and its susceptibility to aureobasidin A. *Rev. Iberoam. Micol.* **2018**, *35*, 68–72. [[CrossRef](#)] [[PubMed](#)]
47. Blankenship, J.R.; Mitchell, A.P. How to build a biofilm: A fungal perspective. *Curr. Opin. Microbiol.* **2006**, *9*, 588–594. [[CrossRef](#)] [[PubMed](#)]
48. Mowat, E.; Lang, S.; Williams, C.; McCulloch, E.; Jones, B.; Ramage, G. Phase-dependent antifungal activity against *Aspergillus fumigatus* developing multicellular filamentous biofilms. *J. Antimicrob. Chemother.* **2008**, *62*, 1281–1284. [[CrossRef](#)]
49. Mukherjee, P.K.; Chandra, J.; Kuhn, D.M.; Ghannoum, M.A. Mechanism of fluconazole resistance in *Candida albicans* biofilms: Phase-specific role of efflux pumps and membrane sterols. *Infect. Immun.* **2003**, *71*, 4333–4340. [[CrossRef](#)]

50. Ramage, G.; Rajendran, R.; Sherry, L.; Williams, C. Fungal Biofilm Resistance. *Int. J. Microbiol.* **2012**, 528521. [[CrossRef](#)]
51. Stepanović, S.; Vuković, D.; Hola, V.; Di Bonaventura, G.; Djukić, S.; Cirković, I.; Ruzicka, F. Quantification of biofilm in microtiter plates: Overview of testing conditions and practical recommendations for assessment of biofilm production by staphylococci. *APMIS* **2007**, *115*, 891–899. [[CrossRef](#)]
52. Dowd, S.E.; Sun, Y.; Smith, E.; Kennedy, J.P.; Jones, C.E.; Wolcott, R. Effects of biofilm treatments on the multi-species Lubbock chronic wound biofilm model. *J. Wound Care* **2009**, *18*, 508–512. [[CrossRef](#)]
53. Peeters, E.; Nelis, H.J.; Coenye, T. Comparison of multiple methods for quantification of microbial biofilms grown in microtiter plates. *J. Microbiol. Methods* **2008**, *72*, 157–165. [[CrossRef](#)]
54. Alves, F.R.F.; Silva, M.G.; Rôças, I.N.; Siqueira, J.F., Jr. Biofilm biomass disruption by natural substances with potential for endodontic use. *Braz. Oral Res.* **2013**, *27*, 20–25. [[CrossRef](#)] [[PubMed](#)]
55. Kirmusaoğlu, S. The Methods for Detection of Biofilm and Screening Antibiofilm Activity of Agents. In *Antimicrobials, Antibiotic Resistance, Antibiofilm Strategies and Activity Methods*; Kirmusaoğlu, S., Ed.; IntechOpen: Rijeka, Croatia, 2019; pp. 1–17. ISBN 978-1-78985-789-4.
56. Salari, S.; Sadat Seddighi, N.; Ghasemi Nejad Almani, P. Evaluation of biofilm formation ability in different *Candida* strains and anti-biofilm effects of Fe₃O₄-NPs compared with Fluconazole: An in vitro study. *J. Mycol. Méd.* **2018**, *28*, 23–28. [[CrossRef](#)] [[PubMed](#)]
57. Alonso, B.; Cruces, R.; Pérez, A.; Sánchez-Carrillo, C.; Guembe, M. Comparison of the XTT and resazurin assays for quantification of the metabolic activity of *Staphylococcus aureus* biofilm. *J. Microbiol. Methods* **2017**, *139*, 135–137. [[CrossRef](#)] [[PubMed](#)]
58. Azeredo, J.; Azevedo, N.F.; Briandet, R.; Cerca, N.; Coenye, T.; Costa, A.R.; Desvaux, M.; Di Bonaventura, G.; Hébraud, M.; Jaglic, Z.; et al. Critical review on biofilm methods. *Crit. Rev. Microbiol.* **2017**, *43*, 313–351. [[CrossRef](#)]
59. Kuhn, D.M.; Balkis, M.; Chandra, J.; Mukherjee, P.K.; Ghannoum, M.A. Uses and Limitations of the XTT Assay in Studies of *Candida* Growth and Metabolism. *J. Clin. Microbiol.* **2003**, *41*, 506–508. [[CrossRef](#)] [[PubMed](#)]
60. Nett, J.E.; Cain, M.T.; Crawford, K.; Andes, D.R. Optimizing a *Candida* biofilm microtiter plate model for measurement of antifungal susceptibility by tetrazolium salt assay. *J. Clin. Microbiol.* **2011**, *49*, 1426–1433. [[CrossRef](#)]
61. Gazdag, Z.; Fujs, S.; Kőszegi, B.; Kálmán, N.; Papp, G.; Emri, T.; Belágyi, J.; Pócsi, I.; Raspor, P.; Pesti, M. The abc1 – /coq8 – respiratory-deficient mutant of *Schizosaccharomyces pombe* suffers from glutathione underproduction and hyperaccumulates Cd²⁺. *Folia Microbiol.* **2011**, *56*, 353–359. [[CrossRef](#)]
62. Fujs, Š.; Gazdag, Z.; Poljšak, B.; Stibilj, V.; Milacic, R.; Pesti, M.; Raspor, P.; Batic, M. The oxidative stress response of the yeast *Candida intermedia* to copper, zinc, and selenium exposure. *J. Basic Microbiol.* **2005**, *45*, 125–135. [[CrossRef](#)]
63. Das, S.; Gazdag, Z.; Szente, L.; Meggyes, M.; Horváth, G.; Lemli, B.; Kunsági-Máté, S.; Kuzma, M.; Kőszegi, T. Antioxidant and antimicrobial properties of randomly methylated β cyclodextrin—Captured essential oils. *Food Chem.* **2019**, *278*, 305–313. [[CrossRef](#)]
64. Das, S.; Horváth, B.; Šafranko, S.; Jokić, S.; Széchenyi, A.; Kőszegi, T. Antimicrobial Activity of Chamomile Essential Oil: Effect of Different Formulations. *Molecules* **2019**, *24*, 4321. [[CrossRef](#)]
65. Lee, J.; Dawes, I.W.; Roe, J.-H. Adaptive response of *Schizosaccharomyces pombe* to hydrogen peroxide and menadione. *Microbiology* **1995**, *141*, 3127–3132. [[CrossRef](#)] [[PubMed](#)]
66. Pesti, M.; Gazdag, Z.; Belágyi, J. In vivo interaction of trivalent chromium with yeast plasma membrane, as revealed by EPR spectroscopy. *FEMS Microbiol. Lett.* **2000**, *182*, 375–380. [[CrossRef](#)] [[PubMed](#)]
67. Rajendran, R.; Sherry, L.; Nile, C.J.; Sherriff, A.; Johnson, E.M.; Hanson, M.F.; Williams, C.; Munro, C.A.; Jones, B.J.; Ramage, G. Biofilm formation is a risk factor for mortality in patients with *Candida albicans* bloodstream infection-Scotland, 2012–2013. *Clin. Microbiol. Infect.* **2016**, *22*, 87–93. [[CrossRef](#)] [[PubMed](#)]
68. Fai, P.B.; Grant, A. A rapid resazurin bioassay for assessing the toxicity of fungicides. *Chemosphere* **2009**, *74*, 1165–1170. [[CrossRef](#)] [[PubMed](#)]

69. Van den Driessche, F.; Rigole, P.; Brackman, G.; Coenye, T. Optimization of resazurin-based viability staining for quantification of microbial biofilms. *J. Microbiol. Methods* **2014**, *98*, 31–34. [[CrossRef](#)] [[PubMed](#)]
70. Appiah, T.; Boakye, Y.D.; Agyare, C. Antimicrobial Activities and Time-Kill Kinetics of Extracts of Selected Ghanaian Mushrooms. *Evid. Based Complement. Altern. Med.* **2017**, *2017*. [[CrossRef](#)]

Sample Availability: Samples of the compounds artemisinin and scopoletin are available from the authors.



© 2020 by the authors. Licensee MDPI, Basel, Switzerland. This article is an open access article distributed under the terms and conditions of the Creative Commons Attribution (CC BY) license (<http://creativecommons.org/licenses/by/4.0/>).

Article

Antimicrobial Activity of Different *Artemisia* Essential Oil Formulations

Sourav Das ^{1,2,†}, Barbara Vörös-Horváth ^{3,†}, Tímea Bencsik ⁴, Giuseppe Micalizzi ⁵,
Luigi Mondello ^{5,6,7}, Györgyi Horváth ⁴, Tamás Kőszegi ^{1,2,*} and Aleksandar Széchenyi ^{3,*}

¹ Department of Laboratory Medicine, University of Pécs, Medical School, Ifjúság u. 13., 7624 Pécs, Hungary; pharma.souravdas@gmail.com

² János Szentágothai Research Center, University of Pécs, Ifjúság u. 20., 7624 Pécs, Hungary

³ Institute of Pharmaceutical Technology and Biopharmacy, University of Pécs, Faculty of Pharmacy, Rókus u. 2., 7624 Pécs, Hungary; barbara.horvath@aok.pte.hu

⁴ Department of Pharmacognosy, University of Pécs, Faculty of Pharmacy, Rókus u. 2., 7624 Pécs, Hungary; timea.bencsik@aok.pte.hu (T.B.); horvath.gyorgyi@gytk.pte.hu (G.H.)

⁵ Chromaleont s.r.l., c/o Department of Chemical, Biological, Pharmaceutical and Environmental Sciences, University of Messina, 98168 Messina, Italy; giuseppe.micalizzi@chromaleont.it (G.M.); lmondello@unime.it (L.M.)

⁶ Department of Chemical, Biological, Pharmaceutical and Environmental Sciences, University of Messina, 98168 Messina, Italy

⁷ Unit of Food Science and Nutrition, Department of Medicine, University Campus Bio-Medico of Rome, 00128 Rome, Italy

* Correspondence: koszegi.tamas@pte.hu (T.K.); szechenyi.aleksandar@gytk.pte.hu (A.S.); Tel.: +36-30-4917719 (T.K.); +36-70-3814462 (A.S.)

† These authors contributed equally to this work.

Academic Editor: Daniela Rigano

Received: 17 April 2020; Accepted: 20 May 2020; Published: 21 May 2020



Abstract: The extreme lipophilicity of essential oils (EOs) impedes the measurement of their biological actions in an aqueous environment. We formulated oil in water type Pickering *Artemisia annua* EO nanoemulsions (AEP) with surface-modified Stöber silica nanoparticles (20 nm) as the stabilizing agent. The antimicrobial activity of AEP and its effects on mature *Candida* biofilms were compared with those of Tween 80 stabilized emulsion (AET) and ethanolic solution (AEE) of the *Artemisia* EO. The antimicrobial activity was evaluated by using the minimum inhibitory concentrations (MIC₉₀) and minimum effective concentrations (MEC₁₀) of the compounds. On planktonic bacterial and fungal cells beside growth inhibition, colony formation (CFU/mL), metabolic activity, viability, intracellular ATP/total protein (ATP/TP), along with reactive oxygen species (ROS) were also studied. *Artemisia annua* EO nanoemulsion (AEP) showed significantly higher antimicrobial activity than AET and AEE. *Artemisia annua* EO nanoemulsions (AEP) generated superoxide anion and peroxides-related oxidative stress, which might be the underlying mode of action of the *Artemisia* EO. Unilamellar liposomes, as a cellular model, were used to examine the delivery efficacy of the EO of our tested formulations. We could demonstrate higher effectiveness of AEP in the EO components' donation compared to AET and AEE. Our data suggest the superiority of the AEP formulation against microbial infections.

Keywords: *Artemisia* essential oil; Pickering emulsion; oxidative stress; mature biofilm; antimicrobial activity

1. Introduction

Artemisia annua L. (Sweet Wormwood, Sweet Annie, Sweet Sagewort, Annual Wormwood, or Qinghaosu) is a very important member of the Asteraceae family, and is widely distributed

throughout Asia, South Africa, Europe and North America [1–3]. The use of this plant for the treatment of malaria has been recorded before 168 BC in Chinese traditional medicine [2–5]. Discovery of the artemisinin, a sesquiterpene with the antimalarial property made this plant to have potential commercial importance [4–7]. The search for other active components has led to the discovery of many phytochemicals including, monoterpenoids, sesquiterpenoids, flavonoids and coumarins, and aliphatic and lipid compounds [6,8]. Apart from its antimalarial activity, the plant has shown anti-tumor, anti-inflammatory, antipyretic, antimicrobial, antiparasitic, antiulcerogenic, and cytotoxic activities [2–10]. Several studies on the chemical composition of the *Artemisia annua* L. essential oil (AE) have been performed, and active components like camphor, artemisia ketone, germacrene D, and 1,8-cineole have been found [11,12]. Variability in the chemical composition of AE depending on the geographical origin and plant's development stages has led to considerable research interests in the investigation of biological properties of AE [3,6].

With the increasing demand for the AE in aromatherapy as complementary and as alternative medicine, people believe in the myth that it is harmless; therefore, it has been used for a long time [1]. Previous studies have reported many drug–drug interactions in essential oils [4,13,14]. Several side effects of essential oils, which include allergic reactions, may occur if administered topically. Furthermore, some essential oils can be poisonous if absorbed through the skin, breathed, or swallowed. Uncontrolled widespread usage and continuous production of essential oils as alternative therapy along with carrier diluents have created severe problems, especially among children [13,15–17]. Additionally, the highly lipophilic nature of the essential oils makes it difficult to examine their biological properties in aqueous environments [18,19]. Therefore, it is highly important to perform research on the formulations for EOs' usage, to determine the exact mode of their action, with such knowledge we can suggest appropriate formulation, and avoid the danger of misuse of EOs.

The antimicrobial effectiveness is often described in terms of minimum inhibitory concentration (MIC). Conventional broth dilution techniques and disc diffusion data have provided numerous antimicrobial activities of the AE. However, the diffusion assay is not suitable for essential oil testing, as the components are partitioned through the agar because of their low affinity to water [20,21]. Furthermore, the ability to compare data from the broth and agar dilution methods are limited due to the wide spectrum of test methodologies and selection criteria for end-point determinations [16,22,23]. Several techniques have been used to overcome the lipophilicity of the AE, by the application of suitable solvents such as ethanol, methanol, and dimethyl-sulfoxide (DMSO) or surfactants like Tween 80 (Polyoxyethylene (80) sorbitan monooleate) and Tween 20 (Polyoxyethylene (20) sorbitan monolaurate) [21,24,25]. However, previous studies have repeatedly reported that usage of the solvents/surfactants in various microbiological experiments may contribute to changes in the physicochemical properties of the testing microenvironment, leading to enhancement or reduction of the antimicrobial properties [26–28]. Furthermore, the evaporation of the essential oils during the assay or the inability of the active components to reach the test microbes might cause some misleading results [29,30].

Thus, novel formulations have been used to enhance the solubility or to emulsify the essential oils in the aqueous environment, resulting in sustained release of the active components in the testing system [29]. The suitability of the organic solvents/surfactants has been questioned, and therefore they are not welcomed in this regard. Efforts to entrap the essential oils by modified cyclodextrins and silica nanoparticles have been made for the precise characterization of the antimicrobial properties [24,31,32].

Approaches to stabilizing the oil-in-water (O/W) and water-in-oil (W/O) emulsions, by the application of solid particles instead of surfactants as stabilizing agents, is novel in the field of essential oil research. The fundamental mechanism involves the adsorption of the solid particles on the oil-water interface, resulting in a significant decrement of the interfacial tension, causing high emulsion stability [21,33]. Decreased evaporation of the essential oils from the nanoparticle-stabilized O/W emulsion formulations, when compared to essential oil-surfactant systems, has been reported

previously [34,35]. By application of inert and biocompatible particles instead of surfactants, the irritative and toxic effect of surfactants can be avoided [36].

Even though numerous studies have been performed on the essential oil–Pickering emulsion, literature data on AE (obtained from *Artemisia annua* L. cultivated in Hungary)–nanoparticle formulations related to their application as antimicrobial and anti-biofilm agents are not found [1,3,6,11,14,19]. The primary aim of our present study is to formulate the Pickering nanoemulsion of AE stabilized with surface-modified spherical silica nanoparticles (AEP) and characterize its antimicrobial activity on Gram-positive and Gram-negative bacteria and fungi as well as its effects on mature *Candida* species' biofilms. We could also demonstrate an effective biofilm-related microbial cytotoxicity and antimicrobial activity of the AEP on planktonic cells and suggest a plausible mode of action of this formulation. Efforts were made in the experiments to support the proposed mode of action.

2. Results

2.1. Artemisia Essential Oil and Its Components

The amount of the essential oil obtained by steam distillation was 3% *w/w* of plant powder. Our gas chromatography–mass spectrometry/flame ionization detection (GC-MS/FID) analyses (Table S1 and Figures S1–S6) has documented β -pinene (1.25%), artemisia ketone (4.43%), yomogi alcohol (1.29%), artemisia alcohol (1.68%), (E)-pinocarveol (7.55%), pinocarvone (3.22%), camphor (7.06%), terpinen-4-ol (1.75%), α -copaene (2.75%), caryophyllene (5.26%), β -farnesene (4.8%), β -selinene (12.27%), spathulenol (1.75%), caryophyllene oxide (8.64%), eudesma-4(15),11-dien-5-ol (1.06%) and mustakone (1.27%) as the major components of the essential oil of *Artemisia annua* L. essential oil, that has been used throughout the experiments.

2.2. Preparation and Stability Studies of O/W Type Pickering Nanoemulsions

We found that AEPs and AETs have the same stability. The droplet size of the prepared emulsions increased when the concentration of AE has been raised (Table 1). Since the volume fraction of AE is very low (0.004 or less), we can be sure that the Pickering emulsion is o/w type, as it has been proven before [37].

Table 1. Stability parameters and droplet sizes of Pickering nanoemulsion and conventional emulsion.

Stabilizing Agent	c_{oil} (mg/mL)	$D_{droplet}$ (nm) \pm SD	Stability
SNP	0.2–3.5	160 ± 2.2 – 670 ± 37.2	2–3 months
Tw80	0.2–3.5	130 ± 0.9 – 590 ± 19.6	2–3 months

2.3. In Vitro Diffusion Study of Artemisia EO (AE) Formulations

We assumed that the different formulations of AE have different diffusion properties, which could cause different activities in biofilm treatment. To confirm this assumption, in vitro diffusion studies were performed with an ethanolic solution of AE (AEE), in addition to AET and AEP. The concentration of AE was the same for all three formulations, and the droplet sizes of AEP and AET were similar, 160 ± 2.2 and 130 ± 0.9 nm, respectively to avoid the droplet size exclusion effect (Figure 1).

The diffusion profiles were very similar in each case. Still, it can be seen that the cumulative amounts (CA) of AE were the highest in the case of AEP in both experimental circumstances. These were 28.71% at bacterial and 32.30% at fungal experimental temperatures, where AET samples showed lower values, 19.36%, and 30.43%, respectively, while for AEE only 17.60% and 22.82% of AE diffused after 24 h.

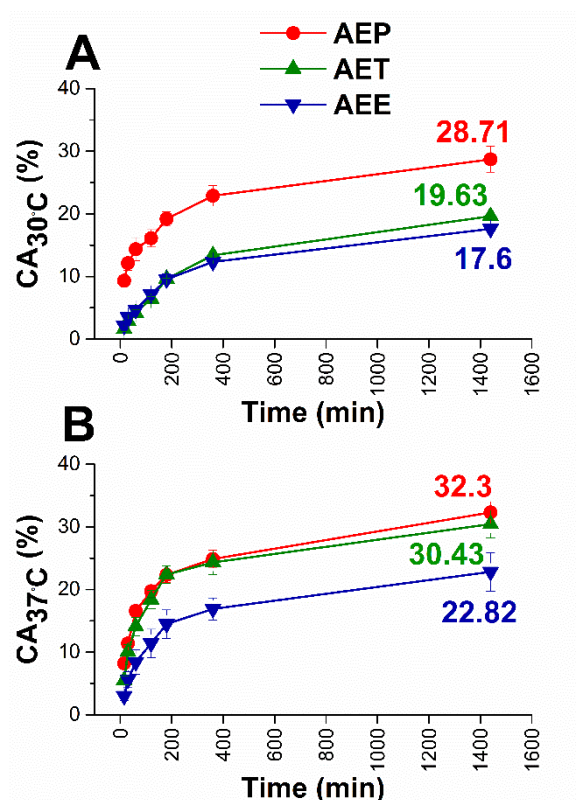


Figure 1. Results of in vitro diffusion studies through agar gel membrane as biofilm model for AEE, AET, and AEP at 30 °C (A) and 37 °C (B), respectively. The AE concentration is 200 µg/mL. CA: cumulative amounts of essential oil in percentage; the experiments were performed in triplicate (mean ± SD).

2.4. Interaction Studies with Unilamellar Liposomes as Cellular Models

Similar to our previous studies, unilamellar liposomes (ULs) were used as a cellular model for studying the intracellular delivery ability of AE for different formulations [20]. We studied the interaction between 3.5 µm sized ULs and different formulations of AE (AEP, AET, AEE) for 48 h at 30 °C and 24 h at 37 °C. The incubation times and temperatures were the same as in the case of cellular microbiological experiments with fungi and bacteria (Figure 2).

For both experimental circumstances, AEP showed the best ability to deliver AE to the internal water phase of ULs; it was 29.8% after 48 hours at 30 °C, and 59.2% after 24 hours at 37 °C. For the AET samples, these values were 25.0% and 27.3%, respectively, and the lowest values were obtained in the case of AEE samples.

2.5. Antibacterial and Antifungal Activities of the Prepared Emulsions

The effects of the *Artemisia* Pickering nanoemulsion, conventional emulsion, and essential oil in ethanol on Gram-positive and Gram-negative bacteria, and on opportunistic fungi were studied. The AEP showed acceptable antibacterial and antifungal activities (MIC₉₀) on *E. coli* PMC 201 (1.68 ± 0.72 µg/mL), *S. aureus* ATCC 29213 (1.62 ± 0.37 µg/mL), *B. subtilis* SZMC 0209 (1.42 ± 0.64 µg/mL), *P. aeruginosa* PMC 103 (1.46 ± 0.22 µg/mL), *S. pyogenes* SZMC 0119 (3.15 ± 0.16 µg/mL), *S. pombe* ATCC 38366 (2.01 ± 0.46 µg/mL), *C. albicans* SZMC 1372 (3.62 ± 0.65 µg/mL), *C. tropicalis* SZMC 1368 (4.29 ± 0.82 µg/mL), *C. dubliniensis* SZMC 1470 (3.63 ± 0.57 µg/mL) and *C. krusei* SZMC 0779 (3.79 ± 0.57 µg/mL), respectively, when compared to AET ($P < 0.01$). The Pickering *Artemisia annua* EO nanoemulsion (AEP) showed higher antimicrobial activity at an average of twelve-fold less concentration when compared to the free essential oil in ethanol (AEE). The comparative dose–response curves are shown in Figures 3 and 4 for bacteria and fungi, respectively.

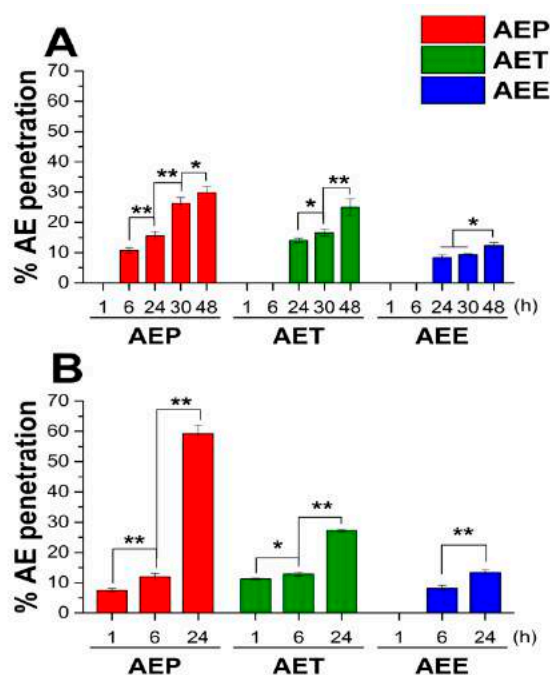


Figure 2. Results of the interaction study between unilamellar liposomes (ULs) and different formulations of *Artemisia* essential oil (AE) at 30 °C for 48 h (A) and at 37 °C for 24 h (B), experiments were performed in triplicate. AEP: Pickering emulsion, AET: conventional emulsion, AEE: ethanolic solution. c[AE] = 200 µg/mL (* $P < 0.05$ and ** $P < 0.01$, mean \pm SD).

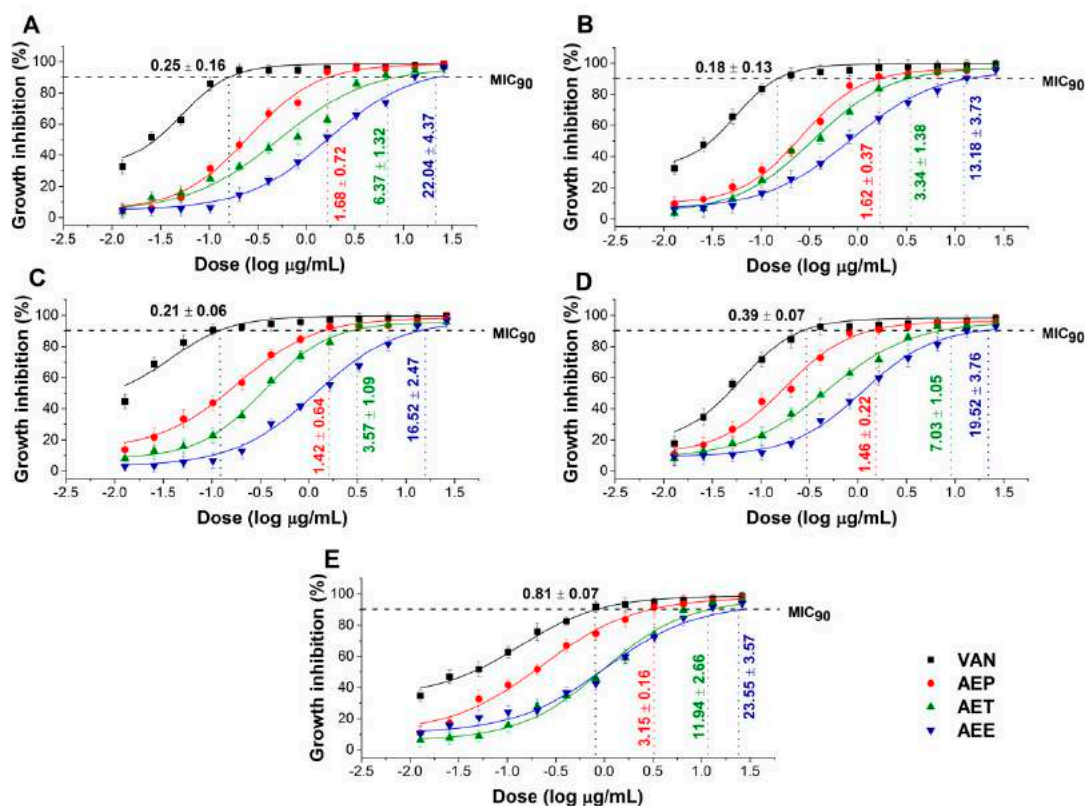


Figure 3. Minimum inhibitory concentration (MIC₉₀) of AEP, AET, AEE, and vancomycin (VAN) in µg/mL on *E. coli* (A), *S. aureus* (B), *B. subtilis* (C), *P. aeruginosa* (D), and *S. pyogenes* (E). Six independent experiments each with three technical replicates were performed (mean \pm SD).

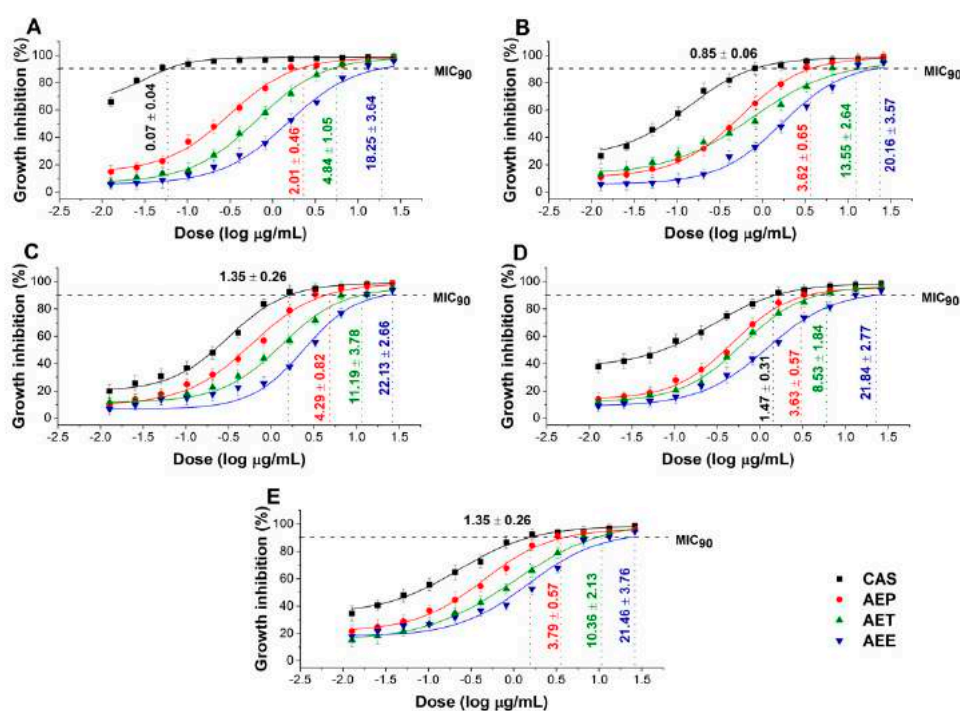


Figure 4. Minimum inhibitory concentration (MIC₉₀) of AEP, AET, AEE, and caspofungin (CAS) in µg/mL on *S. pombe* (A), *C. albicans* (B), *C. tropicalis* (C), *C. dubliniensis* (D) and *C. krusei* (E). Six independent experiments each with three technical replicates were performed (mean ± SD).

2.6. Effects of the Minimum Effective Concentration (MEC₁₀) on Planktonic Microbial Cells

The minimum effective concentration (MEC₁₀) of the *Artemisia* Pickering nanoemulsion, conventional emulsion and essential oil in ethanol on Gram-positive and Gram-negative bacteria, and on opportunistic fungi are shown in Figures 5 and 6. For the AEP the MEC₁₀ concentrations are as follows: *E. coli* (4.05 ± 0.69 µg/mL), *S. aureus* (4.79 ± 0.84 µg/mL), *B. subtilis* (5.54 ± 1.05 µg/mL), *P. aeruginosa* (6.39 ± 0.95 µg/mL), *S. pyogenes* (9.25 ± 1.03 µg/mL), *S. pombe* (7.02 ± 1.55 µg/mL), *C. albicans* (7.12 ± 2.11 µg/mL), *C. tropicalis* (13.79 ± 2.74 µg/mL), *C. dubliniensis* (10.49 ± 3.77 µg/mL) and *C. krusei* (11.67 ± 3.62 µg/mL). The curves expressed a dose-dependent cell survival rate (by CFU quantification) after 60 min exposure to AEP, AET, and AEE. The doses corresponding to MEC₁₀ (average 90% survival rate of the ~10⁵ CFU/mL, mid-log phased cell population) were then used in further study on planktonic cells and on mature biofilms.

2.7. Effects on the Microbial Oxidative Balance

Various reactive oxygen species (ROS) production and accumulation in the bacterial and fungal cells initiate oxidative stress followed by cellular structural damages and apoptosis induction [5]. The oxidative stress generation after 60 min of treatment has been investigated (Figures 7 and 8). Data expressed as % of control are as follows: combined ROS detected by DCFDA (1235.46 ± 133.63%), peroxide by DHR 123 (1053.74 ± 146.26%) and superoxide by DHE (1153.84 ± 142.67%) were the highest in the case of *P. aeruginosa*. The AEP caused an effective increase in the combined ROS, peroxide, and superoxide generations as well, in both Gram-positive and negative bacteria and fungi when compared to AET and AEE ($P < 0.01$). The AEE has generated a three to four-fold increment in oxidative stress compared to the growth control (GC), which was the lowest among all treatments.

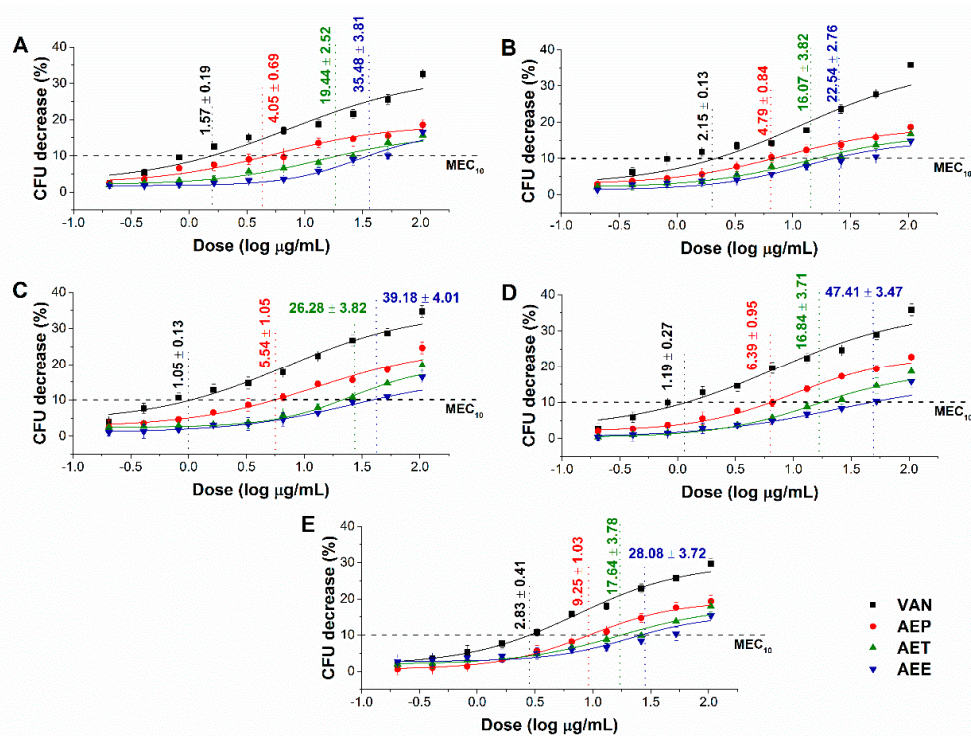


Figure 5. Minimum effective concentration (MEC₁₀) of AEP, AET and AEE (µg/mL) on *E. coli* (A), *S. aureus* (B), *B. subtilis* (C), *P. aeruginosa* (D), and *S. pyogenes* (E). Six independent experiments, each with three technical replicates, compared to vancomycin (VAN) were considered (mean ± SD).

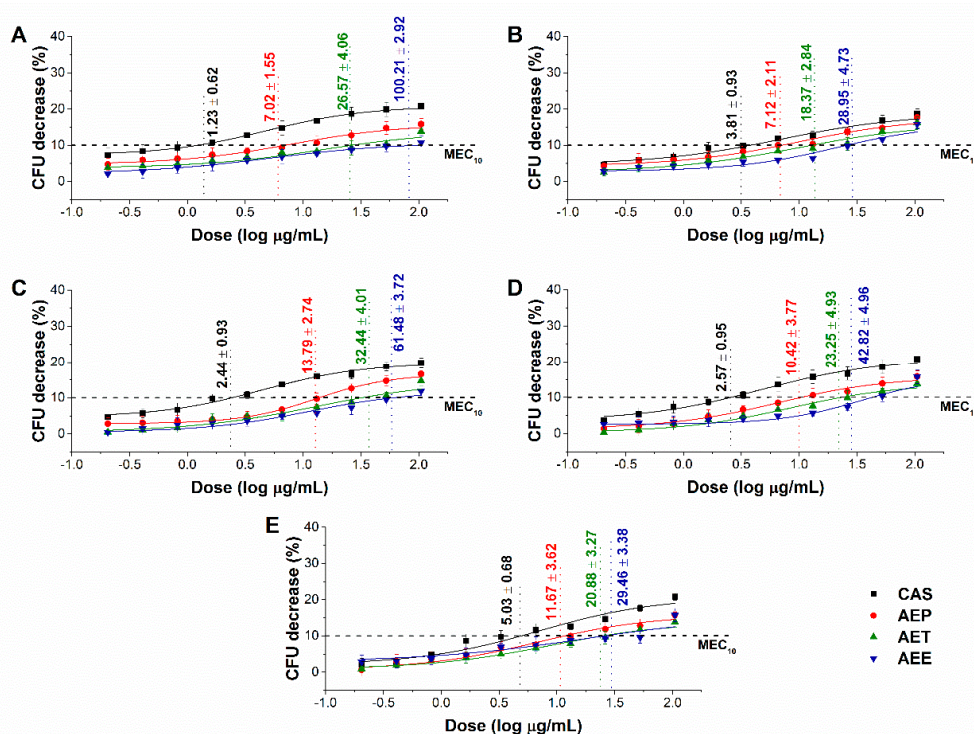


Figure 6. Minimum effective concentration (MEC₁₀) of AEP, AET, and AEE (µg/mL) on *S. pombe* (A), *C. albicans* (B), *C. tropicalis* (C), *C. dubliniensis* (D) and *C. krusei* (E). Six independent experiments, each with three technical replicates, compared to caspofungin (CAS) were considered (mean ± SD).

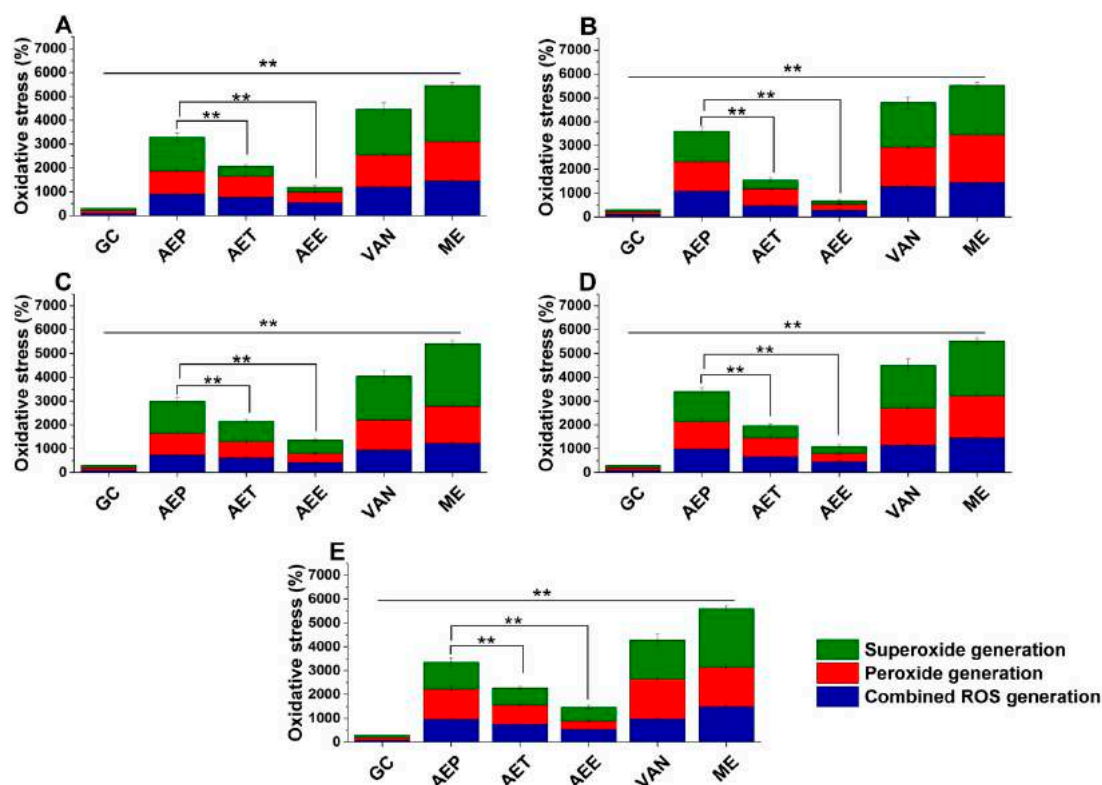


Figure 7. Percentage oxidative stress generation by AEP, AET, AEE, and VAN on *E. coli* (A), *S. aureus* (B), *B. subtilis* (C), *P. aeruginosa* (D), and *S. pyogenes* (E) at their respective MEC₁₀ concentrations after one-hour treatment. All results were compared to those for menadione (ME) and growth control (GC). The three formulations were evaluated separately as well. Six independent experiments, each with three technical replicates (** $P < 0.01$, mean \pm SD).

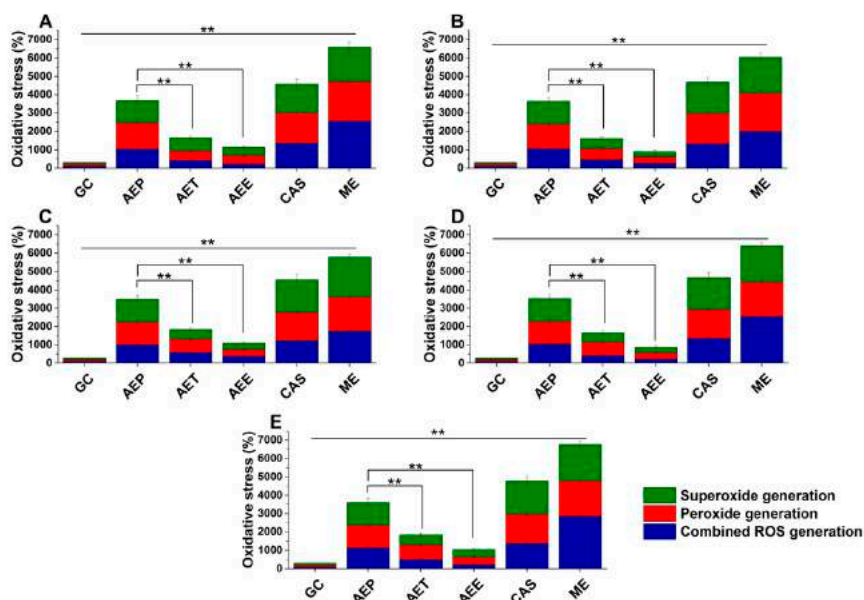


Figure 8. Percentage oxidative stress generation by AEP, AET, AEE, and CAS on *S. pombe* (A), *C. albicans* (B), *C. tropicalis* (C), *C. dubliniensis* (D) and *C. krusei* (E) at their respective MEC₁₀ concentrations and after one-hour treatment. All results were compared to those for menadione (ME) and growth control (GC). The three formulations were evaluated separately as well. Six independent experiments, each with three technical replicates (** $P < 0.01$, mean \pm SD).

2.8. Effects on the Microbial Planktonics' Behavior

2.8.1. Colony Formation Changes

The changes in the colony formation of the microbial cells were followed using a time-kinetic means of investigating the quantity of the living population after a definite time interval under different samples' MEC₁₀ concentrations (Figures 9 and 10). A significant 50% reduction in the bacterial and fungal cell survivability after 6 and 18 h, respectively, was observed in the case of the AEP exposure when compared to that of AET and AEE ($P < 0.01$). AEE was the least effective among all other treatments.

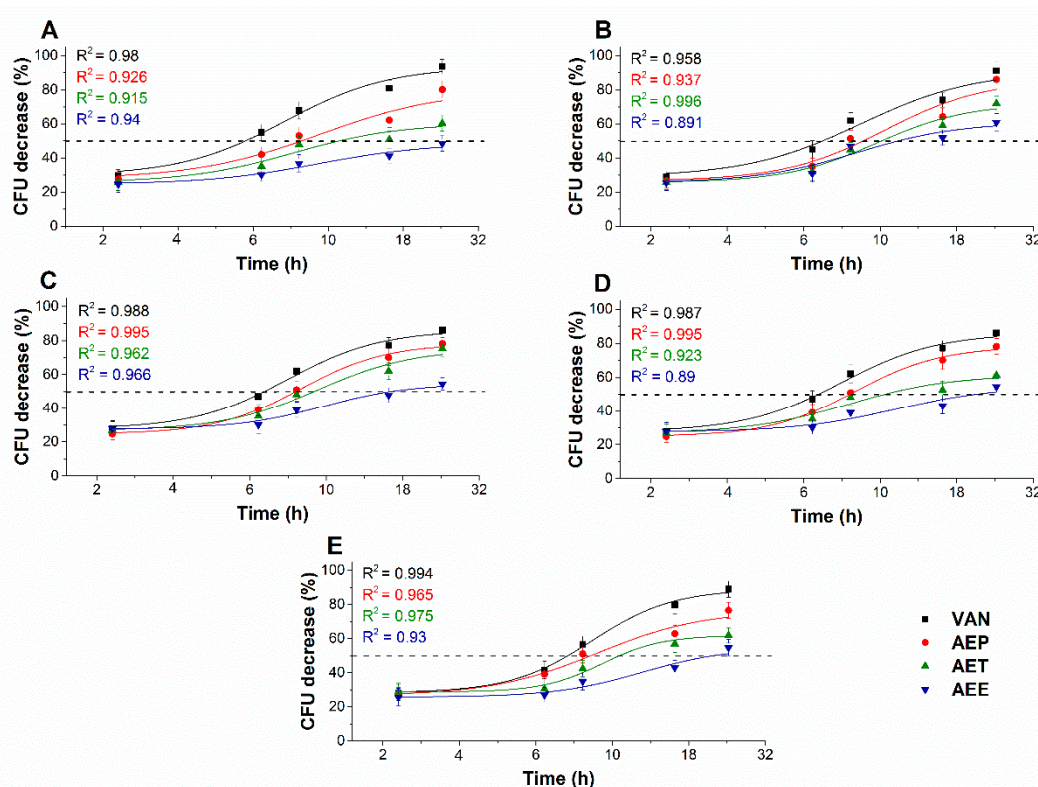


Figure 9. Effects of AEP, AET, and AEE at their MEC₁₀ concentrations on the mean percentage colony-forming unit (CFU/mL) decrement of the planktonic *E. coli* (A), *S. aureus* (B), *B. subtilis* (C), *P. aeruginosa* (D), and *S. pyogenes* (E) compared to their respective 0 h samples and vancomycin (VAN) standard antimicrobial controls after 2, 6, 8, 16 and 24 h of treatment (mean \pm SD, $n = 6$ independent experiments each with three technical replicates).

2.8.2. Variations in the Intracellular ATP to Total Protein Content Ratios

The energy depletive effects of AEP, AET, and AEE at their MEC₁₀ concentrations on the selected Gram-positive and -negative bacteria, and fungi were studied (Figures 11 and 12). Although no significant change in the total protein content (TP) over time in the planktonic cells was observed, a significant $60.37 \pm 5.35\%$ decrement in the ATP/TP ratio was found in the case of the AEP treated samples when compared to the 0 h samples ($P < 0.01$). Both AET and AEE have shown a decrease up to an average of 40% in the ATP/TP ratio in the cases of bacteria and fungi when compared to the 0 h samples.

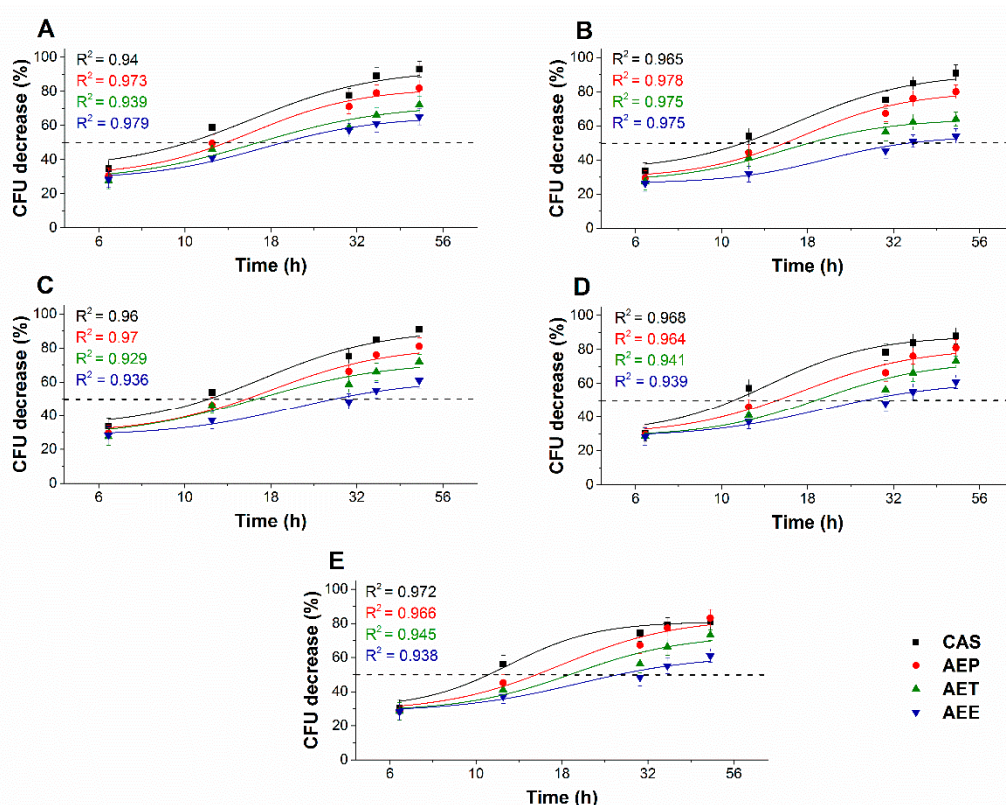


Figure 10. Effects of AEP, AET, and AEE at their MEC₁₀ concentrations on the metabolic activities of the mean percentage colony-forming unit (CFU/mL) decrement of the planktonic *S. pombe* (A), *C. albicans* (B), *C. tropicalis* (C), *C. dubliniensis* (D) and *C. krusei* (E) compared to their respective 0 h samples and caspofungin (CAS) standard antimicrobial controls after 6, 12, 30, 36 and 48 h of treatment (mean \pm SD, $n = 6$ independent experiments each with three technical replicates).

2.8.3. Effects on Microbial Cell Viability and Metabolic Activity

The multi-parametric cytotoxicity assay has been performed to evaluate the viability of the microbial cells using SYBR green I/PI live-dead cell technique while the resazurin fluorometric method was applied for reflecting the metabolic changes caused by the test samples. The cytotoxic effects of AEP, AET, and AEE on the viability (Figures 13 and 14) and on the metabolic activity (Figures 15 and 16) of the selected bacteria and fungi were evaluated. The 50% reduction in the viable cell population was reached at an average of 9.9 ± 0.71 h and 17.09 ± 0.45 h in the case of the Gram-positive and -negative bacteria, and fungi under AEP exposure. A delayed effect at an average of 9.74 ± 1.65 h was observed in the case of AET to initiate a 50% mean non-viability in the microbial populations when compared to AEP ($P < 0.01$). The AEE has shown the slowest induction of microbial non-viability with a delay of 20.63 ± 3.73 h compared to AEP ($P < 0.01$). A significant 50% decrement in the metabolic activity was observed in the case AEP treated bacteria and fungi at an average of 10.63 ± 0.55 h and 26.35 ± 0.36 h, respectively (Figures 15 and 16). The AET treatment showed an average of 7.42 ± 2.63 h delay in reducing metabolic activity by 50% when compared to AEP treated samples ($P < 0.01$). No significant decrease in the metabolic activity was found in the case of the AEE treated fungal samples.

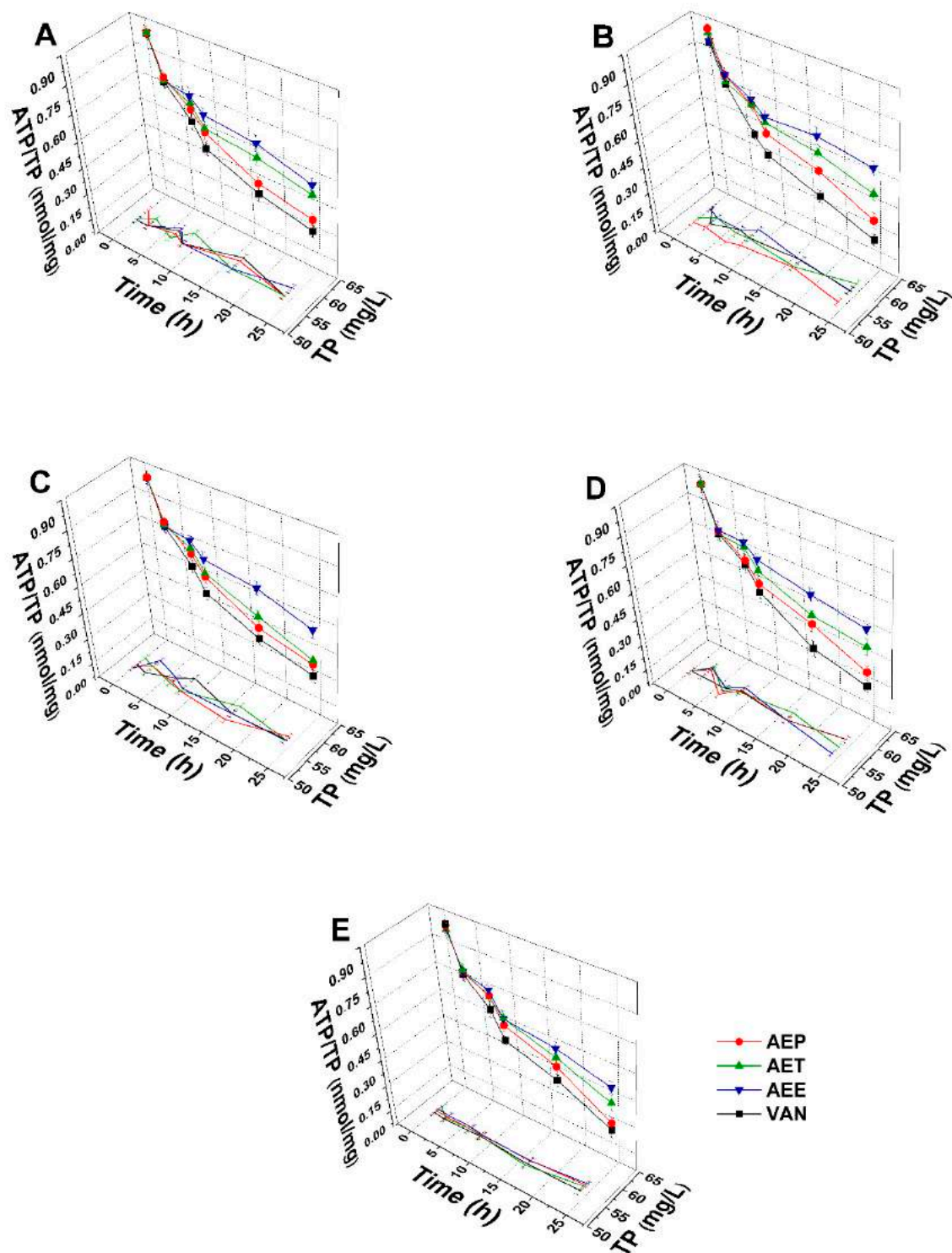


Figure 11. Effects of AEP, AET and AEE at their MEC₁₀ concentrations on the total protein content (TP) and intracellular ATP/TP ratio of the planktonic *E. coli* (A), *S. aureus* (B), *B. subtilis* (C), *P. aeruginosa* (D), and *S. pyogenes* (E) compared to their respective 0 h samples and vancomycin (VAN) standard antimicrobial controls after 2, 6, 8, 16 and 24 h of treatment (mean ± SD, $n = 6$ independent experiments each with three technical replicates).

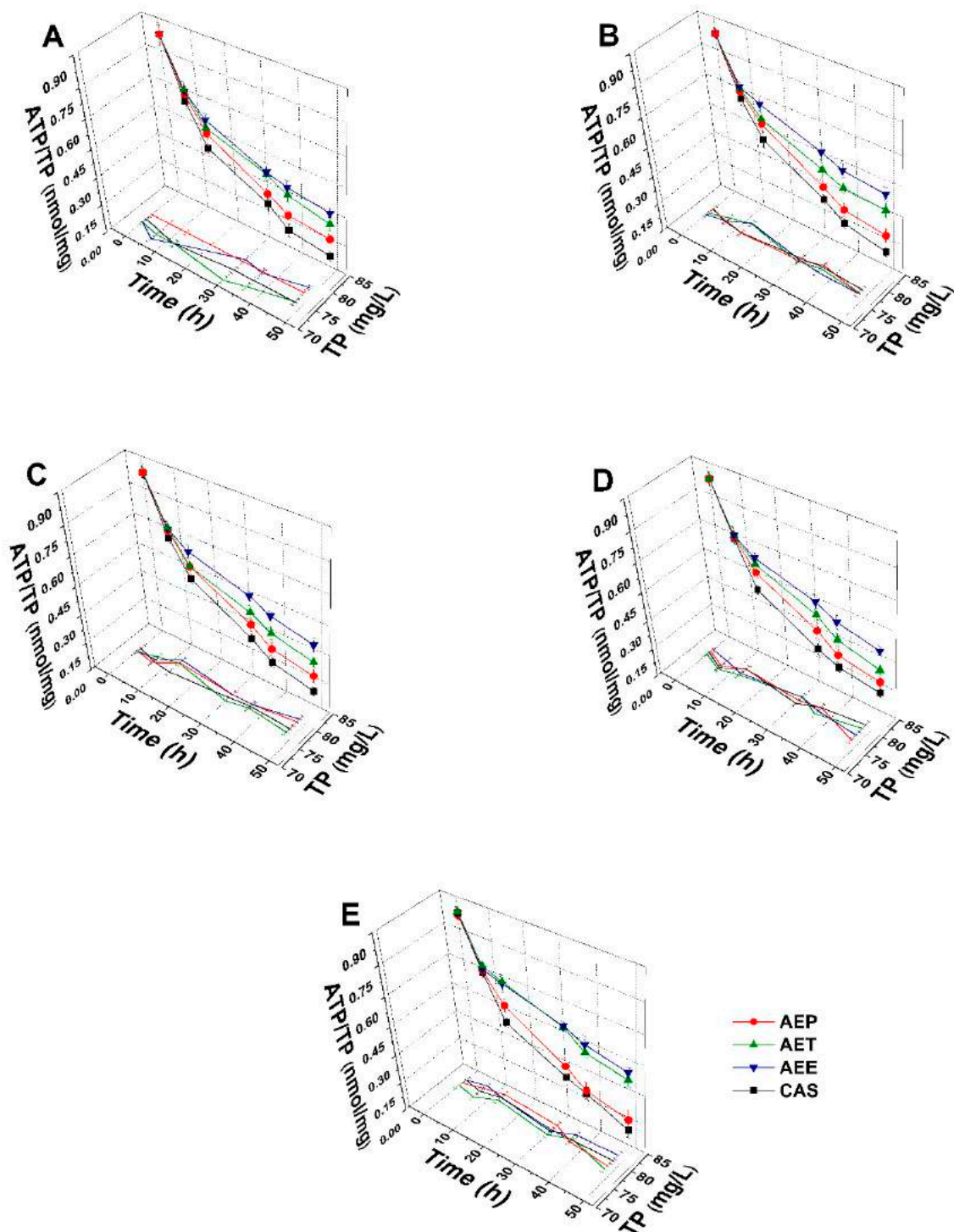


Figure 12. Effects of AEP, AET, and AEE at their MEC₁₀ concentrations on the total protein content (TP) and intracellular ATP/TP ratio of the planktonic *S. pombe* (A), *C. albicans* (B), *C. tropicalis* (C), *C. dubliniensis* (D) and *C. krusei* (E) compared to their respective 0 h samples and caspofungin (CAS) standard antimicrobial controls after 6, 12, 30, 36 and 48 h of treatment (mean ± SD, $n = 6$ independent experiments each with three technical replicates).

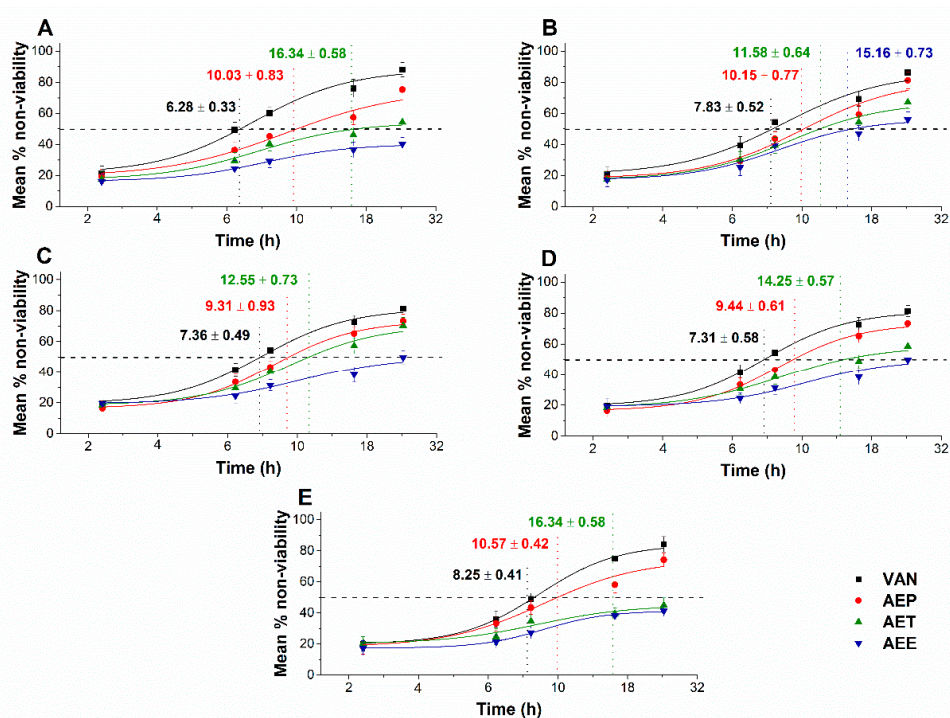


Figure 13. Mean percentage non-viability of AEP, AET and AEE at their MEC₁₀ concentrations on the metabolic activities of the planktonic *E. coli* (A), *S. aureus* (B), *B. subtilis* (C), *P. aeruginosa* (D), and *S. pyogenes* (E) compared to their respective 0 h samples and vancomycin (VAN) standard antimicrobial controls after 2, 6, 8, 16 and 24 h of treatment (mean ± SD, $n = 6$ independent experiments each with three technical replicates).

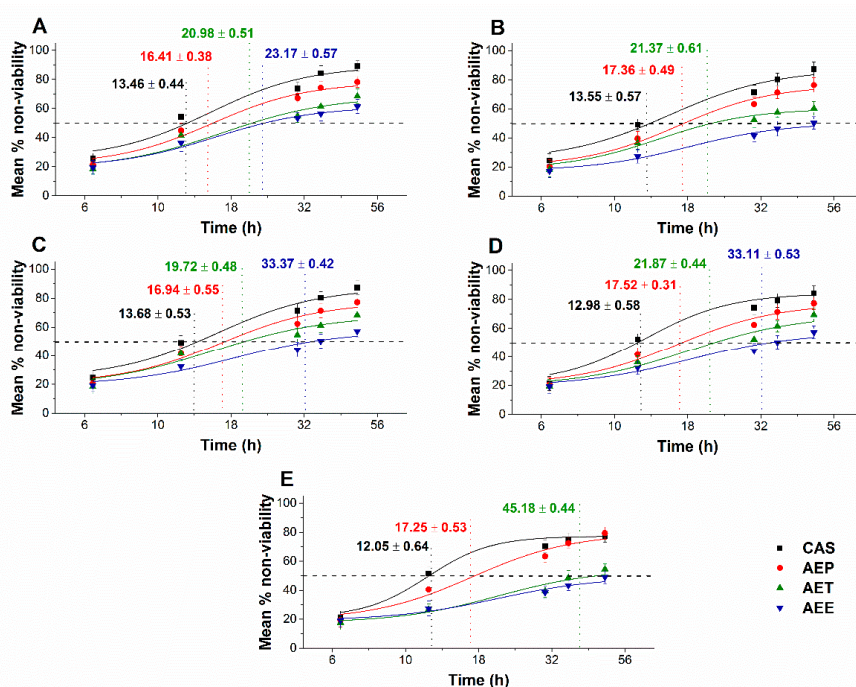


Figure 14. Mean percentage non-viability of AEP, AET, and AEE at their MEC₁₀ concentrations on the metabolic activities of the planktonic *S. pombe* (A), *C. albicans* (B), *C. tropicalis* (C), *C. dubliniensis* (D) and *C. krusei* (E) compared to their respective 0 h samples prior and caspofungin (CAS) standard antimicrobial controls after 6, 12, 30, 36 and 48 h of treatment (mean ± SD, $n = 6$ independent experiments each with three technical replicates).

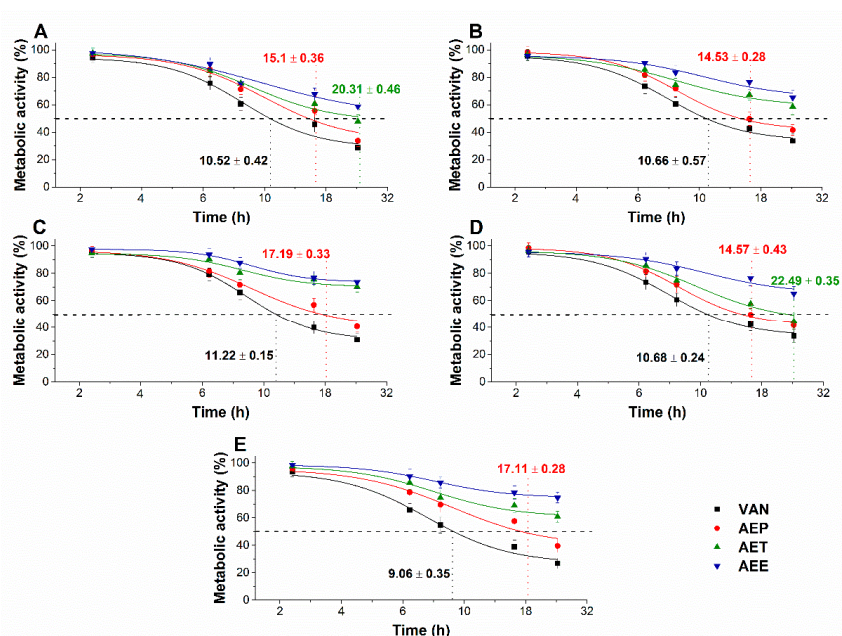


Figure 15. Effects of AEP, AET and AEE at their MEC_{10} concentrations on the metabolic activities of the planktonic *E. coli* (A), *S. aureus* (B), *B. subtilis* (C), *P. aeruginosa* (D), and *S. pyogenes* (E) compared to their respective 0 h samples and vancomycin (VAN) standard antimicrobial controls after 2, 6, 8, 16 and 24 h of treatment (mean \pm SD, $n = 6$ independent experiments each with three technical replicates).

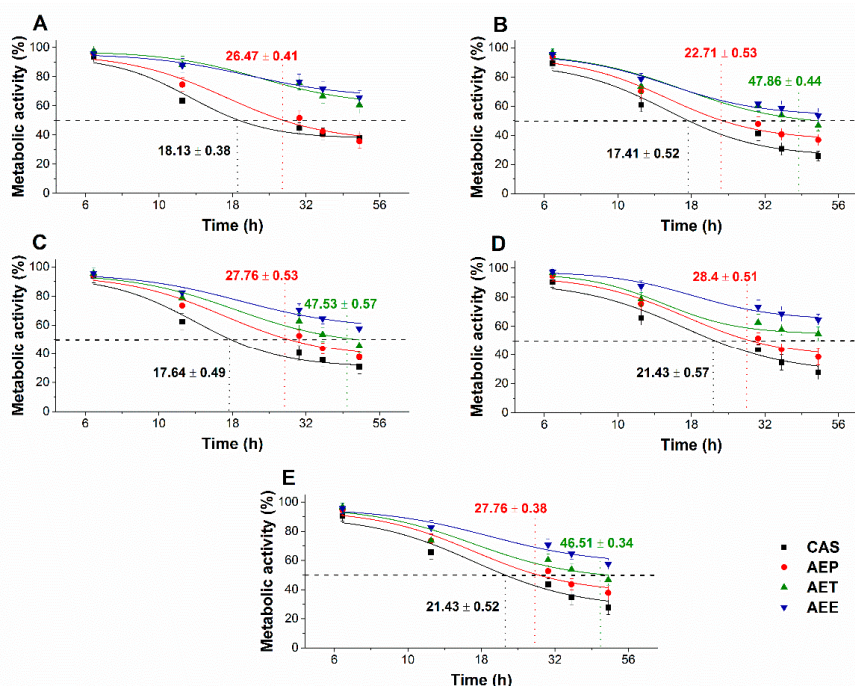


Figure 16. Effects of AEP, AET and AEE at their MEC_{10} concentrations on the metabolic activities of the planktonic *S. pombe* (A), *C. albicans* (B), *C. tropicalis* (C), *C. dubliniensis* (D) and *C. krusei* (E) compared to their respective 0 h samples and caspofungin (CAS) standard antimicrobial controls after 6, 12, 30, 36 and 48 h of treatment (mean \pm SD, $n = 6$ independent experiments, each with three technical replicates).

2.9. Effects on Mature *Candida* Spp. Biofilms

The changes in the metabolic activity, fungal cell viability, total biofilm biomass, total protein content (TP) of the biofilm-attached *Candida* cells, and their ATP content in terms of ATP/TP ratio are

shown in Figures 17 and 18. Variable response to the AEP, AET, and AEE treatments at their respective MEC₁₀ concentrations was observed when compared to the growth control (GC). Although no changes were found in the total biofilm biomass, a significant 40% reduction in the metabolic activity of the AEP treated mature biofilm-attached *Candida* species after 24 h was observed compared to GC. Whereas, AET and AEE treated samples have shown an average of 20% to 30% metabolic activity reduction compared to the AEP treatment ($P < 0.01$). The reduction of the 50% viable biofilm-attached *Candida* cells was also observed compared to the GC after 24 h of the treatment. The killing activity of the AEE treatments was found to be the lowest compared to the AEP treatments ($P < 0.01$). Total protein (reflecting the number of cells, TP) did not change significantly during the treatments, but a significant 60% reduction of the ATP/TP ratio was found in the case of the AEP treated mature biofilm-attached *Candida* samples when compared to the GC ($P < 0.01$). An average of $28.57 \pm 5.26\%$ and $15.34 \pm 4.64\%$ reduction in the ATP/TP ratio for the AET and AEE were recorded, resulting in the AEE treatments to be the least effective among the treatment groups.

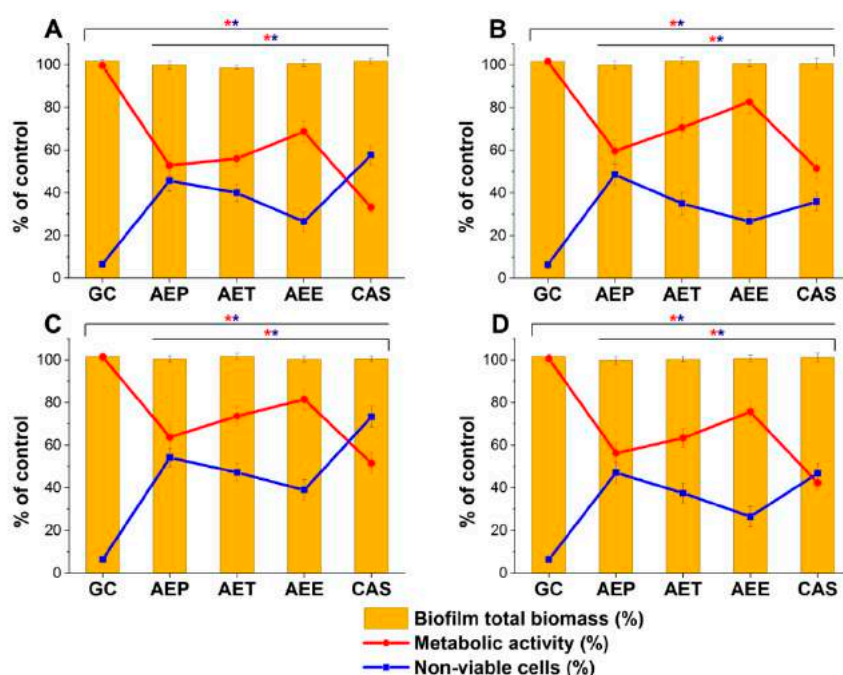


Figure 17. Effects of AEP, AET and AEE after 24 h of treatments at their respective MEC₁₀ concentrations on the metabolic activity, amount of biofilm biomass, and viability of *C. albicans* (A), *C. tropicalis* (B), *C. dubliniensis* (C) and *C. krusei* (D) cell populations (mean \pm SD, $n = 6$ independent experiments each with three technical replicates, data were compared with untreated controls (GC) and with caspofungin (CAS)-treated positive controls. The red (*) and blue (*) asterisks represent a significance value of $P < 0.01$ for the metabolic activity and viability measurements, respectively.

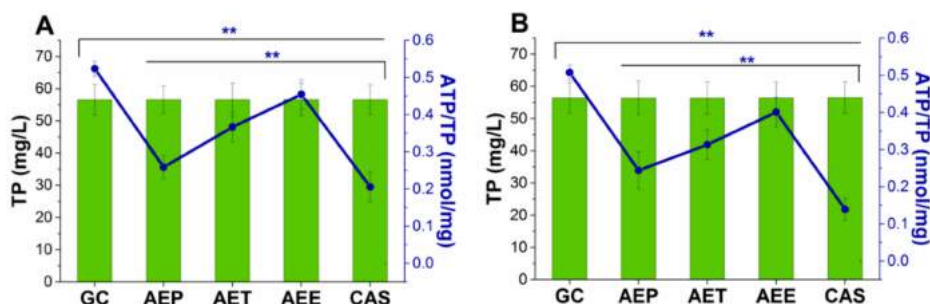


Figure 18. Cont.

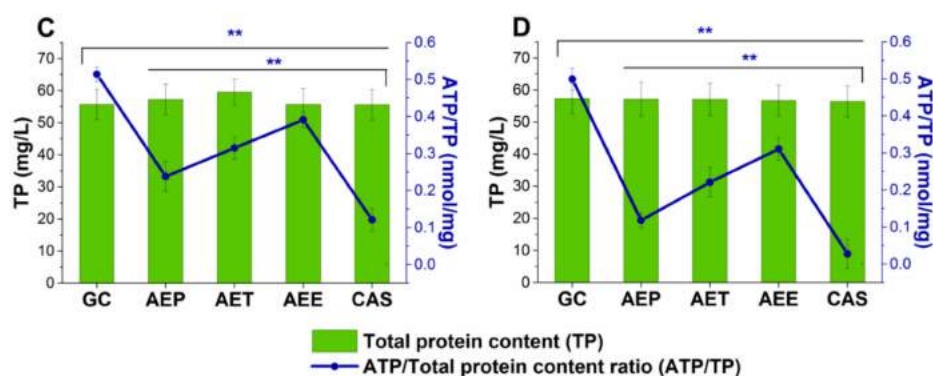


Figure 18. Effects of AEP, AET and AEE after 24 h of treatments at their respective MEC₁₀ concentrations on the ATP and the total protein content (TP) of *C. albicans* (A), *C. tropicalis* (B), *C. dubliniensis* (C) and *C. krusei* (D) cell populations in the mature biofilms (mean \pm SD, $n = 6$ independent experiments each with three technical replicates, data were compared with untreated controls (GC) and with casposungin (CAS)-treated positive controls. The blue double asterisks (**) represent a significance value of $P < 0.01$ for the intracellular ATP/Total protein content (ATP/TP), respectively.

3. Discussion

The effects of three different formulations of *Artemisia annua* EO on mature *Candida* biofilms and antimicrobial activity have been studied. We succeeded in formulating stable Pickering nanoemulsions using surface-modified silica nanoparticles, and the formulation with desired droplet size (160 nm) was examined for its antimicrobial properties. *Artemisia annua* EO Pickering nanoemulsions (AEP) were stable for three months, with a higher effectiveness when compared to AET and AEE.

Based on our analyses, AEP has shown stronger antimicrobial activity at lower concentrations (MICs) compared to that of AET and AEE. Several experiments have been conducted previously; however, the mechanism of action at the sub-inhibitory concentrations has not been studied at all [6,12,13]. Our data suggest an effective microbial killing activity of AEP on selected bacteria and fungi. Previous studies believe that the killing action of the essential oils happens due to the leakage in the cells' cytoplasmic membrane and induction of oxidative stress [38–41]. We have introduced several staining methods to visualize and to understand the mechanism of action of the AEP, AET and AEE. The AEP was able to induce higher oxidative stress compared to AET and AEE followed by metabolic interference, cell wall disruption, ATP depletion and finally cell death in the case of planktonic bacterial and fungal cells as well as in mature biofilm-attached *Candida* cells at their respective sub-inhibitory concentrations.

The results obtained from model experiments have highlighted that the Pickering nanoemulsion of the AE oil is the most effective form for the intracellular delivery and for the transport of EO through biofilms when compared to AET and AEE. On the basis of our observations, it can be postulated that the difference in the antibacterial and antifungal activity against microbial cell may be explained by the different adsorption properties of the essential oil formulations [20,34]. Data for unilamellar liposomes as a cellular model support the phenomenon of adsorption of the Pickering emulsion droplets on the cell membrane that has been reported earlier [33]. It might happen that either the passive diffusion occurs due to higher local concentration gradient of the essential oil or fusion of the AEP droplets with the microbial cells allowing the intracellular delivery of the active components from the AEP. The static Franz diffusion experiments on agar gel membrane as a biofilm model showed that AEP has the best ability to deliver the EO through porous structure. The enhanced transportability of AEP must be related to the difference of the surface properties of AEP and AET since experiments were performed with droplets of similar sizes. Overall, our observations demonstrated that the AEP facilitates the *Artemisia* essential oil in penetrating through the biofilm and the cells, inducing oxidative

stress and disruption of the cell membrane integrity due to the high adsorption efficacy of Pickering nanoemulsion droplets.

4. Materials and Methods

4.1. Plant Collection and Extraction of *Artemisia* Essential Oil

The plant samples were collected in 2017 from Békés county, Orosháza-Nagyszénás, Hungary, from a local farm in the autumn and were dried in the dark, under moisture-free conditions for two months. The plant parts were ground to farinose form and were sieved down. The powdered form of the plant was stored in airtight containers for future use.

The extraction of the *Artemisia annua* L. (*A. annua*) essential oil was done by steam distillation method as described earlier [42]. Briefly, 500 mL of distilled water was added to 50 g dried powder of *A. annua*. The steam distillation was done for 30 min, and the reading in the graduated tube was recorded for the essential oil yield. The yield value was converted to the percentage (%) *w/w* of 1 g of the powdered plant's part.

4.2. GC-MS and GC-FID Studies

The *Artemisia* essential oil was diluted 1:100 in *n*-heptane and injected on the GC-MS and GC-FID systems. The separation and identification of volatile compounds was carried out by using GCMS-QP2020 instrument (Shimadzu, Duisburg, Germany) equipped with a split-splitless injector and an AOC-20i autosampler. For a satisfactory characterization of compounds, two different capillary columns were used. One was a low-polarity column, namely SLB-5ms 30 m × 0.25 mm *id* × 0.25 μm *d_f* (Merck Life Science, Rome, Italy), while the other with a medium polarity was a Supelcowax-10 30 m × 0.25 mm *id* × 0.25 μm *d_f* (Merck Life Science). Both columns operated under a programmed temperature: 50 °C to 280 °C at 3.0 °C/min. Injection volume was of 0.5 μL with a split ratio of 1:10. Helium was used as gas carrier at a constant linear velocity of 30 cm/s and an inlet pressure of 26.7 kPa. MS parameters were as follows: the mass range was 40–650 amu, the ion source temperature was 220 °C and the interface temperature was 250 °C. The GCMSsolution software (version 4.50 Shimadzu, Kyoto, Japan) was used for data collection and handling. Peak identification was carried out by using a double parameter: MS spectra similarity (over 85%) and a LRIs ±5 and ±10 linear retention index (LRI) tolerance window for the SLB-5ms and Supelcowax-10 column, respectively. In this respect, a homologous series C7-C30 *n*-alkanes (Merck Life Science) standard mixture in hexane (1000 g/mL) was used for LRIs calculation on SLB-5ms column, while a C4-C24 even carbon saturated FAMES (Merck Life Science, Rome, Italy) standard solution in hexane (1000 g/mL) on Supelcowax-10 column. For mass spectral identification, *FFNSC 3.01* (Shimadzu Europe, Duisburg, Germany) was mainly used.

The quantification of volatile compounds was carried out by using a GC-2010 Plus (Shimadzu, Kyoto, Japan) equipped a split-splitless injector (280 °C), an AOC-20i autosampler and an FID detector. The GC columns, temperature program, and carrier gas were the same as described for the GC-MS system, except the initial inlet pressure (99.5 kPa) (the average linear velocity was 30 cm/s). The FID temperature was set at 280 °C (sampling rate: 40 ms), while the gas flows were 40 mL/min for hydrogen, 30 mL/min for the make-up gas (nitrogen) and 400 mL/min for air. Data were collected and processed through the LabSolution software (version 5.92, Shimadzu).

4.3. Preparation and Characterization of Pickering Nanoemulsion

We synthesized surface-modified spherical silica nanoparticles (*d* = 20 nm) using the Stöber method [43] and used them as a stabilizing agent of Pickering nanoemulsions. For the stabilization of Pickering nanoemulsions, silica nanoparticles were synthesized as described previously [20]. The surface of hydrophilic silica nanoparticles was modified with propyltriethoxysilane (PTES Alfa Aesar, Haverhill, MA, USA, pur. 99%) with a theoretical surface coverage of 20%. The size distribution of nanoparticles was determined by dynamic light scattering measurements (DLS, Malvern Zetasizer

Nano S, Malvern Panalytical Ltd., Worcester, UK), the particles were suspended in ethanol or water. The following data and settings were used in DLS measurements: temperature 25 °C; disposable polycarbonate cuvette; autocorrelation function; count rate between 200–500 kcps; refractive index and absorption of silica of 1.57 and 0.001, respectively; refractive index of ethanol and water of 1.367 and 1.436, respectively; duration 60 s. Morphology was examined with transmission electron microscopy (TEM, JEM-1400, JEOL Ltd., Tokyo, Japan). The drop of the sample suspension (~1 µL) was drop cast onto 200 mesh copper grid coated with carbon film (EMR Carbon support grids, Micro to Nano Ltd., Haarlem, The Netherlands) and dried overnight in vacuum desiccators. The TEM images of surface modified silica nanoparticles can be seen in Supplementary Material (Figure S7).

For the Pickering emulsions (AEP), the concentration of nanoparticles was kept constant (1 mg/mL) and concentration of *Artemisia* essential oil (AE) was varied between 200 µg/mL and 3.5 mg/mL. The emulsification process was carried out in two steps. In the first step, the mixture was sonicated for 2 min (Bandelin Sonorex RK 52H, BANDELIN electronic GmbH & Co. KG, Berlin Germany). The second step was high shear emulsification, which was performed with an UltraTurrax (IKA Werke T-25 basic, IKA®-Werke GmbH & Co. KG, Germany) high shear homogenizer for 2 min at 13,500 rpm. Conventional emulsions, stabilized by Tween 80 surfactant (AET) (Acros Organics, Thermo Fisher Scientific, Waltham, MA, USA) and ethanolic solution (AEE) were also prepared to compare stability parameters, droplet sizes and microbiological properties with those of AEP. The concentration of Tween 80 surfactant was the same as nanoparticles, 1 mg/mL. The stability of emulsions was studied based on periodical droplet size determination using DLS measurements (Malvern Zetasizer Nano S, Malvern Panalytical Ltd., Worcester, UK). The emulsions were stored in airtight vials, covered with aluminum foil at room temperature (25 °C). We considered the emulsion to be stable when the droplet size did not change in time, creaming, phase separation, or sedimentation and aggregation of nanoparticles could not be observed.

4.4. In Vitro Diffusion Studies—Static Franz Diffusion Cell Method

We carried out the diffusion study with the same parameters as in the in vitro cellular experiments—30 °C/24 h for fungi and 37 °C/24 h for bacteria—to obtain data that could be used to compare with the antimicrobial activities. The examination of diffusion properties was performed in static vertical Franz diffusion cells (Hanson Microette Plus, Hanson Research 60-301-106, Hanson Research Corporation, Chatsworth CA, USA). All experiments were performed in triplicate. As a biofilm model membrane, we have used 2.1 mm thick 2 w/w% agar gel membranes with effective penetration area of 2.54 cm², with a pore size of 1.5–3 µm, as its tortuous pore structure can model the biofilm matrix [44,45]. The agar membrane was prepared as described previously [34]. The volume of the receiver chamber was 7 mL; the receiver solution was phosphate buffered saline (PBS). For PBS preparation the following salts were used: NaCl (high purity, VWR Chemicals Ltd., Debrecen Hungary), KCl (purity 99%–100.5%, VWR Chemicals Ltd., Debrecen Hungary), Na₂HPO₄·2H₂O (AnalaR NORMAPUR®, purity ≥99.0%, VWR Chemicals Ltd., Debrecen Hungary) and KH₂PO₄ (purity ≥99.0%, VWR Chemicals Ltd., Debrecen Hungary). The volume of emulsion or solution sample was placed in the donor chamber (600 µL), and the diffusion was examined for 24 h, the samples were collected at 15 min, 30 min, 1 h, 2 h, 3 h, 6 h and 24 h. The volume of the taken sample was replaced with fresh PBS buffer. The (AE) content was determined with UV-Vis spectroscopy (Jasco V-670 UV/VIS Spectrophotometer, ABL&E-JASCO Ltd., Budapest, Hungary). The absorption wavelength of *Artemisia* essential oil was 248 nm.

4.5. Interaction Study between the Cellular Model (Unilamellar Liposomes) and Different Formulations of AE

Unilamellar liposomes (ULs) were prepared from phosphatidylcholine (Phospholipon 90G, Phospholipid GmbH, Berlin, Germany) as described previously [20,46]. A 5 mL suspension of ULs was mixed with 3 mL Pickering nanoemulsion, conventional emulsion, or ethanolic solution, and the *Artemisia* essential concentration was 200 µg/mL for all examined formulations. In the first set

of experiments, the mixture was stirred at 600 rpm for 24 h at 37 °C, and 1 mL aliquots were taken after 1, 6, and 24 h. In the second set of experiments, the mixture was stirred at 600 rpm for 48 h at 30 °C, and 1 mL aliquots were taken after 1, 6, 24, 30 and 48 h. The samples were centrifuged at 3000 rpm and 20 °C for 5 min, and the ULs were collected and dissolved in absolute ethanol. The *Artemisia* EO content of samples was determined with UV/Vis Spectroscopy at 248 nm (Jasco V-550 UV/VIS Spectrophotometer; ABL&E-JASCO Ltd., Budapest, Hungary). For UV/Vis measurements, we prepared samples without *Artemisia* essential oil, i.e., ULs with silica nanoparticle suspension, Tween 80 solution, or ethanol were also mixed and centrifuged and were used as blanks.

4.6. Materials and Microorganisms Used for the Biological Experiments

Promega BacTiter-Glo microbial cell viability assay kit (Bio-Science, Budapest, Hungary), glass beads (Sigma-Aldrich Chemie GmbH, Steinheim, Germany, reference number: G-8772), sterile petri-dishes (Greiner Bio-One, Kremsmunster, Austria), sterile petri-dishes for the biofilm assays (Sarstedt AG & Co. KG, Numbrecht, Germany, reference number: 83.3900.500), 0.22 µm vacuum filters (Millipore, France), cell scraper (Sarstedt AG & Co. KG, Numbrecht, Germany), sterile microplates (Greiner Bio-One, Kremsmunster, Austria), sterile microplates for the biofilm assays (Sarstedt AG & Co. KG, Numbrecht, Germany, catalog number: 83.3924.500), 96-well optiplates (Perkin Elmer, Waltham, Massachusetts, USA), bovine serum albumin (BSA; Biosera, Nuaille, France), potassium phosphate monobasic, ethanol 96% (Et), methanol, peptone, yeast extract, agar-agar and Mueller-Hinton agar (for the maintenance of the tested bacteria's health, used throughout the experiments) (Reanal Labor, Budapest, Hungary), modified RPMI 1640 (contains 3.4 w/v% MOPS, 1.8 w/v% glucose and 0.002 w/v% adenine), menadione (ME) (Sigma Aldrich, Budapest, Hungary), disodium phosphate, dimethyl-sulfoxide (DMSO) from Chemolab Ltd. (Budapest, Hungary), sodium chloride (VWR International Ltd., Debrecen, Hungary), potassium chloride (Scharlau Chemie S.A, Barcelona, Spain), 3-(N-morpholino) propanesulfonic acid (MOPS) (Serva Electrophoresis GmbH, Heidelberg, Germany), Caspofungin (CAS) from Merck Sharp & Dohme Ltd., Netherlands, vancomycin (VAN) from Fresenius Kabi Ltd., (Budapest, Hungary), SYBR green I 10,000×, propidium iodide, dihydrorhodamine 123 (DHR 123), 2',7'-dichlorofluorescein diacetate (DCFDA) and dihydroethidine (DHE) were purchased from Sigma Aldrich (Budapest, Hungary) and from the above-mentioned sources. All other chemicals applied for the study were of analytical or spectroscopic grade. For fungi, we used an in-house nutrient medium containing 1 w/v% yeast extract, 2 w/v% peptone, 2 w/v% glucose and 2 w/v% agar-agar (for the colony-forming unit assay in the petri-dishes) [47], while phosphate-buffered saline (PBS, pH 7.4) was obtained from Life Technologies Ltd., Budapest, Hungary. Highly purified water (<1.0 µS) was applied throughout the studies.

Escherichia coli (*E. coli*) PMC 201, *Pseudomonas aeruginosa* (*P. aeruginosa*) PMC 103, *Bacillus subtilis* (*B. subtilis*) SZMC 0209, *Staphylococcus aureus* (*S. aureus*) ATCC 29213, *Streptococcus pyogenes* (*S. pyogenes*) SZMC 0119, *Schizosaccharomyces pombe* (*S. pombe*) ATCC 38366, *Candida albicans* (*C. albicans*) SZMC 1372, *Candida tropicalis* (*C. tropicalis*) SZMC 1368, *Candida dubliniensis* (*C. dubliniensis*) SZMC 1470 and *Candida krusei* (*C. krusei*) SZMC 0779 were obtained from Szeged Microbial Collection, Department of Microbiology, University of Szeged, Hungary (SZMC) and Department of General and Environmental Microbiology, Institute of Biology, University of Pecs, Hungary (PMC).

4.7. Determination of Minimum Inhibitory Concentration (MIC₉₀)

We used a previously published protocol [4,20] for measuring the antibacterial activity separately on *E. coli*, *P. aeruginosa*, *B. subtilis*, *S. aureus*, and *S. pyogenes* and antifungal activity against *S. pombe*, and *Candida* species. In brief, for the antibacterial activity determination, a bacterial population of ~10⁵ CFU/mL was inoculated in modified RPMI 1640 medium followed by incubation for 16 h at 35 ± 2 °C Thermo Scientific Heraeus B12 microbiological incubator (Auro-Science Consulting Kft., Budapest, Hungary) with AEP, AET, AEE and VAN over a wide range of concentrations

(26.2–0.01 $\mu\text{g/mL}$). The absorbance was measured by a Thermo Scientific Multiskan EX 355 microplate reader (InterLabSystems, Budapest, Hungary) at 600 nm.

The antifungal activity against *S. pombe* and *Candida* species were also performed according to our previously published method [20]. Briefly, $\sim 10^3$ cells/mL were incubated with AEP, AEE, AET and CAS at a wide concentration range (26.2–0.01 $\mu\text{g/mL}$) in modified RPMI 1640 medium for 48 h at 30 °C (Sanyo MIR-154 microbiological incubator, Auro-Science Consulting Kft., Budapest, Hungary). The absorbance values obtained by the microplate reader at 595 nm were converted to percentages and were compared to the growth control (100%). The data were fitted by a non-linear dose–response curve fitting method to estimate the dose producing $\geq 90\%$ growth inhibition (MIC_{90}). All measurements were performed by applying three technical replicates in six independent experiments. VAN and CAS were used as the standard antibacterial and antifungal drug controls, respectively throughout the experiments.

4.8. Determination of Minimum Effective Concentration (MEC_{10})

The MEC_{10} concentration was obtained according to our previously published protocol [4]. In brief, a wide concentration range (105–0.2 $\mu\text{g/mL}$) of AEP, AET and AEE was used to treat mid-log phased $\sim 10^5$ cells/mL in modified RPMI 1640 medium for an hour, incubated at 35 ± 2 °C and 30 °C for the bacteria and for the fungi, respectively, in an orbital incubator (Sanyo MIR-220RU orbital incubator, Auro-Science Consulting Kft., Budapest, Hungary). Inoculated growth medium without any treatment was considered as growth control. For the colony-forming unit (CFU/mL) quantification, 1 mL of the treated and untreated samples were pipetted out and 10^5 times dilutions were prepared followed by spreading 50 μL of the test samples onto 20 mL respective nutrient-rich agar media containing petri-dishes and were incubated for 24 h at 35 ± 2 °C and 30 °C in the case of bacteria and fungi, respectively. The colony formation data (CFU/mL) were converted to percentages and the data were fitted using a non-linear dose–response curve fitting method to evaluate the drug concentrations producing approximately 90% microbial cell population growth (MEC_{10}) when compared to the untreated microbial cell populations after one hour of treatment. Three technical replicates in six independent experiments were performed in all the measurements. VAN and CAS were used as the standard antibacterial and antifungal drug controls throughout the experiments, respectively.

4.9. Quantification of Microbial Oxidative Stress Production in the Planktonic Cells

4.9.1. Combined ROS Generation Measurement

For the quantification of the combined (not specified separately) reactive oxygen species (ROS) generation, we have followed our previous protocol [4,20]. In brief, for the ROS measurements, mid-log phased $\sim 10^5$ cells/mL were collected and centrifuged at 1500 g (Hettich Rotina 420R bench-top centrifuge, Auro-Science Consulting Ltd., Budapest, Hungary) for 5 min and were re-suspended in PBS. The staining of the cells was done with 2',7'-dichlorofluorescein diacetate (DCFDA) stock solution (20 mM in DMSO) with a final concentration of 25 μM in each well, followed by incubation at 35 ± 2 °C for the bacteria and 30 °C for the fungi in the dark with mild rotation in a test tube rotator (Cole-Parmer Roto-Torque Variable Speed Rotator, InterLabSystems, Budapest, Hungary) for 30 min. The cells were re-suspended in modified RPMI 1640 medium after centrifugation followed by treatment with AEP, AET and AEE at their respective MEC_{10} concentrations for one hour. The fluorescence data were recorded by a fluorescence spectrophotometer/microplate reader (Hitachi F-7000 fluorescent spectrophotometer, Auro-Science Consulting Ltd., Budapest, Hungary) at $\text{Ex/Em} = 485/535$ nm in 96-well optiplates. VAN and CAS were used as the standard antimicrobial controls in the case of bacteria and fungi. ME treated samples were considered as the positive controls. The percentage increase (%) in the ROS generation was measured by comparing the signals obtained from the growth controls (GC). Six independent experiments with three technical replicates in each treatment were performed.

4.9.2. Detection of Peroxide (O_2^{2-}) and Superoxide Anion ($O_2^{\bullet-}$) Generation

Our previously described protocol was adapted for the peroxide and the superoxide anion radicals' measurements [20,47]. AEP, AET and AEE at their respective MEC_{10} concentrations were used to treat the mid-log phased ($\sim 10^5$ cells/mL) microbial cell suspensions followed by incubation in an orbital incubator at 35 ± 2 °C and 30 °C for the bacteria and fungi in modified RPMI 1640 medium for an hour, respectively. VAN and CAS were used as the standard antimicrobial controls in the case of bacteria and fungi. Menadione (ME) (0.5 mmol/L, end concentration) was used as the positive control throughout the experiments. The cells were centrifuged at 1500 g for 5 min at room temperature and were re-suspended in PBS at the original volume of the samples. DHR 123 (10 μ mol/L end concentration) and DHE (15 μ mol/L) were used to stain the microbial cell samples for the peroxide and superoxide determination and were further incubated at 35 ± 2 °C for the bacteria and 30 °C for the fungi in the dark with mild shaking. The samples were centrifuged again and were re-suspended in PBS, followed by even sample distribution into the 96-well microplates. For the peroxide measurements, the fluorescence was measured at Ex/Em: 500/521 nm, whereas, Ex/Em: 473/521 nm was used to detect the superoxide generation by a fluorescence spectrophotometer/microplate reader in 96-well optiplates. The percentage increase (%) in the oxidative stress was measured by comparing the signals obtained from the growth controls (GC). Six independent experiments were performed with three technical replicates for each treatment.

4.10. Microbial Cytotoxicity and Viability Kinetic Assays of Planktonics

The cytotoxicity and the viability of the microbial cells were performed with our previously published method [4,20]. Briefly, AEP, AET, AEE, VAN (bacteria) and CAS (fungi) at their respective MEC_{10} concentrations were used to treat the mid-log phased microbial cell populations ($\sim 10^5$ cells/mL) in modified RPMI 1640 medium followed by incubation in an orbital shaker-incubator at 35 ± 2 °C and 30 °C for the bacteria and fungi in modified RPMI 1640 medium. After that, the multi-parametric cytotoxicity and viability kinetic studies were performed (Sections 4.10.1–4.10.4.).

4.10.1. Determination of the Colony-Forming Unit (CFU/mL)

We followed our previously published protocol for determining the changes in the colony formation (CFU/mL) [4]. Briefly, 1 mL of the treated and the untreated samples were pipetted at the 0, 2, 6, 8, 16 and 24 h for the bacteria, and 0, 6, 12, 30, 36 and 48 h for the fungi, and were diluted 10^5 times followed by spreading 50 μ L onto 20 mL nutrient agar media with a cell spreader and incubation at 35 ± 2 °C (bacteria) and 30 °C (fungi) for 24 h. VAN and CAS were used as the reference controls for the bacteria and fungi. Controls prior to the treatment at 0 h were considered to be 100% and sigmoidal time interval vs. % CFU decrease was established for each test samples. Three technical replicates for each treatment in six independent experiments were performed.

4.10.2. Quantification of the Planktonics' Intracellular ATP and Total Protein Contents

The instructions provided by the manufacturer was followed for the intracellular ATP measurement of the microbial planktonics. In brief, 1 mL of both treated and untreated aliquots were sampled at time intervals of 0, 2, 6, 8, 16 and 24 h (for bacteria), and 0, 6, 12, 30, 36 and 48 h (for fungi) and were centrifuged at 1000 g for 5 min. The pellets were washed and were re-suspended in 1 mL PBS. Equal volume of the freshly prepared BacTiter-Glo reagent was pipetted to 100 μ L of PBS containing the planktonic cells in 96-well optiplates. The microplates were shaken in the dark at 4 °C for 15 min on an orbital shaker and the luminescence was measured using a Perkin Elmer EnSpire Multimode plate reader (Perkin Elmer, Waltham, MA, USA). All the measurements were calculated in terms of nmol/L from an ATP standard calibration curve and were converted to intracellular ATP over total protein content ratio (nmol/mg) followed by comparison with the controls prior to the treatment at 0 h. The PBS, VAN (for bacteria) and CAS (for fungi) were considered as the blank and standard

antimicrobial controls throughout the experiments. Three technical replicates were performed for each treatment in six independent experiments [48].

For the total protein content of the planktonics, we adapted the Bradford protein assay method [49]. One mL of AEP, AET and AEE treated samples were collected at time intervals of 0, 2, 6, 8, 16 and 24 h (for bacteria), and 0, 6, 12, 30, 36 and 48 h (for fungi) and were centrifuged at 1000 g for 5 min. The pellets were washed and were re-suspended in 1 mL NaOH (1 M) containing 100 mg of glass beads (425–600 µm) [50,51]. The collected samples were stabilized on ice for 5 min followed by 5 min vortexing with a mechanical cell disruptor (Scientific Industries SI analog cell disruptor (InterLabsystems, Budapest, Hungary), consecutively. The cycle was repeated three times and then the samples were centrifuged at 20,000 g for 10 min at 4 °C (Heraeus Multifuge 3 S-R bench-top centrifuge, Kendo Laboratory products, Osterode, Germany). The supernatants' microbial cell lysates were collected in separate 1.5 mL centrifuge tubes. Two hundred microliters of the freshly prepared Bradford reagent was added to a new 96-well general microplate containing 20 µL of the test samples lysates. The absorbance was measured at 595 nm by a multimode plate reader. NaOH, VAN and CAS treated samples were used as the blank, standard antibacterial and antifungal controls, respectively. Three technical replicates for each treatment in six independent experiments were performed. All the measurements were calculated in terms of mg/L from a BSA standard calibration curve and were compared to the 0 h samples [48].

4.10.3. Quantification of the Planktonics' Metabolic Activity

For the metabolic activity measurements, AEP, AET and AEE treated samples were pipetted at time intervals of 0, 2, 6, 8, 16 and 24 h (for bacteria), and 0, 6, 12, 30, 36 and 48 h (for fungi) and were centrifuged at 1000 g for 5 min. The pellets were washed and were re-suspended in 200 µL PBS containing resazurin (12.5 µmol/L) followed by 40 min of incubation at 30 °C. The fluorescence was measured with a fluorescence spectrophotometer/microplate reader in 96-well optiplates at an Ex/Em: 560/590 nm wavelengths. The percentage (%) metabolic activity was estimated based on the fluorescence intensities of samples prior to the application of the treatment at 0 h which were considered to be 100%. A sigmoidal time interval vs % metabolic activity was established for each test samples. The PBS, VAN (for bacteria) and CAS (for fungi) were considered as the blank and standard antimicrobial controls throughout the experiments. Three technical replicates for each treatment in six independent experiments were performed [4].

4.10.4. Live/Dead Discrimination of the Planktonic Microbial Cells

Briefly, both untreated, AEP, AET and AEE treated samples were taken at 0, 2, 6, 8, 16 and 24 h (for bacteria), and 0, 6, 12, 30, 36 and 48 h (for fungi) following centrifugation at 1000 g for 5 min, washed and re-suspended in PBS (100 µL/mL). Freshly prepared 100 µL of the SYBR Green I/PI working solutions [4] were added to the samples. For 15 min, the plates were incubated in the dark with mild shaking at room temperature. Fluorescence intensities of the SYBR Green I and PI were measured in 96-well optiplates at an Ex/Em: 490/525 nm and 530/620 nm wavelengths, respectively, by a fluorescence spectrophotometer/microplate reader. The green to red fluorescence ratio for each sample and each dose was established and the % of the dead (non-viable) microbial cells with the response to the applied dose was plotted against the applied test compounds using our previous formula [20]. The VAN and CAS were considered as the standard antimicrobial controls, whereas, PBS was used as the blank. All the treatments were done in triplicates and six independent experiments were performed.

4.11. Determination of the Effects on Preformed Mature *Candida* Biofilms

The effects (Sections 4.10.1–4.10.4) on the mature *Candida* species biofilms and the treatment conditions were adapted from our previously published work [4]. Briefly, 200 µL of 24 h-old late-log phased ($\sim 10^6$ cells/mL) *C. albicans* and non-*albicans* species in modified RPMI 1640 medium were used to culture biofilms in the microplates prior to the treatments for 24 h at 30 °C. The microplates were washed in PBS followed by re-incubation in 200 µL modified RPMI 1640 medium containing AEP, AET

and AEE at MEC₁₀ concentrations (µg/mL) for further 24 h at 30 °C. Modified RPMI 1640 medium, untreated growth sample and CAS treated samples were considered as the blank, growth control (GC) and standard antimicrobial control (CAS), respectively. The biofilm degradation percentage (%) was measured based on the comparison of the values with those of the GC. All the treatments were performed in three technical replicates in six independent experiments.

4.11.1. Evaluation of the Total Fungal Biomass

The change in the biofilm biomass was determined by our previously published crystal violet assay [4]. After 24 h of incubation, the supernatant containing the test samples was pipetted out and the wells were washed with PBS. Two hundred microliters of methanol was added to each well in order to fix the biofilms. The supernatant was removed and 200 µL of 0.1% crystal violet in absolute ethanol was pipetted into each well. The crystal violet solution was pipetted out and 200 µL of acetic acid (33% v/v in double distilled water working stock) was pipetted to the crystal violet pre-stained biofilms to release the bound stains. Subsequently, 20 min later, the acetic acid-dissolved dye from the stained biofilms was pipetted into the wells of general microplates. The absorbance was measured at 590 nm by a multimode plate reader. The CAS was considered as the standard antifungal control. The change in the percentage (%) biofilm biomass was evaluated from the growth control (GC) values which were taken as 100% fungal biofilm biomass. Three technical replicates in each treatment for six independent experiments were considered.

4.11.2. Metabolic Activity in the Biofilms

A resazurin-derived fluorescent technique was adapted from our previously published protocol to determine the metabolic activity in the fungal biofilms [4]. Briefly, after 24 h of the treatment with AEP, AET and AEE at their respective MEC₁₀ concentrations, all of the supernatants were removed followed by rinsing the wells with the PBS. Two hundred microliters of sterile PBS containing resazurin (12.5 µmol/mL) was pipetted into the wells and was incubated at 30 °C for 40 min. The fluorescence intensities were recorded at an Ex/Em: 560/590 nm wavelengths, respectively, by a fluorescent spectrophotometer/microplate reader. The percentage (%) metabolic activity measurements were evaluated based on the fluorescence values recorded by the growth control (GC), which was considered as 100%. The PBS was taken as the blank throughout the measurements. Six independent experiments were performed with three technical replicates for each treatment.

4.11.3. Viability Assay of the Biofilms

For the discrimination of the live/dead fungal cells in the biofilms, we have followed a method previously published [4,17]. After 24 h of treatment with AEP, AET and AEE, at their respective MEC₁₀ concentrations in modified RPMI 1640 medium, the planktonic cells were pipetted out, followed by rinsing and filling of the biofilm-attached wells with 100 µL PBS. One hundred microliters of SYBR Green I/PI working solutions [17] were pipetted into the wells of the microplate. The plates were incubated at room temperature for 15 min in the dark with mild shaking. A fluorescence spectrophotometer/microplate reader was used to measure the fluorescent intensities at an Ex/Em: 490/525 nm and 530/620 nm for SYBR Green I and PI, respectively, into 96-well optiplates. The green to red fluorescence ratio for each sample and each dose was established, and the % of the dead microbial cells with the response to the applied dose was plotted against the applied test compounds using our previous formula [17]. All treatments were done using three technical replicates in six independent experiments.

4.11.4. Determination of the *Candida* Biofilms' Intracellular ATP and Total Protein Contents

The instructions provided by the company was followed for the intracellular ATP measurement of the *Candida* mature biofilms. In brief, after 24 h of the treatment with AEP, AET and AEE, the planktonic cells were pipetted out, followed by rinsing the biofilm and pipetting 100 µL of PBS into every well

of the microplate. An equal volume of the freshly prepared BacTiter-Glo reagent was pipetted into the wells containing the biofilms submerged in the PBS. The microplates were shaken in the dark at 4 °C for 15 min on an orbital shaker. The content of the microplates was transferred to 96-well optiplates and the luminescence was measured using a multimode plate reader. All measurements were quantified by using an ATP standard calibration curve and were converted to intracellular ATP over total protein content ratio (nmol/mg) followed by comparison with the growth control (GC). The PBS and CAS were used as the blank and the standard antifungal controls, respectively. Three technical replicates for each treatment in six independent experiments were performed [49].

For the measurement of the total protein content in the biofilms, parallel to the microplate cultures the biofilms were produced and treated in 35 mm diameter sterile petri dishes with identical surface properties to those of the microplates. We have adapted the Bradford protein assay method [49]. Briefly, after 24-hour treatment of the mature biofilms with AEP, AET and AEE, the planktonic cells were pipetted out and biofilms were rinsed with PBS. The biofilms were scraped out from the petri dishes using a cell scraper into sterile 1.5 mL centrifuge tubes containing 1 mL NaOH (1 M) and 100 mg of glass beads (425–600 µm). The collected samples were stabilized on ice for 5 min, followed by 5 min vortexing, consecutively. The cycle was repeated three times and then the samples were centrifuged at 20,000 g for 10 min at 4 °C. The supernatants' fungal cell lysates were pipetted out and were diluted in NaOH (1 M) up to the initial volume used for the biofilm growth. Two hundred microliters of the homemade freshly prepared Bradford reagent were added to a new 96-well general microplate containing 20 µL of the test sample lysates. The absorbance was measured at 595 nm by a multimode plate reader. All the measurements were calculated in terms of mg/L from a BSA standard calibration curve. Total protein contents were referred to the surface area of the microplates in order to obtain the valid ATP/TP values. The NaOH and CAS treated samples were used as the blank and the standard antifungal controls, respectively. Three technical replicates for each treatment in six independent experiments were performed. All the measurements were calculated in terms of mg/L from a BSA standard calibration curve and were compared to the growth control (GC).

4.12. Statistical Analyses

All data are given as mean ± SD. Graphs and statistical analyses were conducted using OriginPro 2016 (OriginLab Corp., Northampton, MA, USA). All experiments were performed independently six times in triplicates and data were analyzed by one-way ANOVA test. *P*-values of <0.05 were considered statistically significant. The minimum inhibitory concentration (MIC₉₀) and the minimum effective concentration (MEC₁₀) were calculated using a non-linear dose–response curve function as follows:

$$y = A_1 + \frac{A_2 - A_1}{1 + 10^{(LOG_x 0 - x)p}} \quad (1)$$

where A_1 , A_2 , $LOG_x 0$, and p are the bottom asymptote, top asymptote, center, and hill slope of the curve have been considered.

Supplementary Materials: The following are available online, Composition of the *Artemisia annua* L. essential oil analyzed by GC-MS and GC-FID instruments (Supplementary Table S1 and Figures S1–S6). TEM images of surface-modified silica nanoparticles (SNPs), results can be seen in Supplementary Figure S7.

Author Contributions: Conceptualization T.K., and A.S.; methodology S.D., B.V.-H., T.B., G.H., T.K. and A.S.; G.C. analysis G.M., L.M.; software, S.D.; formal analysis, S.D. and B.V.-H.; investigation, S.D. and B.V.-H.; resources, A.S.; data curation, S.D., B.V.-H.; writing—original draft preparation, S.D. and B.V.-H.; writing—review and editing, T.K. and A.S.; visualization, S.D. and B.V.-H.; supervision, T.K., and A.S.; funding acquisition A.S. and T.K. All authors have read and agreed to the published version of the manuscript.

Funding: The present work was funded by the University of Pécs, Medical School grant (KA-2018-17), and was also supported by EFOP 3.6.1-16-2016-00004 project (Comprehensive Development for Implementing Smart Specialization Strategies), University of Pécs. Transmission electron microscopy study was performed using JEOL-1400 TEM electron microscope that was funded by the grant GINOP-2.3.3-15-2016-0002 (New generation electron microscope: 3D ultrastructure).

Acknowledgments: We express our gratitude and many thanks to Mr. Bálint Fekete for his kind supply of *Artemisia annua* L. cultivated at his local farm in Békés county, Orosháza-Nagyszénás, Hungary. The authors gratefully acknowledge Shimadzu Corporation and Merck Life Science for their continuous support.

Conflicts of Interest: The authors declare no conflict of interest.

References

1. Bilia, A.R.; Santomauro, F.; Sacco, C.; Bergonzi, M.C.; Donato, R. Essential Oil of *Artemisia annua* L.: An Extraordinary Component with Numerous Antimicrobial Properties. *Evid. Based Complement. Alternat. Med.* **2014**, *2014*, 1–7.
2. Čavar, S.; Maksimović, M.; Vidic, D.; Parić, A. Chemical composition and antioxidant and antimicrobial activity of essential oil of *Artemisia annua* L. from Bosnia. *Ind. Crops Prod.* **2012**, *37*, 479–485. [[CrossRef](#)]
3. Dib, I.; Angenot, L.; Mihamou, A.; Ziyat, A.; Tits, M. *Artemisia campestris* L.: Ethnomedicinal, phytochemical and pharmacological review. *J. Herb. Med.* **2017**, *7*, 1–10. [[CrossRef](#)]
4. Das, S.; Czuni, L.; Báló, V.; Papp, G.; Gazdag, Z.; Papp, N.; Kőszegi, T. Cytotoxic Action of Artemisinin and Scopoletin on Planktonic Forms and on Biofilms of *Candida* Species. *Molecules* **2020**, *25*, 476. [[CrossRef](#)]
5. Galal, A.M.; Ross, S.A.; Jacob, M.; ElSohly, M.A. Antifungal Activity of Artemisinin Derivatives. *J. Nat. Prod.* **2005**, *68*, 1274–1276. [[CrossRef](#)]
6. Efferth, T. From ancient herb to modern drug: *Artemisia annua* and artemisinin for cancer therapy. *Semin. Cancer Biol.* **2017**, *46*, 65–83. [[CrossRef](#)]
7. Gnonlonfin, G.J.B.; Sanni, A.; Brimer, L. Review Scopoletin—A Coumarin Phytoalexin with Medicinal Properties. *Crit. Rev. Plant Sci.* **2012**, *31*, 47–56. [[CrossRef](#)]
8. De Cremer, K.; Lanckacker, E.; Cools, T.L.; Bax, M.; De Brucker, K.; Cos, P.; Cammue, B.P.A.; Thevissen, K. Artemisinins, New Miconazole Potentiators Resulting in Increased Activity against *Candida albicans* Biofilms. *Antimicrob. Agents Chemother.* **2015**, *59*, 421–426. [[CrossRef](#)]
9. Ham, J.R.; Lee, H.-I.; Choi, R.-Y.; Sim, M.-O.; Choi, M.-S.; Kwon, E.-Y.; Yun, K.W.; Kim, M.-J.; Lee, M.-K. Anti-obesity and anti-hepatosteatosis effects of dietary scopoletin in high-fat diet fed mice. *J. Funct. Foods* **2016**, *25*, 433–446. [[CrossRef](#)]
10. Loewenberg, J.R. Observations on scopoletin and scopolin metabolism. *Phytochemistry* **1970**, *9*, 361–366. [[CrossRef](#)]
11. Héthelyi, E.B.; Cseko, I.B.; Grósz, M.; Márk, G.; Palinkás, J.J. Chemical Composition of the *Artemisia annua* Essential Oils from Hungary. *J. Essent. Oil Res.* **1995**, *7*, 45–48. [[CrossRef](#)]
12. Ho, W.E.; Peh, H.Y.; Chan, T.K.; Wong, W.S.F. Artemisinins: Pharmacological actions beyond anti-malarial. *Pharmacol. Ther.* **2014**, *142*, 126–139. [[CrossRef](#)] [[PubMed](#)]
13. Radulović, N.S.; Randjelović, P.J.; Stojanović, N.M.; Blagojević, P.D.; Stojanović-Radić, Z.Z.; Ilić, I.R.; Djordjević, V.B. Toxic essential oils. Part II: Chemical, toxicological, pharmacological and microbiological profiles of *Artemisia annua* L. volatiles. *Food Chem. Toxicol.* **2013**, *58*, 37–49. [[CrossRef](#)]
14. Wan, X.L.; Niu, Y.; Zheng, X.C.; Huang, Q.; Su, W.P.; Zhang, J.F.; Zhang, L.L.; Wang, T. Antioxidant capacities of *Artemisia annua* L. leaves and enzymatically treated *Artemisia annua* L. in vitro and in broilers. *Anim. Feed Sci. Technol.* **2016**, *221*, 27–34. [[CrossRef](#)]
15. Bouyahya, A.; Abrini, J.; Dakka, N.; Bakri, Y. Essential oils of *Origanum compactum* increase membrane permeability, disturb cell membrane integrity, and suppress quorum-sensing phenotype in bacteria. *J. Pharm. Anal.* **2019**, *9*, 301–311. [[CrossRef](#)]
16. Donsì, F.; Ferrari, G. Essential oil nanoemulsions as antimicrobial agents in food. *J. Biotechnol.* **2016**, *233*, 106–120. [[CrossRef](#)]
17. Das, S.; Gazdag, Z.; Szente, L.; Meggyes, M.; Horváth, G.; Lemli, B.; Kunsági-Máté, S.; Kuzma, M.; Kőszegi, T. Antioxidant and antimicrobial properties of randomly methylated β cyclodextrin—captured essential oils. *Food Chem.* **2019**, *278*, 305–313. [[CrossRef](#)]
18. Dhifi, W.; Bellili, S.; Jazi, S.; Bahloul, N.; Mnif, W. Essential Oils' Chemical Characterization and Investigation of Some Biological Activities: A Critical Review. *Medicines* **2016**, *3*, 25. [[CrossRef](#)]
19. Donato, R.; Santomauro, F.; Bilia, A.R.; Flamini, G.; Sacco, C. Antibacterial activity of Tuscan *Artemisia annua* essential oil and its major components against some foodborne pathogens. *LWT Food Sci. Technol.* **2015**, *64*, 1251–1254. [[CrossRef](#)]

20. Das, S.; Horváth, B.; Šafranko, S.; Jokić, S.; Széchenyi, A.; Kőszegi, T. Antimicrobial Activity of Chamomile Essential Oil: Effect of Different Formulations. *Molecules* **2019**, *24*, 4321. [[CrossRef](#)]
21. Pina-Barrera, A.M.; Alvarez-Roman, R.; Baez-Gonzalez, J.G.; Amaya-Guerra, C.A.; Rivas-Morales, C.; Gallardo-Rivera, C.T.; Galindo-Rodriguez, S.A. Application of a multisystem coating based on polymeric nanocapsules containing essential oil of *Thymus vulgaris* L. to increase the shelf life of table grapes (*Vitis vinifera* L.). *IEEE Trans. NanoBioscience* **2019**, *18*, 549–557. [[CrossRef](#)]
22. Manion, C.R.; Widder, R.M. Essentials of essential oils. *Am. J. Health. Syst. Pharm.* **2017**, *74*, e153–e162. [[CrossRef](#)]
23. Omonijo, F.A.; Ni, L.; Gong, J.; Wang, Q.; Lahaye, L.; Yang, C. Essential oils as alternatives to antibiotics in swine production. *Anim. Nutr.* **2018**, *4*, 126–136. [[CrossRef](#)]
24. Abarca, R.L.; Rodríguez, F.J.; Guarda, A.; Galotto, M.J.; Bruna, J.E. Characterization of beta-cyclodextrin inclusion complexes containing an essential oil component. *Food Chem.* **2016**, *196*, 968–975. [[CrossRef](#)]
25. Wang, T.; Li, B.; Si, H.; Lin, L.; Chen, L. Release characteristics and antibacterial activity of solid state eugenol/ β -cyclodextrin inclusion complex. *J. Incl. Phenom. Macrocycl. Chem.* **2011**, *71*, 207–213. [[CrossRef](#)]
26. Alizadeh Behbahani, B.; Tabatabaei Yazdi, F.; Vasiee, A.; Mortazavi, S.A. Oliveria decumbens essential oil: Chemical compositions and antimicrobial activity against the growth of some clinical and standard strains causing infection. *Microb. Pathog.* **2018**, *114*, 449–452. [[CrossRef](#)]
27. Tang, X.; Shao, Y.-L.; Tang, Y.-J.; Zhou, W.-W. Antifungal Activity of Essential Oil Compounds (Geraniol and Citral) and Inhibitory Mechanisms on Grain Pathogens (*Aspergillus flavus* and *Aspergillus ochraceus*). *Mol. J. Synth. Chem. Nat. Prod. Chem.* **2018**, *23*, 2108. [[CrossRef](#)]
28. Alastruey-Izquierdo, A.; Gomez-Lopez, A.; Arendrup, M.C.; Lass-Flörl, C.; Hope, W.W.; Perlin, D.S.; Rodriguez-Tudela, J.L.; Cuenca-Estrella, M. Comparison of Dimethyl Sulfoxide and Water as Solvents for Echinocandin Susceptibility Testing by the EUCAST Methodology. *J. Clin. Microbiol.* **2012**, *50*, 2509–2512. [[CrossRef](#)]
29. Inouye, S.; Tsuruoka, T.; Uchida, K.; Yamaguchi, H. Effect of Sealing and Tween 80 on the Antifungal Susceptibility Testing of Essential Oils. *Microbiol. Immunol.* **2001**, *45*, 201–208. [[CrossRef](#)]
30. Memar, M.Y.; Ghotaslou, R.; Samiei, M.; Adibkia, K. Antimicrobial use of reactive oxygen therapy: Current insights. *Infect. Drug Resist.* **2018**, *11*, 567–576. [[CrossRef](#)]
31. Dohare, S.; Dubey, S.D.; Kalia, M.; Verma, P.; Pandey, H.; Singh, K.; Agarwal, V. Anti-biofilm activity of *Eucalyptus globulus* oil encapsulated silica nanoparticles against *E. coli* biofilm. *Int. J. Pharm. Sci. Res.* **2014**, *5*, 5013–5018.
32. Astray, G.; Gonzalez-Barreiro, C.; Mejuto, J.C.; Rial-Otero, R.; Simal-Gándara, J. A review on the use of cyclodextrins in foods. *Food Hydrocoll.* **2009**, *23*, 1631–1640. [[CrossRef](#)]
33. Zhou, Y.; Sun, S.; Bei, W.; Zahi, M.R.; Yuan, Q.; Liang, H. Preparation and antimicrobial activity of oregano essential oil Pickering emulsion stabilized by cellulose nanocrystals. *Int. J. Biol. Macromol.* **2018**, *112*, 7–13. [[CrossRef](#)]
34. Horváth, B.; Balázs, V.L.; Horváth, G.; Széchenyi, A. Preparation and in vitro diffusion study of essential oil Pickering emulsions stabilized by silica nanoparticles for *Streptococcus mutans* biofilm inhibition. *Flavour Frag. J.* **2018**, *33*, 385–396. [[CrossRef](#)]
35. Bankier, C.; Cheong, Y.; Mahalingam, S.; Edirisinghe, M.; Ren, G.; Cloutman-Green, E.; Ciric, L. A comparison of methods to assess the antimicrobial activity of nanoparticle combinations on bacterial cells. *PLoS ONE* **2018**, *13*, e0192093. [[CrossRef](#)]
36. Pape, W.J.; Pfannenbecker, U.; Hoppe, U. Validation of the red blood cell test system as in vitro assay for the rapid screening of irritation potential of surfactants. *Mol. Toxicol.* **1987**, *1*, 525–536.
37. Aveyard, R.; Binks, B.P.; Clint, J.H. Emulsions stabilised solely by colloidal particles. *Adv. Colloid Interface Sci.* **2003**, *100–102*, 503–546. [[CrossRef](#)]
38. Drobna, E.; Gazdag, Z.; Culakova, H.; Dzugasova, V.; Gbelska, Y.; Pesti, M.; Subik, J. Overexpression of the *YAP1*, *PDE2*, and *STB3* genes enhances the tolerance of yeast to oxidative stress induced by 7-chlorotetrazolo[5,1-c]benzo[1,2,4]triazine. *FEMS Yeast Res.* **2012**, *12*, 958–968. [[CrossRef](#)]
39. Fujs, Š.; Gazdag, Z.; Poljšak, B.; Stibilj, V.; Milacic, R.; Pesti, M.; Raspor, P.; Batic, M. The oxidative stress response of the yeast *Candida intermedia* to copper, zinc, and selenium exposure. *J. Basic Microbiol.* **2005**, *45*, 125–135. [[CrossRef](#)]

40. Eruslanov, E.; Kusmartsev, S. Identification of ROS Using Oxidized DCFDA and Flow-Cytometry. In *Advanced Protocols in Oxidative Stress II*; Armstrong, D., Ed.; Humana Press: Totowa, NJ, USA, 2010; Volume 594, pp. 57–72. ISBN 978-1-60761-410-4.
41. Orosz, E.; Antal, K.; Gazdag, Z.; Szabó, Z.; Han, K.-H.; Yu, J.-H.; Pócsi, I.; Emri, T. Transcriptome-Based Modeling Reveals that Oxidative Stress Induces Modulation of the AtfA-Dependent Signaling Networks in *Aspergillus nidulans*. *Int. J. Genomics* **2017**, *2017*, 1–14. [[CrossRef](#)]
42. Ács, K.; Bencsik, T.; Böszörményi, A.; Kocsis, B.; Horváth, G. Essential Oils and Their Vapors as Potential Antibacterial Agents against Respiratory Tract Pathogens. *Nat. Prod. Commun.* **2016**, *11*, 1702–1712. [[CrossRef](#)]
43. Stöber, W.; Fink, A.; Bohn, E. Controlled growth of monodisperse silica spheres in the micron size range. *J. Colloid Interface Sci.* **1968**, *26*, 62–69. [[CrossRef](#)]
44. Sanders, E.R. Aseptic Laboratory Techniques: Plating Methods. *J. Vis. Exp. JoVE* **2012**, *63*, 3064. [[CrossRef](#)] [[PubMed](#)]
45. Pernodet, N.; Maaloum, M.; Tinland, B. Pore size of agarose gels by atomic force microscopy. *Electrophoresis* **1997**, *18*, 55–58. [[CrossRef](#)] [[PubMed](#)]
46. Moscho, A.; Orwar, O.; Chiu, D.T.; Modi, B.P.; Zare, R.N. Rapid preparation of giant unilamellar vesicles. *Proc. Natl. Acad. Sci. USA* **1996**, *93*, 11443–11447. [[CrossRef](#)]
47. Stromájer-Rácz, T.; Gazdag, Z.; Belágyi, J.; Vágvölgyi, C.; Zhao, R.Y.; Pesti, M. Oxidative stress induced by HIV-1 F34IVpr in *Schizosaccharomyces pombe* is one of its multiple functions. *Exp. Mol. Pathol.* **2010**, *88*, 38–44. [[CrossRef](#)]
48. Sali, N.; Nagy, S.; Poór, M.; Kőszegi, T. Multiparametric luminescent cell viability assay in toxicology models: A critical evaluation. *J. Pharmacol. Toxicol. Methods* **2016**, *79*, 45–54. [[CrossRef](#)]
49. Kőszegi, T.; Sali, N.; Raknić, M.; Horváth-Szalai, Z.; Csepregi, R.; Končić, M.Z.; Papp, N.; Poór, M. A novel luminol-based enhanced chemiluminescence antioxidant capacity microplate assay for use in different biological matrices. *J. Pharmacol. Toxicol. Methods* **2017**, *88*, 153–159. [[CrossRef](#)]
50. Dobson, A.J.; Boulton-McDonald, R.; Houchou, L.; Svermova, T.; Ren, Z.; Subrini, J.; Vazquez-Prada, M.; Hoti, M.; Rodriguez-Lopez, M.; Ibrahim, R.; et al. Longevity is determined by ETS transcription factors in multiple tissues and diverse species. *PLoS Genet.* **2019**, *15*, e1008212. [[CrossRef](#)]
51. Yu, T.; Zhou, Y.J.; Huang, M.; Liu, Q.; Pereira, R.; David, F.; Nielsen, J. Reprogramming Yeast Metabolism from Alcoholic Fermentation to Lipogenesis. *Cell* **2018**, *174*, 1549–1558.e14. [[CrossRef](#)]

Sample Availability: Samples of AEP, AET and AEE are available from the authors.



© 2020 by the authors. Licensee MDPI, Basel, Switzerland. This article is an open access article distributed under the terms and conditions of the Creative Commons Attribution (CC BY) license (<http://creativecommons.org/licenses/by/4.0/>).